Stability of oxylipins stored on biocompatible solid-phase microextraction (SPME) devices

Oluwatosin Kuteyi

A Thesis

In

the Department

of

Chemistry and Biochemistry

Presented in Partial Fulfillment of the Requirements

For the Degree of Doctor of Philosophy (Chemistry) at

Concordia University

Montreal, Quebec, Canada

March 2025

© Oluwatosin Kuteyi, 2025

CONCORDIA UNIVERSITY

School of Graduate Studies

This is to c	ertify that the thesis p	prepared by:	
Oluwatosir	n Racheal Kuteyi		
Entitled:	Stability of oxylip devices	pins stored on biocompatible solid-p	hase microextraction (SPME
and subm	itted in partial fulfilln	nent of the requirements for the degr	ee of
	Doct	tor of Philosophy (Chemis	try)
-	with the regulations of with the regulations of with the regulations of with the with the with the with the regulations of the with the with the regulations of the with the wi	of the University and meets the accep	pted standards with respect to
Signed by	the final Examining	Committee:	
	Dr. Yves Gélinas		Chair
			External Examiner
	Dr. Ken Yeung		Arm's LengthExaminer
	Dr. Xianming Zha	ang	Aim's Lengui Exammer
	Dr. Cameron Skinne	ar .	Examiner
	——————————————————————————————————————	61	Examiner
	Dr. Brandon Findlay	y	
	Dr. Dajana Vuckovi	ic	Thesis Supervisor
	Approved by	Dr. Louis Cuccia Graduate Program Director	
	<u>Defence date</u>	March 7, 2025	
		Dean, Faculty	

ABSTRACT

Stability of oxylipins stored on biocompatible solid-phase microextraction (SPME) devices

Oluwatosin Kuteyi, PhD.

Concordia University, 2025

Oxylipins are lipid mediators involved in inflammation, immunity, and oxidative stress. Accurately measuring oxylipins in biospecimens is analytically challenging due to their poor stability and susceptibility to enzymatic and non-enzymatic reactions during sampling, storage, and transportation. Recently, in vivo solid-phase microextraction (SPME) has been introduced as an effective method for direct sampling and extraction of oxylipins from biological tissues and fluids. Although in vivo SPME protects oxylipins from enzymatic degradation, it is not known how the storage in the SPME coating affects oxylipin stability and susceptibility to non-enzymatic reactions such as autoxidation, hydrolysis, and isomerization. The objective of this thesis was to evaluate the stability of oxylipins on SPME devices post-extraction and investigate whether the use of antioxidants, such as butylated hydroxytoluene (BHT), is useful in minimizing degradation processes. To evaluate the effect of 3freeze-and-thaw cycles (3-FT), and 18-day room temperature (RT) storage on the stability of oxylipins on SPME devices, oxylipins were extracted from standard solutions or citrated human plasma samples using hydrophobic lipophilic balance (HLB) SPME devices and analyzed by C18 liquid chromatography-high-resolution mass spectrometry (LC-HRMS). The pre- and post-extraction loading methods for antioxidants were successfully developed in order to investigate the ability of BHT to minimize oxylipin autooxidation during storage of SPME devices. Finally, degradation products of selected unstable oxylipins were comprehensively mapped by forced degradation studies including photooxidation (365 nm for 5 and 7 days), copper sulphate oxidation, and elevated temperatures (37°C and 50°C for 3 days). In conclusion, this is the first study to characterize the stability of oxylipins on SPME devices, demonstrating how SPME can effectively improve stability during sample storage, handling, and shipping even without the use of BHT. Importantly, these results also show how the degradation of unstable oxylipins can impact the accurate measurement of stable oxylipins and provide novel insight into major degradation products of PUFAs and selected unstable oxylipins.

Acknowledgements

I want to express my deepest gratitude to my supervisor Dr. Dajana Vuckovic for all the encouragement, support and contribution towards achieving my Ph.D. These 7 years have improved me in every area of my life as a mother and a wife I am very grateful.

I want to thank all my lab colleagues who both graduated and are currently in the laboratory for all their support. This includes Dr. Dmitri Sitnikov, Cian Monnin, Marianna Russo, Dr. Irina Slobodchikova, Ankita Gupta, Rosalynde Sonnenberg, Dr. Shama Naz, Dr. Lise Cougnaud, Alexander Napylov, Reza Maulana, Dr. Ana Carolina Dos Santos, Ekaterina Burovaia, Jesse McLaughlin, Dr. Myriam Mireault, Jordan Kache and Dr. Arianna Cirillo for all their help, collaboration and support.

I would like to thank my committee members, Dr. Cameron Skinner and Dr. Brandon Findlay, for being of great support and believing in me throughout this journey. I really appreciate you both.

Finally, a very big thank you to my family, especially to my family there, for supporting and for believing in me all through these years: my parents Mr. and Mrs. Odesanmi and Mr. Biola and Mrs. Iyabo Kuteyi, my brothers Olaitan Odesanmi, Oluwaseun Odujobi, Kolade and Konyinsola Kuteyi. My sister Oluwakemi Ajakaye and their families. My special thanks to my husband Boyce Ayomide Kuteyi who has supported, loved and provided for me throughout this journey including my son Jesse who began this journey with me. Thanks to you all.

Contribution of Authors

Chapter 4

Chapter 4 entitled "Forced degradation of oxylipins and their precursors using ultraviolet light (UV), copper sulphate oxidation, and elevated temperatures" authored by Oluwatosin Kuteyi and Dr. Dajana Vuckovic, included a collaboration with SCIEX to analyze the 50°C stored forced degradation study samples for PGE2, DHA and EPA at 3 days stored samples analyzed in CID and EAD mode. These sample analyses were performed at Sciex by Dr. Joel Blair, whereas I, Oluwatosin Kuteyi performed data analysis and interpretation of the results.

Table of Contents

ABSTRACT	iii
Acknowledgements	V
Contribution of Authors	vi
Table of Contents	vii
List of Figures	X
List of Tables	xiv
1.0 Oxylipins and eicosanoids	1
1.1 Biosynthesis of oxylipins	2
1.1.1 Enzymatic biosynthesis of oxylipins: Cyclooxygenase (COX)	3
1.1.2 Enzymatic biosynthesis of oxylipins: Lipoxygenases (LOXs)	4
1.1.3 Enzymatic biosynthesis of oxylipins: Cytochrome P450	6
1.2 Non-enzymatic reactions of oxylipins	7
1.2.1 Non-enzymatic reactions of oxylipins: Autoxidation	8
1.2.2 Non-enzymatic reactions of oxylipins: Photooxidation	10
1.3 Analytical techniques for measurement of oxylipins	11
1.3.1 Protein Precipitation (PPT)	12
1.3.2 Liquid-liquid extraction (LLE)	14
1.3.3 Solid-phase extraction (SPE)	15
1.3.4 <i>ln vivo</i> solid-phase microextraction (SPME) for oxylipin profiling	17
1.3.5 Liquid chromatography (LC) methods for oxylipin analysis	21
1.3.6 Mass spectrometry	24
1.3.7 Key LC-MS/MS methods for analysis of oxylipins	29
1.3.8 Quality control (QC) procedures for oxylipin measurement by LC-MS	31
1.4 Stability of oxylipins in biological samples	32
1.4.1 Short and long-term stability studies of biological fluids	33
1.4.2 Short and long-term stability studies of tissue samples	40
1.4.3 Effect of antioxidants on the stability of oxylipins in biospecimens	41
1.5 Research objectives	43
2.0 Stability of oxylipins stored on biocompatible solid-phase microextraction (S	
2.1 Introduction	45

2.2 Materials and methods
2.2.1 Chemicals
2.2.2 Freeze-and-thaw (FT) stability study of oxylipins
2.2.3 Freeze-and-thaw stability study of precursors
2.2.4 Room temperature (RT) stability study
2.2.5 LC-MS analysis of oxylipins
2.2.6 Data analysis
2.3 Results and discussion
2.3.1 3-cycle freeze-and-thaw stability study results after SPME extraction from standard solutions
2.3.2 3-cycle freeze-and-thaw stability study results after SPME extraction from plasma 54
2.3.3 18-day room temperature stability study results after SPME extraction from spiked citrate plasma
2.4 Conclusions
3.0 Effect of antioxidants on oxylipin stability using solid-phase microextraction (SPME) devices
3.1 Introduction 60
3.2 Materials and methods
3.2.1 Chemicals
3.2.2 Selection of antioxidants and optimization of antioxidant loading on SPME fibres 63
3.2.3 Optimization of oxylipin LC-MS method for analysis of BHT and BHA antioxidants64
3.2.4 Optimization of SPME method for pre- and post-extraction loading of BHT and BHA on SPME devices
3.2.5 3-cycle freeze-and-thaw stability study of oxylipins stored on SPME devices with BHT
3.2.6 LC-MS analysis of antioxidants and oxylipins
3.2.7 Data analysis
3.3 Results and discussion
3.3.1 Results of optimization of oxylipin LC-MS method for the analysis of antioxidants 70
3.3.2 Results of the optimization of pre-extraction loading of BHT and BHA on SPME devices
3.3.3 Results of the optimization of post-extraction loading of BHT and BHA on SPME devices

3.3.4 3-cycle freeze-and-thaw stability study to compare the effect of pre-and post-e loading of BHT on oxylipin stability on SPME devices after extraction from standar	
3.3.5 3-cycle freeze-and-thaw stability study of oxylipins extracted from spiked citrat and stored on SPME devices with pre-and post-extraction loading of BHT	_
3.4 Conclusions	88
4.0 Forced degradation of oxylipins and their precursors using ultraviolet light (UV) sulphate oxidation, and elevated temperatures.	
4.1 Introduction	92
4.2 Materials and methods	96
4.2.1 Chemicals	96
4.2.2 Forced degradation study experimental design	96
4.2.3. LC-MS analysis of forced degradation samples using ZenoTOF and EAD fragments.	
4.2.4 LC-MS analysis of oxylipins using CID	
4.2.5 LC-MS analysis of oxylipins using EAD	
4.2.6 SCIEX data analysis for oxylipins after CID and EAD fragmentation	99
4.3. Results and discussion	99
4.3.1 Forced degradation studies of precursors: AA, LA, DHA and EPA	99
4.3.2 Forced degradation studies of unstable oxylipins: PGE2, 11-HDHA, 13-H HoTre, 9-oxoODE, 15-HETE, 11,12-EpETrE, 5-oxoETE, 13-oxoODE, 4-HDoHE 1 9-HETE, LTB4, 16-HDoHE and 11β-PGF2α.	2-HETE
4.3.3 Comparison of forced degradation results to the results of stability studies	113
4.3.4 Additional structural elucidation of selected forced degradation samples us	_
4.4. Conclusions	130
5.0 Conclusions and future work	132
5.1 Conclusions	132
5.2 Future work	136
References	138
Appendix A: Supplementary information for Chapter 2	157
Appendix B: Supplementary information for Chapter 3	166
Appendix C: Supplementary information for Chapter 4	176

List of Figures

Figure 1.1: Structure of precursors.
Figure 1.2: Schematic diagram of oxylipins in our study and their derived pathways via
lipoxygenase (LOX), cyclooxygenase (COX), cytochrome P450 (CYP), and non-enzymatic
oxidation
Figure 1.3: Main steps of autoxidation reactions include a) initiation b) propagation c) termination
reactions
Figure 1.4: A diagram showing the production of 13-hydroperoxide and 9-hydroperoxide from
linoleic acid.
Figure 1.5: Mechanism of singlet oxygen oxidation in the presence of UV light
Figure 1.6: A diagram showing the key components of in vivo and in vitro SPME devices and a
summary of commonly used SPME coatings
Figure 1.7: Principle of extraction of solid phase microextraction (SPME)
Figure 2.1: Experiment design for 3-cycle freeze-and-thaw (FT) stability study
Figure 2.1: Experiment design for 5-cycle freeze-and-thaw (F1) stability study for 49 oxylipins extracted
on HLB SPME devices from the standard mix.
Figure 2.3: Box-plot diagram showing unstable oxylipins extracted on HLB SPME devices in a
3-freeze-and-thaw cycles stability study of Standard
Figure 2.4: Heatmap results of 3-freeze-and-thaw cycle stability study for 29 oxylipins extracted
on HLB SPME devices from spiked plasma samples
Figure 2.5: Heatmap results of room temperature stability study for 35 oxylipins extracted on HLB
SPME devices from spiked plasma
Figure 2.6: Diagrams showing improved oxylipin stability during storage and pre-analytical
handling using SPME
Figure 3.1: Overview of SPME procedure used for the optimization of antioxidant loading on
SPME fibre
Figure 3.2: Overview of SPME procedure for stability testing with pre-and post-extraction loading
of BHT and oxylipins
Figure 3.3: Effects of the fragmentor voltage on the peak area of BHA and BHT and in-source
fragment of BHA (164.0838)71
Figure 3.4: Effects of the gas temperature on the peak area of BHA and BHT and BHA in-source
fragment (164.0838)
Figure 3.5: Optimization of pre-extraction antioxidant loading procedure. Effect of long extraction
times (1-18 h) on the amount of BHA extracted by HLB SPME fibre
Figure 3.6: Optimization of pre-extraction antioxidant loading procedure. Effect of long extraction
times (1-18 h) on the amount of BHT extracted by HLB SPME fibre73
Figure 3.7: Optimization of post-extraction antioxidant loading procedure. Effect of short
extraction times (1-5 min) on the amount of BHA extracted by HLB SPME fibre

Figure 3.8: Optimization of post-extraction antioxidant loading procedure. Effect of short extraction times (1-5 min) on the amount of BHT extracted by HLB SPME fibre
Figure 3.9: Optimization of post-extraction antioxidant loading procedure with extraction of oxylipins. Effect of short extraction times (1-5 min) on the amount of BHT extracted by HLB SPME fibre
Figure 3.10: Comparison of the amount of 33 oxylipins extracted with (n=2) and without (n=4) post-extraction loading of BHT
Figure 3.11: Heatmap results of 3-cycle freeze-and-thaw stability study for 38 oxylipins with pre-extraction loading of BHT
Figure 3.12: Heatmap results of 3-cycle freeze-and-thaw stability study with post-loading of BHT for 38 oxylipins stored on SPME device extracted from standard
Figure 3.13: Box plot results for 3-cycle FT stability of (A) PGE2 and (B) AA stored on SPME devices with pre-and post-extraction loading of BHT
Figure 3.14: Amount of BHT remaining on SPME devices during 3-FT cycle stability study 82 Figure 3.15: Heatmap results of 3-FT cycle stability study for 24 oxylipins for pre-extraction loading of BHT and oxylipins stored on SPME device extracted from spiked citrate plasma 85 Figure 3.16: Heatmap results of 3-FT cycle stability study for 20 oxylipins for post-extraction
loading of BHT and oxylipins stored on SPME device extracted from spiked citrate plasma 86 Figure 3.17: Bar graph results for 3-FT cycle stability with pre- and post-extraction loading of 10 µg/mL BHT
Figure 3.18: Box plot results of oxylipins unstable in 3-FT cycle stability study with pre- and post-extraction loading of oxylipins from 10 $\mu g/mL$ BHT extracted from spiked citrate plasma.
Figure 4.1: Experimental design of forced degradation studies for oxylipins and precursors 96 Figure 4.2: Forced degradation results of PUFAs at various conditions in comparison to control samples
Figure 4.3: Non-enzymatic reaction pathway of AA mapped from the forced degradation study.
Figure 4.4: Non-enzymatic reaction pathway of LA mapped from the forced degradation study.
Figure 4.5: Non-enzymatic reaction pathways of EPA mapped from the forced degradation study
Figure 4.6: Non-enzymatic reaction pathway of DHA mapped from forced degradation study
Figure 4.7: Structures of oxylipins in our in-house library which matched the degradation products observed from the forced degradation of AA
Figure 4.8: Structures of oxylipins in our in-house library which matched the degradation products observed from the forced degradation of LA (9-and 13-HODE), DHA (8,15-DiHETE) and EPA (11-, 20- and 12-HEPE, 9-HODE)
Figure 4.9 : Non-enzymatic reaction pathway of PGE2 mapped from the forced degradation study

Figure 4.10: Non-enzymatic reaction pathway of 15-HETE mapped from the forced degradation
study
study
Figure 4.12: Non-enzymatic reaction pathway of 11-HDHA mapped from the forced degradation study
study
study
Figure 4.14: Non-enzymatic reaction pathway of 11-PGF2α mapped from the forced degradation
study
study
Figure 4.16: Non-enzymatic reaction pathway of 13-HDHA from the forced degradation study.
Figure 4.17: Non-enzymatic reaction pathway of LTB4 mapped from the forced degradation
study
Figure 4.18: Forced degradation study results of PGE2 at various conditions in comparison to
control samples. 80-120% lines show the acceptable stability range
Figure 4.19: Major degradation product of PGE2 is PGJ2 when stored for 3 days at 37°C and
50°C
Figure 4.20: Forced degradation results for 11-HDHA and 13-HDHA at various conditions in
comparison to control samples
Figure 4.21: Forced degradation results of 9-HoTrE and 9-oxoODE at various conditions in
comparison to control samples
Figure 4.22: Forced degradation results of 11,12-EpETrE, 15-HETE, 5-oxoETE, 4-HDoHE and
13-oxoODE at various conditions in comparison to control samples
Figure 4.23: Major degradation product of 11β -PGF2 α is PGE2 when exposed to 365 nm for 7
days
Figure 4.24: Forced degradation results of 12-HETE, 9-HETE, LTB4, 16-HDoHE and 11β -PGF2 α
at various conditions in comparison to control samples
Figure 4.25: Diagrams connecting forced degradation study results of precursors to unstable
oxylipins from stability studies
Figure 4.26: Diagrams connecting forced degradation study results of oxylipins to unstable
oxylipins from literature stability studies.
Figure 4.27: MS/MS spectra of PGE2
Figure 4.28: MS/MS spectra of EPA
Figure 4.29: MS/MS spectra of DPA
Figure 4.30: Chromatogram of unknown degradation product observed in PGE2 forced
degradation sample (50°C) and PGA2 standard analyzed on Agilent 6545 QTOF instrument using
CID in negative ESI mode
Figure 4.31: CID MS/MS spectra obtained for unknown degradation product observed in PGE2
forced degradation sample (50 $^{\circ}$ C) and PGA2 standard analyzed on Agilent 6545 QTOF instrument
using CID in negative ESI mode

igure 4.32: EAD MS/MS spectra results for unknowns with m/z 339.1940 in pooled sample of nurine plasma analyzed on ZenoTOF 7600 instrument in positive ESI mode
upplementary Figure A1: Heatmap results of 3-cycle freeze-and-thaw stability study for 27 xylipins extracted on HLB SPME devices from spiked plasma samples
0% methanol on LC-MS using C18 oxylipin method with optimization of fragmental voltage to 70V
upplementary Figure C1: Chromatogram of 9-oxoODE various forced degradation conditions.
upplementary Figure C2: EAD MS/MS spectra results for unknowns with m/z 361.1790 in lasma of mouse fed control chow diet (CD) analyzed on ZenoTOF 7600 instrument in positive SI mode
etention time of 24.1 min in pooled sample of murine plasma analyzed on ZenoTOF 7600 astrument in positive ESI mode
upplementary Figure C4: EAD MS/MS spectra results for unknowns with m/z 381.2070 in soled sample of murine plasma analyzed on ZenoTOF 7600 instrument in positive ESI mode
upplementary Figure C5: EAD MS/MS spectra results for unknowns with m/z 383.2113 in coled sample of murine plasma analyzed on ZenoTOF 7600 instrument in positive ESI mode.
upplementary Figure C6: EAD MS/MS spectra results for unknowns with m/z 383.2113 in lasma of mouse fed control chow diet (CD) analyzed on ZenoTOF 7600 instrument in positive SI mode
upplementary Figure C7: EAD MS/MS spectra results for unknowns with m/z 399.2150 in lasma of mouse fed control chow diet (CD) analyzed on ZenoTOF 7600 instrument in positive SI mode
upplementary Figure C8: EAD MS/MS spectra results for unknowns with m/z 405.2040 in soled sample of murine plasma analyzed on ZenoTOF 7600 instrument in positive ESI mode

List of Tables

Table 1.1: Summary of LC-MS methods for analysis of oxylipins 31
Table 1.2: Summary table of oxylipin stability studies in blood-derived samples using various
sample collection and storage conditions
Table 2.1: Summary of the results of 18-day room temperature study for oxylipins extracted
using SPME from spiked citrate plasma
Table 3.1: Properties of selected antioxidants 64
Table 3.2: Summary of the results of the 3-cycle freeze-and-thaw stability study for pre-extraction
loading of BHT from standard solution
Table 3.3: Summary of the results of 3-freeze-and-thaw cycle stability study using pre-extraction
loading of BHT and oxylipins extracted using SPME from spiked citrate plasma
Table 3.4: Summary of the results of 3-freeze-and-thaw cycle stability study using post-extraction
loading of BHT and oxylipins extracted using SPME from spiked citrate plasma
Table 3.5: A summary table evaluating the impact of pre-extraction and post-extraction BHT
loading on oxylipin stability on SPME fibres extracted from standard samples
Table 3.6: A summary table evaluating the impact of pre-extraction and post-extraction BHT
loading on oxylipin stability on SPME fibres extracted from spiked citrate plasma samples 91
Table 4.1: Comparison of the results for non-enzymatic oxidation of precursors in our studies
and the literature.
Table 4.2: Results for degradation products of oxylipins identified from the in-house oxylipin
library
Table 4.3: Results for comparison of forced degradation results to stability studies117
Table 4.4 : Summary of oxylipins in our library analyzed using Q-TOFs from both Agilent
(Agilent 6545 Q-TOF) and Sciex (ZenoTOF 7600) and analyzed using negative ESI119
Table 4.5: Comparison of retention time (rt) and masses of oxylipins analyzed on both Agilent
QTOF 6545 and ZenoTOF 7600 instruments
Table 4.6: Summary of product ions observed in PGE2 CID MS/MS spectrum obtained on
ZenoTOF 7600 instrument
Table 4.7: Summary of product ions observed in PGE2 EAD MS/MS spectrum obtained on the
ZenoTOF 7600 instrument
Table 4.8: Summary of product ions observed in the EPA CID MS/MS spectrum obtained on the
ZenoTOF 7600 instrument
Table 4.9: Summary of product ions observed in the EPA EAD MS/MS spectrum obtained on
the ZenoTOF 7600 instrument.
Table 4.10: Summary of product ions observed in the DHA CID MS/MS spectrum obtained on
the ZenoTOF 7600 instrument. 124
Table 4.11: Summary of product ions observed in the DHA EAD MS/MS spectrum obtained by
ZenoTOF 7600 instrument.

Supplementary Table A1: List of oxylipins evaluated during stability studies in Chapter 2 13
Supplementary Table A2: Summary of the results of 3-freeze-and-thaw cycle study for oxyliping
extracted using SPME from standard mix
Supplementary Table A3: Summary of the results of 3-freeze-and-thaw cycle study for oxyliping
extracted using SPME from spiked citrate plasma
Supplementary Table A4: Peak areas of identified in-house oxylipins for precursors' 3-cycle
degradation
Supplementary Table A5: Summary of the results comparing the concentration of
oxylipins of identified from 3-freeze-and-thaw cycle of precursors extracted from
standard solution and stored on SPME devices to concentration measured in HDMB
Supplementary Table A6: Summary of the results of 3-freeze-and-thaw cycle study for
oxylipins extracted using SPME from non-spiked citrate plasma
Supplementary Table B1: List of oxylipins evaluated during the 3-freeze-and-thaw (FT) cycles
stability studies of oxylipins with pre-and post-extraction loading of BHT
Supplementary Table B2: Summary of the results of the 3-freeze-and-thaw cycle study
of pre-loading extraction of BHT(5-h) and identified unstable oxylipins extracted
using SPME from standard solution
Supplementary Table B3: Summary of the results of 3- freeze-and-thaw cycle study of post-
loading extraction of BHT (5 min.) and identified unstable oxylipins extracted using SPME from
standard solution
Supplementary Table B4: Summary result of the average amount of BHT remaining on SPME
fibres (ng) during 3-freeze-and-thaw cycle stability study
Supplementary Table B5: Summary result of the average amount of BHT remaining on SPME
fibres (ng) during 3-freeze-and-thaw cycle stability study
Supplementary Table B6: Summary result of the average amount of BHT remaining on SPME
fibres (ng) during 3-freeze-and-thaw cycle stability study
Supplementary Table B7: Summary result of the average amount of BHT remaining on SPME
fibres (ng) during 3- freeze-and-thaw cycle stability study
Supplementary Table C1: List of oxylipins for forced degradation study
Supplementary Table C1: List of oxymphis for forced degradation study
at various degradation conditions
Supplementary Table C3: Summary of the results of the forced degradation of LA when stored
at various degradation conditions
Supplementary Table C4: Summary of the results of the forced degradation of DHA when
stored at various degradation conditions
Supplementary Table C5: Summary of the results of the forced degradation of EPA when
stored at various degradation conditions. 183
Supplementary Table C6: Summary of the results of the forced degradation of PGE2 when
stored at various degradation conditions

Supplementary Table C7: Summary of the results of the forced degradation of 13-HDHA when
stored at various degradation conditions
Supplementary Table C8: Summary of the results of the forced degradation of 11-HDHA when
stored at various degradation conditions
Supplementary Table C9: Summary of the results of the forced degradation of 9-oxoODE when
stored at various degradation conditions
Supplementary Table C10: Summary of the results of the forced degradation of 9-HoTrE when
stored at various degradation conditions
Supplementary Table C11: Summary of the results of the forced degradation of 15-HETE when
stored at various degradation conditions
Supplementary Table C12: Summary of the results of the forced degradation of 5-oxoETE
stored at various degradation conditions
Supplementary Table C13: Summary of the results of the forced degradation of 13-oxoODE
when stored at various degradation conditions
Supplementary Table C14: Summary of the results of the forced degradation of 4-HDoHE
when stored at various degradation conditions
Supplementary Table C15: Summary of the results of the forced degradation of 11,12-EpETE
when stored at various degradation conditions
Supplementary Table C16: Summary of the results of the forced degradation of LTB4 stored
when stored at various degradation conditions
Supplementary Table C17: Summary of the results of the forced degradation of 16-HDoHE
stored at various degradation conditions
Supplementary Table C18: Summary of the results of the forced degradation of 12-HETE when
stored at various degradation conditions
Supplementary Table C19: Summary of the results of the forced degradation of 9-HETE when
stored at various degradation conditions
Supplementary Table C20: Summary of the results of the forced degradation of $11\text{-PGF}2\alpha$
when stored at various degradation conditions
Supplementary Table C21: Summary of the results of the forced degradation of PGE2 using
SCIEX Zeno trap when stored at 3 days 50°C (%)
Supplementary Table C22: Summary of the results of the forced degradation of EPA using
SCIEX Zeno trap when stored at 3-days 50°C (%)
Supplementary Table C23: Summary of the results of the forced degradation of DHA using
SCIEX Zeno trap when stored at 3 days 50°C (%)
Supplementary Table C24: Summary of the results of the forced degradation pathway using
SCIEX Zeno trap and SCIEX OS software for DHA when stored at 3 days $50^{\circ}\text{C}\ (\%)$ 205
Supplementary Table C25: Summary of the results of the forced degradation pathway using
SCIEX Zeno trap and SCIEX OS software for EPA when stored at 3 days 50°C (%)
Supplementary Table C26: Summary of the results of the forced degradation pathway using
SCIEX Zeno trap and SCIEX OS software for PGE2 when stored at 3 days $50^{\circ}\text{C}\ (\%)$ 206
Supplementary Table C27: Summary table of identified unknown oxylipins from mice plasma
samples in comparison to the forced degradation in standard solution

Supplementary Table C28: Summary table of identified unknown oxylipin from mice plasma	a
samples with comparison to the forced degradation in standard solution	210

List of Abbreviations

AA	Arachidonic acid
HAc	Acetic acid
ACN	Acetonitrile
ALA	Alpha-linoleic acid
ANOVA	Analysis of variance
APCI	Atmospheric pressure chemical ionization
AUDA	Adamantan-1-yl-ureido-dodecanoic acid
BALF	Bronchoalveolar lavage fluid
ВНА	Butylated hydroxyanisole
ВНТ	Butylated hydroxytoluene
BD	Bligh & Dyer
CE	Collision energy
CID	Collision-induced dissociation
COX	Cyclooxygenase
CPLA2	Cytosolic phospholipase A2
CYP450	Cytochrome P450
DDA	Data-dependent acquisition
DGLA	Dihomo-gamma-linoleic acid
DHA	Docosahexaenoic acid
DIA	Data-independent acquisition
DiHETE	Dihydroxy eicosatetraenoic acid
DiHETrE	Dihydroxyeicosatrienoic acid
DiHDPA	Dihydroxydocosapentaenoic acid
DiHOME	Dihydroxyoctadecenoic acid
DP	Declustering potential
DPA	Docopentenoic acid
EA	Ethanolamide
ECD	Electron capture dissociation
EDTA	Ethylenediaminetetraacetic acid
EET	Epoxyeicosatrienoic acid
EpETrE	Epoxyeicosatrienoic acid
ЕрЕТЕ	Epoxyeicosatetraenoic acid
EID	Electron-induced dissociation
EPA	Eicosapentaenoic acid
EpETrE	Epoxyeicosatrienoic acid
ЕрЕТЕ	Epoxyeicosatetraenoic acid
ESI	Electrospray ionization
ETD	Electron-transfer dissociation

FT	Freeze-and-thaw
GC	Gas chromatography
HEDE	Hydroxyeicosadienoic acid
НЕРЕ	Hydroxyeicosapentaenoic acid
HLB	Hydrophilic-lipophilic balance
HODE	Hydroxyoctadecadienoic acid
HDHA/HDoHE	Hydroxydocosahexaenoic acid
HDPA	Hydroxydocosapentaenoic acid
НЕТЕ	Hydroxyeicosatetraenoic acid
HOTrE	Hydroxyoctadecatrienoic acid
HP	Hydroperoxide
НРЕТЕ	Hydroperoxyeicosatetraenoic acid
HPLC	High-performance liquid chromatography
HOTrE	Hydroxyoctadecatrienoic acid
IPA	Isopropanol
IsoF	Isofuran
IsoPs	Isoprostanes
K _{fs}	Fibre/sample distribution coefficient
LC	Liquid Chromatography
LLE	Liquid-liquid extraction
LOD	Limit of detections
LOQ	Limit of quantitation
LOX	Lipoxygenase
LTs	Leukotrienes
MCP	Microchannel plate
МеОН	Methanol
min.	Minute
MP	Mobile phase
MRM	Multiple reaction monitoring
MS/MS	Tandem mass spectrometry
MS	Mass spectrometry
MTBE	methyl tert-butyl ether
m/z	Mass-to-charge ratio
n	number
NP	Normal-phase
oxoETE	Oxoeicatetraenoic acid
oxoODE	Oxooctadecadienoic acid
pg	Picogram
PGs	Prostaglandins
PPT	Protein precipitation
PDs	Protectins

PUFA	Polyunsaturated fatty acid
Q	Quadrupole
QC	Quality control
Q-TOF	Quadrupole-time-of-flight
QQQ	Triple quadrupole
R·	Radicals
RF	Radio frequency
ROS	Reactive oxygen species
ROOH	Lipid hydrogen peroxide
ROO.	Lipid peroxyl radical
RP	Reversed-phase
rpm	Rotation per minute
rt	Retention time
RT	Room temperature
Rv	Resolvins
S	Supplementary
SD	Standard deviation
SP	Stationary phase
SPE	Solid-phase extraction
SPME	Solid-phase microextraction
SRM	Selected reaction monitoring
TOF-MS	Time-of-flight mass spectrometry
PPT	Protein precipitation
TTP	Triphenylphosphine
TXs	Thromboxanes
UHPLC-MS	Ultra high-performance liquid chromatography-mass
	spectrometry
¹ O ₂	Singlet oxygen
0-T	Control

Chapter 1: Introduction

1.0 Oxylipins and eicosanoids

Oxylipins constitute a category of oxygenated lipid mediators derived from polyunsaturated fatty acids (PUFAs), characterized by having more than one double bond in their structure. PUFAs are broadly classified into two main groups, namely omega-3 and omega-6 essential fatty acids. The key precursors of oxylipins in mammalian cells are composed of 18 or more carbon atoms and include arachidonic acid (C20:4n-6, AA), docosahexaenoic acid (22:6n-3, DHA), eicosapentaenoic acid (20:5n-3, EPA), linoleic acid (18:2n-6, LA), dihomo-gamma-linolenic acid (C18:3n-6, DGLA), and alpha-linolenic acid (C18:3n-3, ALA) (Figure 1.1). PUFAs such as AA and EPA produce a special class of oxylipins known as eicosanoids, originating from the Greek word *eicosa i.e.* oxylipins with a 20-carbon atom [1], [2]. The biosynthesis of oxylipins (Figure 1.2) is initiated by cell stimulation, causing an elevation in intracellular calcium (calcium flux), which results in the translocation of cytosolic phospholipase A2 (cPLA2) from the cell to the lipid membrane. Subsequently, the phospholipids are cleaved at the *sn-2* position, releasing free PUFAs for oxidation within the cell and producing lipid products including oxylipins [1], [3].

Figure 1.1: Structure of precursors. (i) arachidonic acid (ii) docosahexaenoic acid (iii) eicosapentaenoic acid (iv) linoleic acid (v) dihomo-gamma-linolenic acid and (vi) alpha-linolenic acid.

The key enzymatic pathways to generate oxylipins include cyclooxygenase (COX), lipoxygenase (LOX), or cytochrome P450 (CYP450) [1], [3], [4] but non-enzymatic oxidation of specific PUFAs may also take place [1]-[7].

Eicosanoids play significant roles in cellular signal regulation [7]. They can be involved in various regulatory mechanisms such as intercellular propagation (binding to G protein-coupled receptors), direct interaction within the cell by activating peroxisome proliferator-activated receptors, and inhibition of platelet regulatory functions [1], [3], [8]. They also have both anti-inflammatory and pro-inflammatory properties, playing significant roles in the central nervous, cardiovascular, gastrointestinal, genitourinary, respiratory, and immune systems [3], [5]. LOX metabolites of EPA and DHA called resolvin E1(RvE1) and protectin D1(PD1) are also responsible for resolving inflammation, and are called pro-resolving oxylipins [3], [9], [10]. Oxylipins produced from DHA by both LOX and COX are called PDs and have important roles in inflammatory disease [1], [11], [12] and tissue repair [1], [13], [14].

Numerous clinical and biomedical research studies have evaluated the involvement of oxylipins in various diseases [3], [15]. Examples of such studies include Alzheimer's disease [5], cardiovascular disease [7], [16], diabetes [17], COVID-19 [18], metabolic syndrome [19], neurodegenerative disease [20] and chronic pain [21]. Oxylipin pathways may also be important targets in drug discovery and development, and several oxylipins may serve as oxidative stress markers or potential biomarkers for several diseases.

1.1 Biosynthesis of oxylipins

The main biosynthetic pathways of oxylipins include COX, LOX and CYP450 enzymes.

1.1.1 Enzymatic biosynthesis of oxylipins: Cyclooxygenase (COX)

There are two predominant forms of the human COX enzymes (COX-1 and COX-2), however, the expression of COX-1 is higher as compared to COX-2 [1], [22], [23]. COX (Figure 1.2) enzymes are responsible for the synthesis of different classes of oxylipins, including prostaglandins (PGs) and thromboxanes (TXs). These enzymes can modulate platelet function, exhibiting either prothrombotic or anti-thrombotic effects[10], [24]. The PGs were the first oxylipins identified in 1930 [25]. For example, acetylsalicylic acid (Aspirin Cardio®) inhibits COX enzymes [9], [3], which are known for their significant roles in inflammation and tumorigenesis [26]. Different PGs and TXs series exist. The 1-series PGs (PGD1 and PGE1) and TXs (TXA1) are produced by COX-1 acting on DGLA, an ω-6 PUFA in human platelets [27], [28]. These compounds inhibit platelet function in humans, both in vivo and in vitro [29]. The 2- series PGs (PGE2, PGD2, PGI2) and TX (TXA2) [16] are COX-1 products derived from prostaglandin endoperoxide-H2 [1], [30]. Depending on its concentration, PGE2 can elicit both pro- and anti-platelet responses [22], [23]. PGD2 can dehydrate to produce compounds such as PGJ2, Δ 12PGJ2, and 15-deoxy- Δ 12,14-PGJ2, which can inhibit platelet activation [27]. PGI2 inhibits platelet function via its receptors and peroxisome proliferator-activated receptors and can be used for treating cardiovascular-related diseases [27]. TXA2 functions to activate platelets, enhancing aggregation and thrombosis [31]. The 3-series PGs (PGE3, PGD3, PGI3) and TX (TXA3) [32] are anti-inflammatory and inhibit platelet aggregation, produced by COX-2 acting on EPA [32], [33]. PGE3 can exert either pro- or anti-thrombotic effects in human platelets [33], [34].

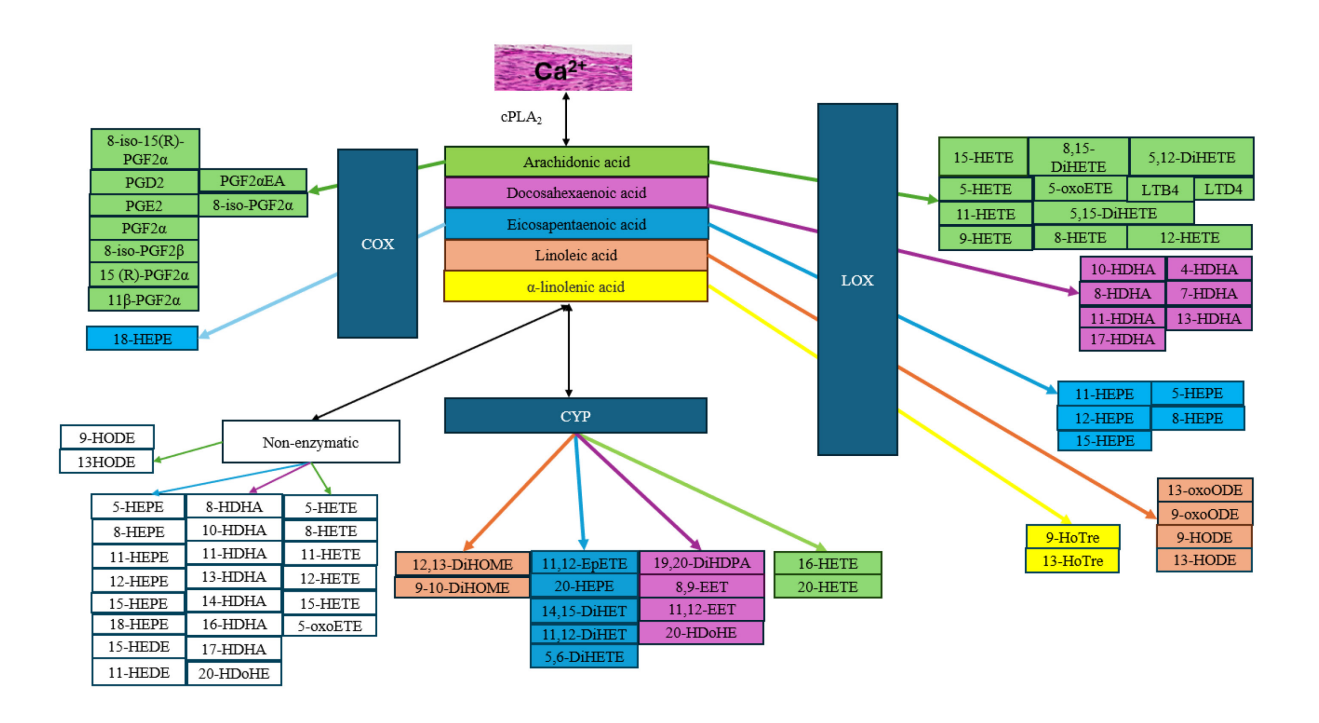


Figure 1.2: Schematic diagram of oxylipins in our study and their derived pathways via lipoxygenase (LOX), cyclooxygenase (COX), cytochrome P450 (CYP), and non-enzymatic oxidation. Colors depict the precursor pathway metabolite families: LA (orange), AA (green), DGLA (yellow), EPA (blue), DHA (purple), and non-enzymatic (colourless). HODE, hydroxyoctadecadienoic acid; oxoODE, keto-octadecadienoic acid; DiHOME, dihydroxyoctadecenoic acid; HOTrE, hydroxyoctadecatrienoic acid; PG, prostaglandin; TX, thromboxane; LT, leukotriene; HpETE, hydroperoxyeicosatetraenoic acids; HETE, hydroxyeicosatetrenoic acid; oxoETE, keto-eicosatetraenoic acid; EET, epoxyeicosatrienoic acids; HEPE. hydroxyeicosapentaenoic acid; HDHA, hydroxyl-docosahexaenoic acid; DiHDHA, hydroxydocosahexaenoic acid; DiHETE, dihydroxyeicosatetraenoic acid and DiHET, dihydroxy eicosatrienoic acid.

1.1.2 Enzymatic biosynthesis of oxylipins: Lipoxygenases (LOXs)

The LOXs (**Figure 1.2**) are enzymes that act on AA to produce oxygenated oxylipins that play significant roles in the activation and regulation of metabolic activities such as hemostasis and thrombosis [24]. LOXs can convert AA into different hydroperoxyeicosatetraenoic (HpETE) oxylipins exhibiting positional isomerism such as 5-, 8-, 9-, 11-, 12- and 15-HpETE metabolites. These isomers can be further converted to their corresponding hydroxyeicosatetraenoic (HETE)

products by the LOXs [1]. The HETE metabolites are converted to oxoeicosatetraenoic (oxoETE) products through the dehydrogenase pathway. Similarly, various LOX enzymes can convert other precursors such as LA, EPA, DHA, and DGLA to their metabolites [1].

Common LOXs which play significant roles in mammals are 5-LOX, 12-LOX, and 15-LOX [1], [35], [36]. The 5-LOX class helps improve airway smooth muscle cell proliferation [30], inflammation, and immune response [37]. 5-LOX acts on AA to generate 5-HpETE which in turn produces 5-HETE which can dehydrogenate to 5-oxoETE [1]. In a similar pathway, 5-HETE can dehydrate to produce leukotrienes (LTs) [5], such as LTA4, which further produces LTB4 and LTC4 [38]. LTC4 synthesizes LTD4 and LTE4 by the removal of the glutamyl residue mediated by dipeptidases [39]. 12-HpETE, a metabolite that inhibits platelet activation and thrombosis [40], is further metabolized to 12-HETE, which is known to exhibit anti-thrombotic and pro-thrombotic effects [40] as well as platelet activation [32].

12(S)-hydroxyeicosatrienoic acid (12(S)-HETrE), a 12-LOX metabolite of DGLA, has been reported to inhibit thrombosis through gas signalling in platelets [36]. It also exhibits anti-platelet or anti-thrombotic effects *in vivo* [41]. 11- and 14-HDPA, 12-LOX products of docosapentaenoic acid (DPA) act as an anti-thrombotic agent in platelets [42], [43]. 12(S)-hydroxyeicosapentaenoic acid (12-HEPE), a metabolite of eicosapentaenoic acid (EPA), exhibits an anti-thrombin effect in washed human platelets [36], [40].

15-LOX exists in two forms in mammalian tissue: leukocyte-type 15-LOX-1 and 15-LOX-2 found in eosinophils, leukocytes, reticulocytes, macrophages, dendritic cells, epithelial cells and epidermis [44], [45]. AA-derived oxylipins mediated by 15-LOX in humans such as 15-HETE and 8,15-8,15-diHETE and 14,15-diHETE help to regulate platelet functions by inhibiting platelet aggregation [46]-[48]. 15-HpETE and its reduced product, 15-HETE, have been reported to

increase platelet aggregation and thrombin generation in macrophages [49]. DHA, via the 15-LOX pathway, produces 17-hydroxy docosahexaenoic acid (17-HDHA) [50], also known to play a critical role in platelet function and pro-thrombotic effects [20]. LA with LOX synthesizes 13-hydroxyoctadecadienoic acid (13-HODE) from precursors in humans [1], [51], [52], a metabolite that affects the stimulation of thrombin in platelets. 15-LOX activity on DGLA generates 15-HETrE which enhances platelet aggregation in humans [53] and inhibits platelet aggregation induced by different agonists [54].

1.1.3 Enzymatic biosynthesis of oxylipins: Cytochrome P450

CYP450 (**Figure 1.2**) is another critical pathway for oxylipin synthesis. The CYP450 enzymes are membrane-bound proteins that derive their unique name from the characteristic absorption peak at 450 nm when they are bound to carbon monoxide in their reduced state [1]. CYP450 enzymes are diverse oxygenases, with over 50 forms identified in both humans and mice [55]. They can be expressed mainly in the liver, with some forms expressed in the heart, lungs, vasculature, kidney, and gastrointestinal tract [26], [32]. They play a significant role in the metabolism of various endogenous and exogenous compounds, such as oxylipins, steroids, fatty acids [55], as well as xenobiotics such as drugs and toxins. They are also involved in enzymatic control of vascular reactivity and systemic blood pressure [55]. CYP450 enzymes mediate the metabolism of AA, DHA and EPA through either the ω-hydoxylase or the epoxygenase pathways [1]. However, for other precursors such as LA and DGLA, only the epoxygenase pathways are utilized [1]. The ω-hydoxylase pathway leads to the formation of the HETE oxylipins while the epoxygenase yields the epoxy-oxylipins (Ep) that can be further metabolized to dihydroxy DiHETEs [1].

Well-known oxylipins derived from CYP450 pathways include 5,6-epoxyeicosatrienoic acid (5,6-EET), 8,9-epoxyeicosatrienoic acid (8,9-EET), 11,12-epoxyeicosatrienoic acid (11,12-EET), and

14,15-epoxyeicosatrienoic acid (14,15-EET). These metabolites have been reported to hyperpolarize platelets by activating Ca²⁺ and K⁺ channels, which leads to a decrease in the expression of platelet surface-bound P-selectin [56]. Other endothelial CYP450-derived oxylipins such as 19-HETE are known to have an anti-thrombotic effect in mouse platelets by activating the prostacyclin (IP) receptor [27], whilst the 20-HETE has shown both pro-and-anti-thrombotic effects on platelet function in humans [28]-[30].

1.2 Non-enzymatic reactions of oxylipins

Oxylipins may also be produced non-enzymatically. This usually occurs under conditions of oxidative stress, where reactive oxygen species (ROS) and other free radicals mediate the peroxidation of PUFAs [57]. A radical is an ion, atom or molecule which contains more than one pair of valence (unpaired) electrons that can occupy a molecular orbital space [57]. This radical ion can take part in various chemical reactions by contributing its unpaired electrons to molecules to achieve stability [57]. Examples of ROS free radicals are superoxide, hydroxyl, hydroperoxyl, peroxyl and singlet oxygen (1O₂) [57], [58]. The non-radical ROS are also oxidizing agents, and include hydrogen peroxides, ozone and organic peroxides. These ROS can be produced both enzymatically (oxidative reaction process in mitochondria) [24] and non-enzymatically and can be either beneficial or harmful once in excess to the body [59]. These ROS are produced nonenzymatically when exposure to radiation such as UV or visible light, enabling the excitation of triplet oxygen to produce (1O2) and can further be reduced to non-radical forms (less reactive) called hydrogen peroxides or hydroxy radicals. Lipids such as oxylipins, can be degraded by their oxidization with the radicals [60], [62]. The increase in the number of double bonds in the fatty acid chain increases the lipid's susceptibility to oxidation by hydrogen abstraction. This makes PUFAs and oxylipins especially vulnerable to autooxidation reactions [63], [64].

1.2.1 Non-enzymatic reactions of oxylipins: Autoxidation

Autoxidation reaction involves three major steps: initiation, propagation, and termination (Figure 1.3) [65]. The initiation step starts with the abstraction of a hydrogen atom from a nonradical lipid [R], typically by ROS such as hydroxyl radicals (•OH), leading to the formation of a lipid radical [65]. The loss of the hydrogen atom depends on its position, as the location determines the energy required to remove it from the compound. The bond type between two elements determines the energy required to break the bonds [66]. For example, for autooxidation of LA (refer to Figure 1.1 iv for structure), the energy required to remove the hydrogen attached to C8 or C14 is 75 kcal/mol, while at C17 or C18 a higher energy such as 100 kcal/mol is needed [65], [67]. The autoxidation of LA with double bonds at C9 and C13 produces 9-hydroperoxide and 13hydroperoxide oxylipins (Figure 1.4), which are primary oxidation products [65]. During propagation, the lipid alkyl radical [R•] reacts with ³O₂ to form a lipid peroxyl radical [ROO•] [65]. In the presence of a lipid or saturated compound with hydrogen atoms, the peroxyl radical abstracts hydrogen to produce hydroperoxide [ROOH], which is considered stable in the absence of reactions with metals such as copper or iron at room temperature (RT) [65], [68], [69]. The autoxidation reaction involves the continuous production of lipid alkyl radicals and hydroperoxides as long as there is oxygen, lipids (to donate hydrogen atoms), and heat; otherwise, the reaction is terminated [65].

In other words, the chain reaction is terminated when two radicals react to form a non-radical product, such as lipid peroxides. The termination phase can be facilitated by the presence of antioxidants which can react with ROO• to produce a non-radical by donating a hydrogen atom [65], [70]. Therefore, the main roles of antioxidants include inhibiting the formation of lipid alkyl

or peroxyl radicals, quenching (¹O₂) and controlling the effects of transition metals if present [65], [71].

Initiation RH
$$\longrightarrow$$
 R· + H·

Propagation R· + 3O_2 \longrightarrow ROO·
ROO· + RH \longrightarrow ROOH + R·

Termination ROO· + R· \longrightarrow ROOR
R· + R· \longrightarrow RR

(Where R: lipid alkyl)

Figure 1.3: Main steps of autoxidation reactions include a) initiation b) propagation c) termination reactions.

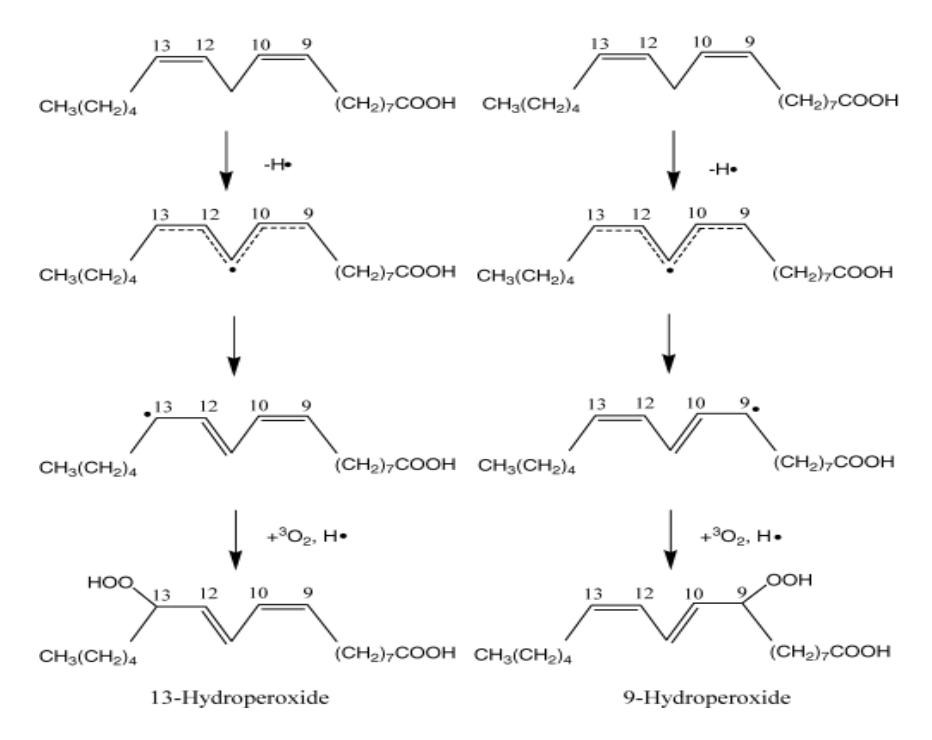


Figure 1.4: A diagram showing the production of 13-hydroperoxide and 9-hydroperoxide from linoleic acid. Diagram reprinted from reference [65].

1.2.2 Non-enzymatic reactions of oxylipins: Photooxidation

Photooxidation is another mechanism of free radical oxidation of PUFAs involving the formation of ${}^{1}O_{2}$ from ${}^{3}O_{2}$ in the presence of light and a photosensitizer [65], [72], [73]. Unlike radicals, ${}^{1}O_{2}$ directly reacts with the isolated double bonds of unsaturated FAs, producing two hydroperoxides for each double bond. The reaction rate correlates with the number of double bonds present in the FA. ${}^{1}O_{2}$ reacts approximately 1500 times faster with dienoic FAs compared to normal ${}^{3}O_{2}$ [74]. Because no free radical intermediates are formed, this reaction is not inhibited by radical chain-breaking antioxidants. Both ${}^{1}O_{2}$ and free radicals yield similar hydroperoxides during FA oxidation. Nevertheless, specific hydroxylated fatty acids such as 10- and 15-OH-FAs, are exclusive markers of ${}^{1}O_{2}$ -dependent FA oxidation [74].

Photooxidation reactions can be classified as Type I and II [65], [75]. With Type I, the sensitizer used is one which easily absorbs light and becomes excited from the singlet state. This follows the acceptance of hydrogen, or an electron, from a reactant, leading to radical formation. The electron transfer process between ${}^{3}O_{2}$ and an excited sensitizer produces superoxide, further creating hydroperoxides in the presence of metals [65], [73], [76]. The hydroperoxides can further react with superoxide to create ${}^{1}O_{2}$ in a process called Haber–Weiss [65], [77]. Sensitizers such as phenols, amines, and easily reducible quinones tend to promote the Type I process due to their oxidation or reduction capabilities [73], [78]. In contrast, olefins, dienes, and aromatic compounds, which are less readily oxidized or reduced, typically favour the Type II process [65]. Type II reaction involves a photosensitizer whereby excited oxygen is oxidized to create ${}^{1}O_{2}$ and later goes back to its singlet ground state [65], [79]. The rates of Type I or II processes varies based on factors such as the types of sensitizers and substrates [65], [75], [79], as well as the concentrations of substrates and oxygen [80].

UV light from direct sunlight, or fluorescent lights, can lead to the decomposition of unsaturated lipids, hydrogen peroxide (ROOH), and other peroxide compounds (ROOR). Via direct photooxidation, the ${}^{1}\text{O}_{2}$ produced from an activated ${}^{3}\text{O}_{2}$ can react directly with the bond of unsaturated fatty acid, by an attachment to the end of the carbon double bond (C=) to produce hydroperoxides. For example, linoleate undergoes oxidation to produce the hydroperoxide isomers such as 9-hydroperoxy-trans-10-cis-12-octadecadienoate (*trans, cis*-9-OOH), 13-hydroperoxy-cis-9-trans-11-octadecadienoate (*cis, trans*-13-OOH), 10-hydroperoxy-trans 8-cis-12-octadecadienoate (*trans, cis*-10-OOH) and 12-hydroperoxy- cis-9-trans-13-octadecadienoate (*cis, trans*-12-OOH) as shown in **Figure 1.5.** This free radical reaction is prevented if there is no availability of UV light or can be stopped if antioxidants are added [74].

Figure 1.5: Mechanism of singlet oxygen oxidation in the presence of UV light. Mechanism reprinted from reference [74].

1.3 Analytical techniques for measurement of oxylipins

Several analytical challenges affect oxylipin accurate quantification in biological matrices for clinical and research studies. The three critical challenges are the presence of isomeric and isobaric oxylipins which make correct identification challenging, low concentration in biological samples necessitating the development of very sensitive assays, and their poor stability during sample collection, transportation, and storage. Common sample preparation methods to extract oxylipins

and potentially increase assay sensitivity include protein precipitation (PPT), liquid-liquid extraction (LLE), solid-phase extraction (SPE), and, more recently, solid-phase microextraction (SPME). To separate various oxylipins, chromatographic techniques such as gas chromatographymass spectrometry (GC-MS) [81]-[83] or chiral chromatography [84] may be employed. To enhance sensitivity, antibody-based methods such as immunoassays including enzyme immunoassay (EIA) and radioimmunoassay (RIA) have been utilized in oxylipin analysis but may provide limited specificity and/or may not be able to measure multiple analytes in one analysis [85], [86]. For example, immunoassays focus on specific oxylipin subclasses such as IsoPs [87], LTs [88]- [90], TxBs [91], and PGs [90]. Some oxylipin classes such as regioisomers of EETs, and DHETs can be separated using capillary electrophoretic methods with long run times such as 196 minutes (min.) [92]. Therefore, immunoassays may provide limited selectivity for oxylipins with high structural similarity and may be used to measure a limited number of oxylipins in the same assay [93]. On the other hand, GC methods require high temperatures that can degrade oxylipins and necessitate derivatization [86]. Due to these various limitations, in the past decade, liquid chromatography (LC) coupled with mass spectrometry (MS) has proven to be more effective and is increasingly used for studying oxylipins. The next subsections will provide a more detailed overview of current sample preparation and LC-MS methods for oxylipin analyses.

1.3.1 Protein Precipitation (PPT)

PPT is a sample extraction approach that generally uses the addition of organic solvent to precipitate proteins and disrupt metabolite protein binding. Centrifugation is then used to remove the precipitated proteins. This prevents protein build-up on the chromatographic column during the chromatography run. PPT can also be performed by addition of acid in lieu of organic solvent. The addition of acids leads to the protonation of amino acid side chains on the protein surface,

reducing their overall charge [94]. This reduction in charge decreases the protein's solubility, causing it to aggregate and precipitate [94]. Also, the acid may alter the native conformation of proteins by disrupting the biomolecule's characteristic hydrophobic interactions or breaking its hydrogen or ionic bonds that maintain its structural integrity. Thus, the biomolecule becomes less soluble leading to precipitation. Another mechanism may involve the formation of insoluble salt complexes when acids react with proteins [94]. Organic solvents such as methanol (MeOH), ethanol (EtOH), acetonitrile (ACN) or isopropanol (IPA) are mostly used for PPT of oxylipins [95], followed by centrifugation and the removal of the supernatant which can then be analyzed on LC-MS [94]. PPT methods do not include an enrichment step, so their limits of quantification (LOQ) may not be sufficient for the measurement of very low abundance oxylipins [96]. Using MeOH, Lee et al. measured 50 oxylipins in serum [97], similar to what was obtained by Chocholouskova et al. who used ACN PPT to measure 50 oxylipins in plasma [98]. Wang et al. measured PUFA precursors such as AA in plasma using ACN [99]. PPT is a simple and rapid extraction method but one of its limitations is the high likelihood of analyte ion suppression when measuring complex biological samples such as plasma due to limited sample clean-up. This can adversely affect assay sensitivity [100]. On the other hand, if acid-based PPT methods are used, this may promote the formation/degradation of oxylipins by non-enzymatic reactions such as hydrolysis, which can impact the accurate quantification of oxylipins. In conclusion, solvent-based PPT methods may be suitable for the measurement of high-abundance PUFA precursors and oxylipins, but low-abundance oxylipins will typically require further sample clean-up and analyte enrichment, which may be provided by LLE or SPE.

1.3.2 Liquid-liquid extraction (LLE)

LLE is a conventional sample extraction technique which depends on the differential solubility of an analyte between two immiscible liquids such as aqueous and water-immiscible organic solvents. With LLE, the analytes separate between aqueous and organic phases based on their interactions with the two phases [101]. Compound properties such as polarity should be considered with performing LLE. To obtain high extraction efficiency of oxylipins, changing the pH of the extraction system is necessary to ensure oxylipins are present in their neutral form to be effectively extracted into the organic phase [95].

LLE is a common technique used for various classes of lipids including oxylipins. The classic Folch and Bligh and Dyer (BD) LLE methods utilize mixtures of chloroform: MeOH [44], [102], [103], and can be used for oxylipin extraction. For example, using red blood cells, 5-HETE, 5-HPETE and 5-oxoETE were quantified using LLE with the replacement of methylene chloride for chloroform in the BD method [45]. In brain samples, PGs (PGE2, 11\beta-PGE2, PGD2) and IsoPs (isoPGE2, 8-isoPGE2) were extracted using LLE with chloroform [23]. Another approach proposed by Jelena et al. confirmed better reproducibility and higher yield with methyl tert-butyl ether (MTBE) LLE in comparison to the BD method using biofluids (human serum and urine) and tissue (whole *Daphnia Magna*) [104]. Specifically, this study compared (MTBE)/methanol/water solvent system (here termed modified Matyash; 2.6/2.0/2.4, v/v/v) to original Matyash method (10/3/2.5, v/v/v) and the conventional chloroform/methanol/water (stepwise BD, 2.0/2.0/1.8, v/v/v). Such LLE methods can be applied for highly abundant oxylipins in biological matrices, however, the measurement of oxylipins with low concentrations in pg/mL can be a challenge [15]. Another limitation of LLE is its incompatibility with direct injection on LC-MS, which necessitates further steps before injection such as evaporation/reconstitution. Other limitations of LLE are the time consumption, the possibility of formation of emulsions, and the use of large volume of organic solvent(s) as compared to PPT. However, although LLE continues to play an important role in the extraction of oxylipins from biological samples, due to the low concentrations of many oxylipins, high enrichment ratios are required. SPE methods, with more easily attained high enrichment values, predominate in oxylipin analysis [15], [105].

1.3.3 Solid-phase extraction (SPE)

Solid-phase extraction (SPE) works on the principle of partitioning of analytes of interest between a liquid-phase sample and a solid-phase sorbent. SPE can enrich analytes of interest while also providing extensive sample clean-up to purify complex matrices. This may improve assay sensitivity and detection limits by removing interfering compounds or impurities that can contribute to the matrix effect [46], [105], [106].

Prior information on the properties of the analytes and selection of type of sorbent is important to ensure interference compounds are removed while the analyte is retained on the cartridge [49]. The main steps of SPE are (i) conditioning the SPE cartridge (containing solid sorbent), (ii) loading the sample to ensure the binding of the analyte of interest to the sorbent, (iii) washing of the cartridge with a solvent having high potential of removing interfering compounds, and (iv) eluting of analytes of interest with an appropriate organic solvent. It is possible to prevent the binding of interfering proteins to the SPE cartridge with the addition of inorganic salts (such as ammonium sulphate, sodium sulphate, or zinc sulphate) or acids (such as formic, perchloric, and trichloroacetic acid) to the washing solvent [15].

The choice of SPE cartridge and sorbent should be based on the chemical properties of the compound of interest. The most widely used cartridges for the extraction of oxylipins in SPE are

(i) reversed-phase (RP), commonly C-18, which enables the interaction of the aliphatic fragment of oxylipins with the non-polar stationary phase; (ii) normal-phase (NP) (silica), used for sample cleanup and polar compound retention; (iii) anion ion exchange, which retain oxylipins based on their interactions with positively charged sorbent and (iv) polymeric sorbents capable of extracting wide range of polar to hydrophobic analytes [15], [105]. Polymeric sorbents that have both lipophilic and hydrophilic functional groups such as Oasis Hydrophilic-Lipophilic Balance (HLB), offer better wetting properties and retention of polar compounds compared to silica-based absorbents, which are more difficult to optimize [15].

SPE has been applied for sample preparation of oxylipins in numerous studies [27], [35], [53], [54], [107]- [115]. For example, Phenomenex C18 cartridges (500 mg, 6 mL) with 20 mL 15% (v/v) MeOH, 20 mL water and 10 mL of hexane as wash solvent followed by elution using 15 mL of methyl formate were successfully used for qualitative and quantitative analysis of twenty monoand poly-hydroxy fatty acid derivatives of LA, AA, EPA, and DHA [54]. Galvao et al. measured 22 oxylipins in human plasma using Sep-Pak C18 (2.8 mL, 500 mg) with modification of elution the solvent composition to 2 mL of 0.1% acetic acid (HAc) in MeOH, which has also been shown to improve the recovery of some classes of oxylipins such as LTs, HETEs, and lipoxin A4 [109]. Weng et al. reported a comprehensive quantitation of 184 oxylipins with 26 deuterated internal standards in plasma with Strata-X- C18 SPE and elution solvent of 1 mL MeOH [86]. Another study compared three SPE types (Strata X-AW, C18 Sep-Pak, and Oasis HLB) for the quantification of 13 oxylipins in urine samples [116]. Strata X-AW showed better reproducibility for isoPGs than other SPE types tested [116]. For solid tissue samples such as brain tissue, care must be taken with the selection of the appropriate solvent with SPE, because there is a need to ensure proper homogenization of tissue for the release of oxylipins [117]. Some disadvantages of SPE include high cost per sample and the use of a large volume of sample and solvents. However, despite these drawbacks, SPE is currently the most widely used approach for analyzing oxylipins because of its reproducibility, high recovery of a broad range of oxylipins, sample clean-up, and high enrichment factor [106].

1.3.4 In vivo solid-phase microextraction (SPME) for oxylipin profiling

Solid-phase microextraction (SPME) is an equilibrium, non-exhaustive technique that can be used for direct *in vivo* and *in vitro* sampling and extraction of analyte(s) of interest from tissue and blood in living systems or *ex vivo* [118], [86]. In recent years, it has become a powerful microextraction technique for metabolomics and lipidomics, although it was first reported in 1989 for coupling with GC-MS [119].

The SPME devices consist of a metal fibre coated with an appropriate sorbent and coating thickness can vary from 5-400 µm. Similar to SPE, the selection of SPME sorbent is based on the properties of the analyte of interest, with the coatings with high partitioning coefficients (K_{fs}) values selected for a given application [120], [121]. The entire coated fibre is then inserted inside a hypodermic needle for protection and to facilitate sampling (**Figure 1.6**). For *in vivo* applications, biocompatible SPME coatings are used. These coatings are designed to minimize the adhesion and extraction of cells and proteins by adding a top layer of biocompatible polymer such as polydimethylsiloxane, polyacrylonitrile, polypyrene or polyethene glycol to completely cover the sorbent. Controlling the pore size of sorbent particles also helps to prevent extraction of proteins. (**Figure 1.6**) [120]. SPME coatings can be classified as adsorptive or absorptive coatings. With adsorptive coatings, analytes only interact with the surface of the sorbent, so they have limited capacity, limited linear range and may be susceptible to competition effects. In absorptive coatings,

analytes can be extracted by the entire volume of the sorbent, so they do not have the same limitations.

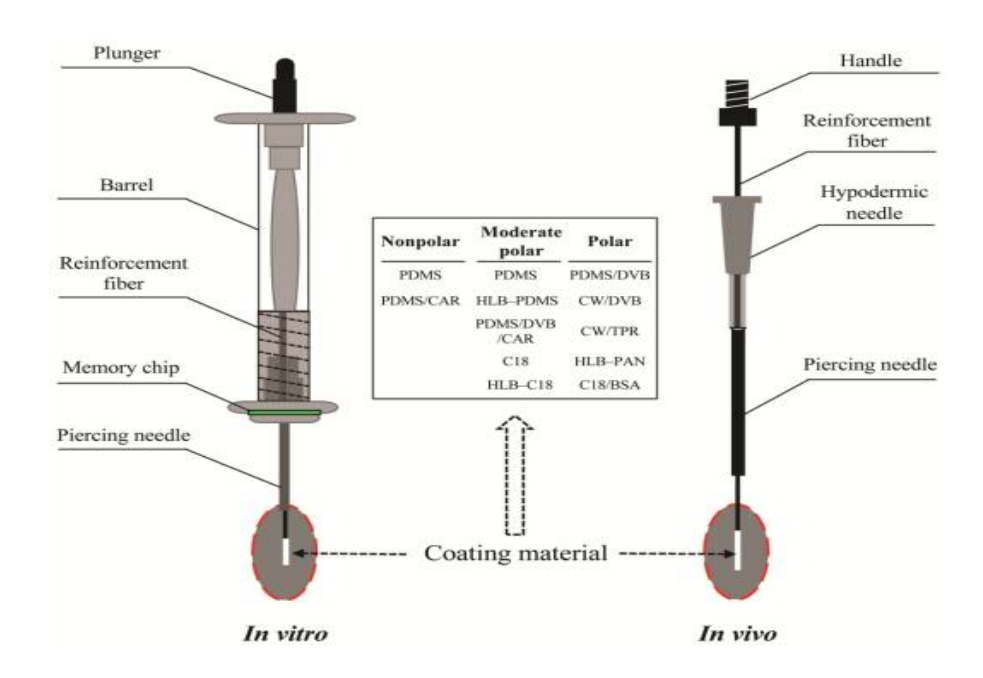


Figure 1.6: A diagram showing the key components of *in vivo* and *in vitro* SPME devices and a summary of commonly used SPME coatings. Reprinted from reference [120].

The SPME principle of extraction is based on the equilibration of analytes of interest between the coated organic polymeric phase fused to the SPME solid-support and the sample matrix [121]. This microextraction process involves the extraction of the analyte onto the coating until equilibrium is reached between the sample matrix and the coated fibre (**Figure 1.7**). For both *in vivo* and *ex vivo* studies, the analyte(s) extracted on SPME sorbent can be desorbed by exposing the sorbent directly to the capillary inlet system (GC) for thermal desorption or indirectly by desorption in an appropriate solvent (GC or LC) [120].

SPME can be performed in headspace or direct immersion mode. For oxylipins, due to their low volatility and poor stability at high temperatures, direct immersion is preferred. The main steps of *in vivo* SPME, employed for oxylipin extraction from the rat brain were: (i) pre-conditioning of

the fibre with an organic solvent to clean the fibre and condition the sorbent, (ii) direct immersion of the fibre into the biological matrix for the selected extraction time, (iii) removal of the fibre after the allocated time and rinse in water to avoid carryover of the matrix into the desorption solvent and (iv) placement of the fibre into the desorption solvent with agitation for a selected length of time to desorb the analytes of interest into solvent [121], [122]. The resulting desorption solvent containing the analytes can then be directly analyzed by injection into LC-MS or if need be, can undergo a reconstitution/evaporation step to improve the limit of detection by increasing the enrichment factor [121], [123].

The amount of the analytes extracted by SPME at equilibrium is given by **Equation 1.1** [121], [124] where different terms are defined in **Figure 1.7**. For large sample volumes, if $K_{fs} \ll V_s$, then **Equation 1.2** is applicable, and does not require the use of a defined sample volume. This allows the use of SPME for *in vivo* studies, for example, sampling directly the flowing blood of an animal, or for environmental studies, such as sampling directly a lake or river. To determine the distribution coefficient K_{fs} **Equation 1.3** is used.

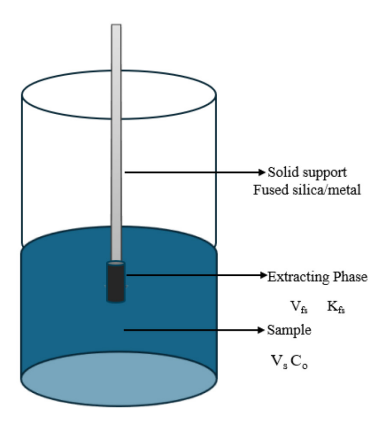


Figure 1.7: Principle of extraction of solid phase microextraction (SPME). Where V_f = volume of fibre coating; K_{fs} = fibre/sample distribution coefficient; V_s = volume of sample; C_0 = initial concentration of analyte in the sample, C_f and C_s = concentration of analyte in the sorbent and sample, n_e = the amount of analyte extracted onto the coating, t = extraction time.

Equation 1.1
$$n_e = \frac{K_{fs}V_fV_sC_0}{K_{fs}V_f+V_s}$$

Equation 1.2
$$n_e = K_{fs}V_fC_0$$

Equation 1.3
$$K_{fs} = \frac{C_f}{C_s}$$

The geometry of the SPME device can be modified depending on the type of sampling required. A syringe-like arrangement has been successfully used for various applications [120], [125], [126], [127] and various specimen types such as human [81], [128], [129], plant [130]-[132] and animal [133], [134].

In vivo SPME is an extraction method which can be employed for the measurement of both exogenous and endogenous compounds present in living systems. It has been applied to various animal studies [87], [92], [126], [135] due to its excellent selectivity and sample enrichment efficiency without the need to sacrifice the animal. Another common in vivo sampling technique is microdialysis, but it is mostly effective for polar analytes, unlike SPME which is suitable for intermediate hydrophobic analytes and hydrophobic compounds [136]. A major development in oxylipin analysis from tissue samples is using SPME for both in vivo sampling and extraction in a single step [123]. In vivo SPME is a promising approach for oxylipin analysis because (i) it is possible to obtain a true concentration of oxylipins in the brain of living animals without sacrificing the animal for the first time, (ii) it enables the study of the changes in oxylipin concentrations in an individual animal in response to a perturbation such as medication, stress or disease onset and (iii) it can protect the oxylipins from enzymatic reactions during the sampling step because the enzymes are not extracted and can avoid post-mortem changes. True oxylipin concentration is the

actual concentration of the oxylipins in the sample present at the time of sampling, ensuring that no artifactual release of oxylipins occurs during the sample collection (See Section 1.4.2). Using this approach, Napylov et al. measured the largest panel of oxylipins in vivo in rat brains with a total of 52 oxylipins obtained, 26 were successfully identified and the remaining 26 require further investigation [123]. Despite these advantages, there are limitations of in vivo SPME including the following: (i) it is a non-exhaustive technique so very small amounts of analyte are extracted, thus requiring analytical methods with excellent limits of detection (LOD), (ii) the inter-fibre variability can be high, especially for very thin coatings and (iii) the concentrations determined in vivo correspond to time-weighted average over the sampling time. In vivo SPME sampling times in flowing blood can be short (0.5-2 min.), because blood flow serves as a means of agitation in the system. In tissue, sampling in interstitial fluid relies on diffusion as the main mass transfer process, thus longer extraction times of 15-30 min. are typically required for tissue sampling and analytes present at low concentrations, such as oxylipins [121], [123]. SPME and SPE both use similar principles for the extraction of oxylipins from the biological milieu, but when considering the amount of solvent used, sample volume required, and ability to directly integrate sampling and extraction, SPME is preferable. A key limitation of SPME, as compared to SPE, is its nonexhaustive nature, which can affect sensitivity [15]. In conclusion, using in vivo SPME for oxylipin measurements in blood and tissue opens up new possibilities to improve oxylipin stability during sampling, transportation and storage.

1.3.5 Liquid chromatography (LC) methods for oxylipin analysis

The analysis and correct identification of oxylipins in biological samples is challenging due to the difficulty in distinguishing various isomers, many of which may have similar MS/MS fragmentation patterns. These could be regioisomers or stereoisomers, and thus often

chromatographic separation may be required for accurate measurement of selected oxylipins. The most common method used for the analysis of oxylipins is LC-MS because it provides better sensitivity and selectivity for various biological sample types for oxylipin studies [86].

The separation of analytes using LC relies on their partitioning between the stationary phase (SP) and mobile phase (MP). Separation with LC requires knowledge of the properties of the compound to aid method development and optimization. The chemical properties of the analytes of interest determine the choice of MP and SP. Depending on the chromatographic mode employed, compounds may be separated based on their polarity, size and/or interactions with both phases. Different modes of LC can be employed in the separation of oxylipins, including normal, reversed-phase (RP) and chiral chromatography [137]. RP-HPLC is the most frequently used for the separation of oxylipins [138]. Normal-HPLC [139] is not typically compatible with MS analysis, so will not be discussed further in this thesis.

Oxylipin analysis can be performed using different flow rates. Using flow rate in nanoliter/min. and reducing column diameter can enhance sensitivity for measuring low-concentration compounds such as oxylipins with nano-LC-MS. Nano-LC allows the use of smaller sample volume, and can offer better sensitivity and separation of compounds [140]- [142], but suffers from very long analyses times and poor retention time (rt) reproducibility which is especially detrimental for accurate oxylipin identification. Thus, the most used LC methods rely on ultrahigh performance liquid chromatography (UHPLC) with conventional flow rates [115], [143], [144]. This includes 2.1 mm x 5-20 cm long chromatographic columns packed with sub-2 µm particles and the use of flow rates ranging from 0.3-0.8 mL/min.

Chiral chromatography can be used for the separation of oxylipin stereoisomers but may require long run times. For example, a 107 min. separation was used to separate 16 isomers of

trihydroxyoctadecenoic acids using same LC-MS/MS instruments to perform both chiral analysis and quantification. The columns used are BEH C18 and Chiralpak AD-RH in two separate analysis [145]. Vickery *et al.* separated 18-R/S-HEPEs and 18R/S-resolvin (Rv) E2 stereoisomer pairs from human sera using the Chiralpak AD-RH column [84]. Another chiral method was developed to characterize S-HETEs in colonic mucosa [146]. Chiral HPLC can also be used for the measurement of oxidative stress biomarkers such as PGs and isoPGs [23], or when chiral information is required.

The most common stationary phases for oxylipin separations with HPLC/UHPLC are octadecyl silica (C18) or octyl silica (C8) RP columns [147]. Using core-shell C18 columns can help achieve good resolution in a shorter analysis time. Shorter analysis times are achieved due to the porosity of the shell layer, which provides a large surface area and allows rapid diffusion (mass transfer) of analytes from the MP to the SP. Better resolution results from the solid core, which limits diffusion of the analyte to only the porous outer layer of the particle. This reduces peak broadening and leads to sharp peaks. For example, Chen et al. successfully quantified 131 endogenous oxylipins in human plasma using an HSS T3 column and reduced the analysis time from 20-60 min. to 4-12 min. [115]. A comparative study of standard C18 column and Kinetex core-shell column by Kortz et al. reported better separation of seven PUFAs and 94 oxylipins with a run time of 7 min. for the core-shell column [148]. Considering the wide range of oxylipin polarities, using gradient elution is common practice with the addition of additives (0.1% formic acid, 0.1% HAc) to the MP which enhances ionization efficiency in the MS. MP A is usually water with an additive, while MP B is the organic solvent such as ACN, IPA, or MeOH. These solvents can be used individually or mixed to enhance the chromatographic resolution of analytes including oxylipins [116]. Monnin et al. compared the performance of ammonium acetate and HAc as MP additives and found that HAc

can enhance lipid ionization by 2-9x as compared to ammonium acetate [149]. Specifically, very low concentrations of HAc (0.02% v/v) are recommended [147], [149] for best LOQs. Another study further demonstrates the efficiency of acetic acid additive in the LC-MS separation of lipids [146]. The use of additive such as ammonium acetate has also shown excellent separation for oxylipins such as 5-HETE, 11,12-EET, 15-HETE, 5,15-DiHETE, 6-transLTB4, 11-HETE, 12-HETE, 4-and 14-HDHA along with other endogenous oxylipins in human plasma [115].

Numerous UHPLC-MS/MS methods have been reported to date. For instance, a large panel of 141 oxylipins was successfully analyzed with C18 LC-MS/MS using a 25 min. run time with MP (A: H₂O/ACN/HAc (70/30/0.02, v/v/v) and B B: ACN/IPA (50/50, v/v) [150]. Another method covering 85 oxylipins used the Agilent Zorbax Eclipse Plus C-18 column and 16 min. run time [49]. Thakare *et al.* quantified 34 oxylipins in human serum, sputum and bronchoalveolar lavage fluid (BALF) using BEH Shield RP18 UHPLC-MS/MS with a 25 min. gradient run [151]. High sensitivity assay on SCIEX Triple Quad[™] 6500 plus QTRAP was developed by Fu *et al.* for the detection of 87 oxylipins within 20 min. run time, with LODs of 0.05-0.5 pg observed [152]. A larger panel of 184 oxylipins, including their deuterated internal standards, was measured within a very short 5 min. run time by Wang *et al.* in human plasma using Acquity UHPLC BEH Shield RP18 [86]. Napylov *et al.* measured 65 oxylipins and 7 internal standards, with successful separation of isomers using Zorbax Eclipse Plus C-18 column in a 40 min. run [123]. In this thesis, the optimized UHPLC-MS/MS method developed in our laboratory by Napylov *et al.* for successful quantification of oxylipins in both *in vivo* [123] and *ex vivo* [153] studies will be used.

1.3.6 Mass spectrometry

MS is an analytical technique used for qualitative and quantitative analysis of a wide range of compounds, including small molecules and large biomolecules such as complex proteins in

biological matrices [154]. The use of MS for metabolomics and lipidomics typically involves coupling MS with separation techniques such as GC or LC [155]. Using appropriate sample preparation is key with MS when applying it to complex matrices. SPE, LLE, PPT [156], or derivatization are frequently used [157] to simplify the sample matrix and potentially enhance analyte concentration.

MS consists of three main components: the ion source, which ionizes the analyte(s); the mass analyzer, which separates the ions based on their m/z ratio; and the detector which detects the ions. The detected ions are displayed on the computer as the mass spectrum chart. The x-axis of the spectrum represents the m/z, and the y-axis represents the count rate, or intensity, of the ions [158]. MS coupled with LC typically uses soft ionization techniques performed at atmospheric pressure, such as electrospray ionization (ESI) and atmospheric pressure chemical ionization [159]. GC-MS uses electron ionization, which involves exposing the analyte molecules to an electron beam with 70 eV typically [160]. For ionization of complex biological samples, ESI-MS is commonly used due to its soft ionization (less kinetic energy applied) causing little or no fragmentation damage to the molecule of analytes of interest [161]. Additionally, no derivatization is required for most analytes of interest, including oxylipins which are commonly detected in negative ESI mode as the deprotonated molecular ion [M-H]. In positive ESI mode, common adduct ions observed are the protonated ion [M+H]⁺, sodium [M+Na]⁺ and ammonium [M+NH₄]⁺ adducts [162], [163]. ESI involves three key steps to ionize the analyte from LC effluent using high voltage: (i) formation of a fine spray of charged droplets, (ii) evaporation of the solvent, typically with the assistance of high temperature and high flow of nitrogen gas, and (iii) ejection of ions from the charged droplets. The resulting gas phase ions are then directed to the mass analyzer [161]. The mass analyzer in MS helps identify compounds by measuring the m/z of ions. Analyte identification can be further

aided by intentionally fragmenting the precursor ion and analyzing the fragmentation patterns produced [164].

Using electric or magnetic fields, mass analyzers can separate ions based on their m/z. Common mass analyzers include quadrupole (Q), time-of-flight (TOF), Fourier transform ion cyclotrons, ion traps, and orbitrap. These mass analyzers can be categorized based on their mass resolving power. Low resolving power mass analyzers include ion traps and quadrupoles which provide nominal resolution (0.1-1.0 Da), whereas TOFs, ion cyclotrons and Orbitraps can provide resolving powers of over a million and 0.01-0.0001 Da accuracy [165].

Using tandem MS (MS/MS), where two or more of the mass analyzers are coupled together can improve both identification and quantification using MS. The selection of the tandem MS is based on the application of interest. These include tandem quadrupole or triple quadrupole (QQQ) mass spectrometers for quantitative analysis, and quadrupole-time of flight (Q-TOF), ion trap-orbitrap, and quadrupole-orbitrap mass spectrometers frequently employed for metabolomic, lipidomic and proteomic studies where both analyte identification and quantification are required. For in-depth structural identification, Fourier-transform ion cyclotron resonance or Orbitrap Tribrids combining ion trap, Q and Orbitrap analyzers with various fragmentation techniques can be preferred.

The two most used tandem mass spectrometers for oxylipin analysis are QQQ and Q-TOF, so these will be described in more detail. The Q mass analyzer is made up of four parallel-positioned rods arranged in circular cross-sections with each opposite rod under the influence of an electric field. The electric field generated between the opposing rods allows ions with specific m/z to pass based on the applied frequency (radiofrequency) and the direct current. Depending on the radiofrequency and direct current applied, only specific m/z have a stable trajectory throughout the quadrupole and can reach the detector [166]. QQQ is made of three quadrupoles, which operate as full

quadrupoles (Q1 and Q3) or allow ion fragmentation and transmission of all resulting ions (Q2). It is frequently employed in selected reaction monitoring (SRM) mode where precursor m/z ion of interest is isolated in the first quadrupole (Q1), this precursor ion is then fragmented in Q2 by introduction of a collision gas such as argon, nitrogen, or helium and lastly the selected product ion is isolated by the third quadrupole and measured by the detector. Q-TOF is made of a quadrupole and time of flight (TOF) mass analyzer, whereby the third quadrupole of QQQ is replaced with a TOF. Briefly, in TOF, ions are accelerated to a uniform kinetic energy into a field-free TOF tube [167]. Lower-mass ions will travel faster and reach the detector earlier than heavier ions, which are slower. The time of arrival of the ions at the detector can be measured very accurately and then converted into m/z value. TOF spectrometers can be equipped with a Reflectron, which is an ion mirror, which helps to improve the resolving power of TOF by (i) doubling the flight path of the ions and (ii) compensating for small differences in kinetic energy of the ions with the same m/z when they are accelerated into the TOF tube. Q-TOF mass spectrometers use a microchannel plate (MCP) detector, which is made up of an array of electron multiplier detectors with large photoelectric surfaces for ion detection [168]. The MCP principle involves an ion hitting the surface and releasing an electron, which in turn creates a cascade of electrons to amplify the signal. The resulting electrons then hit a scintillator surface to convert the electrical signal to an optical signal. This light signal is finally converted back to an electrical signal via a photomultiplier tube to allow signal measurement at ground potential [169]. A Q-TOF was used in this thesis for oxylipin analysis and degradation product characterization. QTOFs can provide excellent sensitivity and fast data acquisition speed. Typical resolving powers achievable by QTOFs depend on the model and range from ~20,000-60,000, with some newer models today capable of resolving

powers up to 200,000, whereas the model used in this thesis can provide resolving power up to 40,000.

MS/MS fragmentation techniques include collision-induced dissociation (CID) and electron-activated dissociation (EAD) such as electron-capture dissociation (ECD), and electron transfer dissociation (ETD). By far, the most used fragmentation method for LC-MS analyses, including oxylipins, is CID. EAD methods were historically more frequently used for protein analyses, but new applications of EAD are gradually surfacing which use low-energy electrons for fragmentation and are applicable for small molecules such as oxylipins. CID fragmentation involves a collision between a neutral gas and the ions. The collision energies of CID range from 1-100 eV [166] to fragment the precursor compound to its product ion(s). CID is applicable for the quantification and identification of various ions in complex matrices [170]. Limitations to the use of CID for metabolomics and lipidomics include structural characterization of analytes, whereby depending on the analyte structure, insufficient information for unambiguous identification may be obtained [171]. For example, for oxylipins, this means that the location of all double bond positions may not be assigned based on CID MS/MS spectra.

ECD is a type of dissociation where ions capture free electrons leading to the formation of a radical, which can further undergo fragmentation. These multiply charged ions are irradiated with electron beams to produce radical cations followed by a cleavage fragmentation process called electron-transfer dissociation [172]. EAD operation involves the collision between ions and electrons. An electron is attracted to the positively charged precursor ions (typically multiply charged precursor ions such as commonly observed for peptides and proteins), leading to a reduction in the charge state and forming a radical product which is dependent on the electron kinetic energy (0-3 eV) applied [171]. For oxylipin structural characterization, EAD has proven to produce more fragment

ions for the structural identification of ring oxylipins such as cis and trans isomers of PGs [173]. Major limitations of EAD versus CID are the need for multiple positively charged precursors and the lack of comprehensive MS/MS databases for compound identification and structural interpretation.

The advantage of Q-TOF versus QQQ for oxylipin analysis is the ability to combine targeted and non-targeted analysis. This allows the targeted measurement of pre-selected oxylipins with authentic standards available for accurate quantification. Additional unknown, or untargeted, oxylipins may also be measured during the same analysis. This is because a full MS1 scan in TOF mass analyzer can collect information on all ions present within a selected wide range of m/z. Precursor ions of interest can be further prioritized to collect MS/MS spectra to aid in the identification of any unknowns of interest. This makes it possible to re-analyze the collected data for future identification of unknown masses in untargeted studies and makes it suitable for forced degradation studies. In contrast, QQQ is run in SRM mode, whereby specific precursor m/z and product ion m/z of interest are selected before starting the analysis. Therefore, it provides information only on targeted oxylipins. The main advantage of QQQ is its high sensitivity, due to its ability to significantly reduce background noise, which increases signal-to-noise ratio and enables the detection of the analyte of interest at low concentrations. Even the best Q-TOF instruments still cannot beat the exquisite sensitivity of QQQ for many analytes.

1.3.7 Key LC-MS/MS methods for analysis of oxylipins

As mentioned in previous sections, the use of MS/MS coupled with HPLC or UHPLC has been the best approach for the analysis of oxylipins to improve resolution, sensitivity, selectivity, and analysis time [105]. LC-MS/MS with QQQ is frequently used for the quantitation of oxylipins in various biological matrices. For urine analysis, PGs were quantitated with C18 UHPLC-SRM-MS (QQQ),

and LODs of 0.002-0.06 ng/mL were achieved [143]. Similarly, Balgoma *et al.* reported LODs of 0.55-154 fmol for 26 lipids in urine samples [174]. For the analysis of oxylipins in whole blood and plasma, various LC-MS methods have been explored (**Table 1.1**). For example, IsoPs and isofuran, which are autoxidation products of PGs, have been quantified by Rund *et al.* [113]. Sens *et al.* used SPE with C18 UHPLC QQQ MS QTRAP 6500 ⁺ for the measurement of 67 oxylipins in whole blood and plasma with a 17 min. run time [175]. In another study, 34 oxylipins were quantified in human serum, sputum and BALF using C18 SPE and C18 UHPLC-MS/MS (Q3-LIT) with LOQs of 0.2-1 ng/mL depending on the matrix evaluated [151]. Solid biological matrices were also successfully analyzed by SPE-LC-QQQ-MS/MS. For example, Arnold *et al.* measured oxylipins in rat heart, kidney, brain, lungs, pancreas, red blood cells, and plasma and achieved 0.05-0.1 ng LODs [27]. PGs and isoPGs were quantified in murine brains with LOD of approximately 3 pg/mg in tissue for five PGs [23]. Fu *et al.* developed a highly sensitive method to evaluate 87 oxylipins, including lipoxins and resolvins, in mouse plasma and liver tissue as well as human plasma samples [152].

In addition to these targeted low-resolution MS methods, in our laboratory, Napylov *et al.* successfully developed an analytical method to measure 62 oxylipins and 7 internal standards using Q-TOF in 40 min. (Table 1.1) [153]. The method also separated critical pairs of isomers, such as 8- and 12-HETE. The same method was also employed in another study for *in vivo* SPME sampling of living rat brain tissue to successfully measure 52 oxylipins, of which 26 were identified and 26 unknowns [123]. The focus of this thesis is on improving the stability of oxylipins and identifying degradation products. Although QQQ is the most used mass spectrometer for oxylipin studies, because of its high sensitivity, since this thesis is focused on both target and non-target oxylipins, Q-TOF will be used as it can provide accurate quantitative information on target

oxylipins while simultaneously helping to monitor any degradation products during my study. QQQ would not be ideal for this research because not all degradation products are known *a priori* so appropriate SRMs cannot be set up. Furthermore, short analysis times on QQQ could also lead to potential interference(s) because some oxylipins have similar fragmentation spectra.

Table 1.1: Summary of LC-MS methods for analysis of oxylipins

Number of oxylipins in each study and references	Extraction method	LC-MS methods	LOD	
35, [113]	Bond Certify II SPE C18 C-18 LC - QQQ-LIT		0.005-1.0 nM	
57, [106]	C-18 SPE	C18 UHPLC-QTRAP5500	0.02-0.2 ng/mL	
131, [115]	HLB SPE	HSST3 UHPLC- QQQ	0.24-156.25 picogram (pg)	
110, [86]	Strata-X-C18 SPE	C-18 UHPLC- Triple Quad™ 6500 plus QTRAP	0.1-300 pg	
87, [152]	HLB-SPE	C-18 UHPLC- Triple Quad™ 6500 plus QTRAP	0.05–0.5 pg	
69, [153]	C-18 SPE	C-18 UHPLC-Q-TOF	0.1-0.8 ng/ml	

1.3.8 Quality control (QC) procedures for oxylipin measurement by LC-MS

The key quality control (QC) strategies which should be incorporated for any study of oxylipins are: running of blank samples including extraction blanks, the addition of internal standards to monitor extraction recovery and LC-MS performance including correction of matrix effects and analysis of calibration standards to establish and verify linear dynamic range of the method. Solvent and extraction blanks are typically analyzed to check for contamination or interferences that could affect accurate quantification. Additionally, solvent blanks are used to evaluate or prevent carryover between samples [176]. Internal standards are used in oxylipin studies to

compensate for any loss of oxylipins during the sample preparation process or to correct for ion suppression. In most cases, stable isotopic labelled standards are used with the same chemical properties as the analyte of interest [177]. Internal standards can also help measure or compensate for any degradation or loss of the analyte during sample preparation and analysis [150]. Stable isotopic labelled standards are not commercially available for all oxylipins of interest so typically one or few internal standards per oxylipin subclass are used for all members of that subclass. Two commonly used calibration methods for the quantification of analytes are internal standard or external standard calibration [178]. For the oxylipin studies presented in this thesis, external standard calibration were mainly used, as it was not desirable to correct for oxylipin degradation using internal standards. In addition to these strategies, ensuring repeatable performance of LC-MS throughout long analytical runs is important. For this purpose, QC samples are usually run periodically (e.g. after every 10 samples) to verify instrument performance. This QC sample could either be a pooled sample prepared by combining aliquots of all study samples or a standard mix of oxylipins prepared at a specific concentration [179].

1.4 Stability of oxylipins in biological samples

Analytical challenges such as the measurement of low concentrations of oxylipins have been successfully resolved by combining an appropriate sample extraction approach with high enrichment and powerful analytical techniques such as LC-MS/MS to improve resolution, sensitivity and selectivity for adequate quantitation [152], [180]. However, the stability of oxylipins remains a critical research problem. Ensuring stability is of keen importance in the study of oxylipins, due to the possible degradation of these compounds during sampling, storage and transportation, affecting their accurate measurement. Resolving this challenge is of great

importance, considering the physiological roles that oxylipins play. **Table 1.2** summarizes various stability studies of oxylipins in plasma samples with and without additives.

1.4.1 Short and long-term stability studies of biological fluids

Blood samples are typically collected into tubes containing anticoagulants, from which plasma can be collected after a short centrifugation step to remove cells. In biological fluids such as blood, serum, and plasma (Table 1.2), enzymatic pathways such as 5-LOX, COX, and CYP450 and nonenzymatic pathways may be activated for some classes of oxylipins. Therefore, prolonged blood storage time and temperature conditions immediately after specimen collection also contribute to the degradation of oxylipins even before the centrifugation process occurs [181], [182]. The use of additives such as ethylenediaminetetraacetic acid (EDTA) helps improve the stability of oxylipins for both blood and plasma, and is common for research and clinical studies [181]. EDTA is an anticoagulant and a chelating agent which binds to metal ions such as calcium and iron to produce soluble complexes. It also helps to prevent or suppress the formation of free radicals, which can participate in chemical reactions such as autoxidation, causing poor stability. EDTA is generally the preferred anticoagulant for oxylipin analysis in blood. Various studies have evaluated short-term stability (up to 120 min.) of whole blood and plasma with EDTA anticoagulant. Several AA-derived subclasses of oxylipins, such as HETEs, LTs and HDHAs were found to be unstable as summarized in Table 1.2 [96], [183]-[185]. 12-HETE was found unstable by both Ramsden et al. and Dorow et al. studies [184], [185] when stored at RT for up to 120 min. in EDTA whole blood. However, 15-HETE was stable in Ramsden et al. study but was found to significantly increase with time by Dorow et al. [184], [185]. Willenberg et al. evaluated the stability of oxylipins in EDTA whole blood when stored for short-term 60 min. at RT [96]. In this study, the concentrations of 15-HETE and 14(15)-EpETrE decreased as compared to the control. Koch et al.

evaluated the stability of 26 oxylipins in EDTA-whole blood for 24 h at 4°C or 4 h at 20°C before centrifugation, and found all tested oxylipins were stable [182]. The effect of other anticoagulants, such as heparin, was also tested. For example, Jonasdottir *et al.* compared the stability of 18 oxylipins at RT (2 and 8 h storage) and 6°C (2, 8, and 24 h storage) with/without EDTA and heparin, and found no significant difference between the two additives [186].

The long-term oxylipin stability at -20°C for EDTA plasma with and without additives for storage of one month to a year has been evaluated [107], [184]. Another long-term storage study of EDTA or heparin plasma with and without additives such as BHT confirmed the stability of all 18 tested oxylipins up to 1 year [186]. Polinski *et al.* studied the stability of 90 oxylipins stored at -80°C up to 356 days and reported significant changes for oxylipins such as 12-HETE, TXB₂, 14-HDHA, and 18-HEPE [183]. Finally, Hewawasam *et al.* investigated RT storage of 12 oxylipins in dried blood spots for up to 2 months and showed all were stable [187]. In summary, for liquid blood-based samples, EDTA is the preferred anticoagulant, while newer studies have also shown promising results for microsampling methods such as dried blood spots.

The presence of enzymes which can promote the enzymatic synthesis/degradation of oxylipins, such as epoxide hydrolase esterase, has been investigated [113], [188]. One possible way to reduce enzymatic activity is the use of organic solvents such as methanol with 12-(3-adamantan-1-yl-ureido)dodecanoic acid (AUDA or Paraoxon), which acts as an acetylcholinesterase inhibitor in human plasma to prevent further degradation [83]. Other inhibitors, such as 12-(3-adamantan-1-yl-ureido) dodecanoic acid and phenylmethylsulphonyl fluoride, were successfully used [83], [188].

Immediate freezing (-80°C) or flash-freezing using liquid nitrogen is recommended for biological samples collected to study oxylipins [83]. However, repeated FT cycles of biospecimens can

contribute to the poor stability of oxylipins. The effect of FT cycles on the concentration of oxylipins in plasma stored at -80°C was investigated by Dorow *et al.* [184], who found that oxylipins such as 12-HETE, 12-HEPE, and 5-HETE increased significantly during the first cycle. Another recent 4-FT cycle study of 46 oxylipins by Polinski *et al.* [183] also identified 12-HETE, 5-HETE, 18-HEPE, and 14-HDHA to be unstable, confirming some of the results previously reported by Dorow *et al.* [184].

In general, for plasma, the recommended storage conditions are to add methanol (50% and above, v/v), avoid FT cycles, and store samples at temperatures of -20 to -80°C [189], [184], [182], [181]. Even if the recommended conditions are employed, some oxylipins may still be unstable and antioxidants or enzyme inhibitors tested to date could not effectively protect all oxylipin subclasses. Therefore, these various stability study results indicate a need to investigate better ways to ensure the stability of oxylipins throughout the analytical process and sample storage.

Table 1.2: Summary table of oxylipin stability studies in blood-derived samples using various sample collection and storage conditions

Number of oxylipins in each study and references	Analytes	Storage conditions	Duration of storage	Sample matrix	Number of freeze and thaw cycles	Type of additive	Identified unstable oxylipins
8, [96]	Non- esterified plasma oxylipins	RT	5, 30, 60, and 120 min.	Pre-processed EDTA plasma (whole blood)	NA	NA	Increase 14,15-EpETrE
	Non- esterified	RT or 4°C	30, 60, 90, and 120 min.	EDTA whole blood processed for plasma	5-cycles	NA	12- and 15-HETE increase
28, [184]	8, [184] plasma and serum oxylipins	RT or 4°C -20 °C, -80°C, and -150°C	30, 60, 90, 120 min. 1 day, 1, 2, and 6 months	EDTA plasma (with and without additives)	NA	ВНТ	@ RT
18, [186]	Non- esterified plasma oxylipins	RT or 4°C 6°C -20°C	2 and 8 h 2, 8, and 24 h @-20°C 24 h and 1 week 1, 4, 12, 26, and 52 weeks 4, 12, 26, and 52 weeks	EDTA and heparin plasma (with and without additives)	NA	ВНТ	TXB2, 12-HETE, 5- HETE, LTB4 and LTE4 (short- and long-term storage without methanol addition)

Number of oxylipins in each study and references	Analytes	Storage conditions	Duration of storage	Sample matrix	Number of freeze and thaw cycles	Type of additive	Identified unstable oxylipins
16, [185]	Non- esterified plasma oxylipins	RT or ice	0, 10, 20, 30, 60, and 120 min.	Whole blood collected in potassium- EDTA tube and centrifuge for plasma	NA	NA	Increase of 12-HETE, 14-HDHA and TXB2 in whole blood @ RT
4, [189]	Non- esterified plasma oxylipins	−80°C	2.5 years	EDTA plasma	NA	NA	Increase of TXB2, 5- HETE, 12-HETE, and 15- HETE
		4°C	24 h	Whole blood collected in potassium- EDTA tubes and centrifuge for plasma	NA	NA	
	Non-	20°C	4 h	Processed EDTA			
	esterified and total plasma oxylipins	−20°C	5 days	plasma (with & without)	NA		Increases in 9-HETE and
		-80°C	1–6, 9, 12, and 15 months	EDTA plasma	NA	ВНТ	8,15-DiHETE

Number of oxylipins in each study and references	Analytes	Storage conditions	Duration of storage	Sample matrix	Number of freeze and thaw cycles	Type of additive	Identified unstable oxylipins
23, [181]	Non- esterified and total plasma and serum oxylipins	Whole blood at RT for 30 min, storage at 4°C	4 and 24 h, or after pneumatic tube system transport	Whole blood collected in potassium-EDTA tubes centrifuge for plasma and serum	NA	NA	Increase of PGE2, TxB2 and 12-HHT,15- HETE, 5-HETE, 11- HETE, 9-HETE in serum compared to plasma
87, [190]	Free and total plasma and oxylipins	4°C	24-120 h	EDTA plasma (with and without additives)	5-FT	внт	Significant increase of 11-HETE, 9-HpOTrE, 5-HETE, 11-HETE, 12-HETE, 11,12-DiHETrE, 12-HEPE, 9-HODE, 13-HODE, 9(10)-EpOME, 12(13)-EpOME, 12,13-DiHOME, after 2-FT cycles
46, [183]	Non- esterified plasma oxylipins	-80°C	3, 7-days, 1, 3, 6 - months, and 1 year 0, 10, 30, 60, and 120 min	EDTA plasma (no additives) Whole blood collected in EDTA, or heparin tubes an centrifuge for	NA 4-cycles	NA	Increase of 12-HETE and 5-HETE after 2-FT cycles Decreases in 18-HEPE and increases in 14- HDHA

Number of oxylipins in each study and references	Analytes	Storage conditions	Duration of storage	Sample matrix	Number of freeze and thaw cycles	Type of additive	Identified unstable oxylipins
Free and total plasma and oxylipins	0°C	0, 20, 60, 120, 240 min. (whole blood and plasma)		NA	NA	Increase of 12-HETE in	
	oxylipins	21°C	60, 240 min. (whole blood and plasma)	K₃EDTA blood and plasma			K ₃ EDTA whole blood @ RT

^{*}RT = Room Temperature *Min. = Minutes *Hour = h *NA=not applicable

1.4.2 Short and long-term stability studies of tissue samples

For tissue samples, the stability of oxylipins can be improved by immediate freezing with liquid nitrogen. During laboratory operations, storage on ice during sample preparation, minimizing FT cycles and long-term storage at -80°C have been recommended to prevent, or reduce, the degradation of these compounds [184]. This is because polyunsaturated precursors such as EPA and DHA are prone to non-enzymatic degradation at -20°C, especially for PGs and Rvs class [191]. However, even at -80°C, not all oxylipins will be stable. A study on brain samples reported a two-fold decrease in prostaglandins after one month of storage at -80°C [110]. The use of a pre-additive such as trans-4-[4-(3-adamantan-1-yl-ureido)cyclohexyloxy]-benzoic acid (t-AUCB) in mouse heart to inhibit the soluble epoxide hydrolase has been reported [192].

Different methods of euthanasia and tissue collection may adversely affect oxylipin measurement. For example, collection of brain tissue using traditional methods such as decapitation [117], [193] can result in artefactual release of oxylipins due to activation of phospholipase cascade. This release can lead to extremely inaccurate measurements of oxylipins which do not reflect true oxylipin concentrations in the brain. Golovko *et al.* [110] compared the use of decapitation and microwave irradiation for euthanized rodents, and showed that the use of head-focused microwave irradiation helped to reduce the PG by 10- to 40-fold in comparison to the use of decapitation due to effective inactivation of enzymes [110]. However, although head-focused microwave irradiation represents one way to ensure accuracy of oxylipin profiling, there is a critical need to develop new strategies that can accurately measure oxylipin profiles over time and without requiring animal sacrifice. In addition, the time required for tissue dissection can also impact the accuracy of oxylipin measurement. For instance, dissection time as short as 10 min drastically increased the

concentration of oxylipins such as diHOMEs, DiHETEs and DiHETES [194]. *In vivo* SPME method provides an attractive alternative to address these challenges.

1.4.3 Effect of antioxidants on the stability of oxylipins in biospecimens

The addition of antioxidants to improve the stability of oxylipins has been commonly employed to reduce their degradation during sample collection, extraction, storage and during transportation. Examples of sensitizers are light (UV) and transition elements as they promote autoxidation to produce ${}^{1}O_{2}$ from O_{2} gas [195]. One approach to measuring the level of oxidation is the determination of the concentration of hydroperoxide plotted against time [195]. Another approach to measuring oxidation is by measuring the consumption of oxygen or the degradation of antioxidant concentration over time [196], [197].

Antioxidants can be classified as primary which are phenolic compounds which prevent oxidative stress even at low concentrations [198]. Examples of primary antioxidants are butylated hydroxytoluene (BHT), butylated hydroxy anisole (BHA), propyl gallate (PG), and tertiary butyl hydroquinone (TBHQ) while tocopherols are a natural antioxidant. For example, 0.01% BHT, and 0.01% BHA were found effective for the stability of a triglyceride called trilinolein [198]. As the temperature plays a significant role in degradation, the thermal stability of these antioxidants has been evaluated at 110°C with PG > TBHQ > BHA > BHT [199]. Secondary antioxidants reduce oxidation reactions by scavenging for oxygen and reduce radical formation to improve stability of lipids [200]. Examples include water soluble antioxidant (ascorbic acid), ascorbyl palmitate (soluble in liquid, solid and alcohols), metabisulfites (sodium and potassium salt), EDTA salts (disodium and calcium), etc. [195]. The combination of antioxidants to obtain synergistic effects can also be useful, for example using EDTA as a metal chelator and primary antioxidants such as TBHO, BHA or BHT can be beneficial [199].

BHT is an artificial phenolic antioxidant which can be used as an additive to potentially improve the stability of oxylipins in plasma [182], [184]. Koch *et al.* focused on 27 oxylipins including 13 unstable oxylipins and determined that the addition of BHT alone to plasma improved the stability of 15-HETE and 18-HEPE compared to indomethacin, EDTA, trans-4-(-4-(3-adamantan-1-ylureido)-cyclohexyloxy)-benzoic acid (t-AUBT), and even the mix of all the additives [182]. Dorow *et al.* [184] and Hulda *et al.* [186] also confirmed that the addition of BHT to plasma improved stability in combination with other additives such as MeOH or EDTA. The addition of antioxidants such as 0.0001% BHT to improve stability with K₃EDTA collected whole blood or plasma at RT and ice up to 240 min. has been reported [175]. An increase of 12-HETE was observed even with BHT addition, while other analyzed HETEs were stable under the conditions tested [175]. The use of natural antioxidants such as vitamin C was also investigated, but vitamin C did not improve the stability of oxylipins prone to oxidative stress in blood samples stored at 4°C for 5-days or plasma samples stored at 4°C for 25-days [201].

If antioxidants are used to help improve the stability of oxylipins they should be added as early as possible to prevent degradation during both sample collection and storage phases. For tissue sample collection, the addition of BHT (stops radical reaction) and triphenylphosphine (reduces peroxides) was used to help prevent peroxyl radical formation and degradation of oxylipins [180]. BHT was also used to improve the stability of HETEs and IsoPs [96]. A recent study by Moran-Garrido *et al.* evaluated 5-FT cycle stability of oxylipins with BHT[190]. Poor stability was reported after 3 or 4-FT cycles for most oxylipins. Short-term stability at -4°C for 120 h or at – 80°C for 98 days reported no significant effect of BHT. However, BHT improved the stability of oxylipins stored at –20°C for 98 days [190]. Of all antioxidants, the most used to improve the stability of oxylipins in biological samples is BHT, which will be further evaluated in this thesis

to examine whether it can improve the stability of oxylipins when stored on SPME devices during various storage conditions.

1.5 Research objectives

Analyte stability is a critically important factor for accurately measuring unstable oxylipins. The goal of this thesis is to investigate and propose new analytical approaches to improve oxylipin stability during sampling, transportation, and storage. The selected oxylipin library (**Figure 1.2**) which was used throughout this thesis includes unstable oxylipins identified in the literature, and various enzymatically and non-enzymatically produced oxylipins, to determine if their stability improves when stored *in vivo* on SPME devices.

The first objective of this thesis was to test the stability of oxylipins when stored on SPME devices and subjected to 3-FT cycles or stored at room temperature (RT) over 18 days without antioxidants. In addition, it was evaluated whether the degradation of unstable oxylipins can adversely impact the quantitation of unstable oxylipins. These studies and results are described in **Chapter 2** of this thesis.

The second objective of this thesis was to investigate whether the stability of the unstable oxylipins can be enhanced by loading antioxidants onto SPME devices. As part of this objective, antioxidant loading procedures, including pre-extraction and post-extraction loading, were optimized for phenolic antioxidants, BHA and BHT. Pre- and post-extraction loading of BHT was then compared to see which method better improves the stability of oxylipins during 3-FT cycle and the RT stability studies. These studies and results are described in **Chapter 3** of this thesis.

Finally, the last objective of this thesis was to conduct forced degradation studies (heating, photooxidation, and copper sulphate oxidation) on the unstable oxylipins determined from the first

and second objectives to map their degradation products and further examine how they may interfere with accurate oxylipin quantification. These studies and results are discussed in **Chapter** 4 of this thesis.

Chapter 2

2.0 Stability of oxylipins stored on biocompatible solid-phase microextraction (SPME) devices.

2.1 Introduction

Oxylipins are oxygenated lipid mediators produced both enzymatically and non-enzymatically from PUFAs such as AA, DHA, EPA and LA [96]. The 20-carbon PUFA precursors such as EPA and AA produce well-known oxylipins called eicosanoids [2]. PUFAs can be oxidized via three main enzyme families: COX which produces PGs and TxA; LOX which synthesizes mid- or multiply-hydroxylated PUFAs such as LTs; and CYP450 enzymes which produce hydroxy- or epoxy-PUFAs [37], [202]. Additionally, non-enzymatic reactions include lipid peroxidation, isomerization, hydrolysis, and photooxidation. Lipid peroxidation reactions involve the initiation stage with the formation of a free radical and the propagation stage by the addition of ROS to an unstable lipid radical to produce fatty acid peroxyl radicals, further reacting with unsaturated fatty acid to form fatty acid hydroperoxide and a new lipid radical [203]. In contrast, photooxidation reactions involve the addition of ROS to a double bond [203]. The non-enzymatic reactions produce numerous hydro(pero)xy-PUFA, epoxy-PUFAs, and IsoPs [204], [205].

Oxylipins play significant roles in health and disease. For example, PGD2 promotes sleeping [206], 9-HODE acts as a proinflammatory mediator [207], and some LA- and AA-derived oxylipins are possible biomarkers of brain injury [208]. On the other hand, an oxylipin can also show different effects depending on its concentration or receptor, for example, PGs such as PGE2 and PGD2 can act as pro-thrombotic or anti-thrombotic agents [209]. Based on these important and dynamic biological roles, the accurate measurement of oxylipins is required in many fields.

Oxylipins are commonly measured using LC-MS/MS due to high assay sensitivity and the ability to separate and distinguish many positional isomers either chromatographically and/or by the differences in MS/MS fragmentation [152]. To ensure adequate sensitivity, SPE with C18 or HLB polymeric sorbents are frequently used for sample clean-up and enrichment of biospecimens prior to LC-MS/MS analysis [210], [211]. A major challenge often encountered when measuring this lipid subclass is their poor stability during sample collection, transportation, and storage. These oxylipins are unstable due to the presence of their polyunsaturated backbone and/or transient functional groups (e.g. epoxides) in their structure, which can promote degradation by enzymatic or non-enzymatic reactions (oxidation, hydrolysis, etc.). For example, HETEs, HODEs, HDoHEs, and HEPEs were previously shown to change over time during pre-analytical handling steps or storage [181], [182], [184], [185]. Pre-analytical steps such as FT cycles play a significant role in the degradation and formation of new compounds [183], [184]. Various studies to date have investigated ways to improve the stability of oxylipins in biospecimens. For example, the use of citrate [184] or EDTA [182], [183], [184], [186] anticoagulants (chelating agents) was shown to improve the stability of oxylipins in human plasma during storage. EDTA helps to suppress or prevent the formation of free radicals, which can promote autoxidation. This is because EDTA helps suppress or prevent the formation of free radicals by strongly chelating metal ions (iron and copper) that can promote autoxidation. EDTA, binds to these metals, inhibiting oxidation and degradation. Citrate is used to minimize platelet activation by weakly binding calcium ions, forming a reversible complex. Also, citrate prevents coagulation during blood collection and reduces the risk of inaccurate quantification of platelet-derived oxylipins, such as 12-LOX products of DHA However, degradation was still observed for some classes, such as HETEs and HODEs [182], [184], [185], despite the use of these anticoagulants. Since non-enzymatic oxidation

involves free radicals, the use of antioxidants such as BHT [182]- [184] to capture the free radicals and terminate further oxidation of oxylipins has also been investigated. BHT improved the stability of oxylipins during long-term storage in combination with other additives such as MeOH or EDTA [182], [184]. Temperature also significantly affects the stability of oxylipins, with the preferred storage temperature at -80°C or lower [182]. Short-term storage at room temperature (≥2 hours) contributed to the degradation of oxylipins even when antioxidants were added in plasma samples [181], [184], [185]. Higher temperatures can increase the oxidation of PUFA precursors to oxylipins and increase the degradation of various oxylipins, especially of the hydroxy and dihydroxy-PUFAs [182]- [186]. In sum, the instability of many oxylipins during common preanalytical steps and storage can severely impact their accurate measurement. Thus, new strategies to ensure oxylipin stability before LC-MS measurement are urgently needed.

In vivo SPME is a non-exhaustive sampling technique that can be used for *in vivo* sampling and extraction of oxylipins in a single step from tissue [123]. This technique represents a major development in oxylipin analysis because it provides an effective approach to measuring true oxylipin concentrations in the brain of living awake animals without the need for tissue collection [123]. Biocompatible SPME devices can minimize the adsorption and extraction of proteins by using biocompatible polymers such as polydimethylsiloxane, polypyrrole, polyacrylonitrile or polyethene glycol, and sorbents with small pore sizes. Such *in vivo* SPME devices thus protect the extracted oxylipins from enzymatic degradation. However, it is currently not known if the oxylipins extracted on the SPME devices may be susceptible to non-enzymatic oxidation and/or degradation. This chapter systematically examines 3-FT cycles and 18-day RT stability of oxylipins stored on SPME devices after extraction from a standard solution and spiked plasma to demonstrate that storage on SPME devices can improve oxylipin stability after extraction.

2.2 Materials and methods

2.2.1 Chemicals

HAc, MeOH, EtOH, water, ACN and IPA, all LC-MS grade, were purchased from Fisher Scientific (Ottawa, Ontario, Canada). All oxylipin standards and PUFA precursors, listed in **Supplementary Table A1**, were purchased from Cayman Chemical Company (Ann Arbor, MI, USA) or their Canadian distributor (Cedarlane, Burlington, Ontario, Canada). A stock standard mix of all oxylipins and precursors was prepared at 10 μg/mL in methanol. Pooled human plasma with sodium citrate as an anticoagulant was purchased from Bioreclamation Inc. (Baltimore, MD, USA). Hydrophilic-lipophilic balanced (30 μm HLB) SPME fibres (10 mm coating length) were obtained from Millipore-Sigma (Bellefonte, PA, USA).

2.2.2 Freeze-and-thaw (FT) stability study of oxylipins

The FT study was performed according to the experimental design shown in **Figure 2.1** using new HLB SPME. 100 ng/ml mix of standards in 10% MeOH was prepared from the stock standard solution. Blank extraction was performed using 10% MeOH in lieu of standard or plasma. The HLB fibres were conditioned for one hour in 1.5 mL EtOH:water (1:1, v/v), prior to use. Conditioned HLB SPME fibres were then inserted into 100 μL of standard solution, plasma or spiked plasma placed in a 250 μL glass insert held within 2 mL HPLC vial and extracted for 30 min at 450 rotations per minute (rpm) on a shaker. All extracted fibres were rinsed by dipping for 5 secs in LC-MS grade water. Control samples (0-T) were desorbed immediately for analysis. For FT stability samples, the fibres were retracted into the needle, wrapped with aluminum foil and stored in a -80°C freezer. The fibres were desorbed using 100 μL of 80% methanol with agitation at 450 rpm for 1 hour and transferred for analysis on LC-MS. Each freeze cycle lasted for a

minimum of 22 h, whereas each thaw cycle lasted 2 h. On the first day, one set of FT fibres was thawed, on the second day two sets were thawed, and on the third day all three sets were thawed, to enable LC-MS analysis on the same day and control the length of storage for all fibres.

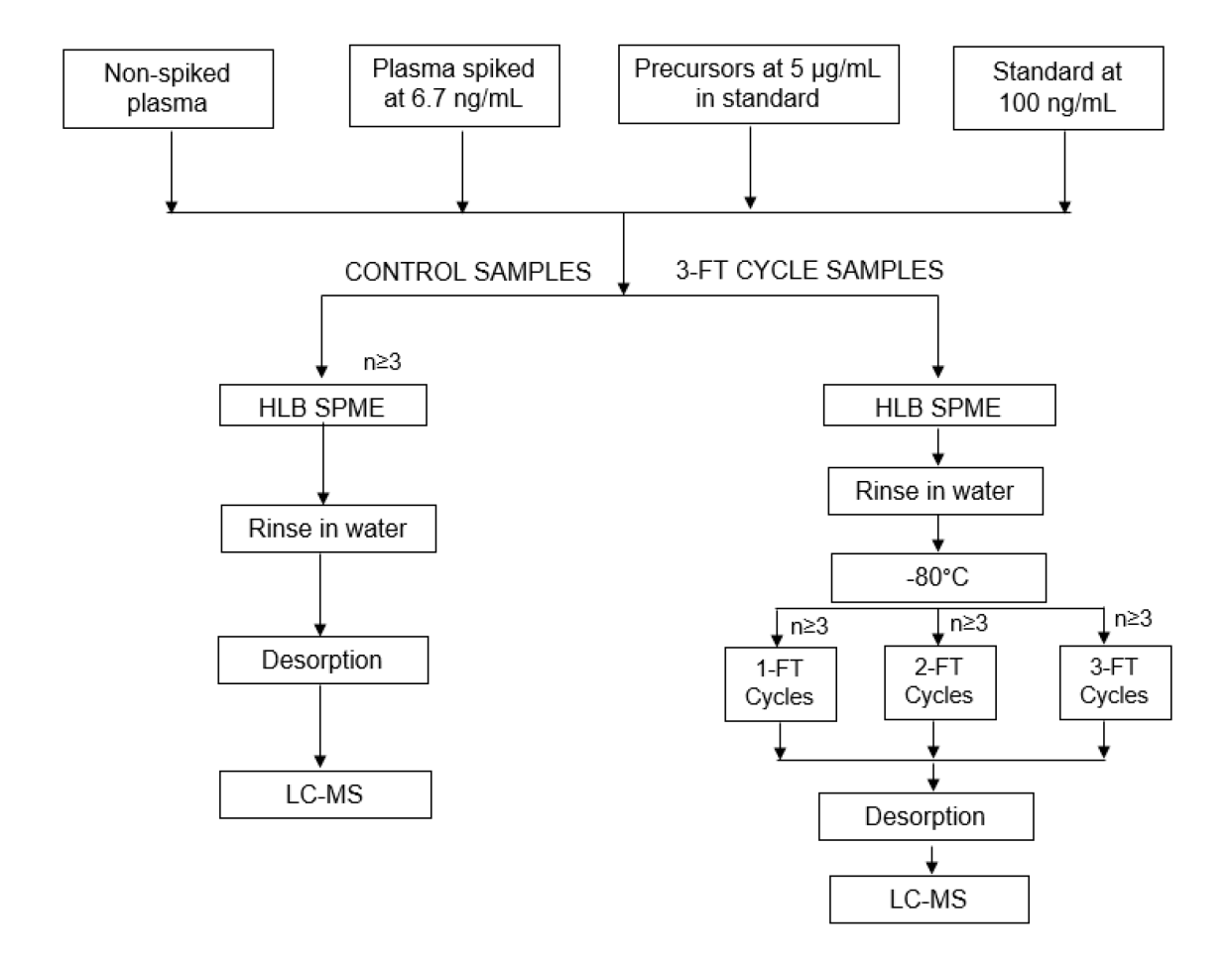


Figure 2.1: Experiment design for 3-cycle freeze-and-thaw (FT) stability study.

2.2.3 Freeze-and-thaw stability study of precursors

One additional FT study was performed according to the experimental design shown in **Figure 2.1** and procedure described in **Section 2.2.2** with reusable HLB SPME fibres but 5 µg/mL standard

of AA, EPA, LA and DHA in 10% MeOH was used for extraction to mimic higher precursor concentrations found in various biospecimens.

2.2.4 Room temperature (RT) stability study

The room temperature stability study was performed for 18 days. Plasma samples spiked with 6.7 ng/mL of standards (140 µL) were extracted using newly conditioned HLB SPME fibres (n≥3) using the same extraction procedure as described in **Section 2.2.2**. One replicate of non-spiked plasma was also extracted. After extraction, fibres were rinsed for 5 seconds and allowed to air dry for 3 seconds before SPME coating was retracted into the needle, capped and then wrapped with aluminum foil. The 0-T were placed in a freezer box stored in a -80°C freezer immediately, while room temperature samples were stored at room temperature for 3, 6, 9, 12 or 18 days before transferring into the -80°C freezer. On the 18th day, all fibres were desorbed using the same procedure as for the FT experiment, followed by LC-MS analysis.

2.2.5 LC-MS analysis of oxylipins

For the quantification of oxylipins, a serial dilution calibration range from 0.1 to 125 ng/mL was performed in 80% MeOH. Oxylipins were separated using UHPLC, model 1290 (Agilent Technologies), with an Agilent ZORBAX Eclipse plus C-18 (1.8 µm particle size, 2.1 mm x 100 mm) equipped with a 2.1 mm x 5 mm guard column containing the same stationary phase. MP A was LC-MS grade water containing 0.02% (v/v) of HAc, and MP B was a mixture of 10% IPA/ 90% ACN/ 0.02% HAc [149]. The flow rate was 0.4 mL/min. while the column temperature was 50°C. The total run time for the analysis was 40 min. The gradient started at 5% of B for 1 min., then increased to 20% over 1 min., followed by a shallow linear gradient from 20% to 80% B over 29.9 min. This was followed by a % B increase to 95% held for 3.9 min., then % B was returned

to 5% over 0.1 min. before column re-equilibration to the initial condition for 5 min. The injection volume was 6 μ L [123].

MS analysis was performed on an Agilent 6545 Q-TOF equipped with dual AJS ESI source operated in negative mode [123]. ESI capillary voltage of 3500 V, nozzle voltage of 500 V, drying gas temperature of 250°C, drying gas flow of 15 L/min, sheath gas temperature of 275°C, sheath gas flow of 12 L/min were used. The mass range was 100 to 1000 m/z, using three-time segments (i) 0-22.08 min. (MS only), (ii) 22.08-22.48 min. (MS/MS at 3 spectra/sec) (iii) 22.48-40 min. (MS only), all performed with an acquisition rate of 2 spectra/sec. For internal calibration, a dual AJS system and an isocratic pump set at 0.3 mL/min. flow rate, with calibrant masses 119.03632 (purine) and 980.01638 (HP-0921 acetate adduct) from Agilent mass reference solution were utilized. Agilent MassHunter software (version B.07.00) was used for data acquisition [123]. Technical repeatability during all studies was monitored using a pooled sample as QC. This QC sample was run after every 10 samples. All oxylipins in QC samples showed relative standard deviation (RSD) below 20% for all studies.

2.2.6 Data analysis

Data analysis was performed using MassHunter software (TOF Qualitative Analysis B.07.00 and QTOF Quantitative Analysis B.07.00), with an extraction window of 10 parts per million (ppm). The calibration curves were prepared using 1/x weighted linear regression except for PGF2αEA, PGE2, PGD2, 20-HEPE, 15(R)-PGF2α, 8-iso-PGF2α, 8-iso-PGF2β, 11,12-EpETE, PGF2α, 13-HODE, 9-oxoODE, 9-HODE,13-oxoODE, LA, DHA, 15-HEDE, 8-iso-15(R)-PGF2α and EPA for which 1/x weighted quadratic models were used to improve accuracy. For stability data analysis, one-way ANOVA and post-hoc t-test were used at a 95% confidence level to compare the amount of oxylipins in the stability test samples against the freshly extracted samples (0-T). ANOVA

testing was performed using JASP statistics 0.18.1 software [212]. The stability acceptance criteria for both RT and the FT study were (i) the mean extracted concentration within 80 to 120% of the control (0-T) samples and (ii) no significant difference using ANOVA. Heat maps were prepared with log transformation with hierarchical clustering using Metaboanalyst 6.0 [213].

2.3 Results and discussion

This study investigated whether it is possible to reduce the non-enzymatic degradation/formation of oxylipins when stored on *in vivo* SPME devices. The stability evaluations were performed after SPME extraction from (i) standard solutions of defined composition and (ii) human plasma, to mimic a relevant complex biological matrix. All experiments were performed using 30 min. extraction time to ensure suitable amount of oxylipins was extracted for subsequent LC-MS analysis. Also, a 1h desorption time was selected to ensure complete desorption of oxylipins from the fibre. Precise control of both the extraction and desorption timing are important to ensure accurate quantitation of oxylipins during all stability studies.

2.3.1 3-cycle freeze-and-thaw stability study results after SPME extraction from standard solutions

A standard mix of 49 oxylipins (**Supplementary Table A1**), including numerous oxylipins reported to be unstable in the literature under various conditions, were extracted using HLB SPME devices. The devices were stored in a -80°C freezer and then subjected to no (0-T), one, two, or three FT cycles. Each FT cycle included 22 h of FT for 2 h. The results obtained are summarized in the heatmap shown in **Figure 2.2**. Statistical analysis using ANOVA (p<0.05) showed that out of the 49 oxylipins extracted only AA and PGE2 were unstable (**Supplementary Table A2**). AA

decreased over 3-FT cycles whereas PGE2 showed an increase across three FT cycles. The box plot representation of the change in concentration of AA and PGE2 is shown in **Figure 2.3**.

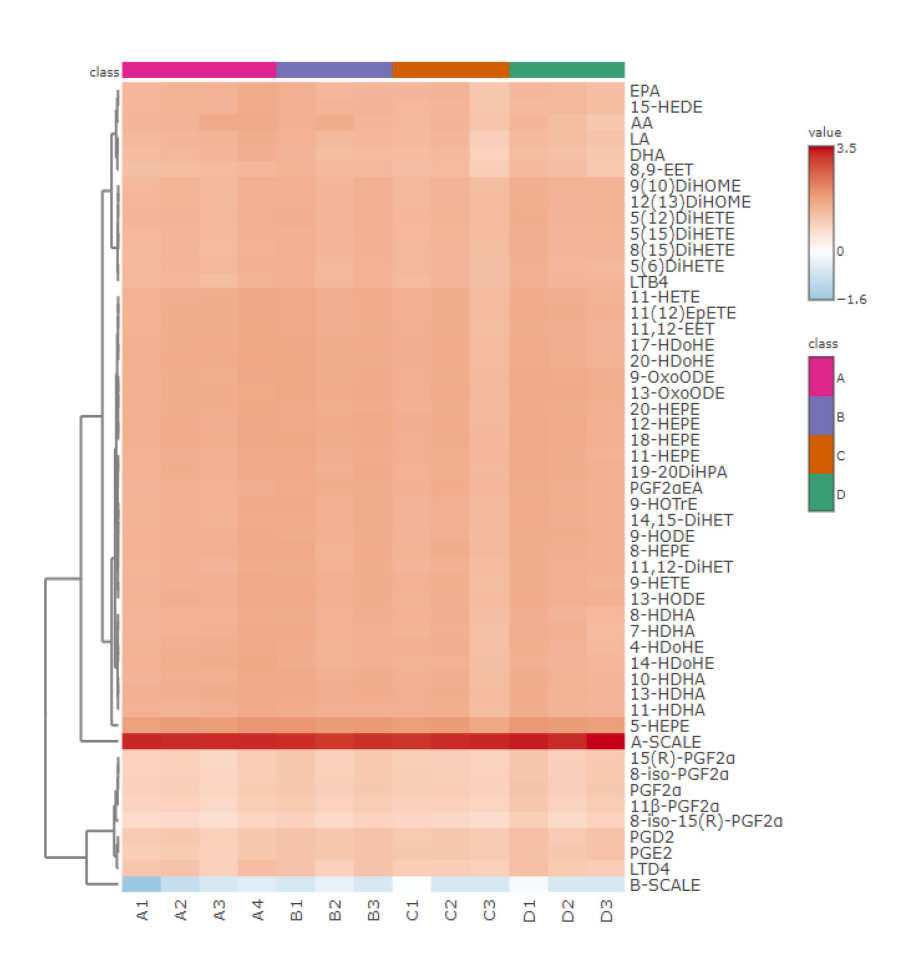


Figure 2.2: Heatmap results of 3-cycle freeze-and-thaw stability study for 49 oxylipins extracted on HLB SPME devices from the standard mix. Heatmap was built using log transformation with hierarchical clustering and Euclidean distance using MetaboAnalyst, where A = control (0-T), B = 1-FT cycles, C = 2-FT cycles, and D = 3-FT cycles. The row A-SCALE and B-SCALE were added to the raw data to show all hierarchical maps in this chapter on the same scale.

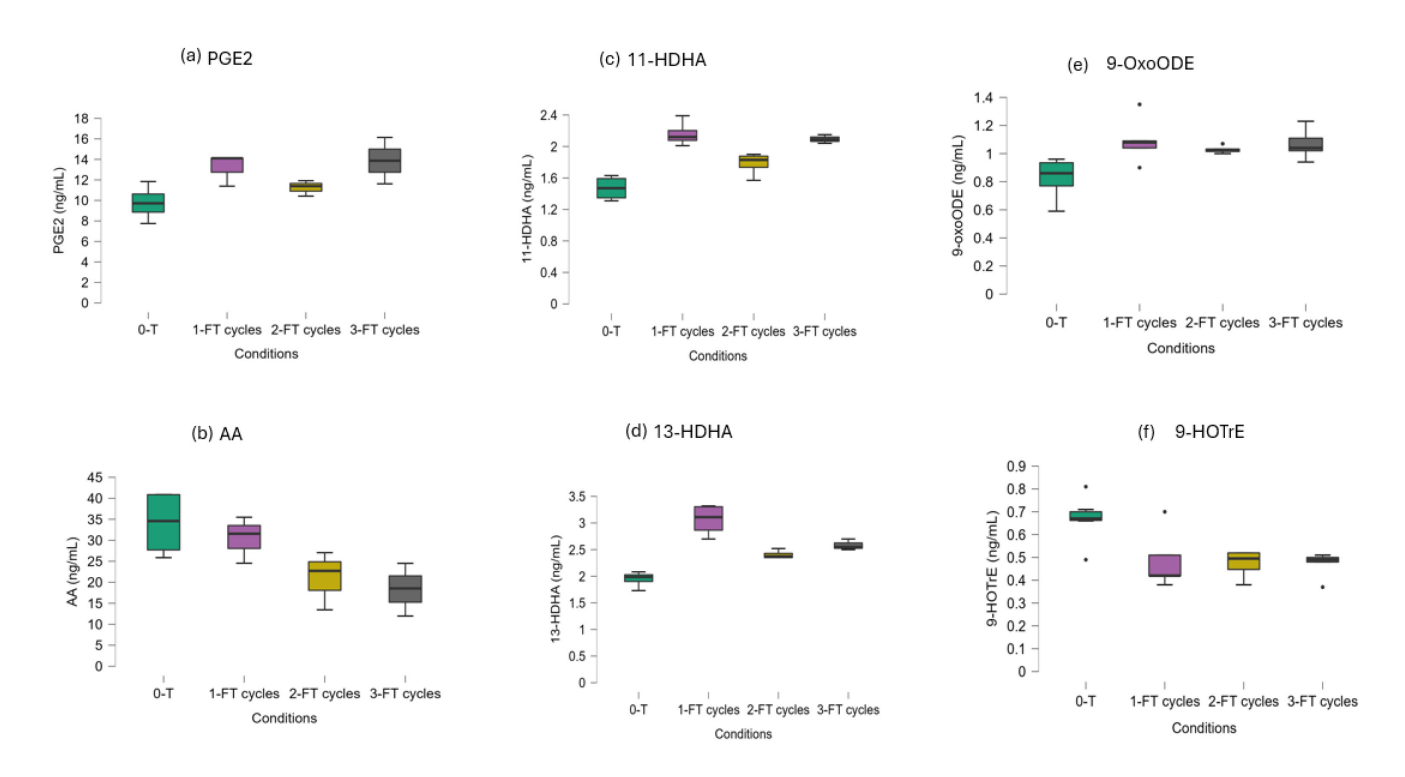


Figure 2.3: Box-plot diagram showing unstable oxylipins extracted on HLB SPME devices in a 3-freeze-and-thaw cycles stability study of Standard (a) PGE2 and (b) AA. Spiked plasma (c) 11-HDHA and (d)13-HDHA, non-spiked plasma and (e) 9-oxoODE and (f) 9-HOTrE. The Y-axis shows the concentration (ng/mL) of the stated oxylipin extracted using SPME.

2.3.2 3-cycle freeze-and-thaw stability study results after SPME extraction from plasma

Next, it was examined whether other co-extracted compounds from a complex biological matrix may further influence oxylipin stability on SPME devices. Thus, 3-FT cycle stability experiment was repeated using spiked citrate plasma. Out of the 49 oxylipins spiked in citrate plasma, 26 oxylipins (**Supplementary Table A1**) were measured due to inadvertent low concentration used for spiking and 3 additional oxylipins, which were not spiked, were detected (5-HETE, 15-HETE and 5-oxoETE), as shown in **Figure 2.4**. Two oxylipins out of 29 measured oxylipins failed the acceptance criteria as shown in **Supplementary Table A3** and **Figure 2.4**. 8,9-EET, 11,12-EET, 7-HDHA, 8-HDHA, PGE2, PGD2, 12,13-DiHOME, 9-10-DiHOME, 19,20-DiHDPA, PGF2αEA, PGF2α, 8-isoPGF2α, 12-HEPE, 20-HEPE, 11,12-EPETE, 15-HEDE, 11-HEPE, 5,6-DiHETE,

LTDA, 18-HEPE, 14,15-DiHET, 8-iso-15-(R)-PGF2α and 8-HEPE were not measured, so no stability determination was made for these compounds.

In the spiked plasma results, two metabolites; 13-HDHA and 11-HDHA were identified as being unstable. These are metabolites of DHA, and they increased as compared to the 0-T. We investigated the degradation of the precursors, without the presence of oxylipins, to identify the degradation products formed and whether the degradation of precursors can explain the observed increases of 13-HDHA and 11-HDHA. The results for the 3-FT cycle stability evaluation of precursors are shown in **Supplementary Table A4**. The apparent increase of both 11- and 13-HDHA, could not be linked to the degradation of DHA precursor itself.

The typical concentrations of the precursors, such as AA (14 μM) [214], LA (83.8 μM) [214], DHA (94.2 μM) [215] and EPA (0.44 μM) [216] in plasma are significantly higher than most oxylipins (≥0.0001μM). If even a small fraction of these precursors degrades, it can significantly interfere with (increase) the oxylipins detected. A good example is reported in **Supplementary Table A5**, summarizing how the degradation of precursors may interfere with the measurement of oxylipins obtained from the 3-FT cycle precursor stability study when stored on SPME devices.

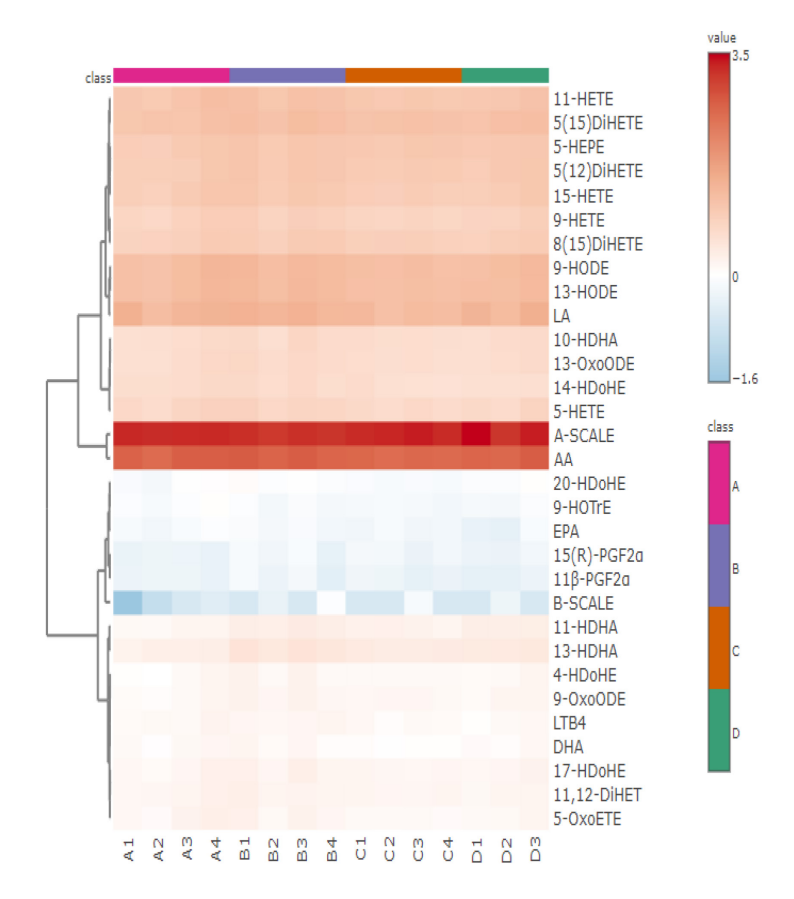


Figure 2.4: Heatmap results of 3-freeze-and-thaw cycle stability study for 29 oxylipins extracted on HLB SPME devices from spiked plasma samples. Heatmap was built using log transformation with hierarchical clustering, and Euclidean distance using MetaboAnalyst, where A = control (0-T), B = 1-FT cycles, C = 2-FT cycles, and D = 3-FT cycles. The row A-SCALE and B-SCALE were added to the raw data to show all hierarchical maps in this chapter on the same scale.

For non-spiked plasma, 27 endogenous oxylipins were measured as shown in **Supplementary** Figure A1. 11βF2α, 15(R)-PGF2α, and were not quantified because their concentrations were below the limit of quantitation (LOQ), so their levels of stability in non-spiked plasma could not be determined. 9-oxoODE and 9-HoTrE are unstable, 9-oxoODE increased while 9-HoTrE decreased shown in **Supplementary Table A6** and **Figure 2.3**.

Prior studies have shown 5-HETE to be unstable during short-term storage in plasma [185], [186] but it was stable in our study. This shows SPME can improve the stability of oxylipins and even the HETE classes, which were also stable in our study when stored on an SPME device.

As shown in **Figures 2.2** to **2.4**, inter-fibre SPME variability may be high with some fibres extracting lower or higher amounts than average, depending on the exact amount of sorbent deposited on each fibre. This is a well-known challenge with single-use SPME fibres. Although the use of an internal standard of oxylipins could have been introduced for this purpose, however stability of oxylipins using an internal standard would not be possible. This is why 80-120% criteria were applied in addition to ANOVA.

2.3.3 18-day room temperature stability study results after SPME extraction from spiked citrate plasma

35 oxylipins were measured after the extraction of pooled spiked citrate plasma with HLB SPME devices. The fibres were then kept at room temperature for 0, 3, 6, 10, or 18 days. Figure 2.5 shows the results of this study. All oxylipins were stable for 18 days at room temperature except for 4-HDHA acid, 13-oxoODE, 5-oxoETE, 15-HETE, and 11,12-EpETE, as shown in Table 2.1. These oxylipins showed significant differences when comparing 0 and 18-day conditions. The results obtained from this study showed that even known auto-oxidation products such as 11-HDHA, 13-HDHA, and 9-HODE were stable. This confirms that SPME devices can effectively protect oxylipins after extraction and that cold-chain storage, at least for short-term storage and transportation, is not required. In summary, we observed improved stability for non-enzymatically derived oxylipins during 3-FT cycle and RT stability studies, including some unstable oxylipins from literature studies (Figure 2.6).

Table 2.1: Summary of the results of 18-day room temperature study for oxylipins extracted using SPME from spiked citrate plasma. The results are shown as mean concentration $(ng/mL) \pm SD$ for oxylipins that failed accepted criteria of concentration within 80-120% of 0-T and ANOVA <0.05.

Oxylipins	Control	3 days	6 days	10 days	18 days	ANOVA
	(0-T)					p-value
11,12-EpETE	4.9±0.7	5.2±2	7.6±1.6	6.8±1.4	4.2±0.8	0.033
13-oxoODE	7.2±0.9	8.7±3.4	11.7±2	11.2±1.9	6.7±3	0.044
4-HDHA	4.1±0.4	2.6±0.7	1.9±0.5	1.75±0.9	4.4±1.7	0.006
15-HETE	28.3±2.7	30.9±8.7	39.9±6.6	37.6±3.1	24.5±7	0.028
5-oxoETE	5.7±0.7	6.2±0.4	8.4±1.4	8.0±1.8	6.1±0.3	0.013

^{*} The number of replicates was n=4 for control and 6-day while n=3 for 3, -10- and 18 days room temperature conditions.

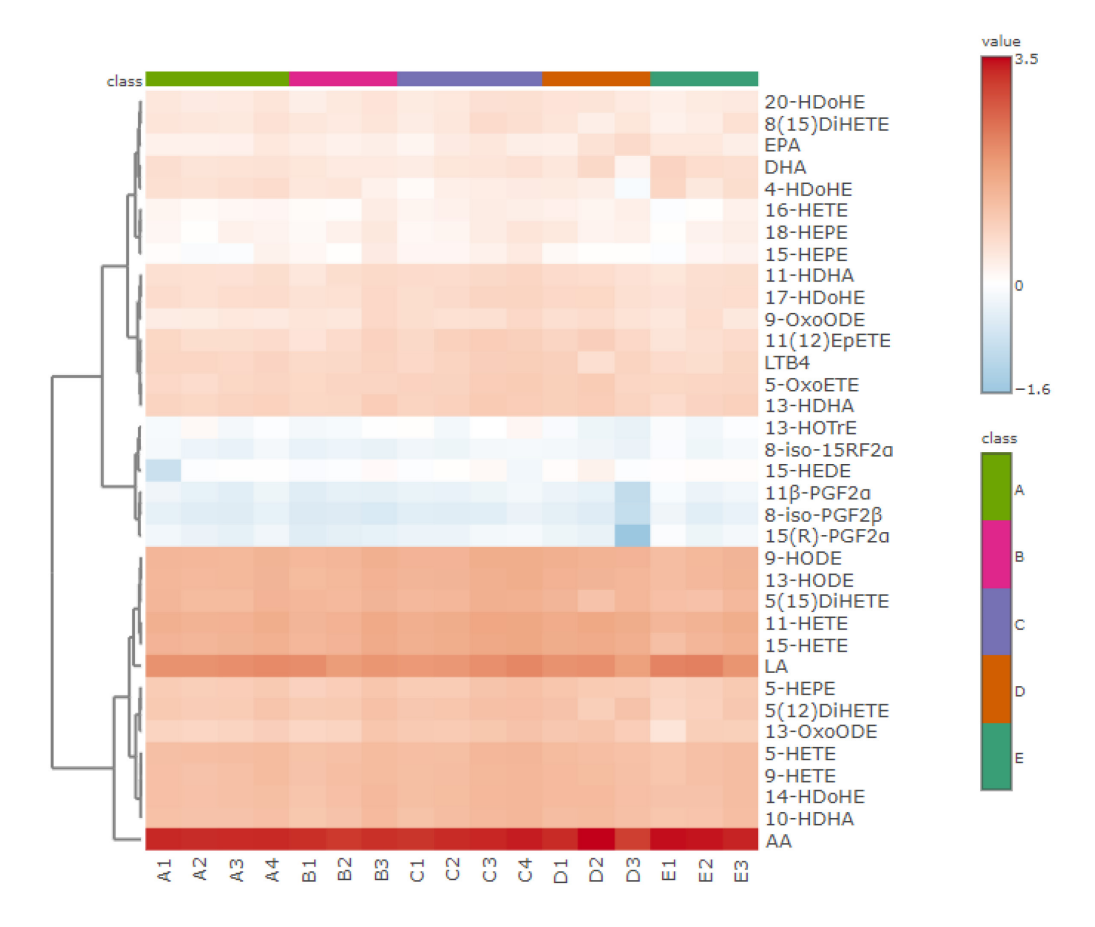


Figure 2.5: Heatmap results of room temperature stability study for 35 oxylipins extracted on HLB SPME devices from spiked plasma. Heatmap was built using log transformation with hierarchical clustering, and Euclidean distance using MetaboAnalyst, where A = control, B = 3 days, C = 6 days, D = 10 days, and E = 18 days. The number of replicates was n=4 for all days except 10 - and 18 days, where n=3.

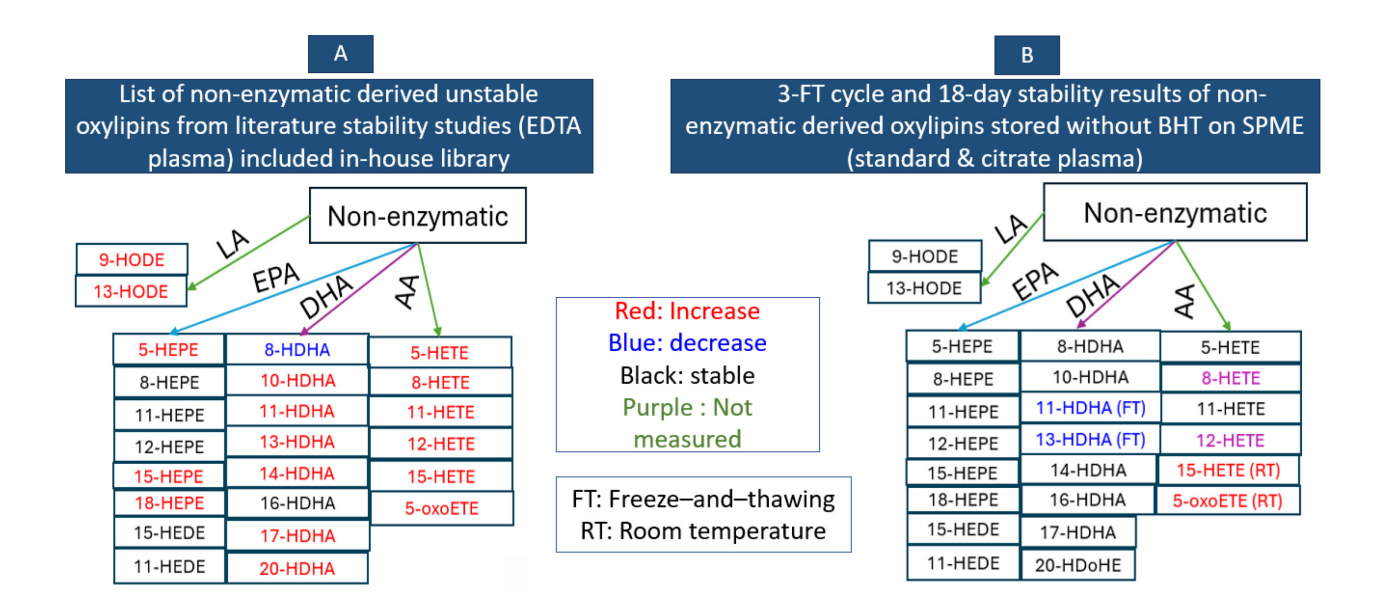


Figure 2.6: Diagrams showing improved oxylipin stability during storage and pre-analytical handling using SPME. Where A = identified unstable oxylipins from literature studies and B = stability results for 3-FT cycle and RT of oxylipins study on SPME devices extracted from standard or citrate plasma samples.

2.4 Conclusions

Overall, our results show that SPME facilitates the quantitative analysis of oxylipins by improving their stability during storage. Therefore, repeated FT cycles of SPME devices should be avoided when comprehensive oxylipin coverage is required, especially if oxylipins such as AA, PGE2, 9-oxoODE, 9-HoTrE, 13-HDHA, and 11-HDHA are of interest. The room temperature stability results are particularly important, as SPME simplifies sample collection, shipping, and short-term storage procedures by eliminating the need for ultra-cold temperatures.

In future, SPME-based devices may facilitate at-home sampling of oxylipins and provide a new approach for easier longitudinal monitoring of oxylipin concentrations in clinical and biomedical studies.

Chapter 3

3.0 Effect of antioxidants on oxylipin stability using solid-phase microextraction (SPME) devices

3.1 Introduction

Oxylipins are oxygenated derivatives of polyunsaturated fatty acids. These precursors of oxylipins include both omega 3 and 6 fatty acids and are typically made of 18-22 carbon atoms and contain two or more double bonds. Oxylipins are produced by enzymatic (LOX, COX, and CYP450) and non-enzymatic oxidation of their precursors such as AA, LA, DHA, and EPA [217]. The type of enzyme can determine the specific oxylipins produced in biosynthetic reactions. Oxylipins play a significant role in many biological processes [218], [219]. The CYP450 oxidation of the ωterminal of LA can synthesize 11-HETE which is responsible for vasoconstriction, and vascular dysfunction [219]. Other classes of oxylipins produced by the CYP450 enzymes such as EpOMEs were shown to be vascular endothelial cell oxidative stress elevators [220] and EETs were shown to have cardioprotective effects on ischemia [221]. PGE₂ which is produced by the COX oxidation of AA, is involved in inflammation, infection, and pain [34], [222]. LA produces HODEs, including 9-HODE with pro-inflammatory [219] and 13-HODE [223] with anti-inflammatory roles in humans. Non-enzymatic oxidation reactions of precursors with ROS can produce oxylipins such as 9-HETE and IsoPs from AA [204] and 9-HODE from LA which are biomarkers of stress [217]. Interestingly, some precursors can be converted into other precursors. For example, LA is converted to AA, and α-LA produces DHA, which can further be converted into EPA in the presence of enzymes such as delta-5 desaturase and delta-6 desaturase [224]. Given their significant roles such as lipid mediators, studying oxylipins is important in many biomedical and clinical studies.

The challenges in studying oxylipins lie in their correct identification due to the existence of numerous isomers and/or isobars, and their low concentrations in biological samples, requiring the use of highly selective, sensitive, and robust analytical techniques such as LC-MS/MS [54], [123], [149]. In addition, some members of oxylipin classes are short-lived, creating a need for appropriate sample collection, transportation, and storage to ensure adequate measurement of these compounds. This makes sample stability a crucial challenge. Developing (pre-)analytical approaches to enhance the stability of oxylipins during storage and transportation, such as using anticoagulants, solvents and antioxidants to minimize degradation/formation during sampling, transportation, and storage of tissues and biological fluids, has been investigated [180], [182]-[184], [186], [190], [201]. However, successful stabilization of some classes has yet to be achieved. Anticoagulants are commonly added for blood sample collection to prevent platelet activation and reduce lipid oxidation in the presence of trace metals such as iron and copper. For instance, the use of EDTA and heparin has been investigated to prevent lipid oxidation in blood samples during short and long-term storage conditions [186]. EDTA also reduced lipid oxidation in whole blood compared to citrate plasma [184], [225]. Antioxidants are added to prevent/minimize further oxidation of oxylipins, especially during sampling and storage [190]. Antioxidants may be classified as natural and synthetic. Natural antioxidants such as ascorbic acid were used in biological matrices such as blood and tissue [201], [226]. Synthetic phenolic antioxidants such as triphenylphosphine minimized peroxidation and autoxidation of oxylipins in both blood and biofluids such as BALF during sample collection [180]. Synthetic phenolic antioxidants BHT and BHA are common antioxidants used to scavenge free radicals. As discussed in **Section 1.4.3**, reported antioxidants tested for the stability of oxylipins are ascorbic acid [201], t-AUBT [182] and BHT. Among these, BHT was the most commonly used antioxidant to improve the stability of oxylipins in biofluids [180], [182], [184],

[186] or tissues [180], [96]. BHT is often used with other additives such as methanol or anticoagulants such as EDTA [186]. However, the effectiveness of BHT to reduce lipid and oxylipin oxidation is questionable. For instance, Moran-Garrido *et al.* showed that the addition of BHT for storing oxylipins at -80°C did not result in a significant difference and therefore, did not notably improve oxylipin stability [190].

One novel approach to simultaneously sample and extract oxylipins directly from tissues, used *in vivo*, is SPME, which can accurately measure oxylipin concentrations in living rat brains [123]. Such SPME devices protect oxylipins from enzymatic reactions immediately after the sampling step. This is possible because enzymes are not co-extracted by the device due to the use of biocompatible polymer materials and sorbents with small pore sizes, such as HLB. *Post-mortem* changes that can contribute to the degradation/formation of oxylipins are thus avoided [194], [227]-[229]. However, it is currently not known how stable the extracted oxylipins are on SPME devices post-extraction and whether the devices can reduce degradation due to auto-oxidation, isomerization and other non-enzymatic processes.

Oxylipins can degrade during the sampling, storage, and sample handling process. The loading of antioxidants onto the SPME devices before extraction (pre-extraction loading) may assist in preventing any degradation processes that can occur during sampling, transportation or storage. However, small amounts of the preloaded antioxidant(s) will be desorbed during the sampling process, requiring the use of antioxidants safe for consumption. Alternately, it is possible to load antioxidant(s) onto the SPME devices after *in vivo* extraction (post-extraction loading), for example during a rinsing step. In this approach, antioxidant(s) may help improve the stability of oxylipins during storage and/or transportation.

This study first aimed to develop methods for pre- and- post-loading of phenolic antioxidants, BHA and BHT, on SPME devices. The optimized pre- and -post-loading procedures of BHT were then used to investigate the stability of oxylipins on SPME devices after extraction from standards and spiked plasma samples during a 3-FT cycle stability study and RT stability study. In addition, the LC-MS oxylipin method was modified to enable simultaneous measurement of the BHA and BHT antioxidants.

3.2 Materials and methods

3.2.1 Chemicals

All oxylipin standards and organic solvents were purchased as reported in **Section 2.2.1** and **Supplementary Table B1**. Antioxidants (**Figure 3.1**) were purchased from Cayman Chemical Company. For the 3-cycle FT and RT stability study, citrate plasma was purchased from BioIVT (Westbury, New York, US). The HLB SPME fibres, with 37 µm coating thickness, were obtained from Millipore-Sigma (Bellefonte, PA, USA).

3.2.2 Selection of antioxidants and optimization of antioxidant loading on SPME fibres

BHT and BHA antioxidants were chosen because of their free radical scavenger properties, their logP values, and their solubility properties, which will ensure their efficient loading by HLB SPME (Table 3.1), and their frequent use as food additives to ensure their safe use in *in vivo* SPME workflows. These antioxidants are a good choice for either pre- or post-extraction loading on SPME. However, these are not water-soluble antioxidants as shown in Table 3.1. For this study, BHA was also selected as a backup synthetic antioxidant for BHT, just in case loading enough BHT on the SPME fibre was not achieved due to its poor aqueous solubility. Considering organic solvents must be used to dissolve these antioxidants, the optimization of the solvent composition

of standards used for antioxidant loading onto SPME fibre was required. In general, increasing the organic solvent proportion decreases K_{fs} , thus reducing the amount of antioxidants loaded. Therefore, it was important to determine the appropriate solvent composition to effectively dissolve the antioxidants of interest during the loading step while maintaining as high a K_{fs} as possible (**Supplementary Figure B1**). However, if sufficient BHT can be loaded on SPME using optimized conditions, then BHA will not be further investigated.

Table 3.1: Properties of selected antioxidants

Antioxidant	Formula	Antioxidant class	Solubility	Structure	logP
Butylated	$C_{15}H_{24}O$	Phenolic	Organic	ОН	5.3
hydroxytoluene		antioxidant	solvent	(CH ₃) ₃ C C(CH ₃) ₃	
(BHT)			(methanol)	CH,	
(====)			()	**************************************	
Butylated	$C_{11}H_{16}O_2$	Phenolic	Organic		2.3
			_	ОН	
hydroxyanisole		antioxidant	solvent	C(CH ₃) ₃	
(BHA)			(methanol)	OCH,	

^{*}Log P values obtained from www.pubchem.com.

3.2.3 Optimization of oxylipin LC-MS method for analysis of BHT and BHA antioxidants

To investigate if BHA and BHT could be analyzed using the existing oxylipin method to ensure their adequate quantitation during the stability study, a stock mixture of 5 μ g/mL of BHT and BHA in 80% methanol was prepared and analyzed using the oxylipin method. BHT was successfully measured in negative ESI mode with m/z of 219.1781 using the oxylipin method as described in **Section 2.5** while for BHA, the [M-H]⁻ mass 179.1073 (C₁₁H₁₅O₂⁻) was not detected, but its demethylated ion corresponding to the loss of CH₃ with m/z of 164.0838 (C₁₀H₁₂O₂⁻) was detected

in negative ESI mode. To reduce the observed in-source fragmentation, two ESI parameters: gas temperature (175°C, 200°C, and 250°C) and fragmentor voltage (170 V, 190 V, and 210 V) were optimized while other ESI parameters were kept constant. The impact of changing these parameters on oxylipin measurement was also investigated (**Supplementary Figure B2**).

3.2.4 Optimization of SPME method for pre- and post-extraction loading of BHT and BHA on SPME devices

The antioxidant pre- and post-extraction loading procedures and full SPME workflow for determination of the amount of antioxidant loaded are shown in **Figure 3.1**. To determine when equilibrium was reached for antioxidant loading onto the SPME devices and to load the maximum possible amount of antioxidants, long extraction times of 1, 3, 5, and 18 h were tested for pre-extraction loading. Two replicates per time point were used. Antioxidant loading was incorporated using reused SPME fibre for conditioning procedure as follows. SPME fibres were immersed in 1.5 mL of 5 µg/mL of BHT and BHA standard prepared in 50% MeOH (v/v), and the extraction times were varied from 1 to 18 h with agitation of 450 rpm. 2.0 mL HPLC glass vials were used for the antioxidant loading step. This was followed by fibre rinsing in water for 5 secs, followed by desorption in 80% MeOH for 1 h on a shaker (450 rpm) and immediate analysis on LC-MS.

For post-extraction loading of antioxidants, very short extraction times of 1, 2, and 5 min. were tested. These short times and low proportions of organic solvent were investigated to prevent the desorption of oxylipins from the fibres during the post-extraction antioxidant loading approach. In this approach, the fibre rinsing step was removed and replaced with the antioxidant loading step before desorption or storage. The SPME fibres for post-extraction loading of antioxidants were conditioned in 50% EtOH (v/v), followed by antioxidant loading from 1.5 mL of 5 μ g/mL BHT and BHA standard solution prepared in 5% MeOH (v/v) for the selected times ranging from 1 to 5

min. with 450 rpm agitation. 2.0 mL HPLC glass vials were used for the antioxidant loading step. A similar desorption approach, as reported for pre-extraction loading, was used, and the samples were immediately analyzed by LC-MS.

The amount of antioxidants loaded was calculated by multiplying the concentration of the antioxidant found in the SPME extract (obtained from the calibration curve prepared from 10 µg/mL mix of BHT and BHA in 80% MeOH) by the volume of the desorption solvent. The goal was to achieve a minimum BHT-to-oxylipin ratio of 10:1 for both standard and plasma samples. For example, in standard samples, an average concentration of 40 ng/mL of each oxylipin was found after desorption. This corresponds to ~4 ng (40 ng/mL x 0.1 ml) of each oxylipin loaded. When multiplied by the total oxylipins measured (33), a total of ~132 ng of oxylipins is extracted onto the SPME fibre. To achieve the mole ratio of BHT-to-oxylipin ratio (10:1), meaning that ~992 ng of BHT must be loaded per SPME device. In the spiked plasma sample, the total extracted amount of oxylipins and PUFA precursors was 103 ng. Therefore, the loading of >992 ng of BHT, as calculated for standard, will also be sufficient for plasma samples to achieve a minimum of 10:1 molar ratio of antioxidant: oxylipin.

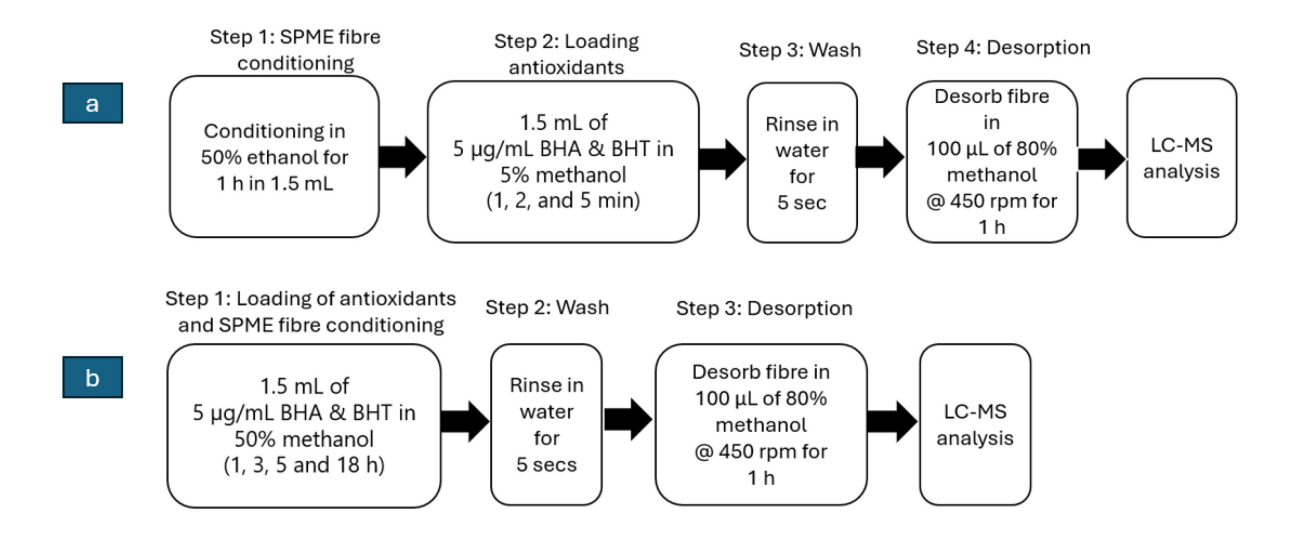


Figure 3.1: Overview of SPME procedure used for the optimization of antioxidant loading on SPME fibre for (a) short antioxidant loading during the fibre rinsing step to be incorporated for the post-extraction antioxidant loading procedure and (b) conditioning and pre-loading of antioxidant procedure for pre-extraction loading of antioxidant.

The next step was to further optimize the post-extraction loading of BHT and evaluate which extraction time yields the highest antioxidant loading, without inducing inadvertent oxylipin desorption during this short antioxidant loading step. To achieve this, the desorption of oxylipins during all the post-extraction loading time points of BHT was investigated, as 5% of organic solvent was used in the post-extraction procedure, in lieu of typical fibre rinsing with pure water. Prolonged time and the increase in the volume and organic solvent proportion may altogether promote undesirable oxylipin desorption during antioxidant loading. To investigate this possibility, $100 \,\mu$ L of a $100 \,n$ g/mL standard mix containing 33 oxylipins was extracted using SPME (n = 2), followed by post-extraction BHT loading. For the post-extraction loading, the same approach as shown in **Figure 3.1** was used, but with an optimized loading concentration of BHT at $10 \,\mu$ g/mL in 5% methanol. This adjustment was made for all three time points to ensure a high antioxidant-to-oxylipin ratio. Next, BHT and oxylipins were desorbed using $100 \,\mu$ L of 80% MeOH for 1 h on

a shaker (450 rpm) and analyzed on LC-MS to measure the amount of BHT and oxylipins extracted on SPME devices.

3.2.5 3-cycle freeze-and-thaw stability study of oxylipins stored on SPME devices with BHT

This experiment was performed to investigate the effect of pre- and -post-extraction loading of BHT on the stability of oxylipins during 3-FT stability study. The study was performed using oxylipin extraction from standard solution, to mimic a less complex matrix for easy monitoring of the effect of BHT on the stability of oxylipins when stored on new batch of SPME devices.

The 3-FT cycle stability was performed as follows. After SPME fibre conditioning, oxylipins were extracted onto SPME devices from 100 μL of 300 ng/mL oxylipin standard containing 38 oxylipins including precursors prepared in 10% MeOH. The selection of 5 h for pre-loading and 5 min for post-loading conditions was based on the results discussed in Section 3.2.5. The 3-FT cycle study was then repeated after SPME extraction of spiked citrate plasma. 140 μL of citrate plasma was spiked with 10 μL of 20 ng/mL of the oxylipin standard mix, extracted and stored on SPME with replicate n=4. Figure 3.2 summarizes the complete SPME procedure incorporating either pre-extraction loading of BHT or post-extraction loading of BHT. The same 3-FT cycle stability study experimental design was used as reported in Section 2.2.2.

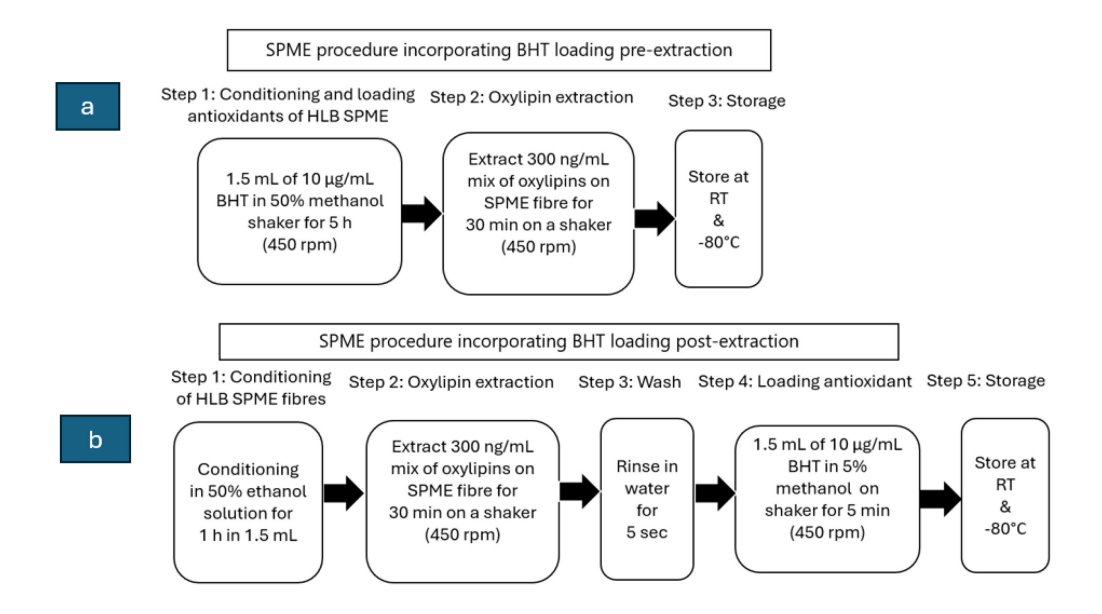


Figure 3.2: Overview of SPME procedure for stability testing with pre-and post-extraction loading of BHT and oxylipins where (a) antioxidant loading during SPME conditioning procedure before extraction of oxylipins and (b) oxylipin extraction before short antioxidant loading of BHT.

3.2.6 LC-MS analysis of antioxidants and oxylipins

For the quantification of oxylipins, a serial dilution calibration in the range from 0.17 to 350 ng/mL in 80% MeOH was performed. 80% MeOH was run periodically as blank sample during LC-MS analysis [123]. BHT calibration standards in the range from 17 ng/mL to 20 µg/mL in 80% MeOH were prepared while the BHA calibration curve ranged from 17 ng/mL to 10 µg/mL in 80% MeOH. An example of calibration for BHA and BHT is shown in **Supplementary Figure B3**. LC-MS analysis was performed on an Agilent 6545 QTOF [123], [149] as described in **Section 2.2.5**, all parameters fixed as BHT was measured successfully with the existing oxylipin method. Agilent MassHunter software (version B.07.00) was used for data acquisition [123]. Technical repeatability during all studies was monitored using 100 ng/mL oxylipin standard as a QC. This

QC sample was run after every 10 samples. All oxylipins in QC samples showed a relative standard deviation (RSD) below 20% for all studies.

3.2.7 Data analysis

Data analysis was performed using MassHunter software (TOF Qualitative Analysis B.07.00 and QTOF Quantitative Analysis B.07.00), with an extraction window of 100 ppm. The calibration curves were prepared using 1/x weighted linear regression except for PGE2, PGD2, 20-HEPE, 15(R)-PGF2α, 8-iso-PGF2α, 8-iso-PGF2β, 11,12-EpETE, PGF2α, 13-HODE, 9-oxoODE, 9-HODE,13-oxoODE, LA, DHA, 15-HEDE, 11-HDHA, AA and EPA for which 1/x weighted quadratic models were used. For stability data analysis, one-way ANOVA and post-hoc t-test were used at a 95% confidence level to compare the amount of oxylipins in the stability test samples against the freshly extracted samples (0-T). ANOVA testing was performed using JASP statistics 0.16.1 software [212]. The stability acceptance criteria for all studies were (i) the mean extracted concentration within 80 to 120% of the 0-T samples and (ii) no significant difference using ANOVA. Heat maps were prepared using hierarchical clustering using Metaboanalyst 6.0 [213].

3.3 Results and discussion

3.3.1 Results of optimization of oxylipin LC-MS method for the analysis of antioxidants

BHA and BHT can be measured using LC-MS [226] and LC-HRMS/MS [230] for *in vitro* studies. The suitability of the oxylipin LC-MS method to measure the amounts of BHA and BHT antioxidants loaded and remaining on SPME fibres after the completion of stability studies were evaluated. Standard solutions of BHA and BHT were analyzed using the oxylipin method and showed rt of 25.78 min. for BHT and 13.11 min. for BHA and suitable chromatographic peak shape (**Supplementary Figure B4**). However, for BHA, in-source fragmentation was observed

whereby no parent [M-H]⁻ ion was detected. Instead, only its fragment ion m/z (164.0838) corresponding to CH₃ loss was observed. To investigate whether in-source fragmentation can be minimized, ESI conditions were optimized, with focus on fragmentor voltage (170-250 V) and gas temperature (175-250 °C) as shown in **Figures 3.3** and **3.4** respectively. Lowering of fragmentor voltage to 170 V reduced the amount of in-source fragmentation and m/z 179.1073 (BHA-H⁻) could be detected with considerably reduced in-source fragmentation (**Figure 3.3**). For BHT, fragmentor voltage did not significantly impact its observed signal intensity. In summary, the optimization of gas temperature and in-source fragmentation for BHT (m/z) showed no significant effect on the detected peak area compared to the existing oxylipin method (250°C and 250V). However, for BHA (m/z 179.1073), in-source fragmentation optimization at 170 V showed a significant improvement compared to the existing oxylipin method. Based on these results, since BHT, the primary antioxidant of focus, showed no impact from the optimization, all parameters in the oxylipin method were kept constant.

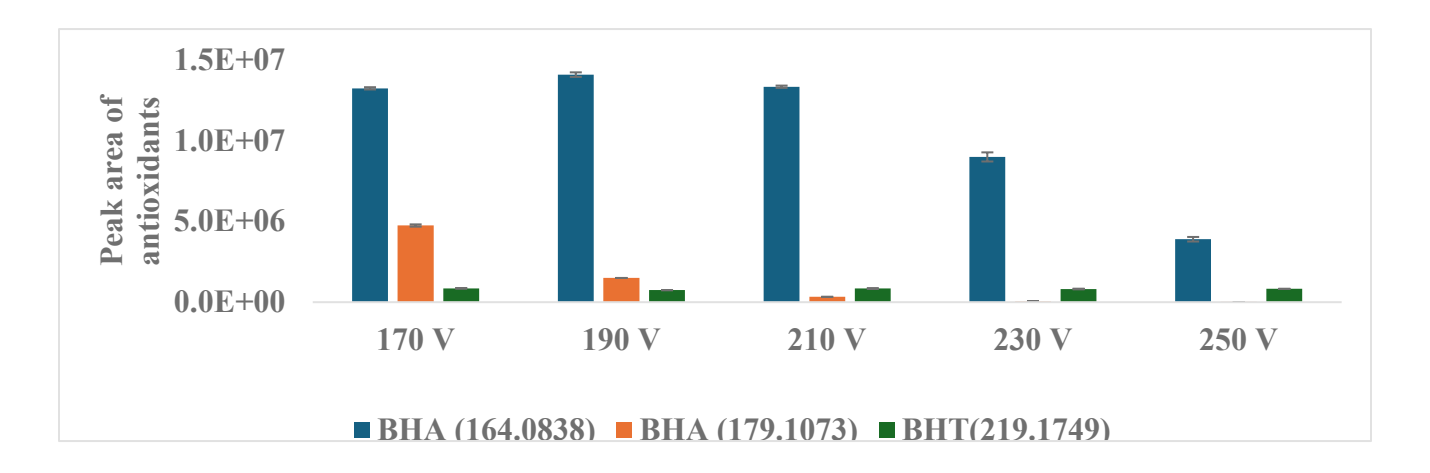


Figure 3.3: Effects of the fragmentor voltage on the peak area of BHA and BHT and in-source fragment of BHA (164.0838). A 5 μ g/mL standard mix of BHA and BHT in 80% MeOH was analyzed on LC-MS, and all ESI settings were kept as described in Section 3.2.9 except fragmentor voltage which was varied from 170-250V. The mean of 2 replicates is shown, and error bars represent the standard error. The initial fragmentor setting of oxylipin LC-MS assay was set at 250 V, showing that this resulted in excessive in-source fragmentation of BHA, whereas it was suitable for the analysis of BHT.

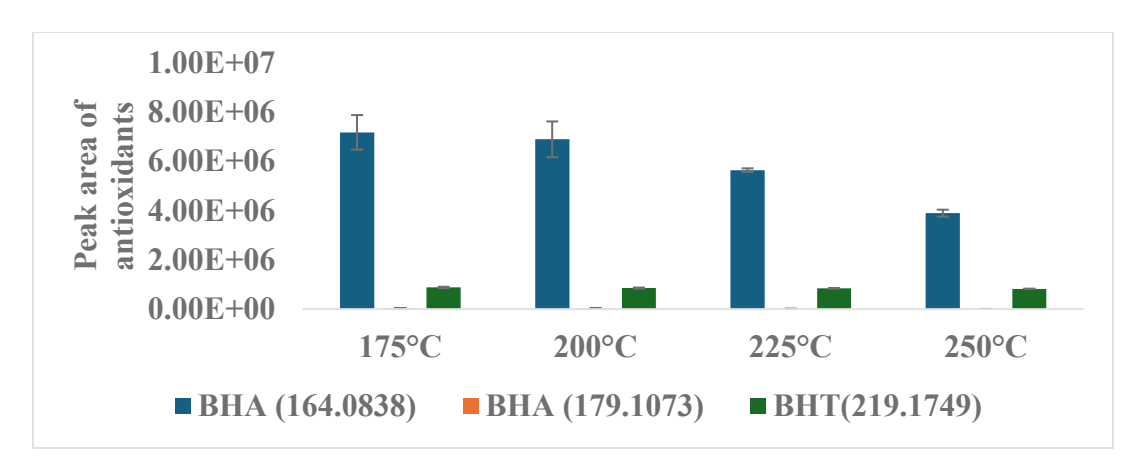


Figure 3.4: Effects of the gas temperature on the peak area of BHA and BHT and BHA in-source fragment (164.0838). A 5 μ g/mL standard mix of BHA and BHT in 80% MeOH was analyzed on LC-MS, and all ESI settings were kept as described in Section 3.2.9 except gas temperature, which varied from 175-250°C. The mean of 2 replicates is shown, and error bars represent the standard deviation. The initial gas temperature setting of oxylipin LC-MS assay was set at 250 °C, showing that this resulted in the decreased signal of BHA in-source fragment (164.0838), whereas gas temperature did not impact the signal intensity of BHT.

3.3.2 Results of the optimization of pre-extraction loading of BHT and BHA on SPME devices

The extraction time is a crucial factor in determining the amount of analyte extracted using SPME. One option to pre-load antioxidants before extraction is to combine the SPME fibre conditioning procedure and antioxidant loading into a single step. If this approach is used, long loading times can be employed to load the maximum possible amount of antioxidant(s) using equilibrium extraction. The effect of long extraction times (1-18 h) on the amount of BHA or BHT loaded on the SPME fibre using 1.5 mL volume of 5 μg/mL of BHT and BHA standard in 50% MeOH is shown in **Figure 3.5** and **Figure 3.6** respectively. As expected, increasing the extraction time significantly increased the amount extracted on SPME devices. For both BHA and BHT, equilibrium was reached by 5 h as there was no significant difference in the amount extracted at 5 h compared to the 18 h extraction. Based on these results, 5 h extraction time was selected for the pre-loading of BHT in subsequent experiments. The minimum desired amount of BHT to load on SPME fibre was calculated as 992 ng in order to reach 10:1 mole ratio of BHT to oxylipin., As

shown in **Figure 3.6**, about 1276 ng of BHT was loaded after 5 hr. This exceeds the target amount and no further optimization of this procedure was required.

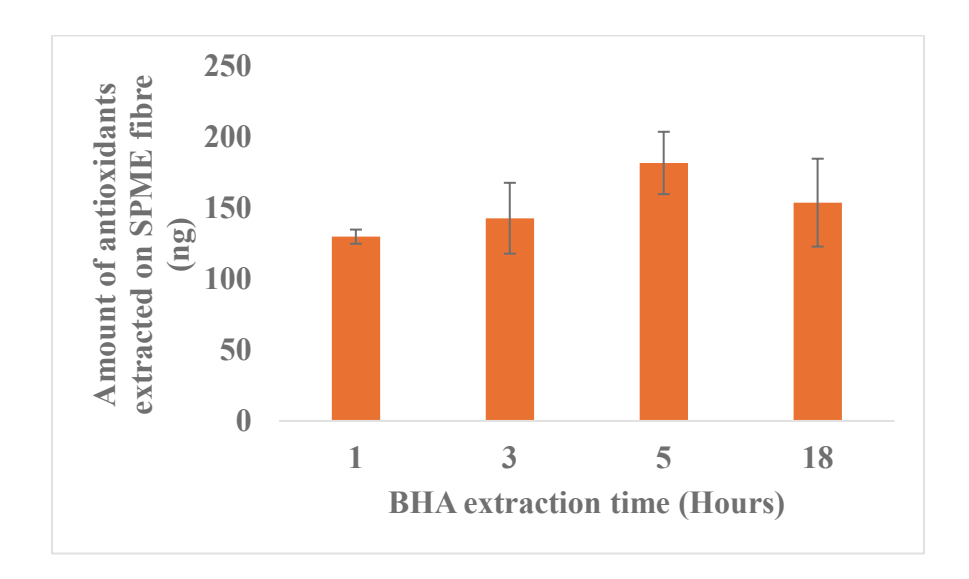


Figure 3.5: Optimization of pre-extraction antioxidant loading procedure. Effect of long extraction times (1-18 h) on the amount of BHA extracted by HLB SPME fibre (n=2 per time point). A 5 μ g/mL standard mix of BHA and BHT in 80% MeOH was used for antioxidant loading and fibre conditioning.

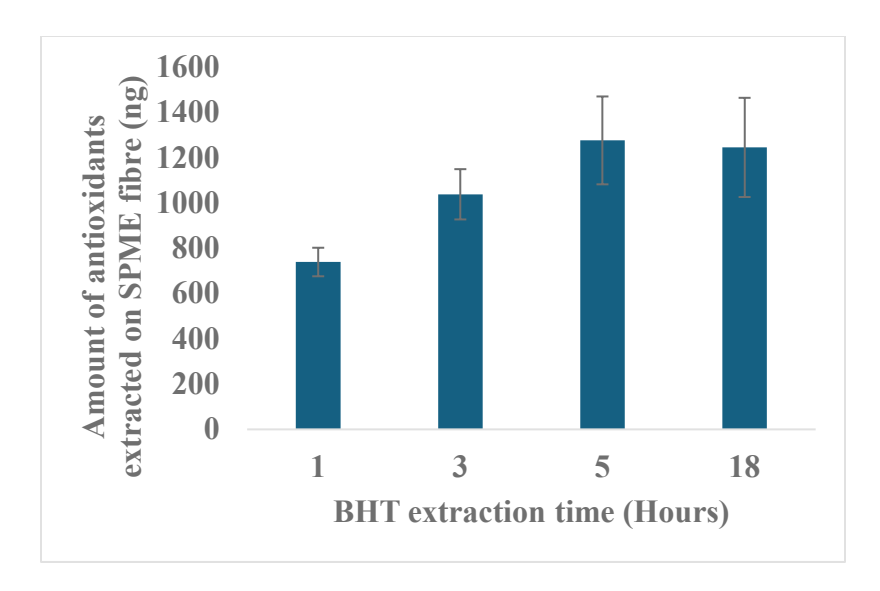


Figure 3.6: Optimization of pre-extraction antioxidant loading procedure. Effect of long extraction times (1-18 h) on the amount of BHT extracted by HLB SPME fibre (n=2 per time point). A 5 μ g/mL standard mix of BHA and BHT in 80% MeOH was used for antioxidant loading and fibre conditioning.

3.3.3 Results of the optimization of post-extraction loading of BHT and BHA on SPME devices

The selection of an appropriate loading time is crucial for the post-extraction loading of antioxidants on SPME. The selected loading time must ensure that enough antioxidant is loaded on the SPME device while also ensuring that it is short enough to avoid the desorption of oxylipins during the antioxidant loading. To meet the latter criterion, low concentration of organic solvent should also be used in this approach, as normally high proportion of organic solvent is required to efficiently desorb oxylipins from HLB SPME fibres. To determine the loading time, which is the most suitable for post-extraction antioxidant loading, short loading times of 1, 2 and 5 min. were tested, and the loading was performed using a 1.5 mL of 5 µg/mL of BHT and BHA standard in 5% MeOH. The results for BHA and BHT are shown in Figure 3.7 and Figure 3.8 respectively. As expected, the post-extraction loading of BHA and BHT showed an increase in the amounts of oxylipins extracted as proportional to extraction time. 5 min. loading successfully loaded approximately 425 ng of BHA and 538 ng of BHT. For the desired ratio of BHT to oxylipin (10:1), the required amount to load is 992 ng per SPME fibre. This amount was not successfully loaded and further increase in the concentration of BHT extraction solution was required to achieve this goal.

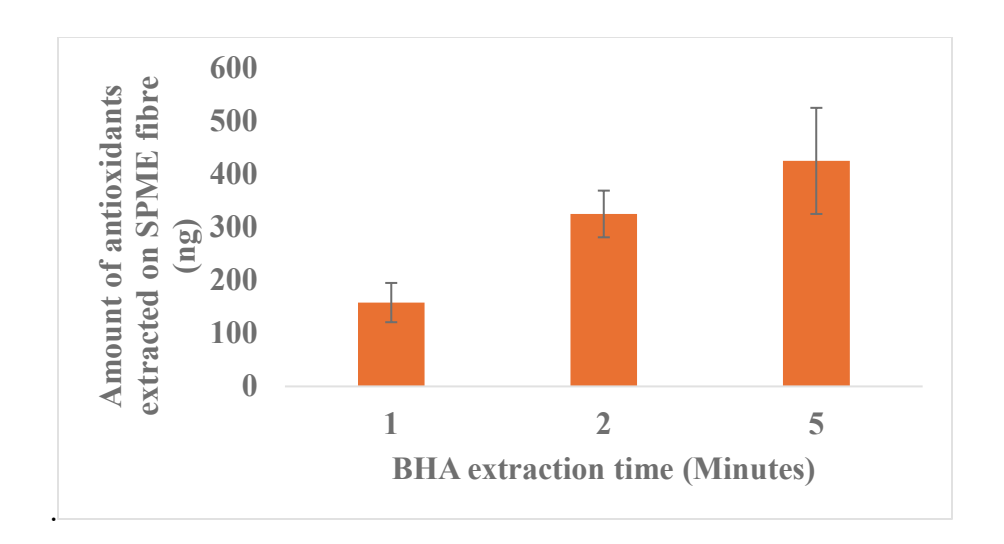


Figure 3.7: Optimization of post-extraction antioxidant loading procedure. Effect of short extraction times (1-5 min) on the amount of BHA extracted by HLB SPME fibre (n=2 per time point). A 5 μ g/mL standard mix of BHA and BHT in 80% MeOH was used for antioxidant loading and fibre conditioning.

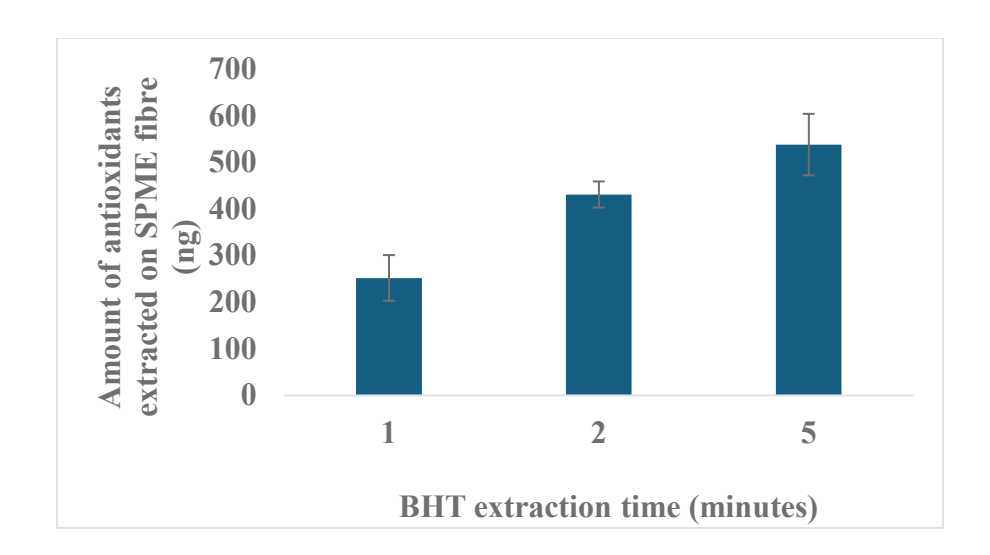


Figure 3.8: Optimization of post-extraction antioxidant loading procedure. Effect of short extraction times (1-5 min) on the amount of BHT extracted by HLB SPME fibre (n=2 per time point). A 5 μ g/mL standard mix of BHA and BHT in 80% MeOH was used for antioxidant loading and fibre conditioning.

The next experiment aimed to determine which of the post-extraction loading conditions of BHT would result in sufficient BHT being loaded on SPME devices while also ensuring minimal or no

loss of oxylipins during the BHT loading procedure. To investigate this, a standard mix containing 33 oxylipins was extracted on SPME followed by post-extraction loading of BHT for 1-5 min. For BHT loading, the same results as reported in **Figure 3.9** were obtained with 5 min. loading time resulting in the highest amount of BHT extracted across the tested extraction times.

Next, the amount of 33 oxylipins extracted by SPME with/without post-extraction loading of BHT was compared as shown in the bar graph (Figure 3.10). Similar amounts of oxylipins were extracted with and without BHT for most oxylipins. The t-test of all oxylipins for all short extraction conditions was performed. Oxylipins that failed t-test with reported p-values shown in brackets were 18-HEPE (0.04), 13-oxoODE (0.04) 17-HDoHE (0.03), 13-HDHA (0.02), 11,12-EPETE (0.04), 11-HDHA (0.04), EPA (0.04), and LA (0.03) (Figure 3.10). Although the results were not significant for most oxylipins, (Figure 3.10) shows that there is a small decrease in the amount extracted of oxylipins when BHT is loaded post-extraction. To determine if oxylipins were desorbed during the loading of BHT, the 1.5 mL solution of 10 µg/mL BHT in 5% methanol which was used for post-extraction loading of BHT was also analyzed by LC-MS. In this experiment, all oxylipins were below the limit of quantification. This result shows that 5 min. post-extraction loading of BHT is suitable for measurement of oxylipins as it minimizes the desorption of oxylipins during antioxidant loading step while ensuring an adequate amount of BHT is loaded, with minimal impact on the amount of oxylipins extracted. In future, the loss of oxylipins during BHT loading could be further reduced by (i) reducing loading time while increasing the concentration of BHT standard used for antioxidant loading or (ii) decreasing the volume of solution used for BHT loading. Fundamentally, PUFA precursors are more hydrophobic than oxylipins with higher K_{fs} values and lower solubility in highly aqueous solutions. Therefore, we would expect to see lower % desorbed as the hydrophobicity of the analyte increases. In general,

we see the expected trend for PUFAs with % desorbed <5%, but the highest amount desorbed appears to belong to several oxylipins of intermediate polarity such as PGE2 and HDHA sub-class.

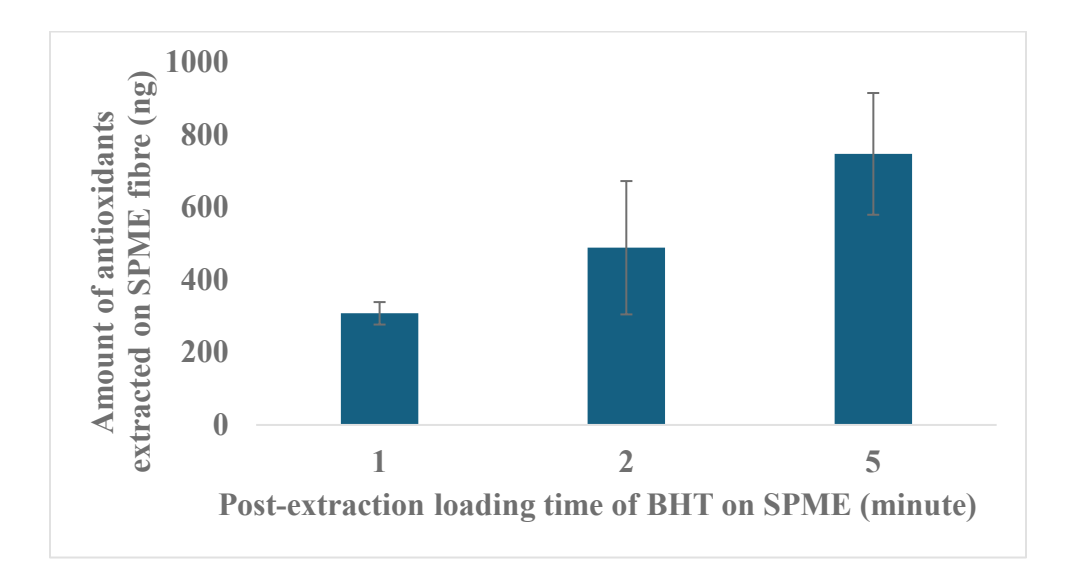


Figure 3.9: Optimization of post-extraction antioxidant loading procedure with extraction of oxylipins. Effect of short extraction times (1-5 min) on the amount of BHT extracted by HLB SPME fibre (n=2 per time point). A 5 μ g/mL standard mix of BHA and BHT in 80% MeOH was used for antioxidant loading and fibre conditioning. Oxylipins were extracted from 100 μ L of 100 ng/mL of standard mix of 33 oxylipins on SPME devices.

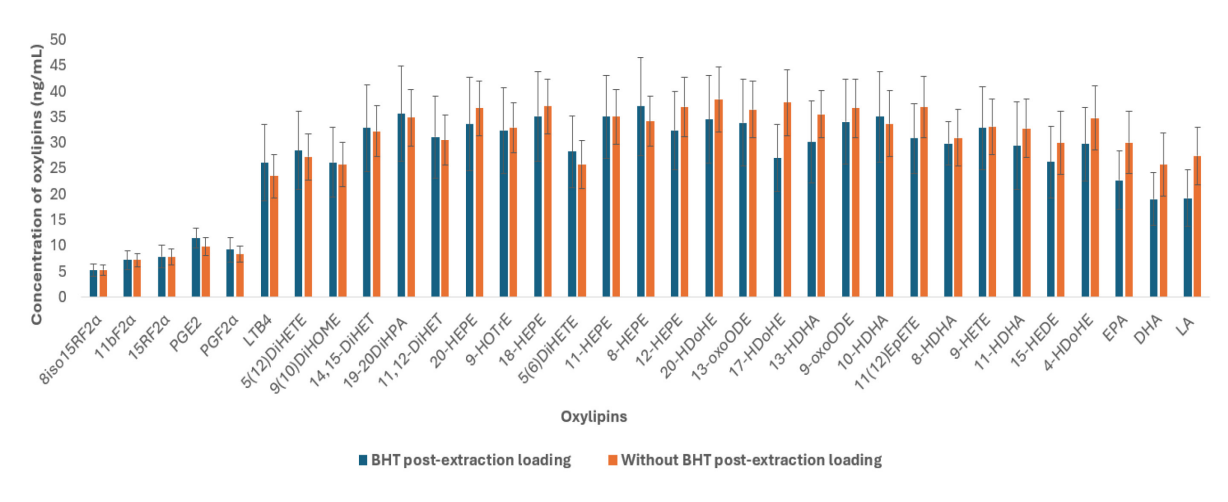


Figure 3.10: Comparison of the amount of 33 oxylipins extracted with (n=2) and without (n=4) post-extraction loading of BHT. The result for using BHT antioxidants was obtained from the average value for all short loading times for each oxylipin respectively. Oxylipins were extracted from $100 \,\mu\text{L}$ of $100 \,\text{ng/mL}$ standard mix for 30 minutes on a shaker.

To reach a high BHT-to-oxylipin ratio of 10:1, our results showed that for 33 oxylipins, approximately 992 ng of BHT was required for the standard sample and for the pooled plasma sample. This was successfully achieved for pre-extraction loading (5 h) but not in post-extraction loading (5 min.), so loading BHT concentration needs to be further increased. The amount of oxidant required for loading can be calculated for different tissue types, expected levels of oxylipins and/or different SPME coatings. In addition, having the ability to measure the amount of unreacted BHT remaining on SPME fibres using the same LC-MS assay as for oxylipins, allows to quickly verify that sufficient BHT was loaded, and that sufficient amount of antioxidant remains on the fibre to protect the oxylipins from oxidation during the storage period.

3.3.4 3-cycle freeze-and-thaw stability study to compare the effect of pre-and post-extraction loading of BHT on oxylipin stability on SPME devices after extraction from standard

Although pre-and post-extraction loading procedures were optimized for both BHA and BHT, BHT was selected for further evaluation in stability studies due to its reported ability in the literature to help protect some oxylipins from degradation [182], [190] and its higher K_{fs} value, which allows the loading of higher amounts of antioxidant(s). The stability study was conducted to determine whether pre- or post-loading of BHT would enhance the stability of oxylipins stored on SPME devices. 38 oxylipins were extracted from the standard solution by SPME devices and subjected to 3-FT cycles. For pre-extraction loading of BHT, all 38 oxylipins tested were found to be stable, except 11β -PGF2 α which was found unstable with a decrease in concentration as compared to the control (**Table 3.2**). For the post-extraction loading of BHT, all oxylipins were stable with stability within the range of 80 to 120% of control and passing the ANOVA test. The heatmap for both pre-and post-extraction loading is shown in **Figure 3.11** and **Figure 3.12**.

Table 3.2: Summary of the results of the 3-cycle freeze-and-thaw stability study for pre-extraction loading of BHT from standard solution. The results are shown as mean oxylipin concentration $(ng/mL) \pm SD$ for oxylipins that failed the acceptance criteria of concentration within 80-120% of 0-T and ANOVA < 0.05.

Oxylipin	Control 0-T (ng/mL)	1-FT cycle (ng/mL)	2-FT cycles (ng/mL)	3-FT cycles (ng/mL)	ANOVA p-value (Control and 3 FT cycles)
11β-PGF2α	58.8±7	42.2±9	40.1±11	38.6±4	0.014

^{*} The number of replicates was n=4 for all conditions

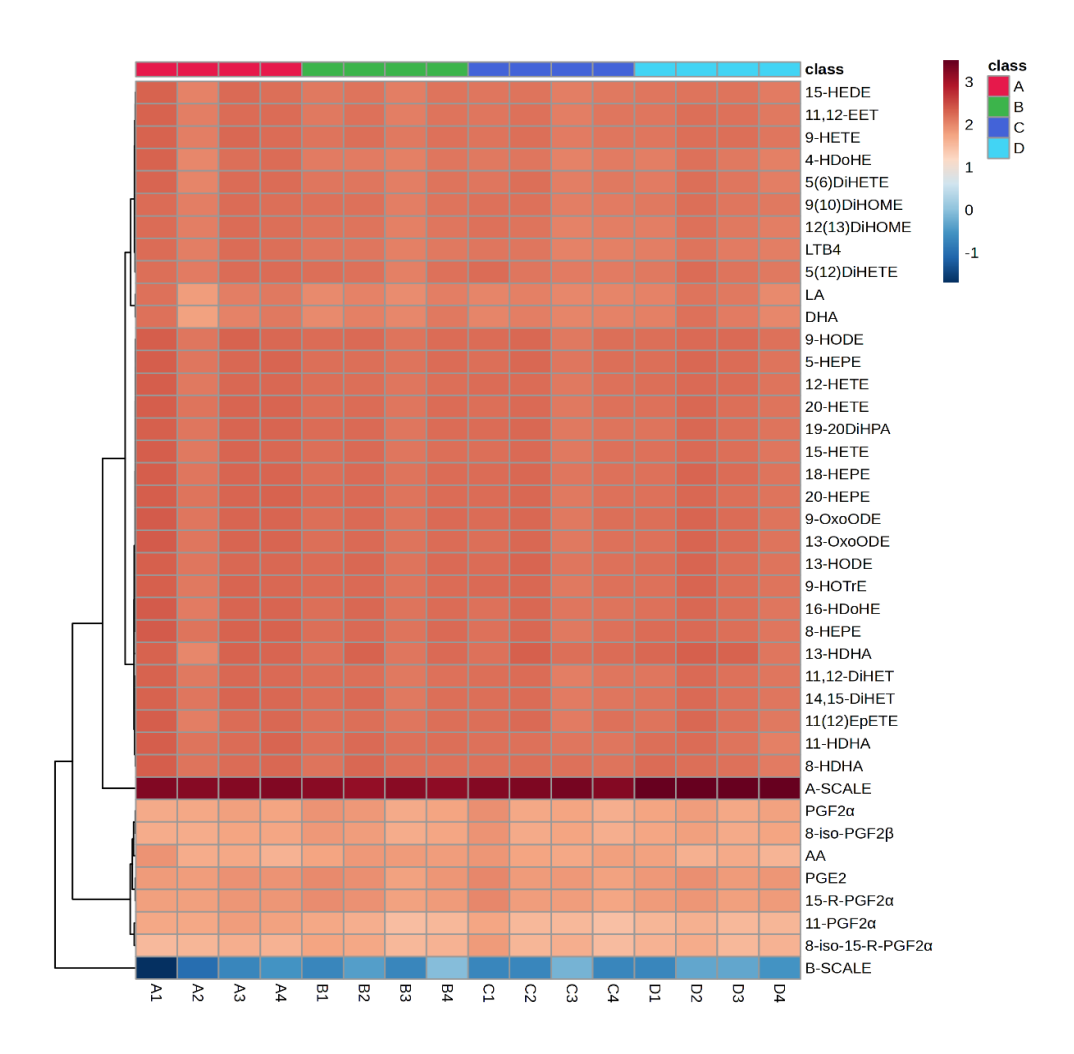


Figure 3.11: Heatmap results of 3-cycle freeze-and-thaw stability study for 38 oxylipins with pre-extraction loading of BHT. Oxylipins were extracted from standard after pre-extraction loading of BHT. Where A= control, B= 1-FT cycle, C =2-FT cycles and D =3-FT cycles. Heatmap was built using log transformation with hierarchical clustering, and Euclidean distance using MetaboAnalyst software. The row A-SCALE and B-SCALE were added to the raw data to show all hierarchical maps in this chapter on the same scale.

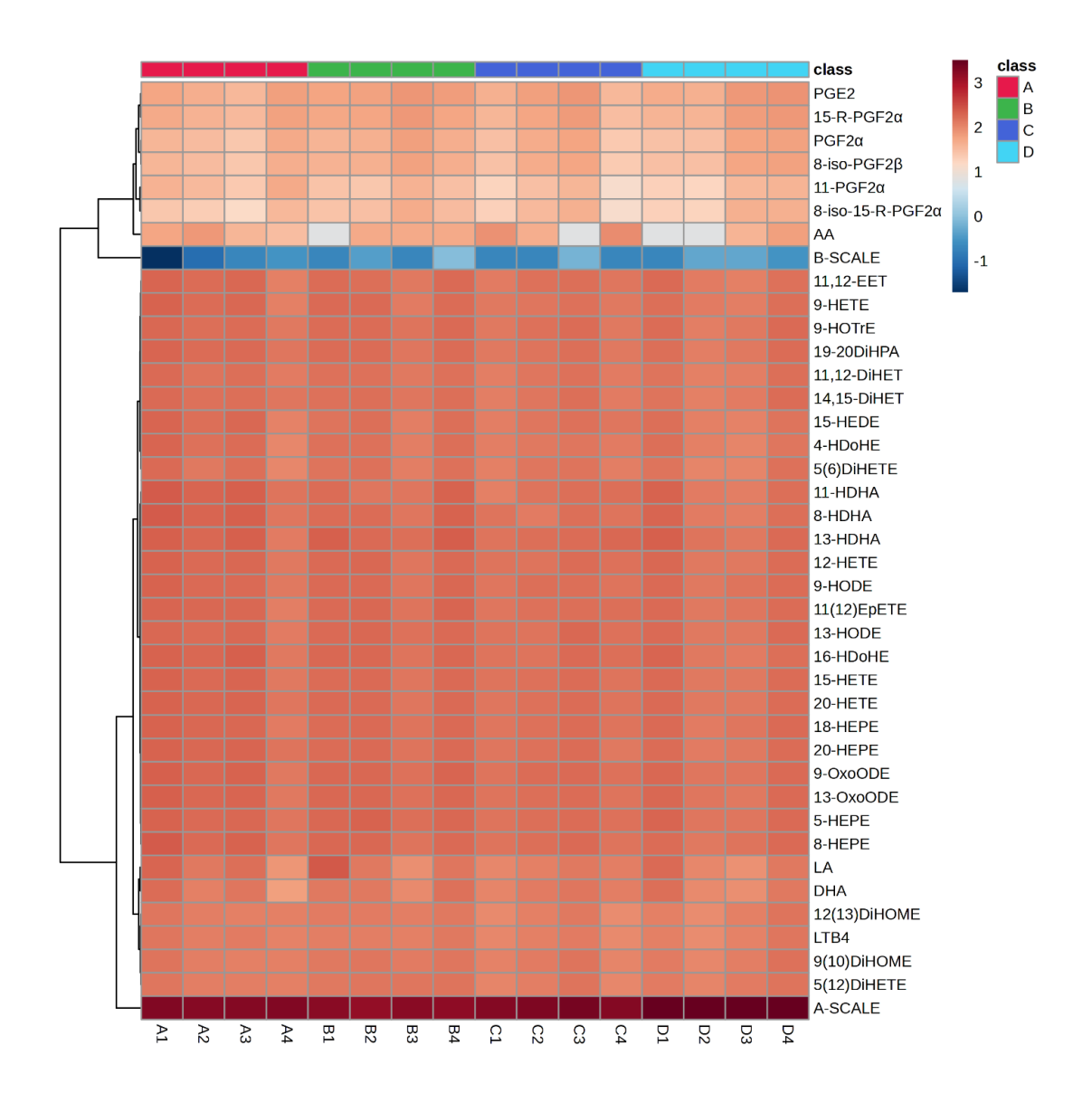


Figure 3.12: Heatmap results of 3-cycle freeze-and-thaw stability study with post-loading of BHT for 38 oxylipins stored on SPME device extracted from standard. Where A= control, B= 1-FT cycle, C =2-FT cycles and D =3-FT cycles. Heatmap was built based on log transformation with hierarchical clustering, and Euclidean distance using MetaboAnalyst software. The row A-SCALE and B-SCALE were added to the raw data to show all hierarchical maps in this chapter on the same scale.

In my previous stability study in **Chapter 2**, PGE2 and AA (**Section 2.3.1**) were identified to be unstable during the 3-FT cycle stability test of oxylipins extracted and stored on SPME after extraction from a standard solution. The results in this section show that PGE2 and AA were stable

using both BHT loading approaches as shown in **Figure 3.13** and the summary tables for pre-and post-extraction loading of PGE2 and AA (**Supplementary Tables B2** and **B3**). In general, when possible, pre-extraction BHT loading is preferred as it (i) ensures the stability of analytes even during the sampling step, (ii) allows higher amounts of BHT to be loaded to ensure excess antioxidant is present and (iii) improves overall method precision as it avoids desorption of oxylipins during loading step.

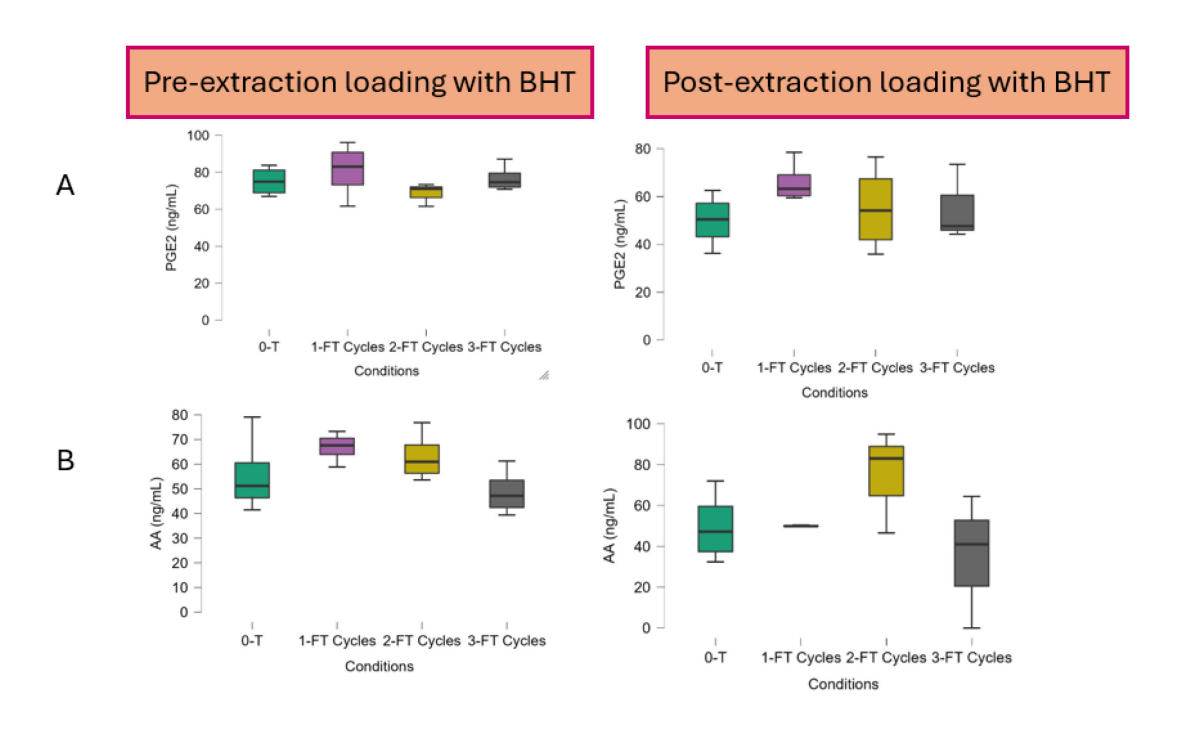


Figure 3.13: Box plot results for 3-cycle FT stability of (A) PGE2 and (B) AA stored on SPME devices with pre-and post-extraction loading of BHT (n=4). Oxylipins were extracted from the standard mix of 300 ng/mL. Pre-extraction loading of BHT was from 1.5 mL of 50% methanol and the post-extraction loading of BHT was from 1.5 mL of 5% MeOH.

Next, the amount of BHT remaining on all SPME fibres was determined. As shown in **Figure 3.14** there was no significant difference in the amount of BHT desorbed between the control and 3-FT cycle samples when BHT was pre-loaded on SPME fibres. However, for the post-extraction

loading of BHT, there was a significant loss of BHT in fibres that underwent 1-FT to 3-FT cycles which could explain why most of the oxylipins were stable as the decrease might have contributed to their stability (**Figure 3.14**). The BHT summary results for both pre-and post-extraction loading are shown in **Supplementary Tables B4** and **B5**.

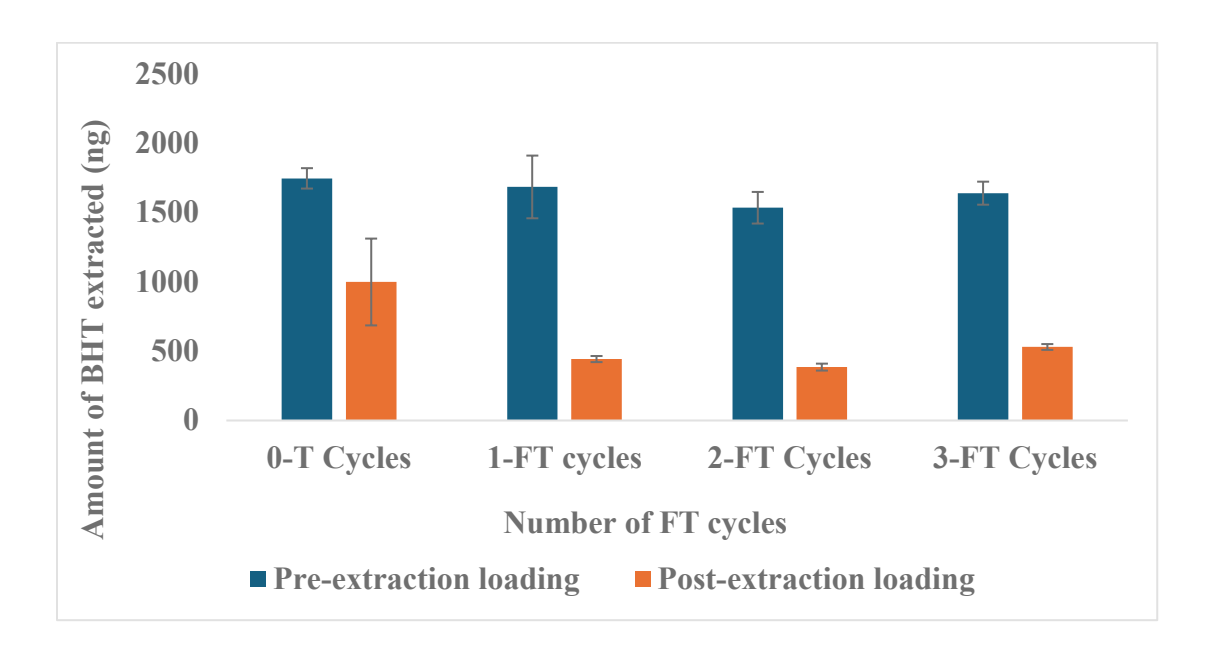


Figure 3.14: Amount of BHT remaining on SPME devices during 3-FT cycle stability study comparing pre- (n=4) and post-extraction (n=4) loading of BHT. Oxylipins were extracted from 300 ng/mL standard mix. Pre-extraction loading of BHT was performed using 1.5 mL of 10 μ g/mL BHT standard in 50% MeOH for 5 h and the post-extraction loading of BHT was performed using 1.5 mL of 10 μ g/mL BHT standard 5% methanol for 5 min.

3.3.5 3-cycle freeze-and-thaw stability study of oxylipins extracted from spiked citrate plasma and stored on SPME devices with pre-and post-extraction loading of BHT

The 3-FT cycle stability study was conducted to determine whether pre- or post-loading of BHT would enhance the stability of oxylipins stored on SPME devices when extracted from spiked plasma. 38 oxylipins were spiked into citrate plasma, and the resulting samples were subjected to SPME with both pre- and post-extraction loading of BHT, followed by 3-FT cycles. Our results from both studies on pre- and post-extraction BHT loading showed some oxylipins that did not

meet the stability criteria i.e. within the range of 80 to 120% of the control and failed the ANOVA test in both approaches. For the pre-extraction loading of BHT, out of the 38 spiked oxylipins, 24 oxylipins were measured. 8 oxylipins out of the 24 measured showed an increase as compared to control, including PGF2α, 8-iso-15-R-PGF2a, 14,15-DiHET, 13 HODE, 13-HDHA, 12-HETE, 5-HETE, and LA. On the other hand, AA, 16-HDoHE and 11-HDHA showed decreasing amounts as compared to the control (**Table 3.3** and **Figure 3.15**). For the post-extraction loading, 20 oxylipins were measured out of 38 spiked from the standard study. Seven oxylipins failed the stability criteria. An increase was noted in 13-HDHA, while LTB4, 9-HETE, 12-HETE, 16-HDoHE, 11-HDHA, and DHA showed a decrease compared to the control samples (**Table 3.4** and **Figure 3.16**).

Table 3.3: Summary of the results of 3-freeze-and-thaw cycle stability study using pre-extraction loading of BHT and oxylipins extracted using SPME from spiked citrate plasma. The results are shown as mean concentration (ng/mL) \pm SD for oxylipins that failed the accepted criteria of concentration within 80-120% of 0-T and ANOVA <0.05.

Oxylipins	Control 0-T (ng/mL)	1-FT cycles (ng/mL)	2-FT cycles (ng/mL)	3-FT cycles (ng/mL)	ANOVA p-value (Control and 3 FT cycles)	ANOVA p-value (Between FT cycles
8-iso-15-R- PGF2α	0.9±0.1	0.6±0.1	0.47±0.2	0.5±0.2	0.007	0.460
PGF2α	1.3±0.2	1.0±0.2	0.7 ± 0.2	0.9 ± 0.2	0.014	0.169
14,15-DiHET	0.3±0.1	0.7 ± 0.1	0.3 ± 0.2	0.5 ± 0.2	0.027	0.052
16-HDoHE	3.7±0.6	2.0 ± 0.4	1.9 ± 0.4	1.8 ± 0.2	0.003	0.803
13-HDHA	2.1±0.6	4.7 ± 0.7	4.5±1	4.2±0.6	0.004	0.801
12-HETE	2.9±0.2	5.3±0.9	4.5±0.3	4.2±0.3	< 0.001	0.081
11-HDHA	6.8±0.7	5.0±0.5	4.3±0.5	4.6±0.3	< 0.001	0.216
5-HETE	8.1±0.6	12.3±2	11.8 ± 2.3	11.6±0.4	0.005	0.841
13-HODE	8.8±0.5	12.3±2	11.3±2.3	11.9 ± 0.7	0.038	0.731
LA	41.9±7	63.1±9	67.9±11	61.9±6	0.004	0.606
AA	73.5±4	42.5±7	36.9±8	42.0±11	< 0.001	0.692

^{*} The number of replicates was n=4 for all conditions

Table 3.4: Summary of the results of 3-freeze-and-thaw cycle stability study using post-extraction loading of BHT and oxylipins extracted using SPME from spiked citrate plasma. The results are shown as mean concentration (ng/mL) \pm SD for oxylipins that failed the accepted criteria of concentration within 80-120% of 0-T and ANOVA <0.05.

Oxylipins	Control 0-T (ng/mL)	1-FT cycles (ng/mL)	2-FT cycles (ng/mL)	3-FT cycles (ng/mL)	ANOVA p-value (Control and 3 FT cycles)	ANOVA p-value (3-FT cycles)
LTB4	2.7±0.2	1.5 ± 0.1	1.2±0.1	1.4±0.2	< 0.001	0.046
16-HDoHE	2.9±0.1	1.7 ± 0.3	1.6±0.3	1.7±0.2	< 0.001	0.962
13-HDHA	2.3±0.2	4.0±0.8	4.2±0.7	4.1±0.7	0.005	0.882
12-HETE	6.4±1	3.5±1.3	3.2±0.3	4.2±0.6	0.001	0.334
11-HDHA	7.2±0.7	4.4±0.6	4.3±0.7	4.6±0.7	< 0.001	0.749
9-HETE	3.5±0.2	2.7±0.4	2.7±0.2	2.6±0.3	0.001	0.932
DHA	2.4±0.1	1.7±0.2	1.8±0.3	1.7±0.2	< 0.001	0.863

^{*} The number of replicates was n=4 for all conditions.

11- and 13-HDHA which were unstable from the 3-FT cycle stability study in spiked citrate plasma without BHT in Section 2.3.2 were investigated. Using the pre-and post-extraction loading with BHT, we observed poor stability for these two compounds (Table 3.3 and 3.4) when comparing the control samples and the 3-FT cycles. ANOVA between the 3-FT cycles for these two compounds showed no significant difference with the increasing number of FT cycles (Table 3.3 and 3.4), indicating no effect of FT when stored on SPME devices.

ANOVA between the 3-FT cycles samples, excluding the control for both BHT loading approaches was investigated to identify if the poor stability of the unstable oxylipins can be connected to the number of FT cycles. Only LTB4 (**Table 3.4**) in the post-extraction loading failed the ANOVA between the cycles. The extracted BHT amounts are presented in **Figure 3.17**, and the summary tables are shown in **Supplementary Tables B6** and **B7**. Also, for the post-extraction loading of BHT, there was no significant loss of BHT in fibres that underwent 1-FT to 3-FT cycles (0.485), which could explain why most of the oxylipins were stable, as the decrease might have contributed

to their stability. This suggests the possibility of a systematic error on the control day, as there was no significant difference or decrease in the amount of BHT across all three cycles.

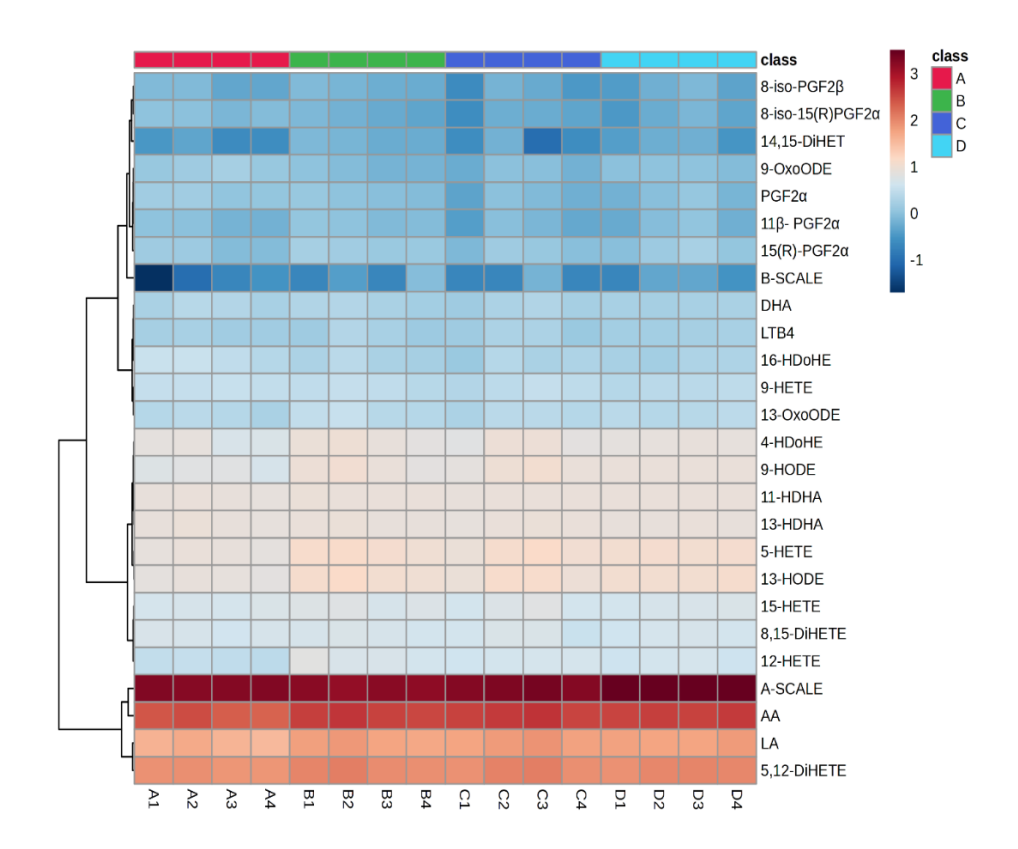


Figure 3.15: Heatmap results of 3-FT cycle stability study for 24 oxylipins for pre-extraction loading of BHT and oxylipins stored on SPME device extracted from spiked citrate plasma. Where A= control, B= 1-FT cycle, C=2-FT cycle and D=3-FT cycle. Heatmap was built based on log transformation, hierarchical clustering, and Euclidean distance using MetaboAnalyst software. The row A-SCALE and B-SCALE were added to the raw data to show all hierarchical maps in this chapter on the same scale.

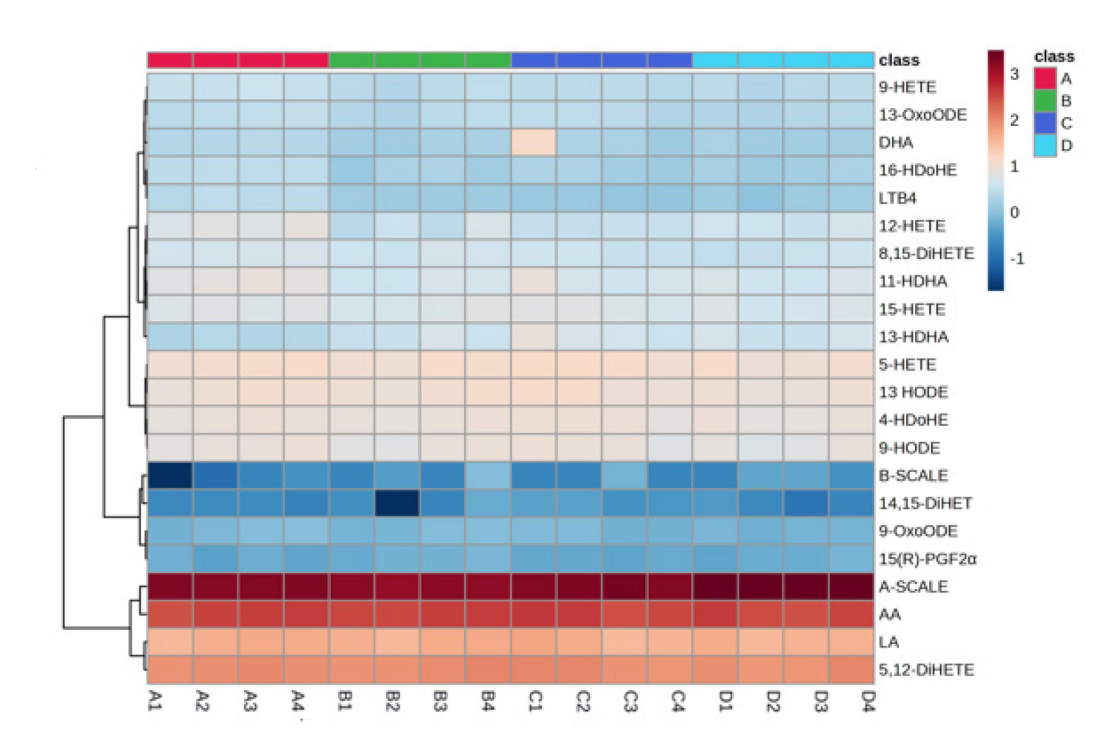


Figure 3.16: Heatmap results of 3-FT cycle stability study for 20 oxylipins for post-extraction loading of BHT and oxylipins stored on SPME device extracted from spiked citrate plasma. Where A= control, B= 1-FT cycle, C =2-FT cycle and D =3-FT cycle. Heatmap was built based on log transformation, hierarchical clustering, and Euclidean distance using MetaboAnalyst software. The row A-SCALE and B-SCALE were added to the raw data to show all hierarchical maps in this chapter on the same scale.

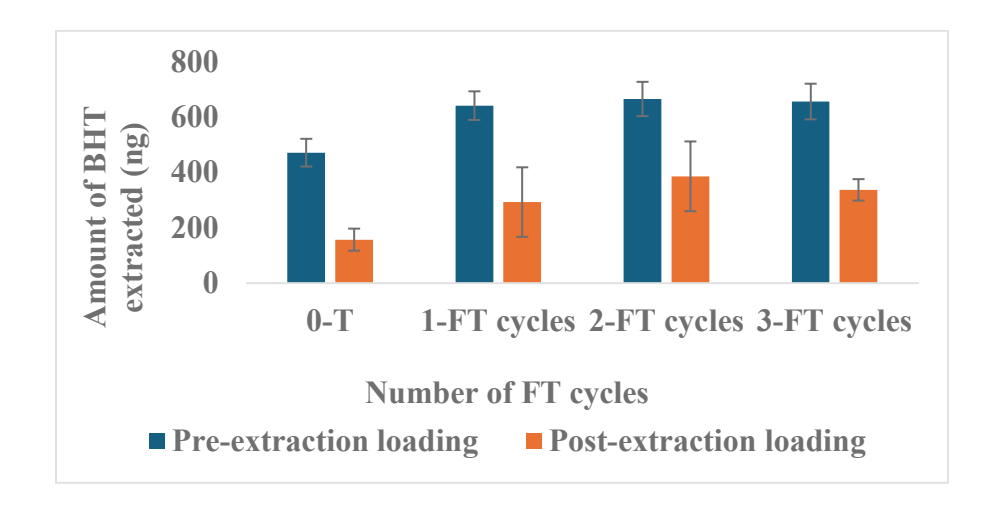


Figure 3.17: Bar graph results for 3-FT cycle stability with pre- and post-extraction loading of 10 μg/mL BHT (n=4). Oxylipins were extracted from spiked citrate plasma. Pre-extraction loading of BHT was from 1.5 mL of 50% MeOH and the post-extraction loading of BHT was from 1.5 mL of 5% methanol.

Comparing our study to the FT cycle stability in literature, Polinski *et al.* performed a 4-FT cycle with EDTA and heparin plasma without BHT and identified an increase of 12-HETE and 5-HETE after 2-cycle FT [183], [190]. Our study also confirmed a similar trend in the pre-extraction loading approach, but a decrease in 12-HETE as compared to the control in the post-extraction loading with BHT. 5-HETE was stable in combination with the post-extraction loading of BHT when stored on the SPME devices. Dorow *et al.* reported an increase in 12- and 15-HETE when stored at RT with no effect of BHT [184] and our result showed stability of 15-HETE using both pre-and post- and post-extraction loading with BHT when stored on SPME. Jonasdottir *et al.* reported poor stability of 12-HETE, 5-HETE, and LTB4 using EDTA and heparin plasma when stored for the short- and long-term without methanol [186]. Similarly, LTB4 and 12-HETE were identified to be unstable in the 3-FT cycle with post-extraction loading with BHT in our study.

Additionally, EDTA was shown to improve the stability of oxylipins, as it prevents platelet activation and may reduce lipid oxidation. However, our study was performed with citrate plasma, to eliminate the effects of EDTA from the results. Our results showed stability for most of the LOX-synthesized oxylipins in our library, including 15-HETE (unstable as reported in literature) for both loading approaches when compared to control samples. 5-HETE and 5,12-DiHETE were stable using post-extraction loading with BHT, while LTB4 remained stable with pre-extraction loading with BHT. 5-HETE, and 12-HETE have been reported to increase after 2-FT cycles using EDTA plasma [183], [190] were also found unstable with citrate in either loading approaches. Some unstable oxylipins, such as 16-HDoHE, 13-HDHA, 11-HDHA, and 12-HETE, failed stability criteria for both pre-and post-extraction loading when compared to control (Figure 3.18). Non-enzymatic pathways oxylipins such as 9-HODE and 13-HODE were stable using post-extraction loading with BHT when stored on SPME devices during the 3-FT cycle. Although,

Moran-Garrido *et al.* reported a significant increase of these compounds after 3, 4 and 5-FT cycles [190].

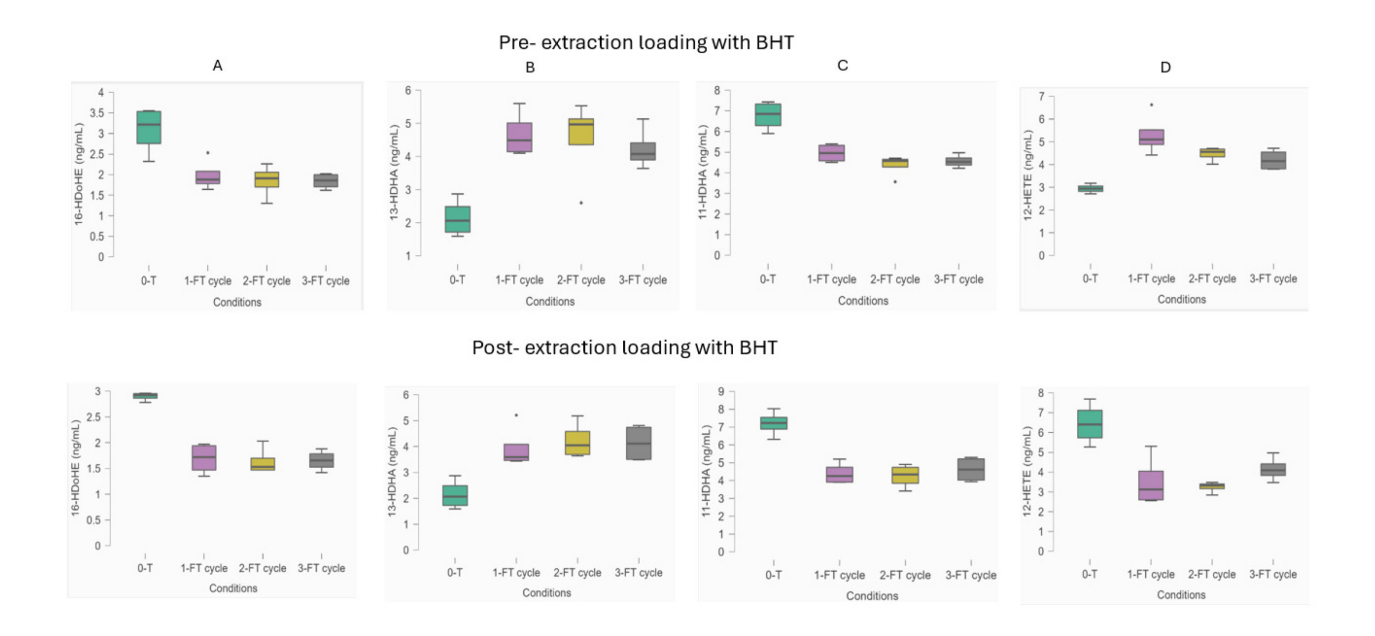


Figure 3.18: Box plot results of oxylipins unstable in 3-FT cycle stability study with pre- and post-extraction loading of oxylipins from 10 μ g/mL BHT extracted from spiked citrate plasma. (A) 16-HDoHE, (B) 13-HDHA, (C) 11-HDHA and (D) 12-HETE.Oxylipins were extracted from citrate plasma spiked with 300 ng/ml of standard mix. Pre-extraction loading of BHT was from 1.5 mL of 50% MeOH (5 h) and the post-extraction loading of BHT was from 1.5 mL of 5% MeOH (5 min). The number of replicates n=4.

3.4 Conclusions

In conclusion, pre- and post-extraction loading procedures for BHT were successfully developed for SPME devices. The application of these procedures to improve the stability of oxylipins when stored on SPME devices was evaluated in 3-FT cycle stability study after extraction from both standard and spiked citrate plasma samples. In the 3-FT cycle stability study with standard samples, all oxylipins were stable in combination with post-extraction loading of BHT. In the more complex plasma matrix, several unstable oxylipins, such as 16-HDoHE, 13-HDHA, 11-HDHA, and 12-HETE, failed stability criteria in combination with both pre- and post-extraction BHT

loading. Additionally, other unstable oxylipins identified for pre-extraction loading included 8-iso-15-R-PGF2α, PGF2α, 14,15-DiHET, 5-HETE, 13-HODE, AA, and LA. For post-extraction loading, LTB4, 9-HETE, and DHA were unstable. Comparing the results in **Chapters 2** and **3**, better stability was observed in standard samples, as shown in **Table 3.5** below. However, BHT did not improve the stability of oxylipins after extraction from complex biological samples **Table 3.6**. Therefore, the loading of BHT might be useful for selected oxylipins but not a necessity for improving the stability of oxylipins when stored on SPME devices for broad oxylipin profiling.

Table 3.5: A summary table evaluating the impact of pre-extraction and post-extraction BHT loading on oxylipin stability on SPME fibres. All samples were extracted from standard samples.

Oxylipins	3-FT cycle stability of oxylipins without loading of antioxidants	3-FT cycle stability of oxylipins with pre- loading of BHT	3-FT cycle stability with post-loading of BHT
LA	Stable	Stable	Stable
9-HOTrE	Stable	Stable	Stable
9-oxoODE	Stable	Stable	Stable
13-oxoODE	Stable	Stable	Stable
9-HODE	Stable	Stable	Stable
13-HODE	Stable	Stable	Stable
EPA	Stable	ND	ND
AA	Unstable	Stable	Stable
12,13-DiHOME	Stable	Stable	Stable
9,10-DiHOME	Stable	Stable	Stable
18-HEPE	Stable	Stable	Stable
11,12-EpETE	Stable	Stable	Stable
8-НЕРЕ	Stable	Stable	Stable
20-HEPE	Stable	Stable	Stable
5-HEPE	Stable	Stable	Stable
11-HEPE	Stable	ND	ND
12-HEPE	Stable	ND	ND
12-HETE	ND	Stable	Stable
15-HETE	ND	Stable	Stable
11-HETE	Stable	ND	ND
9-НЕТЕ	Stable	Stable	Stable
11,12-EET	Stable	Stable	Stable
8,9-EET	Stable	ND	ND
15-HEDE	Stable	Stable	Stable

Oxylipins	3-FT cycle stability of oxylipins without loading of antioxidants	3-FT cycle stability of oxylipins with pre- loading of BHT	3-FT cycle stability with post-loading of BHT
DHA	Stable	Stable	Stable
LTB4	Stable	Stable	Stable
8,15-DiHETE	Stable	ND	ND
5,15-DiHETE	Stable	ND	ND
5,12-DiHETE	Stable	Stable	Stable
5,6-DiHETE	Stable	Stable	Stable
11,12-DiHET	Stable	Stable	Stable
14,15-DiHET	Stable	Stable	Stable
7-HDHA	Stable	ND	ND
8-HDHA	Stable	Stable	Stable
13-HDHA	Stable	Stable	Stable
11-HDHA	Stable	Stable	Stable
10-HDHA	Stable	ND	ND
14-HDoHE	Stable	ND	ND
20-HDoHE	Stable	ND	ND
17-HDoHE	Stable	ND	ND
4-HDoHE	Stable	Stable	Stable
PGE2	Unstable	Stable	Stable
PGD2	Stable	ND	ND
8-iso-15(R)-PGF2α	Stable	Stable	Stable
8-iso-PGF2α	Stable	ND	ND
8-iso-PGF2β	ND	Stable	Stable
11β-PGF2α	Stable	Unstable	Stable
15(R)-PGF2α	Stable	Stable	Stable
PGF2α	Stable	Stable	Stable
19,20-DiHDPA	Stable	Stable	Stable
PGF2αEA	Stable	ND	ND
LTD4	Stable	ND	ND

Where: ND (not measured).

Table 3.6: A summary table evaluating the impact of pre-extraction and post-extraction BHT loading on oxylipin stability on SPME fibres. All samples were extracted from spiked citrate plasma samples.

Oxylipins	3-FT cycle stability of oxylipins without loading of antioxidants	3-FT cycle stability of oxylipins with pre- loading of BHT	3-FT cycle stability with post-loading of BHT
LA	Stable	Unstable	Stable
9-HOTrE	Stable	ND	ND
9-oxoODE	Stable	Stable	Stable
13-oxoODE	Stable	Stable	Stable
9-HODE	Stable	Stable	Stable
13-HODE	Stable	Unstable	Stable
EPA	Stable	ND	ND
AA	Stable	Unstable	Stable
5-НЕРЕ	Stable	ND	ND
12-HETE	ND	Unstable	Unstable
5-HETE	Stable	Unstable	Stable
15-HETE	Stable	Stable	Stable
5-oxoETE	Stable	ND	ND
11-HETE	Stable	ND	ND
9-HETE	Stable	Stable	Unstable
DHA	Stable	Stable	Unstable
LTB4	Stable	Stable	Unstable
8,15-DiHETE	Stable	Stable	Stable
5,15-DiHETE	Stable	ND	ND
5,12-DiHETE	Stable	Stable	Stable
11,12-DiHET	Stable	ND	ND
14,15-DiHET	ND	Unstable	ND
13-HDHA	Stable	Unstable	Unstable
11-HDHA	Stable	Unstable	Unstable
10-HDHA	Stable	ND	ND
14-HDoHE	Stable	ND	ND
20-HDoHE	Stable	ND	ND
17-HDoHE	Stable	ND	ND
16-HDoHE	ND	Unstable	Unstable
4-HDoHE	Stable	Stable	Stable
8-iso-15(R)-PGF2α	ND	Unstable	ND
8-iso-PGF2β	ND	Stable	ND
11β-PGF2α	Stable	Stable	ND
15(R)-PGF2α	Stable	Stable	Stable
PGF2α	ND	Unstable	ND

CHAPTER 4

4.0 Forced degradation of oxylipins and their precursors using ultraviolet light (UV), copper sulphate oxidation, and elevated temperatures.

4.1 Introduction

Oxylipins are oxygenated lipid mediators which are produced from omega-3 (ω-3) and omega-6 (ω-6) polyunsaturated fatty acids such as AA, 20:4 (ω-6), DHA, 22:6 (ω-3), EPA, 20:5 (ω-3), and linoleic acid LA, 18:2 (ω-3) [1]. These mediators are of keen interest due to their roles in health and are possible biomarkers of diseases such as cancers[98], [231], neurodegenerative disorders [232], etc. Many oxylipins are highly unstable because they contain PUFA backbone and may contain peroxide or epoxide functional groups. This instability can lead to rapid degradation/formation, resulting in primary or secondary degradation products through enzymatic and non-enzymatic oxidation reactions [69], [233]. The enzymatic oxidation reactions of COX, LOX, and CYP450 produce various classes of oxylipins [2]. The non-enzymatic reaction of precursors with reactive oxygen species can also produce various oxylipins. For example, the oxidation of EPA produces HEPEs such as 18-HEPE, 8-HEPE, and 9-HEPE, while the oxidation of DHA can produce HDoHEs such as 4-HDoHE, 20-HDoHE [3].

Lipids undergo non-enzymatic reactions such as autooxidation, photooxidation, hydrolysis, reduction, and isomerization. In non-enzymatic reactions, lipids with more unsaturated bonds tend to oxidize faster due to the rate of formation and concentration of the primary oxidation product being dependent on the number of double bonds present in the lipid [67]. Autoxidation reaction is a common non-enzymatic pathway to produce oxylipins and involves three major steps: initiation, propagation, and termination. In the initiation step, a non-radical lipid [R] undergoes the removal

of a hydrogen atom, transforming it into a lipid free radical. The energy required for this cleavage depends on the position of the hydrogen atom within the compound structure. The next phase is the propagation stage, where the lipid alkyl radical [R·] further reacts with molecular oxygen 3O_2 to produce a lipid peroxyl radical [ROO]. This is a fast reaction at normal atmospheric conditions, resulting in increased peroxyl radical concentrations [65]. In an autoxidation reaction, the lipid alkyl radical and hydroperoxide synthesis is continuous as long as oxygen and lipid are available to donate hydrogen atoms and heat; otherwise, the reaction terminates [65], [234]. Photooxidation involves a free radical reaction induced by UV light radiation, whereby exposure to direct sunlight or fluorescent light (i.e. the left-over UV from the mercury in fluorescent light) can cause the degradation of unsaturated lipids, forming hydrogen peroxide (ROOH) and other peroxide compounds (ROOR). Exposure to UV light generates activated triplet oxygen, which produces 1O_2 . Hence, 1O_2 can further break the double bond of unsaturated fatty acids by photooxidation reaction.

This free radical reaction ceases in the absence of UV light radiation or in the presence of antioxidants [74]. Heating can also lead to the degradation of oxylipins as higher temperatures increase reaction rates of various chemical reactions. Primary products of oxidation (lipid peroxides) are generally stable at room temperature but at elevated temperatures, these peroxides promote homolytic cleavage of oxygen bonds, leading to degradation into alkoxyl and hydroxyl radicals, which further degrade into aldehydes and ketones [65]. Alternatively, the alkoxy radical can undergo homolytic β-scission of carbon-carbon bonds, producing oxo-compounds and other alkyl radicals [74]. Copper sulphate (CuSO₄) can induce oxidative stress and initiate oxidation reactions in plants [235] and promote low-density lipoprotein (LDL) oxidation in humans [236]-, 238].

To date, a limited number of studies in literature have examined the degradation pathways of oxylipins using forced degradation studies but PUFAs were well-studied. For example, Yin et al. identified autoxidation products of EPA in vitro and in vivo studies using thin-layer chromatography. They identified bicyclic endoperoxides by two-5-exo cyclization and oxidation and 5-, 8-, 9-, 11-, 12-, 14-, and 15-hydroperoxides of EPA [239]. The non-enzymatic degradation of hydroperoxyl and hydroxyl DHA-derived oxylipins was studied using photooxidation and LC-MS [240]. Another study focused on the oxidation of DHA in mackerel using photooxidation incubation (LED) for 24, 48 and 72 h at 4°C, 2000 lx and heating for 4, 6 and 8 min. at 100°C [241]. Their results showed the successful formation of DHA photooxidation products after reaction with ¹O₂. Rober et al. evaluated the in vivo oxidation of DHA to produce IsoPs [242]. Miyamoto et al. studied the autoxidation of LA to produce LA peroxyl radicals and ¹O₂ by reacting linoleic acid hydroperoxides under various conditions [243], [244] including photooxidation of isotopic labelled of LA hydroperoxides [245], peroxynitrite [246] and hypochlorous acid reaction [243], [244]. Esterbauer et al. evaluated the autoxidation of aldehydes that can be produced nonenzymatically [247]. Weiny et al. evaluated the autoxidation of AA to EETs such as 14,15-EET,-11,12-EET, 8,9-EET and 5,6-EET after heating at 60°C for 45 min. or air incubation for 6 h [248]. Hennebelle et al. studied the degradation of LA, AA, 13-HODE, and PGE2 in artificial cerebrospinal fluid, with constant bubbling of 95% oxygen at 37°C for 10 min. to track any potential degradation products [249]. The resulting LC-MS analysis revealed significant degradation of PGE2, with PGD2 as the major degradation product. These results highlight the large number of degradation products that may arise from PUFA autoxidation.

To characterize oxylipin degradation pathways, untargeted LC-MS can be used. MS/MS involves the isolation of a precursor compound, which is then fragmented to produce product ions [250].

For a given molecular formula, many oxylipin isomers may exist which makes the characterization difficult and co-elution of several isomeric species possible. The use of MS/MS fragmentation can help to distinguish isomers which give characteristic fragments depending on the position of the modification of the PUFA backbone. However, some isomers may produce similar fragmentation spectra, in which case other separation approaches may be required. The most common type of fragmentation used for small molecule identification in ESI-MS is collision-induced (CID), whereby ion collisions with gases such as argon or nitrogen provide the internal kinetic energy for unimolecular fragmentation (1-100 eV) [251] that can break the weakest chemical bond(s) in an ion [252], [253]. Newer electron-activated dissociation (EAD) methods were introduced recently as they can provide additional complementary information to CID to aid structural determination [254].

The objective of this study was to map non-enzymatic degradation products of selected unstable oxylipins and their precursors. The study employs forced degradation studies in combination with LC-MS/MS analysis using both CID and EAD fragmentation techniques to characterize both standard and plasma samples. In addition to the systematic mapping of the forced degradation products of oxylipins and their precursors in standard solutions exposed to the conditions that promote degradation, the study also examines if the observed degradation products interfere with the analysis of stable oxylipins of interest in our panel. These findings contribute to a more detailed understanding of oxylipin degradation processes, examine the utility of EAD fragmentation to aid in structural determination of oxylipins and may improve the accuracy of oxylipin measurements in future studies.

4.2 Materials and methods

4.2.1 Chemicals

Acetic acid, methanol, ethanol, water, acetonitrile, and isopropanol, all LC-MS grade were purchased from Fisher Scientific (Ottawa, Ontario, Canada). 15-HETE, PGE2, 5-oxoETE, 9-HoTrE, 9-oxoODE, 4-HDoHE, 13-HDHA, 13-oxoODE, 11β-PGF2α, 11,12-EpETrE, 16-HDoHE, 9-HETE, LTB4, 12-HETE and 11-HDHA oxylipin standards and PUFA precursors (AA, LA, EPA, and DHA) were purchased from Cayman Chemical Company (Michigan, US) via their Canadian distributor (Cedarlane, Burlington, Ontario, Canada). All oxylipins with their full names and abbreviations are listed in **Supplementary Table C1**.

4.2.2 Forced degradation study experimental design

For each of the oxylipins mentioned **Section 4.1.1**, individual stocks were prepared at 100 ng/mL in 20% MeOH (v/v) and subjected to the conditions likely to promote their degradation described in **Figure 4.1**. These oxylipins were selected for the forced degradation studies based on the findings of our previous studies in **Chapters 2** and **3**, where they were found unstable in some of the conditions tested.

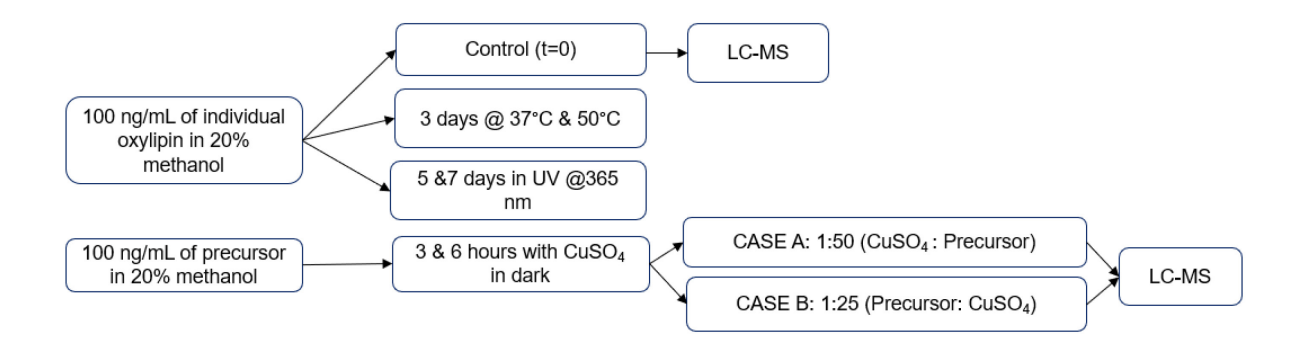


Figure 4.1: Experimental design of forced degradation studies for oxylipins and precursors.

Experimental conditions selected were (i) UV using a wavelength of 365 nm for 5 and 7 days to promote photooxidation including reactions such as lipid peroxidation, generation of free radicals and ROS [74], (ii) storage at 37°C (to mimic in vivo conditions and/or exposure to elevated temperatures during storage) and 50°C as higher temperature to promote more extensive degradation, and (iii) CuSO₄ incubation in a dark room using two different concentration ratios of CuSO₄ to precursor (1:50) CASE A and (25:1) CASE B for 3 and 6 h respectively which acts as an oxidizing agent to promote oxidation process [238]. The control sample for each degradation study was an aliquot of individual oxylipin standard prepared in 20% methanol and stored immediately at -80°C until the analysis day. These conditions were selected to over-stress the samples and promote not only the primary degradation products but also other possible degradation products of unstable oxylipins. The concentration of 100 ng/mL was selected to obtain a high signal within the linear range of the detector and enable direct measurement of the amount of precursor compound remaining and its degradation products. Also, our method LOQ is below 1 ng/mL for oxylipins, to enable the detection of minor degradation products even if only 5%, or less, is converted. A 20% methanol blank sample was also subjected to the various conditions described above as negative control. Samples were analyzed by direct injection using the oxylipin LC-MS method in Section 2.2.5. To confirm the identification of unknowns observed during degradation such as PGA2 (Cayman Chemicals), 1 µg/mL solution of PGA2 in 100% methanol was prepared and analyzed using the same LC-MS method. The rt and MS/MS spectra were collected for both compounds and compared.

4.2.3. LC-MS analysis of forced degradation samples using ZenoTOF and EAD fragmentation

In addition to LC-MS/MS analysis using CID fragmentation described in **Section 4.1**, forced degradation samples of selected oxylipins (PGE2, DHA and EPA at 50°C for 3 days) were also analyzed using the same chromatographic method and the same run time (40 min.) on a ZenoTOF 7600 (Sciex, Vaughan, Canada) using both CID and EAD fragmentation, but an injection volume of 10 µL was used. In addition, pooled murine plasma samples were analyzed to identify unknown oxylipins of interest.

4.2.4 LC-MS analysis of oxylipins using CID

A series of oxylipin calibration standards (0.05 to 100 ng/mL) containing all oxylipins for this study was analyzed to determine the rt of oxylipins in our library **Supplementary Table A1.** The source and gas parameters were 50 psi and 70 psi for the ion source gas 1 and 2, respectively. The curtain gas was 35 psi, CAD gas was 9 psi and the temperature was set at 450°C. For the high-resolution multiple-reaction monitoring (MRM-HR), the source was set for negative ESI polarity and spray voltage of -4500V. A total scan time of 0.506 s was used, to collect 4743 estimated cycles over 40 min. run time. The TOF MS m/z range was 50 to 500 Da with 0.025 seconds accumulation time (ii) TOF MS/MS declustering potential (DP) -40V, collision energy (CE) of -10 V with both DP and CE spread set to 0 V and CE -25 V depending on the oxylipin categories for TOF MS/MS setting.

4.2.5 LC-MS analysis of oxylipins using EAD

The EAD fragmentation was performed using post-column addition of 0.5 mM sodium acetate to obtain the disodiated ion adducts for the oxylipin analysis as previously reported [173]. EAD

fragmentation of disodiated ions was performed using an electron beam of 5000 nA, and a threshold (non-IDA) of 20000 cps. The TOF start-to-end mass was 50-480 Da with 0.125 sec accumulation time. The DP was set to 40 V and CE to 12 V. The electron kinetic energy was 14 eV with the time of bins set to 8 and EAD radio frequency (RF) was 80 Da and reaction time was 30 milliseconds. For the plasma samples, the TOF start-to-end m/z range was 50-410 Da with 0.095 sec accumulation time. The electron kinetic energy was 14 eV with the time of bins set to 4-8 depending on the precursor masses. The DP, CE, RF EAD and reaction times were the same as for the forced degradation samples of standard.

4.2.6 SCIEX data analysis for oxylipins after CID and EAD fragmentation

Data analysis was performed using SCIEX OS software to obtain the MS and MS/MS spectra for both CID and EAD and to identify unknowns in both the plasma and forced degradation standard study using CID by searching public libraries such as Metabolite, NIST and Natural Products. In addition, molecular finder was used to identify possible biotransformation reactions in the forced degradation study from the CID fragmentation.

4.3. Results and discussion

4.3.1 Forced degradation studies of precursors: AA, LA, DHA and EPA

The results for PUFA precursors show significant degradation using 50°C and CuSO₄ oxidation using 25:1 ratio (CASE B) for all precursors, and for AA after 7-day UV exposure as shown in **Figure 4.2.** Among the precursors tested, AA is the most susceptible to degradation. Extensive degradation of precursors was observed using oxidation with high concentrations of CuSO₄ in CASE B (25:1) over 3 and 6 h. Under these conditions, total degradation of AA was observed, whereas DHA, EPA, and LA, showed extensive degradation of 30% or more. A similar degradation

trend was observed for all precursors when exposed to elevated temperatures for extended periods. However, despite extensive degradation of precursors using CuSO₄ oxidation under Case B conditions, these conditions did not yield a comprehensive list of degradation products, possibly due to further extensive degradation of these species. For AA, 6-h incubation with CuSO₄ (Case A condition), showed too high a result above 120%, suggesting a likely outlier as it is not possible to produce more AA than the starting amount. The experiment for this condition will be repeated.

Thus, based on these results, photooxidation and heating provided more relevant degradation pathway results, so only these conditions were used for forced degradation studies of oxylipins reported in **Section 4.3.2.** Overall, the forced degradation studies with heating confirm that the storage temperature and prolonged exposure to high temperatures can promote the extensive degradation of precursors. The rates of these reactions can be calculated using this data for other temperatures, including 4°C and -80°C.

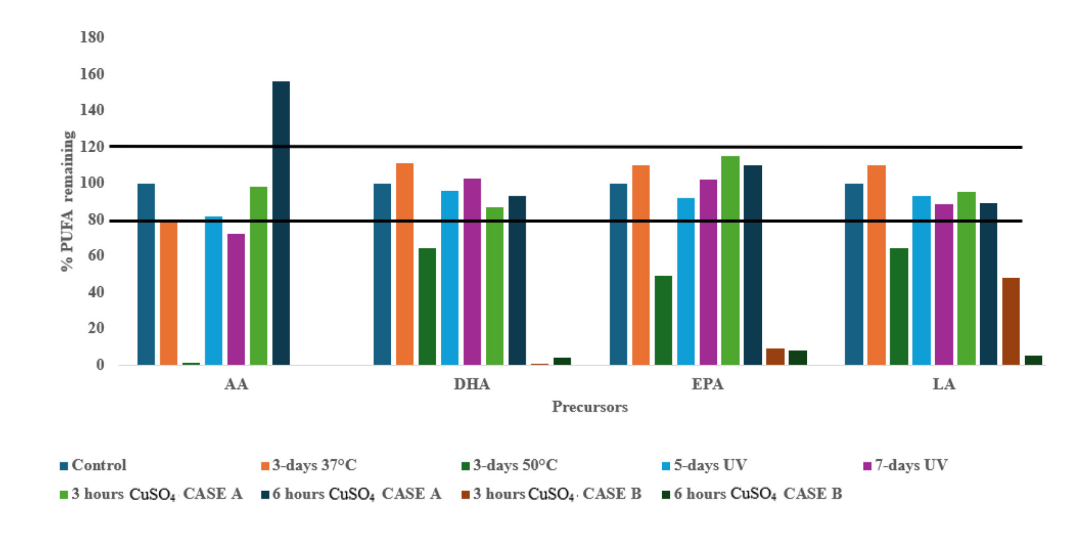


Figure 4.2: Forced degradation results of PUFAs at various conditions in comparison to control samples, where % is the percentage of each precursor remaining after exposure to the selected forced degradation condition in comparison to the control. 80-120% lines show the acceptable stability range. CuSO₄ incubations were performed in a dark room for 3 and 6 hours using two different concentration ratios of CuSO₄ to oxylipin: CASE A (1: 50) and CASE B (25:1). For AA, CuSO₄ CASE B incubations resulted in no AA remaining, so no results are shown for these two conditions.

Heating, photooxidation and copper sulphate oxidation were selected to promote degradation and map possible degradation products for all oxylipins and precursors of interest using various possible degradation pathways. The observed degradation products for the degradation of AA, LA, DHA, and EPA are shown in Supplementary Tables C2-C5. The investigation of the nonenzymatic reaction pathways of precursors under the forced degradation study conditions included non-enzymatic reactions corresponding to mass differences of specific elements—such as oxygen (15.9949), hydrogen (1.00783) and water molecules (18.01056). Both gains and losses of these elements relative to the precursor or degradation mass products were considered within a mass extraction window range of ± 5 ppm. For all PUFAs, possible degradation pathways were mapped, including oxidation (+O/-H), reduction (-O/+H), dehydration (-H₂O), and hydrolysis (+H₂O), as illustrated in Figure 4.3 for AA. The main degradation product of AA under UV photooxidation appears to result from an isomerization reaction, while heating for 3 days at 37°C resulted in two major products at m/z 317.2116 (+2O-H₂O). Longer exposure to heating promoted the formation of numerous minor products corresponding to various combinations of oxidation, reduction, hydrolysis and dehydration.

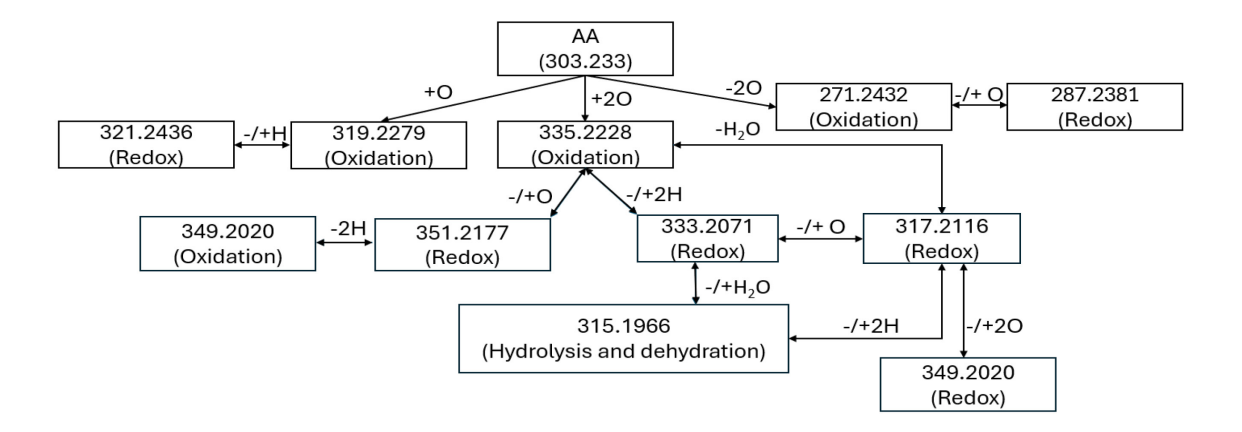


Figure 4.3: Non-enzymatic reaction pathway of AA mapped from the forced degradation study. This pathway includes only degradation products m/z that were observed in the study.

For LA, the annotated degradation products obtained at 37 and 50°C showed degradation pathways such as dehydration or hydrolysis, as well as oxidation reactions (**Figure 4.4**). The exposure to UV photooxidation resulted in the isomerization of LA. For EPA and DHA, the mapped non-enzymatic reactions were oxidation for EPA (**Figure 4.5**) and reduction for DHA (**Figure 4.6**).

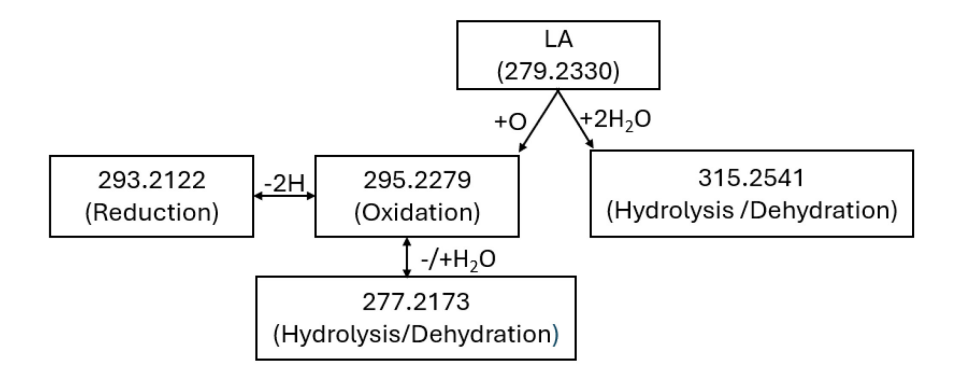


Figure 4.4: Non-enzymatic reaction pathway of LA mapped from the forced degradation study. This pathway includes only degradation products m/z that were observed in the study. The pathway for the conversion of LA to m/z (367.1925) is unknown.

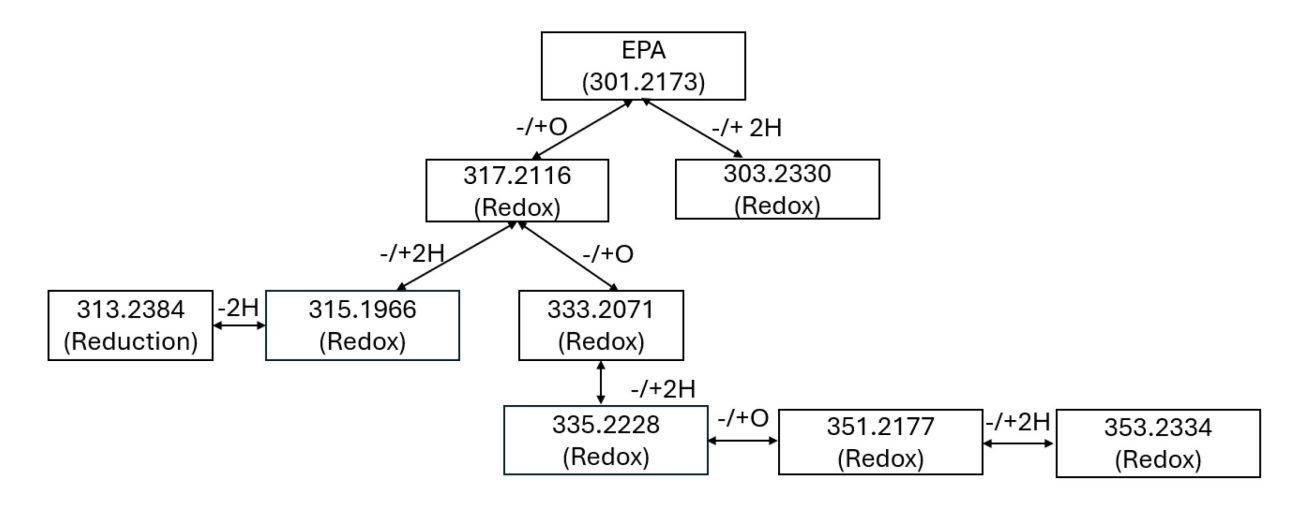


Figure 4.5: Non-enzymatic reaction pathways of EPA mapped from the forced degradation study. This pathway includes only degradation products m/z that were observed in the study. m/z of 264.1582, 269.2275, 293.1760 and 295.2278 were not reported in the diagram because their degradation pathways are unknown.

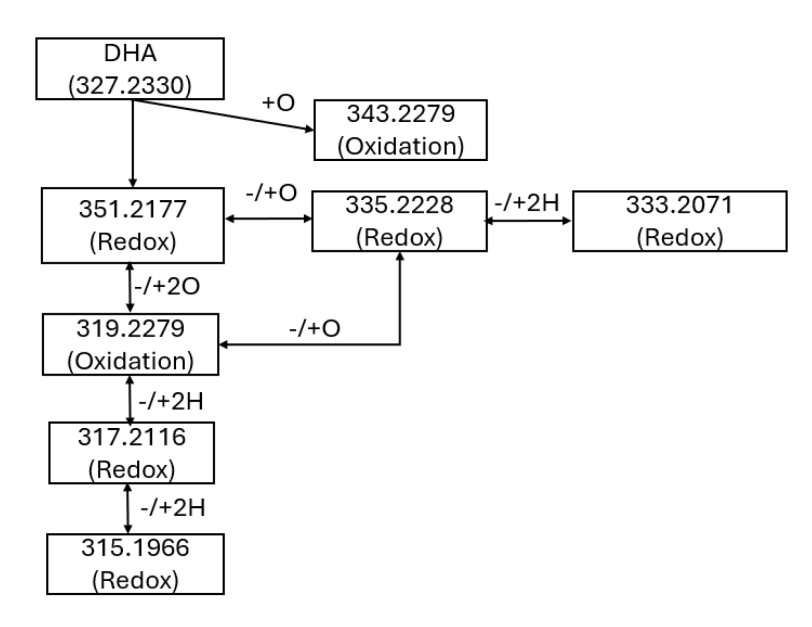


Figure 4.6: Non-enzymatic reaction pathway of DHA mapped from forced degradation study. DHA degradation products such as the addition of 2O and 2+H₂O were investigated but not observed in the current study. The pathway for the conversion of DHA to 351.2177 is unknown.

Also, the observed degradation products (m/z, rt) of precursors were compared against known oxylipins using our in-house library of authentic standards. As expected, some of the observed degradation products correspond to known oxylipins within our in-house oxylipin library. The structures of these forced degradation products, which match authentic standards in our library, are shown in **Figures 4.7** and **4.8**.

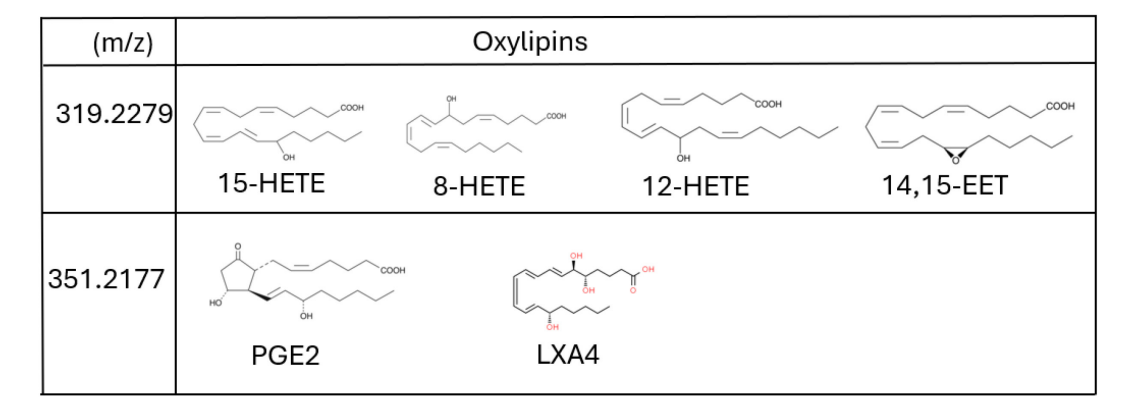


Figure 4.7: Structures of oxylipins in our in-house library which matched the degradation products observed from the forced degradation of AA

(m/z)	Oxylipins		
295.2278	9-HODE 13-HODE		
335.2228	8,15-DiHETE		
317.2122	COOH COOH COOH		
	11-HEPE 12-HEPE 20-HEPE		

Figure 4.8: Structures of oxylipins in our in-house library which matched the degradation products observed from the forced degradation of LA (9-and 13-HODE), DHA (8,15-DiHETE) and EPA (11-, 20- and 12-HEPE, 9-HODE).

Investigating the degradation of precursors is crucial in the quantification of oxylipins, as even small amounts of precursor degradation into known oxylipins of interest can be problematic. Choe *et al.* demonstrated that LA can degrade into secondary products (hydroperoxides), such as 13-and 9-HpODE [65], [66]. These products can further be converted to 9- and 13-HODE through autoxidation and were observed in our study. Therefore, improper or prolonged storage of biospecimens containing high levels of LA may result in artefactually elevated concentrations of 9- and 13-HODE. Similarly, degradation of AA, DHA or EPA using heating also resulted in the formation of detectable quantities of 8-, 12- and 15-HETEs, 14,15-EET, PGE2, LXA2, 8,15-diHETE and 11- and 12-HEPEs. Any degradation of EPA, DHA and AA during sample handling and storage, can therefore complicate the accurate measurement of these oxylipins. Comparing our

studies to literature, **Table 4.1** summarizes some non-enzymatic oxidation of precursors in our studies and the literature.

Table 4.1: Comparison of the results for non-enzymatic oxidation of precursors in our studies and the literature.

	Oxylipins identified in literature	Oxylipins identified in our
Precursor	degradation studies and references	forced degradation study
AA	14,15-EET, 11,12-EET, 8,9-EET, 15-	15-НЕТЕ, 8-НЕТЕ,
	HETE, 5-HETE, 15-HpETE and 5-	12-HETE, 14,15-EET,
	HpETE [248]	PGE2, LXA4
DHA	4- HDHA [240]	8,15-DiHETE

4.3.2 Forced degradation studies of unstable oxylipins: PGE2, 11-HDHA, 13-HDHA, 9-HoTre, 9-oxoODE, 15-HETE, 11,12-EpETrE, 5-oxoETE, 13-oxoODE, 4-HDoHE 12-HETE, 9-HETE, LTB4, 16-HDoHE and 11β-PGF2α.

Forced degradation studies were next performed for all the unstable oxylipins reported in **Chapters 2** and **3**. For all oxylipins, potential degradation pathways were mapped, including oxidation (+O/-H), reduction (-O/+H), dehydration (-H₂O), and hydrolysis (+H₂O). Their possible degradation pathways are illustrated in **Figures 4.9** to **4.17**.

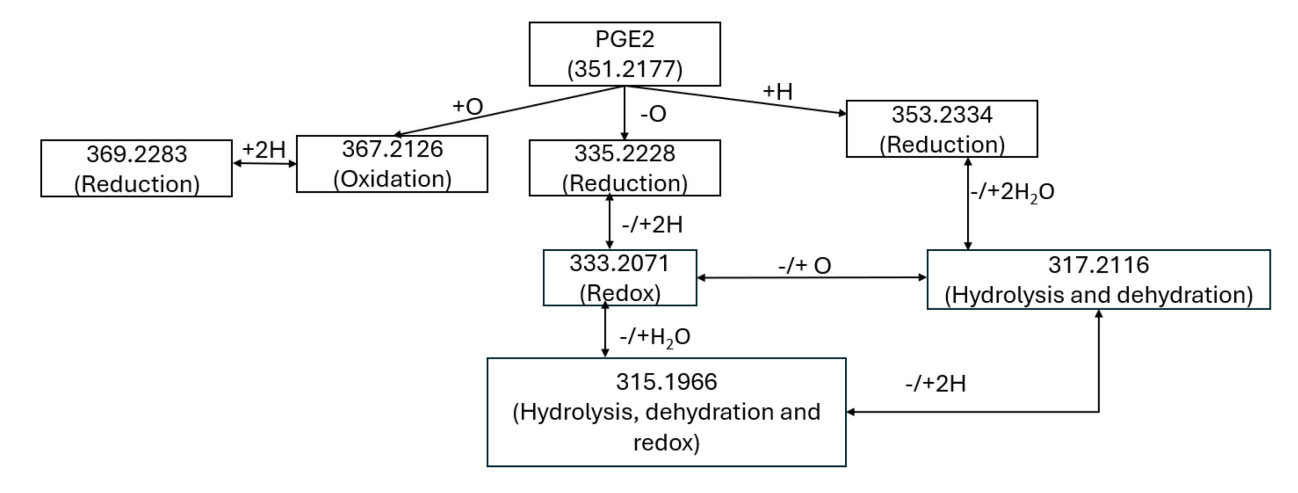


Figure 4.9: Non-enzymatic reaction pathway of PGE2 mapped from the forced degradation study. The pathway for the conversion of PGE2 to 343.2273 is unknown.

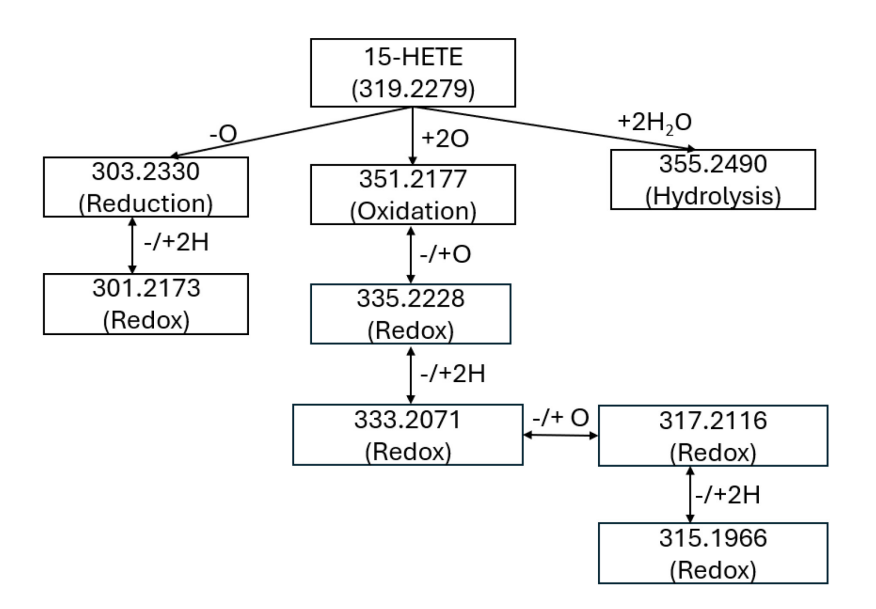


Figure 4.10: Non-enzymatic reaction pathway of 15-HETE mapped from the forced degradation study. 15-HETE degradation products such as the addition/loss -2H₂O and +2H₂O were investigated but not observed in the current study.

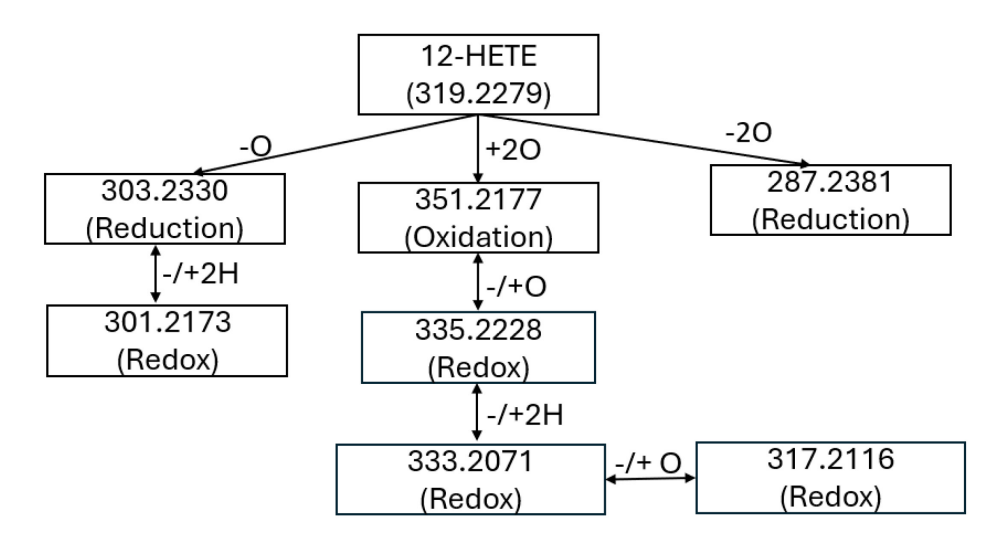


Figure 4.11: Non-enzymatic reaction pathway of 12-HETE mapped from the forced degradation study. 12-HETE degradation products such as the addition/loss of $-2H_2O$ and $+2H_2O$ were investigated but not observed in the current study.

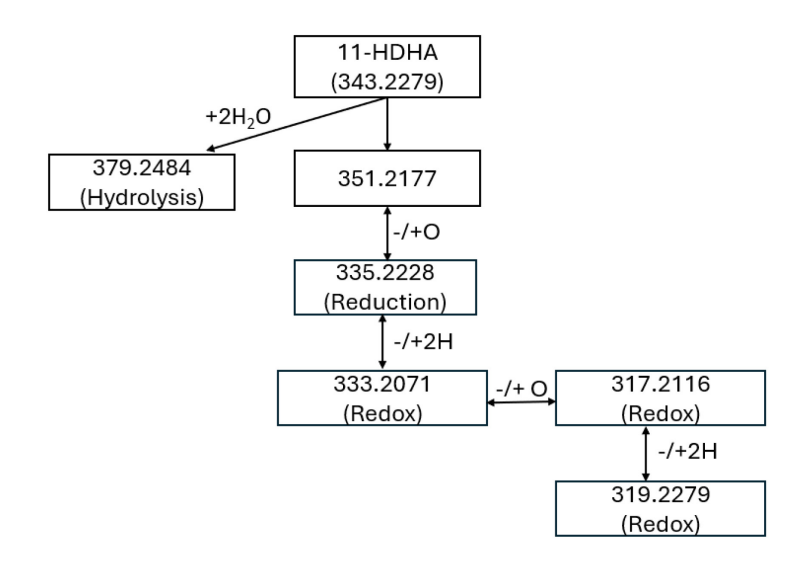


Figure 4.12: Non-enzymatic reaction pathway of 11-HDHA mapped from the forced degradation study. 11-HDHA degradation products such as the addition/loss of -2H₂O, -2O and +2O were investigated but not observed in the current study. The pathway for the conversion of 11-HDHA to 293.2122 and 351.2177 is unknown.

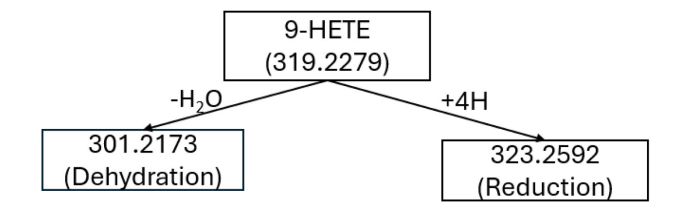


Figure 4.13: Non-enzymatic reaction pathway of 9-HETE mapped from the forced degradation study. 9-HETE degradation products such as the addition/loss -O, +O, +H, -H, -2H, +2H, -2H₂O, + 2H₂O and +H₂O, were investigated but not observed in the current study.

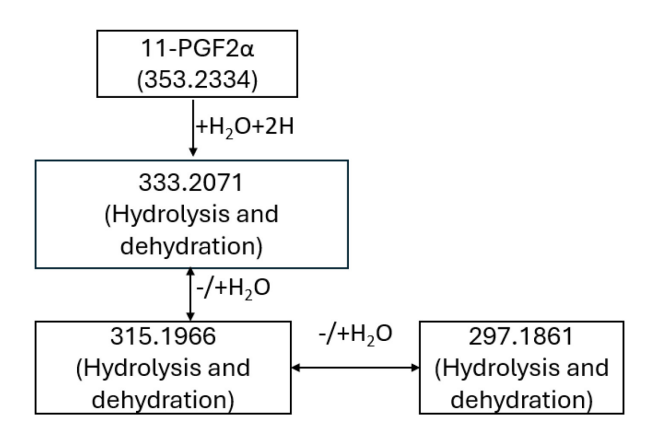


Figure 4.14: Non-enzymatic reaction pathway of 11-PGF2 α mapped from the forced degradation study. 11-PGF2 α degradation products such as the addition/loss of -O, +O, +H, -H, -2H, +2H, were investigated but not observed in the current study.

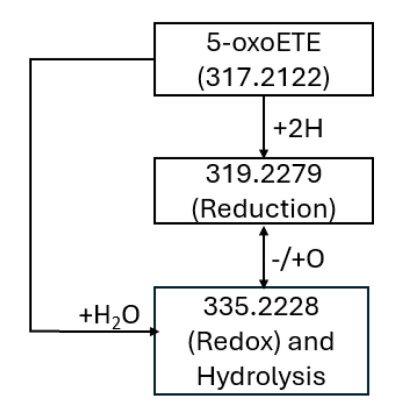


Figure 4.15: Non-enzymatic reaction pathway of 5-oxoETE mapped from forced degradation study. 5-oxoETE degradation products such as the addition/loss of +H, -H, -2H, -H₂O, 2H₂O and +2H₂O, were investigated but not observed in the current study.

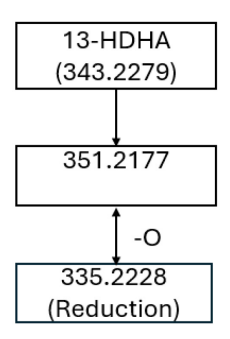


Figure 4.16: Non-enzymatic reaction pathway of 13-HDHA from the forced degradation study. 13-HDHA degradation products such as the addition/loss of +O, -2O, +2O, +2H, -2H, $+H_2O$ and $-H_2O$, were investigated but not observed in the current study. The pathway for the conversion of 13-HDHA to 351.2177 is unknown.

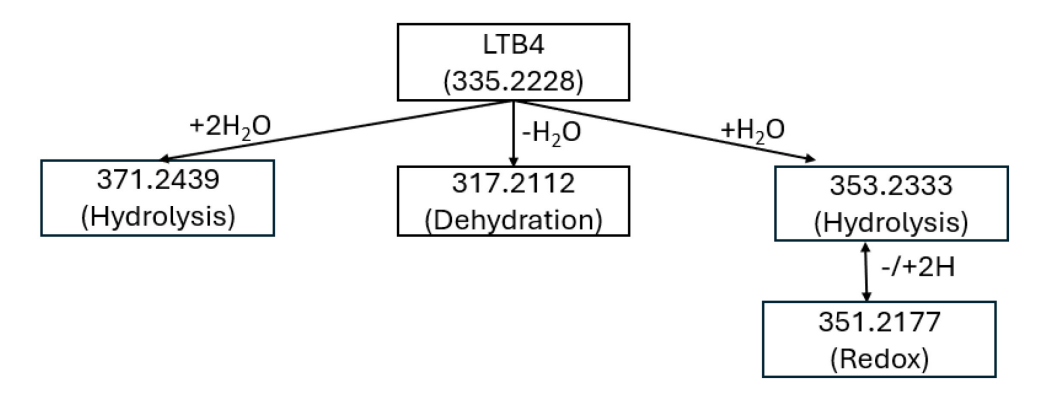


Figure 4.17: Non-enzymatic reaction pathway of LTB4 mapped from the forced degradation study. LTB4 degradation products such as the addition/loss of -O, +O, +2H, -2H, + H_2O and - $2H_2O$, were investigated but not observed in the current study.

In the 3-FT cycle stability study of oxylipins on SPME devices reported in **Chapter 2**, AA and PGE2 were found to be unstable, with a decrease in AA concentration and an increase in PGE2 compared to the control samples in **Section 2.3.1**. The degradation pathway of AA reported in **Section 4.3.1** explains both results very well. Furthermore, a forced degradation study of PGE2 was also carried out to investigate its possible degradation products. PGE2 showed 2% remaining after 7 days under UV conditions, 63% remaining after 3 days at 37°C and 6% remaining at 50°C (**Supplementary Table C6, Figure 4.18**). 20% of PGJ2 at 50°C and 7% at 37°C were produced by PGE2 using the dehydration pathway (**Figure 4.19**).

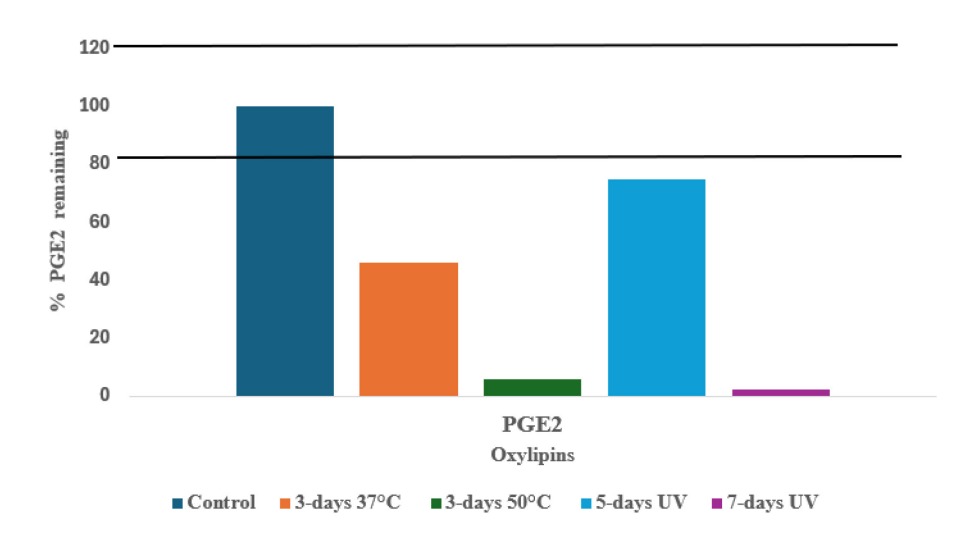


Figure 4.18: Forced degradation study results of PGE2 at various conditions in comparison to control samples. 80-120% lines show the acceptable stability range.

Figure 4.19: Major degradation product of PGE2 is PGJ2 when stored for 3 days at 37°C and 50°C.

In Section 2.3.2, two oxylipins derived from DHA, 11-HDHA and 13-HDHA were identified as unstable and showed increased levels compared to the control in the 3-FT cycle of spiked plasma. Forced degradation studies of DHA did not explain the observed increases in these compounds as their rt was not identified, even though the m/z (343.2279) was observed. Next, these compounds were subjected to the same forced degradation conditions. The results revealed significant degradation of both compounds when stored at 50°C for 3 days. 11-HDHA degraded by 50%, while 13-HDHA degraded by more than 95% (Figure 4.20). The degradation of products for 11-and 13-HDHA are reported in Supplementary Tables C7 and C8.

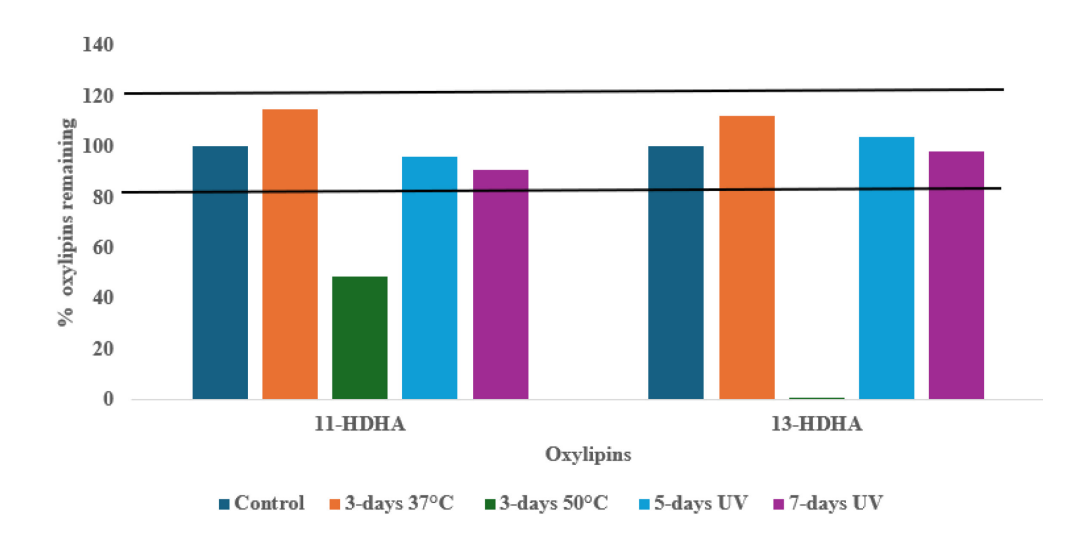


Figure 4.20: Forced degradation results for 11-HDHA and 13-HDHA at various conditions in comparison to control samples. 80-120% lines show the acceptable stability range.

In **Section 2.3.2,** 9-oxoODE and 9-HoTrE were identified as unstable during the 3-FT cycle stability of oxylipins stored on SPME after extraction from non-spiked plasma. For 9-oxoODE, a decrease was observed, whereas for 9-HoTre an increase was observed when compared to the control. Both oxylipins were subjected to all forced degradation conditions and the observed degradation products are reported in **Supplementary Tables C9** and **C10.** The forced degradation results showed significant degradation of 9-oxoODE under UV conditions when stored for 5 and

7 days at 365 nm (**Figure 4.21**), and slight degradation of 9-HoTrE at 50°C. For both 5- and 7-days UV conditions, the identified unknown isomers for 9-oxoODE are reported in **Supplementary Figure C1**.

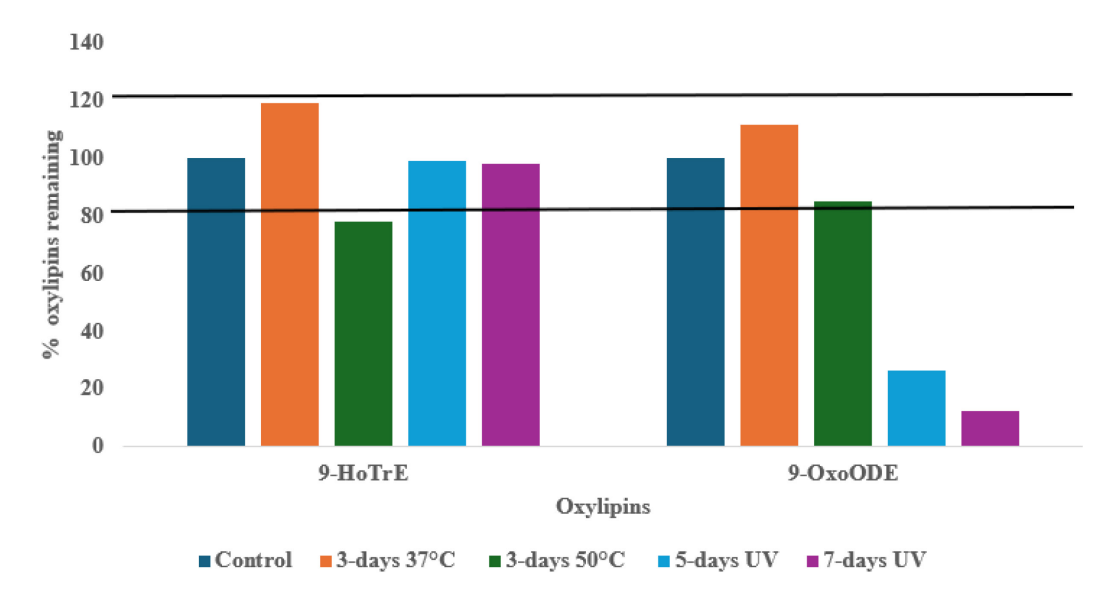


Figure 4.21: Forced degradation results of 9-HoTrE and 9-oxoODE at various conditions in comparison to control samples. 80-120% lines show acceptable stability.

According to the results of a 18-day RT stability study on SPME devices reported in **Section 2.3.3**, with an increase in 15-HETE, 11,12-EpETrE, 5-oxoETE, 13-oxoODE and decrease in 4-HDoHE reported. All of these oxylipins were subjected to forced degradation conditions. The results obtained show significant degradation for 15-HETE with heating (**Figure 4.22**). 5-oxoETE and 13-oxoODE showed significant degradation under UV conditions for both 5 days and at 7 days, with only ~20% remaining after 7 days. Heating at 50°C also degraded both 5-oxoETE and 13-oxoETE as compared to control. Unknown isomers were identified during the degradation of 5-oxoETE and 13-oxoODE **Supplementary Tables C12** and **C13**. On the other hand, 4-HDoHE and 11,12-EpETE showed no significant degradation under all conditions. All degradation products for all unstable oxylipins in RT stability are shown in **Supplementary Tables C11** to **C15**.

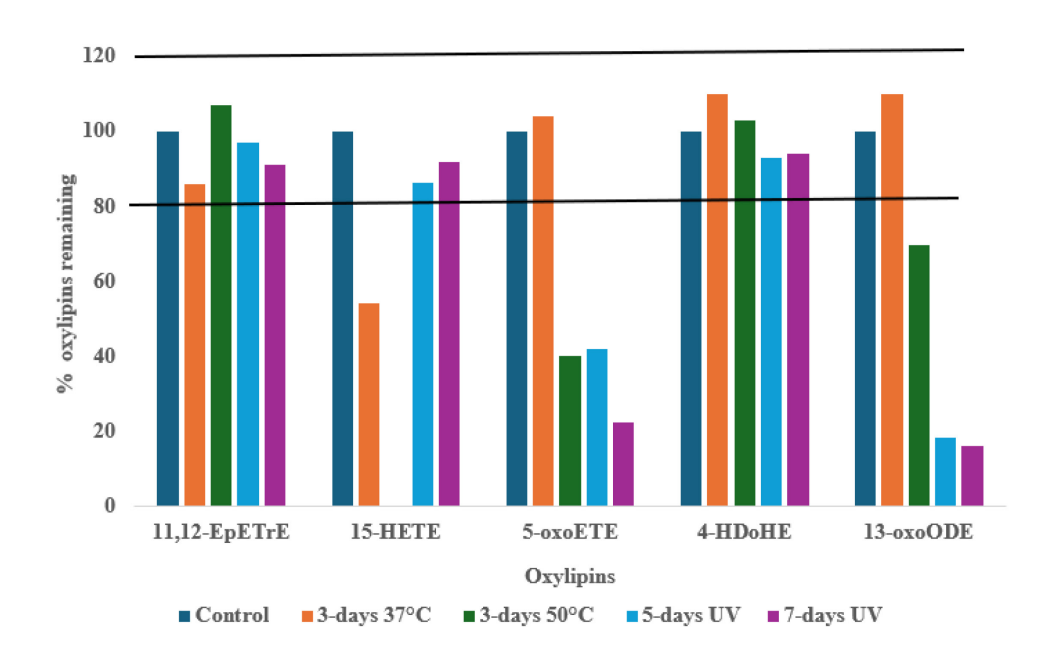


Figure 4.22: Forced degradation results of 11,12-EpETrE, 15-HETE, 5-oxoETE, 4-HDoHE and 13-oxoODE at various conditions in comparison to control samples. 80-120% lines show the acceptable stability range.

Next, the only unstable oxylipin from studies reported in **Section 3.3.4**, 11β-PGF2α, observed to decrease, was subjected to forced degradation study conditions. The forced degradation results showed that PGE2 was produced as a major degradation product when 11β-PGF2α was exposed to 365 nm for 7 days (**Figure 4.23**), and that 11β-PGF2α was completely degraded under these conditions (**Figure 4.24**). In the 3-FT cycle stability study with post-extraction loading of BHT, after oxylipin extraction from citrate plasma, LTB4, 16-HDoHE, 12-HETE, 11-HDHA and 9-HETE were observed to decrease. **Figure 4.24** shows the forced degradation results for these oxylipins, except 11-HDHA which was shown in **Figure 4.20**. Heating caused significant degradation of HETEs, similar to what was observed for 15-HETE in **Figure 4.22**. Furthermore, the degradation products of LTB4, 16-HDoHE, 12-HETE, 9-HETE and 11β-PGF2α are

summarized in **Supplementary Tables C16** to **C20**, while 11-HDHA is summarized in **Supplementary Table C8**.

$$\frac{\text{PGF2}}{\text{OH}}$$
 $\frac{\text{Reduction}}{7\text{-days}}$ $\frac{\text{Reduction}}{\text{OH}}$ $\frac{\text{COOH}}{\text{OH}}$ $\frac{\text{COOH}$

Figure 4.23: Major degradation product of 11β -PGF2α is PGE2 when exposed to 365 nm for 7 days.

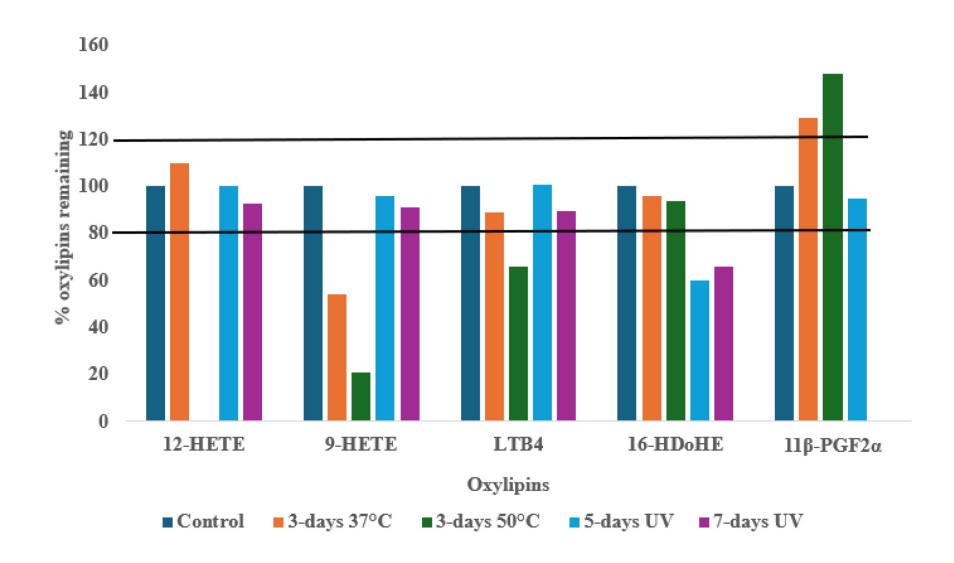


Figure 4.24: Forced degradation results of 12-HETE, 9-HETE, LTB4, 16-HDoHE and 11β-PGF2 α at various conditions in comparison to control samples. 80-120% lines show the acceptable stability range.

4.3.3 Comparison of forced degradation results to the results of stability studies

Summarizing the results obtained for all PUFAs and oxylipins tested, several trends emerge. Heating at 37 or 50°C provided the results which were the most relevant for the interpretation of stability studies and explained some of the observed results for oxylipins which were found to be

unstable when stored on SPME devices. HETEs, HDHAs, PGE2 and precursor PUFAs were particularly sensitive to heating among all the compounds tested. Photooxidation at 365 nm significantly degraded 11β-PGF2α, PGE2, all oxo-compounds and AA.

Next, it was investigated whether the compounds identified during the forced oxylipin or precursor degradation studies matched other oxylipins present in our in-house library. **Table 4.2** summarizes and shows that non-enzymatic degradation of compounds tested can produce known oxylipins. Therefore, if such degradation occurs during storage, this may lead to inaccurate quantification of those oxylipins. This finding has important implications as it demonstrates unequivocally that the measurement of stable oxylipins can be impacted by the degradation of unstable oxylipins during storage. Even if a small (negligible) percentage of precursor degrades, it can introduce a huge amount of inaccuracy to the determination of oxylipins present at low concentrations (see **Section 2.3.2**, and the **Supplementary Table A4** and **A5**. For example, degradation of EPA resulted in a twofold increase in the concentration of 5-HEPE measured in blood. Additionally, all observed degradation products for the unstable oxylipins investigated are listed in **Table 4.2**, along with their relative abundances (in percentages) and corresponding degradation conditions, which are summarized in **Supplementary Tables C2** to **C21**.

Table 4.2: Results for degradation products of oxylipins identified from the in-house oxylipin library.

Oxylipins	Oxylipin products present in the library
AA	15-HETE, 8-HETE, 12-HETE, 14,15-EET, PGE2, LXA4
EPA	9-HODE, 20-HEPE, 11-HEPE, 12-HEPE
DHA	8,15-DiHETE
LA	9-HODE, 13-HODE
13-HDHA	7-HDHA, 12,13-DiHOME
11-HDHA	10-HDHA, 13-HoTrE, 12,13-DiHOME, 9-HEPE, 5-HEPE, 14,15-EET,
	11/15-HEDE, LXB4, 5-HETE
4-HDHA	None
16-HDHA	None
PGE2	PGJ2, 8-iso-PGA1, 8,15-DiHETE, LTB4
9-oxoODE	None
13-oxoODE	None
11-PGF2α	PGE2
9-HoTrE	None
11,12-EpETE	None
15-HETE	PGJ2, 8,15-DiHETE, and LXA4
9-НЕТЕ	None
LTB4	PGE2, 5,15-DiHETE and 5,12-DiHETE
5-oxoETE	11,12-EpETE
12-HETE	15-HETE, PGE2, and PGJ2

Connecting forced degradation studies to stability in **Chapters 2** and **3**, the increase observed for oxylipins such as 15-HETE, 12-HETE, and PGE2 was mapped to degradation of AA and 13-HODE to LA (**Figure 4.25**).

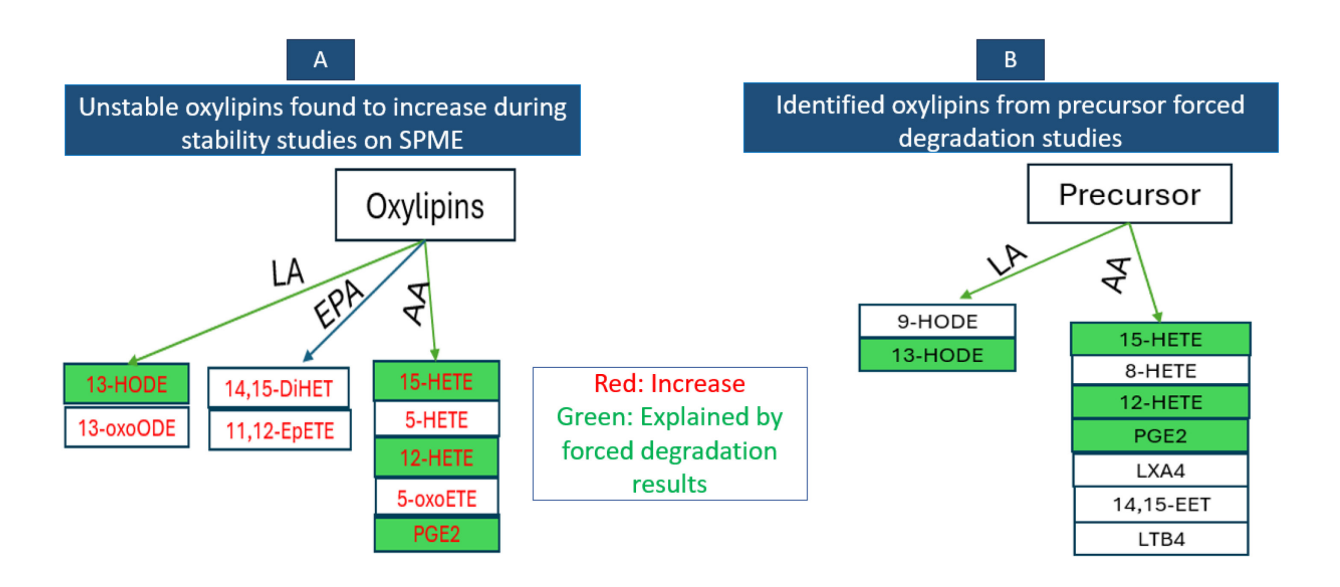


Figure 4.25: Diagrams connecting forced degradation study results of precursors to unstable oxylipins from stability studies. A = elevated unstable oxylipins identified from stability studies and B = identified oxylipins from forced degradation of LA and AA.

Furthermore, the results of our forced degradation studies also explain many unstable oxylipins, which were found to be elevated in the literature studies (**Table 1.2**) as shown in **Figure 4.26**.

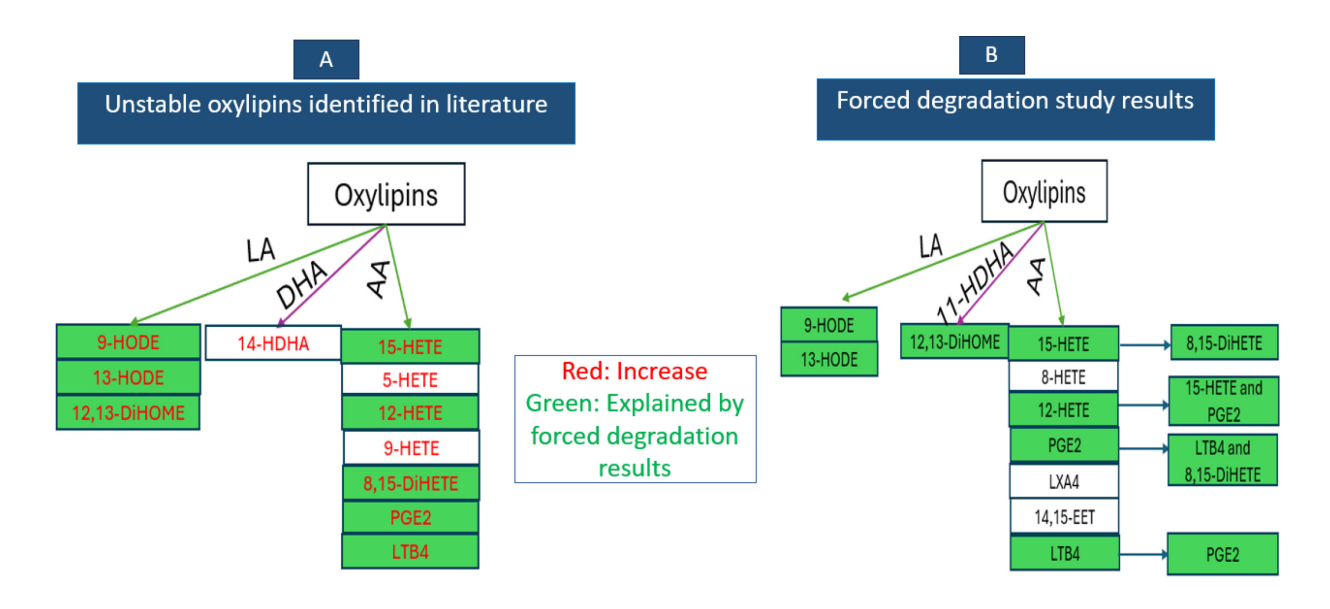


Figure 4.26: Diagrams connecting forced degradation study results of oxylipins to unstable oxylipins from literature stability studies. A = elevated unstable oxylipins identified from literature stability studies, and B = identified oxylipins from forced degradation of LA, 11-HDHA and AA.

Over 400 unknowns were identified from the forced degradation studies (Supplementary Tables C1 to C26). These unknowns were searched using m/z and rt (min.) in all the stability studies for further identification. Table 4.3 shows 18 oxylipins identified from oxylipin degradation and present in stability studies that will be prioritized for future work.

Table 4.3: Results for comparison of forced degradation results to stability studies

Unknown m/z	rt (min.)	The stability study in which unknown was observed	Forced degradation
287.2381	17.85	10-days (RT)	AA
321.2436	26.73	3-FT cycles (Standard)	AA
333.2071	13.93	10-days (RT)	AA
333.2071	13.83	3-FT cycles (Standard)	AA
317.2116	17.56	3-FT cycles plasma (Post BHT loading)	LTB4
317.2116	16.56	3-FT cycles plasma (Post BHT loading)	DHA
335.2228	17.57	3-FT cycles plasma (Post BHT loading)	12-НЕТЕ
335.2228	14.98	3-FT cycles plasma (Post BHT loading)	11-HDHA
335.2228	14.46	3-FT cycles precursor	DHA
335.2228	12.42	3-FT cycles plasma (Pre BHT loading)	LTB4
349.2020	18.74	3-FT cycles precursor	EPA
293.2122	21.75	3-FT cycles precursor	4-HDHA
293.2122	22.72	3-FT cycles precursor	4-HDHA
315.1966	13.73	3-FT cycles plasma post BHT	11-PGF2α
315.1966	18.65	3-FT cycles plasma (Post BHT loading)	DHA SCIEX
287.2381	17.85	10-days (RT)	AA
321.2436	26.73	3-FT cycles (Standard)	AA
333.2071	13.93	10-days (RT)	AA

4.3.4 Additional structural elucidation of selected forced degradation samples using EAD 4.3.4.1 Investigation of 50°C forced degradation samples using CID on Agilent 6545 Q-TOF and Sciex ZenoTOF 7600 instruments

To examine whether EAD fragmentation can provide additional insight to aid the structural characterization of unknown degradation products, three forced degradation samples were selected for further analysis on a Sciex ZenoTOF 7600 instrument. The three selected samples were EPA, DHA and PGE2 exposed to 50°C, because these three samples showed significant degradation and have well-studied oxidation pathways. This preliminary evaluation would allow side-by-side evaluation of CID and EAD, and whether it may be beneficial to use this technique in future forced oxylipin degradation studies. The same column and chromatographic method which was used for our study were implemented on the ZenoTOF system. First, we compared LOQs obtained on Agilent and Sciex Q-TOFs as shown in **Table 4.4.** Next, the rt and masses from both experiments were compared to check for the differences in rt across the two instruments due to different tubing, pump dead volumes and gradient mixing and to verify whether oxylipins can be successfully ionized in positive mode with sufficient intensity as required by EAD. Table 4.5 shows how rt profiles differ on the two instrument platforms despite the use of the same column and gradient. It also confirms that PUFAs and oxylipins can be successfully ionized as disodiated adducts in positive ESI mode.

Table 4.4: Summary of oxylipins in our library analyzed using Q-TOFs from both Agilent (Agilent 6545 Q-TOF) and Sciex (ZenoTOF 7600) and analyzed using negative ESI.

	Agilent 6545 Q-TOF			ZenoTOF 7600	
Abbreviation	rt (min.)	LOQs (ng/ mL)	rt (min.)	TOF-MS (LOQs)	MRMHR (LOQs) ng/mL
LA	29.79	0.48	31.8	0.025	0.025
9-HOTrE	19.04	0.24	22.27	0.5	0.05
EPA	27.33	0.24	29.12	0.5	0.025
AA	29.49	0.95	30.91	0.05	0.1
15-Δ12,14 PGJ2	10.73	0.195	15.17	0.025	0.05
12-HEPE	20.46	0.48	23.56	0.5	0.1
18-HEPE	19.36	0.24	22.52	0.5	0.1
20-HEPE	18.84	0.48	22.08	0.5	0.025
8-НЕРЕ	20.33	0.48	23.07	0.5	0.1
15-HETE	21.68	0.195	NA	NA	NA
DHA	29.07	0.24	30.53	0.5	0.1
PGJ2	13.8	3.9	15.17	0.025	0.1
8-iso-PGA1	13.79	0.39	15.16	1	50
11-HDHA	22.77	0.48	25.36	0.5	0.05
10-HDHA	22.36	0.48	25	0.5	0.5
13-HDHA	22.16	0.24	24.66	0.5	0.05
7-HDHA	22.94	0.48	25.5	0.5	1
PGE2	10.74	0.48	15.17	0.025	0.025
15(R)-PGF2α	10.31	0.195	14.79	0.025	1
19-20 DiHPA/DiHDOPE	17.94	0.098	21.32	0.025	0.5
RvD1	12.39	1.56	NA	NA	NA
LTE4	14.31	6.25	NA	NA	NA
LTD4	12.89	0.24	16.92	0.5	1
13-HOTrE	19.3	0.12	22.49	0.5	1
13-oxoODE	21.72	0.195	24.52	0.5	0.025
9-oxoODE	22.21	0.195	24.94	0.5	0.5
13 HODE	21.04	0.098	23.93	0.5	0.025
9-HODE	21.17	0.195	24.06	0.5	0.025
12,13-DiHOME	16.83	0.195	20.4	5	NA
9,10-DiHOME	17.27	0.195	20.79	5	0.025
11,12-EpETE	22.47	0.78	25.27	0.1	0.05
11-HEPE	20.14	0.48	23.17	0.5	0.05

	Agilent 6545 Q-TOF			ZenoTOF 7600	
Abbreviation	rt (min.)	LOQs (ng/ mL)	rt (min.)	TOF-MS (LOQs)	MRMHR (LOQs) ng/mL
12-oxoETE	22.89	3.125	26.13	0.1	0.05
15-HEPE	20.01	0.391	22.53	0.5	0.05
5-НЕРЕ	20.83	0.24	23.83	0.5	0.05
5-oxoETE	24.39	0.098	26.73	0.1	0.1
8,9-ЕрЕТЕ	22.64	0.78	25.27	0.5	0.5
9-НЕРЕ	20.58	0.39	NA	NA	NA
11,12-EET	24.65	0.39	27.13	0.5	0.5
11-HETE	22.18	0.195	24.87	0.025	0.025
12-HETE/8-HETE	22.43	0.39	NA	NA	NA
14,15-EET	23.93	0.195	26.34	0.5	0.5
16-HETE	20.63	0.195	NA	NA	NA
20-HETE	19.91	0.195	NA	NA	NA
5-HETE	23.17	0.39	25.15	0.5	0.025
8,9-EET	24.88	0.39	27.13	0.5	0.5
9-НЕТЕ	22.79	0.39	27.13	0.1	0.5
11-HEDE/15-HEDE	24.58	0.195	26.83	0.025	0.025
5,12-DiHETE	16.83	0.195	20.42	0.5	0.5
5,15-DiHETE	15.85	0.48	19.57	0.1	0.1
5,6-DiHETE	19.72	0.48	22.87	0.1	0.025
8,15-DiHETE	15.46	0.098	18.98	0.05	0.05
LTB4	16.28	0.098	19.94	0.025	0.025
11,12-DiHET	19.62	0.24	21.91	0.5	0.05
14,15-DiHET	17.91	0.098	21.31	0.025	0.025
14-HDoHE	22.36	0.78	25.23	0.5	0.1
16-HDoHE	21.88	0.78	24.18	0.025	0.1
17-HDoHE	21.96	0.24	24.82	0.1	0.5
20-HDoHE	21.38	0.39	NA	NA	NA
4-HDoHE	23.67	0.195	NA	NA	NA
LXA4	12.24	1.56	16.50	0.025	0.05
8-iso-15(R)-PGF2α	9.13	0.098	13.45	0.025	0.025
8-iso-PGF2α	9.31	0.195	13.89	0.025	0.025
PGD2	11.19	1.92	15.17	0.025	0.025
11β- PGF2α	9.59	0.098	14.14	0.05	0.05
PGF2α EA	7.89	0.24	12.29	0.1	0
8-iso-PGF2β	9.42	0.39	13.98	0.025	0.025
PGF2α	10.44	0.098	14.90	0.025	0.5

Agilent 6545 Q-TOF				ZenoTOF 7600	
Abbreviation	rt (min.)	LOQs (ng/ mL)	rt (min.)	TOF-MS (LOQs)	MRMHR (LOQs) ng/mL
10,17- DiHDHA/Maresin 1	16.05	0.391	19.70	0.05	0.05

^{*}NA: Not measured

Table 4.5: Comparison of retention time (rt) and masses of oxylipins analyzed on both Agilent QTOF 6545 and ZenoTOF 7600 instruments

Oxylipin or PUFA precursor	Formula	m/z ESI (-) (CID)	m/z ESI (+) (EAD)	rt Agilent 6545 Q-TOF (min.)	rt ZenoTOF 7600 TOF-MS (min.)
EPA	$C_{20}H_{30}O_2$	301.2173	347.1967	27.22	28.91
DHA	$C_{22}H_{32}O_2$	327.2330	373.2124	28.95	30.53
PGE2	$C_{20}H_{35}O_5$	351.2177	397.1971	10.69	14.79

All degradation products obtained from the ZenoTOF CID analysis for PGE2, EPA, and DHA are summarized in **Supplementary Tables C21** to **C23**. Comparing both analyses unknown with m/z of 315.1966 was detected using both instruments for DHA, whereas unknown m/z of 333.2063 and PGJ2 were detected in PGE2 forced degradation samples by both instruments. Next, the degradation pathways for these compounds were analyzed using SCIEX OS software, focusing on various Phase 1 biotransformation reactions. The common reactions observed were hydrolysis, oxidation and ketone formation. A detailed summary of the possible degradation pathways for all three compounds is provided in **Supplementary Table C24** to **C26**.

4.3.4.2 Comparison of CID and EAD MS/MS spectra for PGE2, DHA and EPA

Both CID and EAD MS/MS spectra were collected for EPA, DHA and PGE2 and are shown in **Figures 4.27 to 4.29** and **Tables 4.6** to **4.11.** The comparison of CID and EAD fragmentation for these three standards showed that limited additional information could be obtained from EAD, with more extensive fragmentation for EAD only observed below 110 Da. The full localization of double bond positions in EPA and DHA was not possible from EAD spectrum.

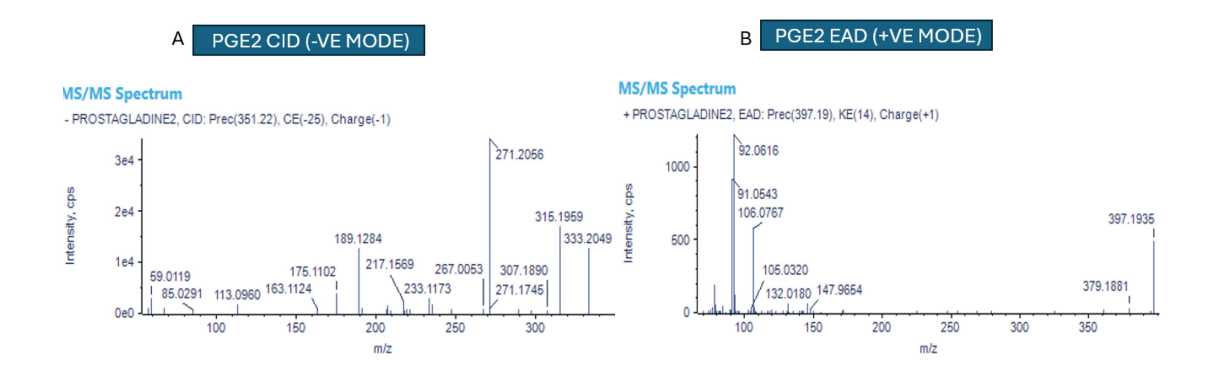


Figure 4.27: MS/MS spectra of PGE2 (a) using CID in negative ESI mode (CE=25) and (b) using EAD in positive ESI mode (KE=14).

Table 4.6: Summary of product ions observed in PGE2 CID MS/MS spectrum obtained on ZenoTOF 7600 instrument

Product ion m/z	Formula for fragment	Difference from precursor mass
351.2177	$C_{20}H_{31}O_5$	PGE2
59.0119	$C_2H_3O_2$	292.2058
85.0291	$C_4H_5O_2$	266.1886
113.0960	$C_7H_{13}O$	238.1217
163.1124	$C_{11}H_{15}O$	188.1053
175.1102	$C_{12}H_{15}O$	176.1075
189.1284	$C_{13}H_{17}O$	162.0893
217.1569	$C_{15}H_{21}O$	134.0608
233.1173	$C_{14}H_{17}O_3$	118.1004
267.0053	$C_{18}H_3O_3$	84.2124
271.2056	$C_{19}H_{27}O$	80.0121
307.1890	$C_{18}H_{27}O_4$	44.0287
315.1959	$C_{20}H_{27}O_3$	36.0218
333.2049	$C_{20}H_{29}O_4$	18.0128

Table 4.7: Summary of product ions observed in PGE2 EAD MS/MS spectrum obtained on the ZenoTOF 7600 instrument.

Product ion m/z in EAD spectrum	Fragment mass without 2Na ⁺	Formula for fragment	Difference from precursor mass in CID
92.0618	46.0824	C ₂ H ₆ O	305.1317
106.0767	60.0973	C ₃ H ₈ O	291.1168
132.018	86.0386	C ₄ H ₆ O ₂	265.1755
147.9654	101.986	$C_3H_2O_4$	249.2281
379.1881	333.2087	C ₂₀ H ₂₉ O ₄	18.0054
397.1935	351.2141	$C_{20}H_{31}O_5$	PGE2

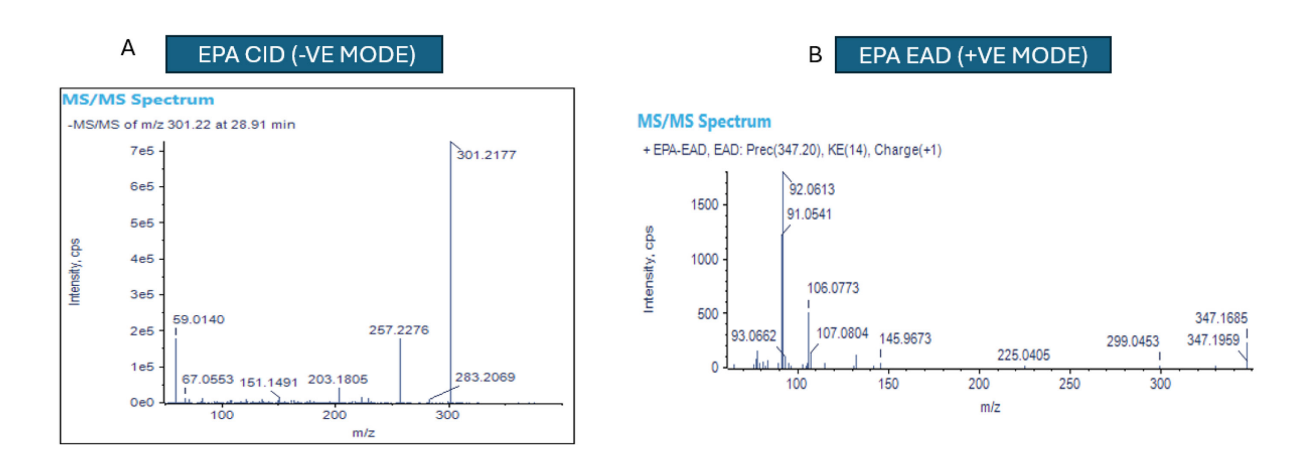


Figure 4.28: MS/MS spectra of EPA (a) using CID in negative ESI mode (CE=25) and (b) using EAD in positive ESI mode (KE=14).

Table 4.8: Summary of product ions observed in the EPA CID MS/MS spectrum obtained on the ZenoTOF 7600 instrument.

Product ion m/z	Formula for fragment	Difference from precursor mass
301.2173	$C_{20}H_{29}O_2$	EPA
59.0140	$C_2H_3O_2$	242.2033
67.0553	C ₄ H ₃ O	234.1620
151.1491	$C_{11}H_{19}$	150.0682
203.1805	$C_{15}H_{23}$	98.0368
257.2276	$C_{19}H_{29}$	43.9897
283.2069	$C_{20}H_{27}O$	18.0104

Table 4.9: Summary of product ions observed in the EPA EAD MS/MS spectrum obtained on the ZenoTOF 7600 instrument.

Product ion m/z in EAD	Fragment mass without 2Na ⁺	Formula for fragment	Differences from precursor mass in CID
92.0662	47.0868	CH ₃ O ₂	255.1297
106.0773	60.0979	C_3H_8O	241.1186
145.9673	99.9879	$C_4H_4O_3$	201.2286
225.0406	179.0612	$C_6H_{11}O_6$	122.1553
299.0453	253.0659	C ₁₉ H ₉ O	48.1506
347.1959	301.2165	$C_{20}H_{29}O_2$	EPA

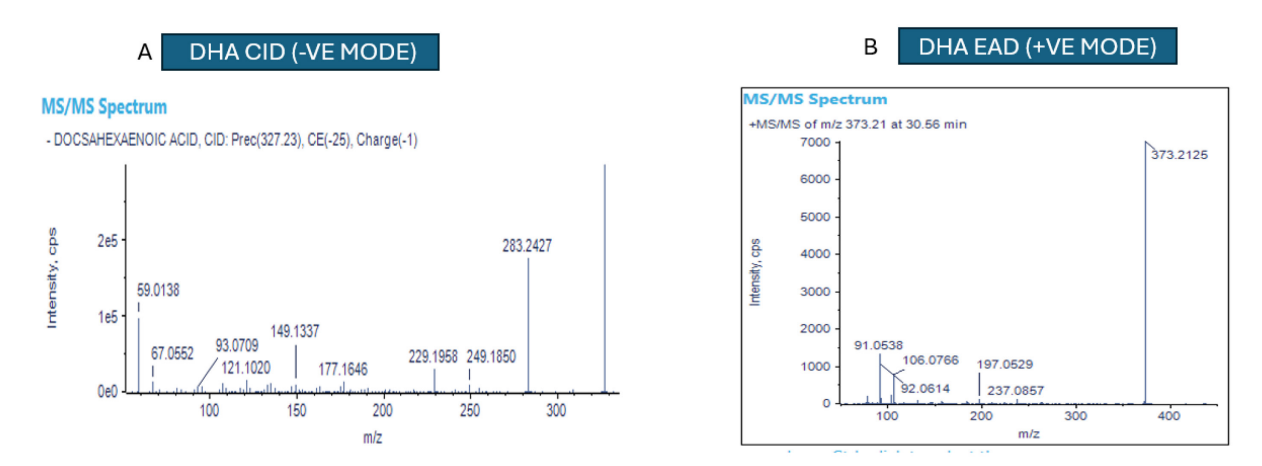


Figure 4.29: MS/MS spectra of DPA (a) using CID in negative ESI mode (CE=25) and (b) using EAD in positive ESI mode (KE=14).

Table 4.10: Summary of product ions observed in the DHA CID MS/MS spectrum obtained on the ZenoTOF 7600 instrument.

		Difference from precursor
Product ion m/z	Formula for fragment	mass
327.233	$C_{22}H_{31}O_2$	DHA
59.0138	$C_2H_3O_2$	268.2192
67.0552	C ₄ H ₃ O	260.1778
93.0709	C ₇ H ₉	234.1621
121.1020	C ₉ H ₁₃	206.1310
149.1337	$C_{11}H_{17}$	178.0993
177.1646	$C_{13}H_{21}$	150.0684
229.1958	C ₁₇ H ₂₅	98.0372
249.1850	$C_{16}H_{25}O_2$	78.0480
283.2427	C ₂₁ H ₃₁	43.9903

Table 4.11: Summary of product ions observed in the DHA EAD MS/MS spectrum obtained by ZenoTOF 7600 instrument.

Product ion m/z	Fragment mass	Formula for	Difference from
in EAD	without 2Na+	fragment	precursor mass in CID
91.0538	45.0744	C ₂ H ₅ O	282.1587
106.0766	60.0972	C ₃ H ₈ O	267.1359
192.05	146.0735	$C_{10}H_{10}O$	181.1596
237.0857	191.1063	$C_{12}H_{15}O_2$	136.1268
373.2125	327.2331	$C_{22}H_{31}O_2$	DHA

4.3.4.3 Identification of unknown oxylipins from forced degradation studies

Using the SCIEX OS software, several putative identifications of the unknowns from the forced degradation studies of PGE2 and DHA were made. For example, PGA2 was matched as a degradation product of PGE2, formed after 3 days of storage at 50°C with mass 333.2071 and RT 13.293 min. This compound was not present in our in-house oxylipin library. To confirm its identification, a commercial standard of PGA2 from Cayman Chemicals was purchased and analyzed. The rt of these two compounds were closely matched (**Figure 4.30**), and their MS/MS spectra were compared to confirm the identification (**Figure 4.31**). Despite close rt of unknown and authentic standard and very similar MS/MS spectra, two major fragment ions present in PGA2 standard (271.2068 and 189.1279) were absent in the MS/MS spectrum of our unknown. Thus, the identity of unknown could not be confirmed as PGA2.

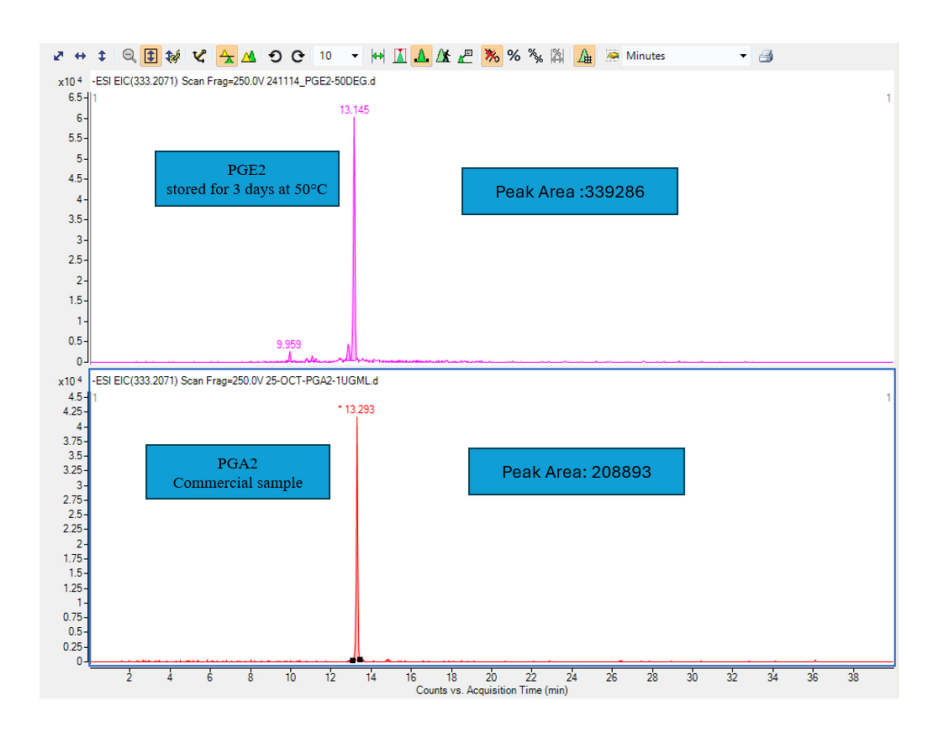


Figure 4.30: Chromatogram of unknown degradation product observed in PGE2 forced degradation sample (50°C) and PGA2 standard analyzed on Agilent 6545 QTOF instrument using CID in negative ESI mode.

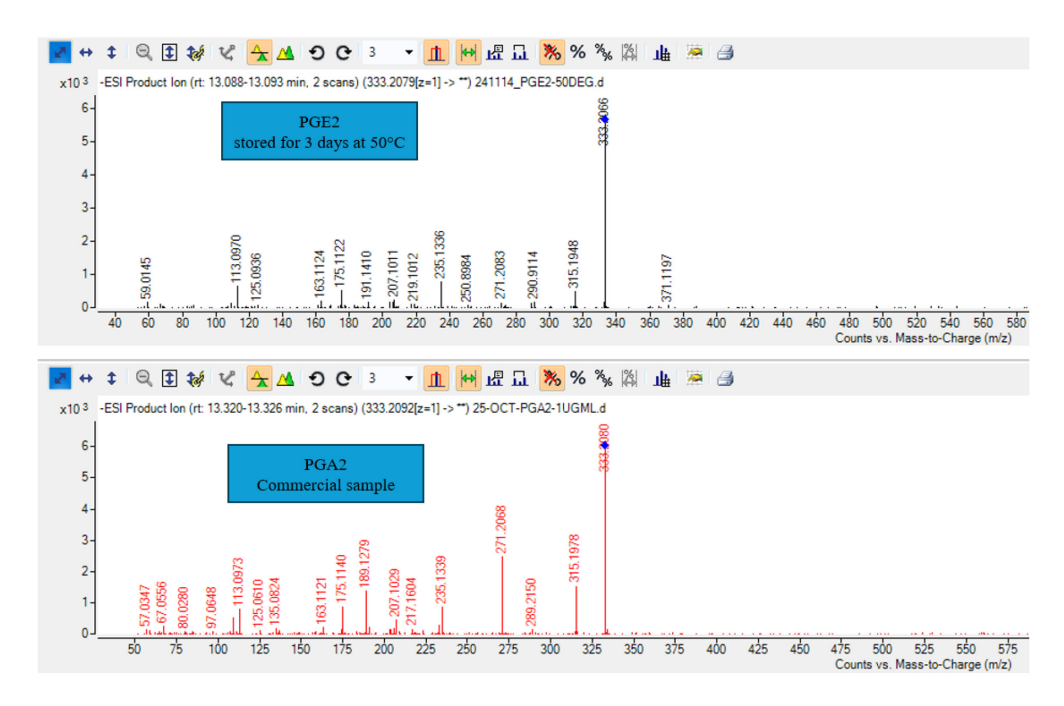


Figure 4.31: CID MS/MS spectra obtained for unknown degradation product observed in PGE2 forced degradation sample (50°C) and PGA2 standard analyzed on Agilent 6545 QTOF instrument using CID in negative ESI mode.

4.3.4.4 Identification of unknown oxylipins in murine plasma samples

In addition to the selected forced degradation samples, selected murine plasma samples [255] were also analyzed using CID and EAD on ZenoTOF to characterize several unknowns of interest (Supplementary Table C27). Unfortunately, none of these unknowns were identified using the SCIEX software. The list of 21 unknown compounds was then compared to the results from the forced degradation study to identify any common compounds (Supplementary Table C27). The EAD MS/MS spectra for several unknowns were collected in murine plasma samples (Supplementary Table C28, Figures C2 to C8). As shown in Figure 4.32-4.33, multiple unknowns eluting with rt ranging from 16.86 to 22.36 min showed extremely similar spectra, with only fragments at 78.0457, 91.0536, 92.0610, and 106.0770 detectable. Although these fragments showed some differences in intensities across different isomers, they did not provide sufficient information for de novo structural identification. Similarly, the analysis of unknowns with m/z 359.220 provided the same fragmentation pattern, and EAD could not be used for their identification (Figure 4.33). We also attempted to match the rt and masses of the identified MS/MS spectra collected in EAD mode to our in-house library of oxylipins to see if any spectra could be matched to those in the library.

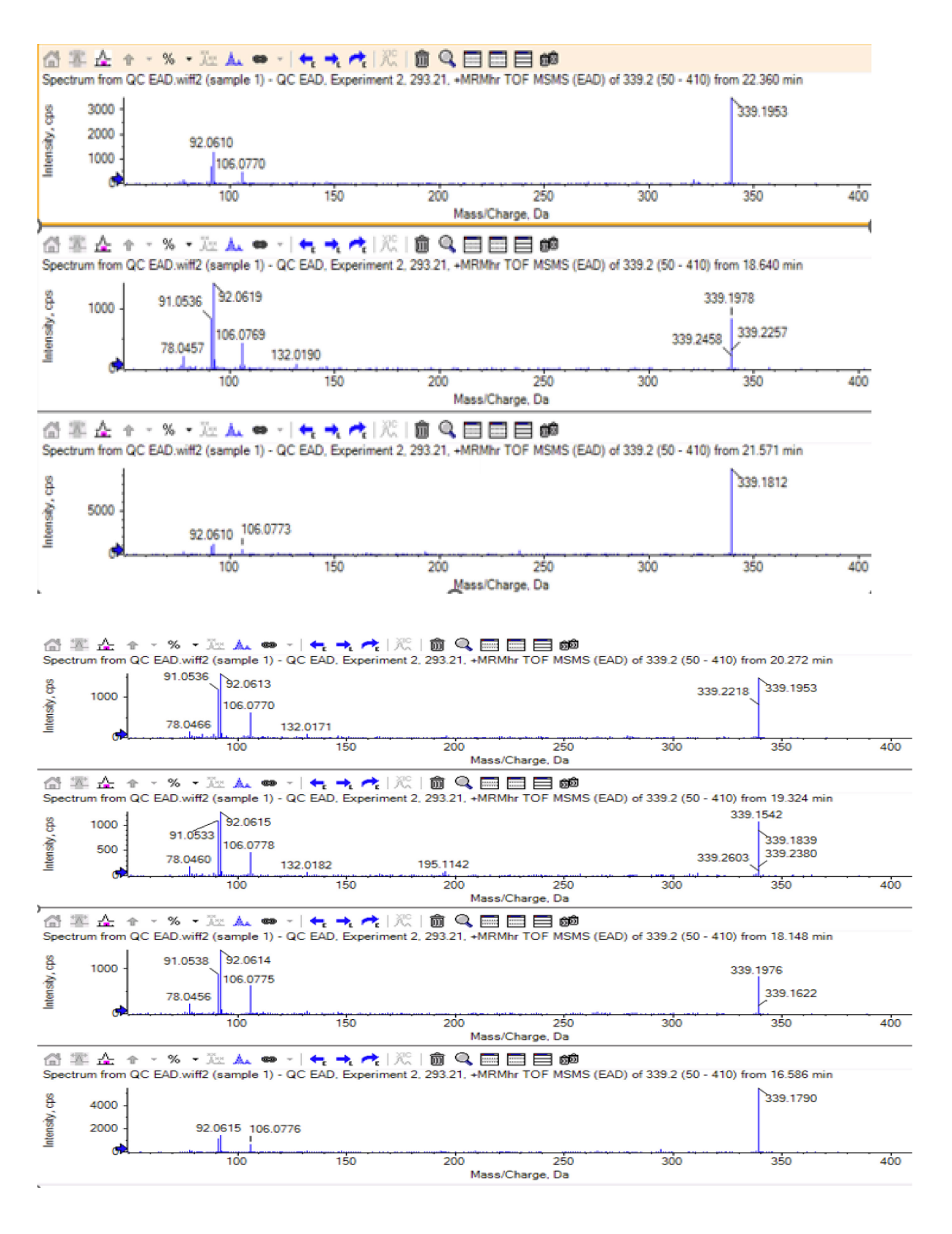


Figure 4.32: EAD MS/MS spectra results for unknowns with m/z 339.1940 in pooled sample of murine plasma analyzed on ZenoTOF 7600 instrument in positive ESI mode.

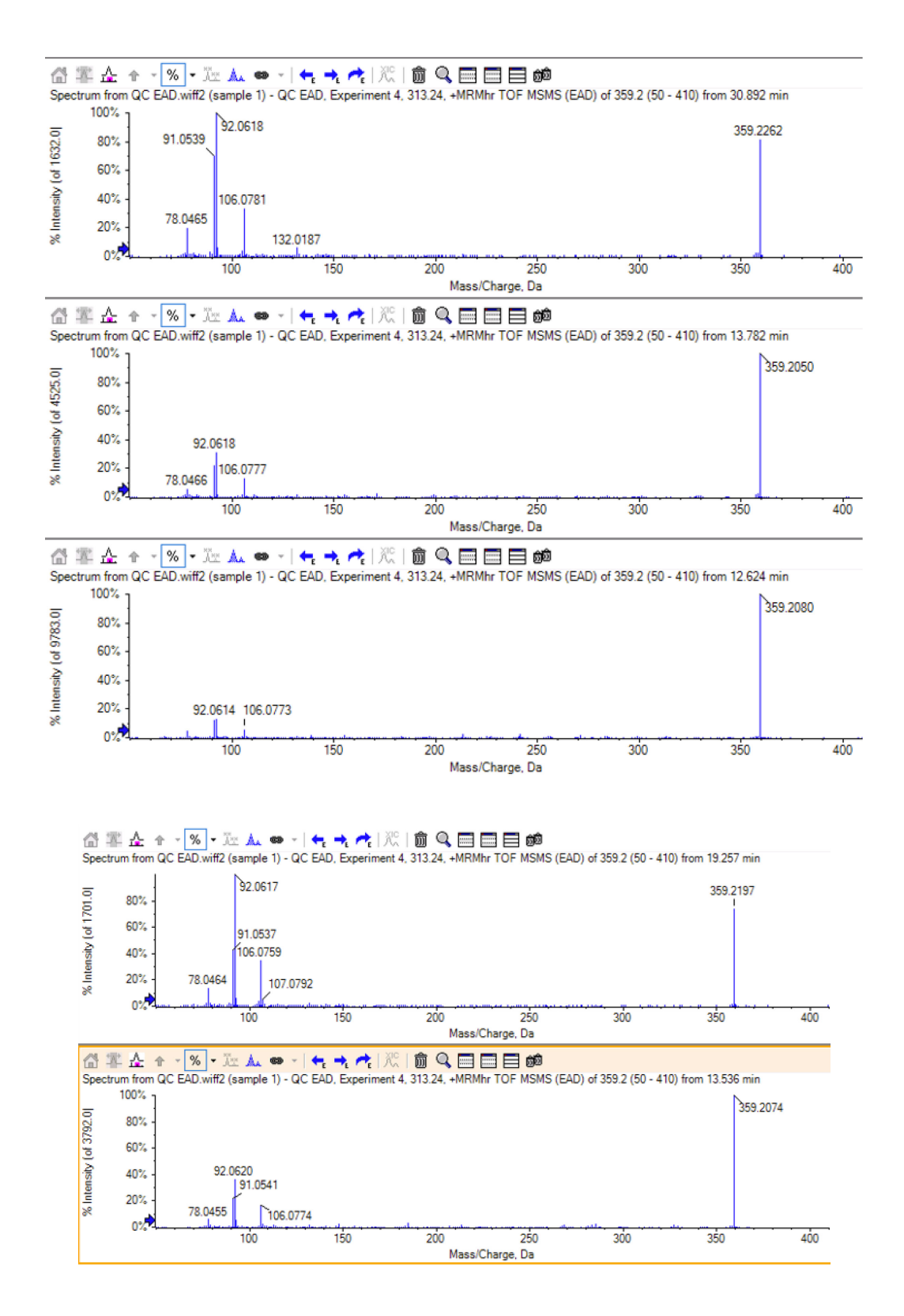


Figure 4.33: EAD MS/MS spectra results for unknowns with m/z 359.220 in pooled sample of murine plasma analyzed on ZenoTOF 7600 instrument in positive ESI mode.

4.4. Conclusions

The stability of polyunsaturated fatty acids and their derivatives, oxylipins, presents a significant challenge for their accurate measurement. In addition, limited information currently exists on nonenzymatic degradation products of oxylipins. In this study, the degradation pathways and products of selected oxylipins (15-HETE, PGE2, 5-oxoETE, 9-HoTrE, 9-oxoDE, 4-HDoHE, 13-HDHA, 13-oxoODE, 11,12-EpETrE, 16-HDoHE, 9-HETE, LTB4, 12-HETE and 11-HDHA) and their precursors (AA, LA, EPA and DHA) were mapped after the exposure to elevated temperatures or UV light. The observed degradation products included oxidation, reduction, hydrolysis, isomerization, and dehydration. Among the oxylipins tested, the degradation with 365 nm UV was particularly notable for 9-oxoODE and 13-oxoODE, with degradation isomers identified for both compounds and degradation of 80% and above for both compounds. In addition, the dehydration of PGE2 to PGJ2 and unknown m/z and rt (333.2071, 13.24 min.) using elevated temperature (50°C for 3 days) and 11β-PGF2α to PGE2 after 7 days of exposure to UV light were successfully mapped. A comparison was made between oxylipins identified in the forced degradation study of precursors (Chapter 4, Supplementary C2 to C5) and those identified as degradation products during 3-FT cycles (Chapter 2, Supplementary A4) to determine any overlap. However, no matching oxylipins were found. The results of these forced degradation studies of oxylipins and precursors successfully explained many of the elevated oxylipins found in this thesis (Chapters 2 and 3) and literature studies, especially for hydroxyl-derived oxylipins. Unfortunately, EAD fragmentation provided very similar fragmentation patterns across many unknown oxylipin isomers, so it could not be successfully used in this study for the more detailed elucidation of unknown structures (e.g. assignment of double-bond position or hydroxyl position).

Several of the observed degradation products of precursors and oxylipins can also affect the quantification of other oxylipins, including stable oxylipins in our library. This research highlights the importance of identifying oxylipin degradation products, monitoring degradation pathways, and understanding non-enzymatic reactions that could affect the accurate and precise quantification of oxylipins in future studies.

5.0 Conclusions and future work

5.1 Conclusions

The stability of polyunsaturated fatty acids and their derivatives, known as oxylipins, presents a significant challenge for their accurate measurement. These metabolites are important due to their notable role in the immune system and inflammation and their potential as biomarkers for various health conditions. This thesis addresses the challenge of oxylipin stability, particularly given their poor stability during sampling, transportation, and storage. **Chapter 2** of this thesis demonstrated that SPME can effectively protect extracted oxylipins, minimizing degradation during sample collection, storage (3-cycles freeze-thaw), and transportation (up to 18 days at room temperature). For this evaluation, the tested oxylipins included both stable and unstable oxylipins, including those prone to degradation, which have been reported in the literature.

With the knowledge that the FT processes contribute to the significant degradation of these compounds and the recommendation to avoid repeated FT cycles [184], [190], this study showed that many oxylipins were not impacted by even 3-FT cycles when stored on SPME devices without the aid of antioxidants. During the 3-FT cycles, the only unstable oxylipins were AA and PGE2 in standard samples, and 13-HDHA, 11-HDHA, 9-oxoODE, and 9-HOTrE in plasma samples. These results showed the effect of FT cycles with regards to the stability of oxylipins and suggest that it is important to limit the number of the FT cycles to a single cycle during analysis to ensure stability when stored on SPME devices. The stability results at RT are particularly important because most clinical and research biological samples are collected from participants at room temperature. Thus, it is essential to minimize degradation before storage. We observed that most of the tested oxylipins remained stable during 18 days of RT storage on SPME devices without loading of antioxidants

in spiked plasma samples. However, certain oxylipins, 11,12-EpETE, 13-oxoODE, 4-HDoHE, and 5-oxoETE, showed increased levels. Our results highlight the potential of SPME devices to simplify sample collection, shipping, and short-term storage by eliminating the need for ultra-cold temperatures. Next, Chapter 3 successfully demonstrated the feasibility of loading and quantitatively measuring oxylipins and antioxidants on SPME devices using both pre- and postloading extraction of BHT. The advantage of pre-extraction over post-extraction loading is that this approach allows sufficient antioxidants to be loaded onto the SPME devices before sampling, preventing degradation through all steps of the procedure. This makes it suitable for in vivo research study. However, the amount of BHT loaded should be carefully considered to ensure it remains at an acceptable level for ingestion by the species of interest in in vivo analysis. On the other hand, the post-extraction approach offers an alternative option but can only protect PUFAs and oxylipins during storage and transportation. The results for the FT stability study show that both pre- and post-loading extraction with BHT can be used with SPME but that addition of BHT adversely impacts the stability of some oxylipins on the devices. In spiked citrate plasma, several oxylipins, 16-HDoHE, 13-HDHA, 11-HDHA, and 12-HETE were identified as unstable, failing the stability criteria regardless of whether BHT was loaded pre- or post- extraction. Other unstable oxylipins were identified for each approach: 8-iso-15RPGF2α, PGF2α, 14,15-DiHET, 5-HETE, 13-HODE, AA, and LA were unstable when BHT was pre-loaded, whereas LTB4, 9-HETE, and DHA were unstable when post-loading of BHT was used. When comparing the results for standard and spiked citrate plasma, oxylipin stability when stored on SPME devices was better with postloading extraction of BHT. Overall, these results do not show clear benefits of BHT loading, especially when broad oxylipin profiling is of interest. Reflecting on the stability study results from Chapter 2 (without BHT loading) and Chapter 3 (with pre- and post-extraction loading of BHT), the stability of oxylipins such as AA and PGE2 was improved in the standard samples, while the stability of 11-PGF2α was affected by pre-extraction loading of BHT. In the spiked plasma results, 11-HDHA and 13-HDHA were unstable using both approaches, along with 16-HDoHE and 12-HETE, while the stability of other oxylipins depended on the loading approach. Thus, the overall suggestion is to avoid loading BHT onto the SPME devices for the analysis of complex biological samples such as blood or plasma. However, if targeted assays are being developed for specific oxylipins which were stabilized by BHT, then the appropriate BHT loading approach can be incorporated. Generally, when using SPME, precursors such as AA, EPA, LA, and DHA showed better stability in spiked plasma samples without the addition of antioxidants, both in the 3-FT cycles and RT stability studies. However, poor stability was observed for AA, LA, and DHA during the 3-FT cycles when BHT was loaded onto the SPME device. For oxylipins produced by non-enzymatic reactions, we identified 13-HDHA, 11-HDHA, 12-HETE, 5-HETE, 13-HODE, 9-HETE, and 5-oxoETE as unstable, regardless of with antioxidants were loaded. Better stability was observed for 5-HETE and 13-HODE in plasma samples without antioxidants. This suggests that when using SPME devices for sampling, transportation, and storage, it is important to select the appropriate approach. In summary, our results showed that for both enzymatically and non-enzymatically produced oxylipins, stability is generally better without BHT as some classes showed poor stability when BHT was loaded on the SPME devices.

Finally, **Chapter 4** of this thesis maps the degradation products of the identified unstable oxylipins. This helps explain the results observed in **Chapters 2** and **3**, ultimately enhancing the reliability of the study's conclusions. These forced degradation studies used heating, oxidation by CuSO₄ and UV exposure to intentionally degrade oxylipins. Suitable degradation conditions to map the degradation products, such as prolonged elevated temperatures and long-term storage

under UV conditions were successfully identified. For precursors, mapping degradation products is crucial because even minimal degradation can lead to one, or more, degradation products, as demonstrated in our forced degradation study. While enzymatic pathways for these precursors are commonly reported in the literature, this study examined non-enzymatic pathways and identified degradation products resulting from reactions such as oxidation, reduction, hydrolysis, and isomerization. The resulting degradation products included several in-house oxylipins based on their rt and m/z in our library. In addition, numerous unknowns were detected during the study. These findings suggest that the quantification of several oxylipins can suffer from interferences and inaccuracy due to degradation. One of the successes of this thesis was the mapped hydrolysis of PGE2 to PGJ2 using elevated temperature (50° for 3 days). EPA, DHA and PGE2 samples which showed significant degradation using elevated temperatures (50° for 3 days) were subjected to EAD fragmentation on a SCIEX ZenoTOF 7600 Trap to evaluate the utility of EAD in structural determination of unknown oxylipin degradation products. Unfortunately, the resulting spectra showed very similar fragmentation spectra, and did not provide much structural information. This shows further development of EAD and/or other fragmentation strategies may be beneficial for oxylipin structural characterization.

In summary, the results of this thesis demonstrate the potential of SPME devices, with or without BHT loading, as a promising tool for the collection, transportation, and storage of oxylipins. Additionally, potential degradation products that could interfere with their accurate quantification have been identified in this study.

5.2 Future work

Despite the promising results presented in this thesis, there are several key areas for future work related to this thesis. First, while SPME has shown immense potential for *in vitro* studies, there is a need to perform further stability studies for SPME concerning long-term storage over months and possibly years. Secondly, the stability of oxylipins using other antioxidants, beyond BHT, tested in this study, has not been explored in combination with SPME. For instance, vitamin C is a water-soluble antioxidant and can be a good choice for pre-loading antioxidants for in vivo studies. There is a need to increase the spiked concentration for both FT and 18-day RT studies to ensure a larger panel of oxylipins can be evaluated for stability when stored on SPME devices. Another important future direction is to perform stability studies in whole blood samples, which is a more relevant matrix for blood microsampling studies. Our results also provided valuable insights into how SPME is a promising device/tool for sampling, storage and transportation of oxylipins at RT. This opens up a new and important direction in the development of SPME-based home-sampling tools, which could maintain oxylipin stability even at RT, as demonstrated in our 18-day stability study. However, the design of these sampling devices should be tailored to the specific class of oxylipins, with potential versions that include or exclude antioxidants. Such devices could support biomedical and clinical research for diseases where oxylipins have been identified as potential biomarkers. Comparing SPME with the current sample collection used for oxylipins, SPME has proven to be a sample collection approach suitable for improving stability from both enzymatic and non-enzymatic degradation. Thus, more applications of in vivo SPME to study oxylipins in both biofluids and tissue may be developed in future.

Finally, forced degradation studies performed in this thesis successfully mapped some degradation pathways of various oxylipins. However, as illustrated in **Chapter 4**, the critical challenge is the identification of the large panel of unknowns and the lack of commercial standards for many possible oxidation products of oxylipins. The issue of unknown identification is a major challenge with all untargeted studies, but is especially problematic for oxylipins, considering the large number of possible sites of modification and a large number of isomers which may have very similar fragmentation spectra. Our results identified different major and minor unknown degradation products with various rt and m/z. If sufficient quantities of unknowns of interest can be generated, the use of NMR could be applied for further characterization of the unknowns. Future confident identification of prioritized 18 unknowns from the stability studies requires the chemical synthesis of standards to help match the rt, m/z and MS/MS results for appropriate identification. Further expansion of spectral libraries and molecular networking approaches, such as GNPS, can help prioritize unknown oxylipin structures which merit more confident identification [254].

References

- [1] M. Gabbs, S. Leng, J. G. Devassy, M. Monirujjaman, and H. M. Aukema, "Advances in Our Understanding of Oxylipins Derived from Dietary PUFAs," *Adv. Nutr. Bethesda Md*, vol. 6, no. 5, pp. 513–540, Sep. 2015, doi: 10.3945/an.114.007732.
- [2] W. L. Smith, "The eicosanoids and their biochemical mechanisms of action," *Biochem. J.*, vol. 259, no. 2, pp. 315–324, Apr. 1989, doi: 10.1042/bj2590315.
- [3] S. M. Camunas-Alberca, M. Moran-Garrido, J. Sáiz, A. Villaseñor, A. Y. Taha, and C. Barbas, "The role of oxylipins and their validation as biomarkers in the clinical context," *TrAC Trends Anal. Chem.*, p. 117065, Apr. 2023, doi: 10.1016/j.trac.2023.117065.
- [4] J. Revol-Cavalier, A. Quaranta, J. W. Newman, A. R. Brash, M. Hamberg, and C. E. Wheelock, "The Octadecanoids: Synthesis and Bioactivity of 18-Carbon Oxygenated Fatty Acids in Mammals, Bacteria, and Fungi," *Chem. Rev.*, vol. 125, no. 1, pp. 1–90, Jan. 2025, doi: 10.1021/acs.chemrev.3c00520.
- [5] Y. Saito, H. Yamamoto, Y. Imai, and E. Niki, "Hydroxyoctadecadienoic acid and oxidatively modified peroxiredoxins in the blood of Alzheimer's disease patients and their potential as biomarkers," *Neurobiol. Aging*, vol. 30, no. 2, pp. 174–185, Feb. 2009, doi: 10.1016/j.neurobiolaging.2007.06.012.
- [6] C. A. Rouzer and L. J. Marnett, "Cyclooxygenases: structural and functional insights," *J. Lipid Res.*, vol. 50 Suppl, no. Suppl, pp. S29-34, Apr. 2009, doi: 10.1194/jlr.R800042-JLR200.
- [7] C. M. Jenkins, A. Cedars, and R. W. Gross, "Eicosanoid signalling pathways in the heart," *Cardiovasc. Res.*, vol. 82, no. 2, pp. 240–249, May 2009, doi: 10.1093/cvr/cvn346.
- [8] H. Tian, Y. Lu, S. P. Shah, and S. Hong, "Novel 14S,21-dihydroxy-docosahexaenoic acid rescues wound healing and associated angiogenesis impaired by acute ethanol intoxication/exposure," *J. Cell. Biochem.*, vol. 111, no. 2, pp. 266–273, Oct. 2010, doi: 10.1002/jcb.22709.
- [9] J. R. Vane and R. M. Botting, "The mechanism of action of aspirin," *Thromb. Res.*, vol. 110, no. 5–6, pp. 255–258, Jun. 2003, doi: 10.1016/s0049-3848(03)00379-7.
- [10] F. Seuter, "Inhibition of Platelet Aggregation by Acetylsalicylic Acid and other Inhibitors," *Pathophysiol. Haemost. Thromb.*, vol. 5, no. 2, pp. 85–95, Apr. 2009, doi: 10.1159/000214122.
- [11] S. Hong, K. Gronert, P. R. Devchand, R.-L. Moussignac, and C. N. Serhan, "Novel Docosatrienes and 17S-Resolvins Generated from Docosahexaenoic Acid in Murine Brain, Human Blood, and Glial Cells: AUTACOIDS IN ANTI-INFLAMMATION *," *J. Biol. Chem.*, vol. 278, no. 17, pp. 14677–14687, Apr. 2003, doi: 10.1074/jbc.M300218200.
- [12] S. Krishnamoorthy *et al.*, "Resolvin D1 binds human phagocytes with evidence for proresolving receptors," *Proc. Natl. Acad. Sci. U. S. A.*, vol. 107, no. 4, pp. 1660–1665, Jan. 2010, doi: 10.1073/pnas.0907342107.
- [13] P. Chen *et al.*, "Full characterization of PDX, a neuroprotectin/protectin D1 isomer, which inhibits blood platelet aggregation," *FEBS Lett.*, vol. 583, no. 21, pp. 3478–3484, Nov. 2009, doi: 10.1016/j.febslet.2009.10.004.
- [14] P. Chen, E. Véricel, M. Lagarde, and M. Guichardant, "Poxytrins, a class of oxygenated products from polyunsaturated fatty acids, potently inhibit blood platelet aggregation," *FASEB J. Off. Publ. Fed. Am. Soc. Exp. Biol.*, vol. 25, no. 1, pp. 382–388, Jan. 2011, doi: 10.1096/fj.10-161836.

- [15] I. Liakh, A. Pakiet, T. Sledzinski, and A. Mika, "Modern Methods of Sample Preparation for the Analysis of Oxylipins in Biological Samples," *Molecules*, vol. 24, no. 8, Apr. 2019, doi: 10.3390/molecules24081639.
- [16] R. N. Schuck *et al.*, "Cytochrome P450-derived eicosanoids and vascular dysfunction in coronary artery disease patients," *Atherosclerosis*, vol. 227, no. 2, pp. 442–448, Apr. 2013, doi: 10.1016/j.atherosclerosis.2013.01.034.
- [17] J. Morgenstern *et al.*, "Sensitive mass spectrometric assay for determination of 15-deoxy-Δ12,14-prostaglandin J2 and its application in human plasma samples of patients with diabetes," *Anal. Bioanal. Chem.*, vol. 410, no. 2, pp. 521–528, Jan. 2018, doi: 10.1007/s00216-017-0748-1.
- [18] D. Biagini *et al.*, "MS-based targeted profiling of oxylipins in COVID-19: A new insight into inflammation regulation," *Free Radic. Biol. Med.*, vol. 180, pp. 236–243, Feb. 2022, doi: 10.1016/j.freeradbiomed.2022.01.021.
- [19] C. Dalle *et al.*, "The Plasma Oxylipin Signature Provides a Deep Phenotyping of Metabolic Syndrome Complementary to the Clinical Criteria," *Int. J. Mol. Sci.*, vol. 23, no. 19, Art. no. 19, Jan. 2022, doi: 10.3390/ijms231911688.
- [20] E. Pourmand, F. Zhang, M. Sarparast, J. K. Alan, and K. S. S. Lee, "Quantitative Profiling Method for Oxylipins in Neurodegenerative Diseases by Liquid Chromatography Coupled with Tandem Mass Spectrometry," *bioRxiv*, p. 2023.10.02.560544, Oct. 2023, doi: 10.1101/2023.10.02.560544.
- [21] J. R. Jensen, M. H. Pitcher, Z. X. Yuan, C. E. Ramsden, and A. F. Domenichiello, "Concentrations of oxidized linoleic acid derived lipid mediators in the amygdala and periaqueductal grey are reduced in a mouse model of chronic inflammatory pain," *Prostaglandins Leukot. Essent. Fatty Acids*, vol. 135, pp. 128–136, Aug. 2018, doi: 10.1016/j.plefa.2018.07.015.
- [22] D. Wang and R. N. DuBois, "Prostaglandins and Cancer," *Gut*, vol. 55, no. 1, pp. 115–122, Jan. 2006, doi: 10.1136/gut.2004.047100.
- [23] S. A. Brose, B. T. Thuen, and M. Y. Golovko, "LC/MS/MS method for analysis of E2 series prostaglandins and isoprostanes," *J. Lipid Res.*, vol. 52, no. 4, pp. 850–859, Apr. 2011, doi: 10.1194/jlr.D013441.
- [24] A. Katoh, H. Ikeda, T. Murohara, N. Haramaki, H. Ito, and T. Imaizumi, "Platelet-derived 12-hydroxyeicosatetraenoic acid plays an important role in mediating canine coronary thrombosis by regulating platelet glycoprotein IIb/IIIa activation," *Circulation*, vol. 98, no. 25, pp. 2891–2898, Dec. 1998, doi: 10.1161/01.cir.98.25.2891.
- [25] S. Bergström *et al.*, "The Isolation of Prostaglandin.," *Acta Chem. Scand.*, vol. 11, pp. 1086–1086, 1957, doi: 10.3891/acta.chem.scand.11-1086.
- [26] S. Wu, C. R. Moomaw, K. B. Tomer, J. R. Falck, and D. C. Zeldin, "Molecular cloning and expression of CYP2J2, a human cytochrome P450 arachidonic acid epoxygenase highly expressed in heart," *J. Biol. Chem.*, vol. 271, no. 7, pp. 3460–3468, Feb. 1996, doi: 10.1074/jbc.271.7.3460.
- [27] C. Arnold *et al.*, "Arachidonic acid-metabolizing cytochrome P450 enzymes are targets of {omega}-3 fatty acids," *J. Biol. Chem.*, vol. 285, no. 43, pp. 32720–32733, Oct. 2010, doi: 10.1074/jbc.M110.118406.
- [28] E. Hill, F. Fitzpatrick, and R. C. Murphy, "Biological activity and metabolism of 20-hydroxyeicosatetraenoic acid in the human platelet.," *Br. J. Pharmacol.*, vol. 106, no. 2, pp. 267–274, Jun. 1992.

- [29] M. L. Schwartzman, J. R. Falck, P. Yadagiri, and B. Escalante, "Metabolism of 20-hydroxyeicosatetraenoic acid by cyclooxygenase. Formation and identification of novel endothelium-dependent vasoconstrictor metabolites," *J. Biol. Chem.*, vol. 264, no. 20, pp. 11658–11662, Jul. 1989.
- [30] J. H. Capdevila, J. R. Falck, and R. C. Harris, "Cytochrome P450 and arachidonic acid bioactivation. Molecular and functional properties of the arachidonate monooxygenase," *J. Lipid Res.*, vol. 41, no. 2, pp. 163–181, Feb. 2000.
- [31] B. Eklund and L. A. Carlson, "Central and peripheral circulatory effects and metabolic effects of different prostaglandins given I.V. to man," *Prostaglandins*, vol. 20, no. 2, pp. 333–347, Aug. 1980, doi: 10.1016/S0090-6980(80)80051-7.
- [32] J. Yeung, M. Hawley, and M. Holinstat, "The expansive role of oxylipins on platelet biology," *J. Mol. Med. Berl. Ger.*, vol. 95, no. 6, pp. 575–588, Jun. 2017, doi: 10.1007/s00109-017-1542-4.
- [33] P. Yang, Y. Jiang, and S. M. Fischer, "Prostaglandin E3 metabolism and cancer," *Cancer Lett.*, vol. 348, no. 0, pp. 1–11, Jun. 2014, doi: 10.1016/j.canlet.2014.03.010.
- [34] D. Iyú, J. R. Glenn, A. E. White, A. Johnson, S. Heptinstall, and S. C. Fox, "The role of prostanoid receptors in mediating the effects of PGE3 on human platelet function," *Thromb. Haemost.*, vol. 107, no. 4, pp. 797–799, Apr. 2012, doi: 10.1160/TH11-11-0794.
- [35] F. Rauzi *et al.*, "Aspirin inhibits the production of proangiogenic 15(S)-HETE by platelet cyclooxygenase-1," *FASEB J. Off. Publ. Fed. Am. Soc. Exp. Biol.*, vol. 30, no. 12, pp. 4256–4266, Dec. 2016, doi: 10.1096/fj.201600530R.
- [36] L. Sun, Y.-W. Xu, J. Han, H. Liang, N. Wang, and Y. Cheng, "12/15-Lipoxygenase metabolites of arachidonic acid activate PPARγ: a possible neuroprotective effect in ischemic brain," *J. Lipid Res.*, vol. 56, no. 3, p. 502, Mar. 2015, doi: 10.1194/jlr.M053058.
- [37] M. W. Buczynski, D. S. Dumlao, and E. A. Dennis, "Thematic Review Series: Proteomics. An integrated omics analysis of eicosanoid biology," *J. Lipid Res.*, vol. 50, no. 6, pp. 1015–1038, Jun. 2009, doi: 10.1194/jlr.R900004-JLR200.
- [38] B. Samuelsson, S. E. Dahlén, J. A. Lindgren, C. A. Rouzer, and C. N. Serhan, "Leukotrienes and lipoxins: structures, biosynthesis, and biological effects," *Science*, vol. 237, no. 4819, pp. 1171–1176, Sep. 1987, doi: 10.1126/science.2820055.
- [39] H. E. Cummings *et al.*, "Leukotriene C4 Activates Mouse Platelets in Plasma Exclusively Through the Type 2 Cysteinyl Leukotriene Receptor," *J. Immunol. Baltim. Md* 1950, vol. 191, no. 12, p. 10.4049/jimmunol.1302187, Dec. 2013, doi: 10.4049/jimmunol.1302187.
- [40] J. Yeung *et al.*, "12-lipoxygenase activity plays an important role in PAR4 and GPVI-mediated platelet reactivity," *Thromb. Haemost.*, vol. 110, no. 3, pp. 569–581, Sep. 2013, doi: 10.1160/TH13-01-0014.
- [41] J. Yeung *et al.*, "12(S)-HETrE, a 12-Lipoxygenase Oxylipin of Dihomo-γ-Linolenic Acid, Inhibits Thrombosis via Gαs Signaling in Platelets," *Arterioscler. Thromb. Vasc. Biol.*, vol. 36, no. 10, pp. 2068–2077, Oct. 2016, doi: 10.1161/ATVBAHA.116.308050.
- [42] S. Akiba, T. Murata, K. Kitatani, and T. Sato, "Involvement of lipoxygenase pathway in docosapentaenoic acid-induced inhibition of platelet aggregation," *Biol. Pharm. Bull.*, vol. 23, no. 11, pp. 1293–1297, Nov. 2000, doi: 10.1248/bpb.23.1293.
- [43] S. Fischer, C. v. Schacky, W. Siess, Th. Strasser, and P. C. Weber, "Uptake, release and metabolism of docosahexaenoic acid (DHA, C22:6ω3) in human platelets and neutrophils," *Biochem. Biophys. Res. Commun.*, vol. 120, no. 3, pp. 907–918, May 1984, doi: 10.1016/S0006-291X(84)80193-X.

- [44] J. Folch, M. Lees, and G. H. Sloane Stanley, "A simple method for the isolation and purification of total lipides from animal tissues," *J. Biol. Chem.*, vol. 226, no. 1, pp. 497–509, May 1957.
- [45] L. M. Hall and R. C. Murphy, "Electrospray mass spectrometric analysis of 5-hydroperoxy and 5-hydroxyeicosatetraenoic acids generated by lipid peroxidation of red blood cell ghost phospholipids," *J. Am. Soc. Mass Spectrom.*, vol. 9, no. 5, pp. 527–532, May 1998, doi: 10.1016/S1044-0305(98)00013-0.
- [46] O. Ai, K. E, R. Km, K. L, M. M, and S. Nh, "Targeting esterified oxylipins by LC-MS Effect of sample preparation on oxylipin pattern," *Prostaglandins Other Lipid Mediat.*, vol. 146, Feb. 2020, doi: 10.1016/j.prostaglandins.2019.106384.
- [47] E. Vericel and M. Lagarde, "15-Hydroperoxyeicosatetraenoic acid inhibits human platelet aggregation," *Lipids*, vol. 15, no. 6, pp. 472–474, Jun. 1980, doi: 10.1007/BF02534075.
- [48] P. Y. Wong, P. Westlund, M. Hamberg, E. Granström, P. H. Chao, and B. Samuelsson, "15-Lipoxygenase in human platelets," *J. Biol. Chem.*, vol. 260, no. 16, pp. 9162–9165, Aug. 1985.
- [49] A. I. Ostermann, I. Willenberg, and N. H. Schebb, "Comparison of sample preparation methods for the quantitative analysis of eicosanoids and other oxylipins in plasma by means of LC-MS/MS," *Anal. Bioanal. Chem.*, vol. 407, no. 5, pp. 1403–1414, Feb. 2015, doi: 10.1007/s00216-014-8377-4.
- [50] Y. Yang, C. Cruickshank, M. Armstrong, S. Mahaffey, R. Reisdorph, and N. Reisdorph, "New sample preparation approach for mass spectrometry-based profiling of plasma results in improved coverage of metabolome," *J. Chromatogr. A*, vol. 1300, pp. 217–226, Jul. 2013, doi: 10.1016/j.chroma.2013.04.030.
- [51] W. S. Powell, "Extraction of eicosanoids from biological fluids, cells, and tissues," *Methods Mol. Biol. Clifton NJ*, vol. 120, pp. 11–24, 1999, doi: 10.1385/1-59259-263-5:11.
- [52] O. Reinaud, M. Delaforge, J. L. Boucher, F. Rocchiccioli, and D. Mansuy, "Oxidative metabolism of linoleic acid by human leukocytes," *Biochem. Biophys. Res. Commun.*, vol. 161, no. 2, pp. 883–891, Jun. 1989, doi: 10.1016/0006-291x(89)92682-x.
- [53] K. Strassburg *et al.*, "Quantitative profiling of oxylipins through comprehensive LC-MS/MS analysis: application in cardiac surgery," *Anal. Bioanal. Chem.*, vol. 404, no. 5, pp. 1413–1426, 2012, doi: 10.1007/s00216-012-6226-x.
- [54] M. Masoodi, A. A. Mir, N. A. Petasis, C. N. Serhan, and A. Nicolaou, "Simultaneous lipidomic analysis of three families of bioactive lipid mediators leukotrienes, resolvins, protectins and related hydroxy-fatty acids by liquid chromatography/electrospray tandem mass spectrometry," *Rapid Commun. Mass Spectrom. RCM*, vol. 22, no. 2, pp. 75–83, 2008, doi: 10.1002/rcm.3331.
- [55] D. R. Nelson, D. C. Zeldin, S. M. G. Hoffman, L. J. Maltais, H. M. Wain, and D. W. Nebert, "Comparison of cytochrome P450 (CYP) genes from the mouse and human genomes, including nomenclature recommendations for genes, pseudogenes and alternative-splice variants," *Pharmacogenetics*, vol. 14, no. 1, pp. 1–18, Jan. 2004, doi: 10.1097/00008571-200401000-00001.
- [56] F. Krötz *et al.*, "Membrane-potential-dependent inhibition of platelet adhesion to endothelial cells by epoxyeicosatrienoic acids," *Arterioscler. Thromb. Vasc. Biol.*, vol. 24, no. 3, pp. 595–600, Mar. 2004, doi: 10.1161/01.ATV.0000116219.09040.8c.

- [57] K. Murotomi, A. Umeno, M. Shichiri, M. Tanito, and Y. Yoshida, "Significance of Singlet Oxygen Molecule in Pathologies," *Int. J. Mol. Sci.*, vol. 24, no. 3, Art. no. 3, Jan. 2023, doi: 10.3390/ijms24032739.
- [58] C. Nathan and A. Cunningham-Bussel, "Beyond oxidative stress: an immunologist's guide to reactive oxygen species," *Nat. Rev. Immunol.*, vol. 13, no. 5, pp. 349–361, May 2013, doi: 10.1038/nri3423.
- [59] L. A. Pham-Huy, H. He, and C. Pham-Huy, "Free Radicals, Antioxidants in Disease and Health," *Int. J. Biomed. Sci. IJBS*, vol. 4, no. 2, pp. 89–96, Jun. 2008.
- [60] B. Halliwell and J. M. C. Gutteridge, *Free Radicals in Biology and Medicine*, Fifth Edition, Fifth Edition. Oxford, New York: Oxford University Press, 2015.
- [61] J. M. Gutteridge and B. Halliwell, "Free radicals and antioxidants in the year 2000. A historical look to the future," *Ann. N. Y. Acad. Sci.*, vol. 899, pp. 136–147, 2000, doi: 10.1111/j.1749-6632.2000.tb06182.x.
- [62] P. Pospíšil, A. Prasad, and M. Rác, "Mechanism of the Formation of Electronically Excited Species by Oxidative Metabolic Processes: Role of Reactive Oxygen Species," *Biomolecules*, vol. 9, no. 7, p. 258, Jul. 2019, doi: 10.3390/biom9070258.
- [63] R. Domínguez, M. Pateiro, M. Gagaoua, F. J. Barba, W. Zhang, and J. M. Lorenzo, "A Comprehensive Review on Lipid Oxidation in Meat and Meat Products," *Antioxidants*, vol. 8, no. 10, Art. no. 10, Oct. 2019, doi: 10.3390/antiox8100429.
- [64] P. W. Harlina *et al.*, "Exploring oxylipins in processed foods: Understanding mechanisms, analytical perspectives, and enhancing quality with lipidomics," *Heliyon*, vol. 10, no. 16, p. e35917, Aug. 2024, doi: 10.1016/j.heliyon.2024.e35917.
- [65] E. Choe and D. B. Min, "Mechanisms and Factors for Edible Oil Oxidation," *Compr. Rev. Food Sci. Food Saf.*, vol. 5, no. 4, pp. 169–186, 2006, doi: 10.1111/j.1541-4337.2006.00009.x.
- [66] Marcel Müller, Fabrice Stefanetti and Ulrich K. Krieger, "Oxidation pathways of linoleic acid revisited with electrodynamic balance–mass spectrometry," *Environ. Sci.: Atmos*, no. 3, p. 85, 2023.
- [67] D. B. Min and J. M. Boff, "Lipid oxidation of edible oil.," *Food Lipids Chem. Nutr. Biotechnol.*, no. Ed.2, pp. 335–363, 2002.
- [68] S. J. J. Madhavi S. S. Nimbalkar, A. D. Kulkarni, D. L., "Lipid Oxidation in Biological and Food Systems," in *Food Antioxidants*, CRC Press, 1996.
- [69] R. R. Hiatt, T. Mill, and F. R. Mayo, "Homolytic decompositions of hydroperoxides. I. Summary and implications for autoxidation," *J. Org. Chem.*, vol. 33, no. 4, pp. 1416–1420, Apr. 1968, doi: 10.1021/jo01268a022.
- [70] E. A. Decker, "Antioxidant Mechanisms," in *Food Lipids*, 2nd ed., CRC Press, 2002.
- [71] G. R. Buettner, "The pecking order of free radicals and antioxidants: lipid peroxidation, alpha-tocopherol, and ascorbate," *Arch. Biochem. Biophys.*, vol. 300, no. 2, pp. 535–543, Feb. 1993, doi: 10.1006/abbi.1993.1074.
- [72] E. E. Farmer and M. J. Mueller, "ROS-Mediated Lipid Peroxidation and RES-Activated Signaling," *Annu. Rev. Plant Biol.*, vol. 64, no. Volume 64, 2013, pp. 429–450, Apr. 2013, doi: 10.1146/annurev-arplant-050312-120132.
- [73] H. R. Rawls and P. J. Van Santen, "A possible role for singlet oxygen in the initiation of fatty acid autoxidation," *J. Am. Oil Chem. Soc.*, vol. 47, no. 4, pp. 121–125, 1970, doi: 10.1007/BF02640400.

- [74] E. N. Frankel, "Chapter 3 Photooxidation of unsaturated fats," in *Lipid Oxidation* (Second Edition), E. N. Frankel, Ed., in Oily Press Lipid Library Series., Woodhead Publishing, 2012, pp. 51–66. doi: 10.1533/9780857097927.51.
- [75] Y. Chen, S. Xu, L. Li, M. Zhang, J. Shen, and T. Shen, "Active oxygen generation and photo-oxygenation involving temporfin (m-THPC)," *Dyes Pigments*, vol. 51, no. 2–3, pp. 63–69, Nov. 2001, doi: 10.1016/S0143-7208(01)00071-7.
- [76] S. H. Lee and D. B. Min, "Effects, quenching mechanisms, and kinetics of nickel chelates in singlet oxygen oxidation of soybean oil," *J. Agric. Food Chem.*, vol. 39, no. 4, pp. 642–646, Apr. 1991, doi: 10.1021/jf00004a002.
- [77] E. W. Kellogg and I. Fridovich, "Superoxide, hydrogen peroxide, and singlet oxygen in lipid peroxidation by a xanthine oxidase system," *J. Biol. Chem.*, vol. 250, no. 22, pp. 8812–8817, Nov. 1975.
- [78] E. c. Lee and D. B. Min, "Quenching Mechanism of β-Carotene on the Chlorophyll Sensitized Photooxidation of Soybean Oil," *J. Food Sci.*, vol. 53, no. 6, pp. 1894–1895, 1988, doi: 10.1111/j.1365-2621.1988.tb07868.x.
- [79] I. E. Kochevar and R. W. Redmond, "[2] Photosensitized production of singlet oxygen," in *Methods in Enzymology*, vol. 319, in Singlet Oxygen, UV-A, and Ozone, vol. 319., Academic Press, 2000, pp. 20–28. doi: 10.1016/S0076-6879(00)19004-4.
- [80] C. S. Foote, "Definition of type I and type II photosensitized oxidation," *Photochem. Photobiol.*, vol. 54, no. 5, p. 659, Nov. 1991, doi: 10.1111/j.1751-1097.1991.tb02071.x.
- [81] E. Duffy, G. Albero, and A. Morrin, "Headspace Solid-Phase Microextraction Gas Chromatography-Mass Spectrometry Analysis of Scent Profiles from Human Skin," *Cosmetics*, vol. 5, no. 4, Art. no. 4, Dec. 2018, doi: 10.3390/cosmetics5040062.
- [82] W. T. Fothergill, "Gas chromatography. Technique," *Proc. R. Soc. Med.*, vol. 61, no. 5, pp. 525–528, May 1968.
- [83] M. J. Mueller, L. Mène-Saffrané, C. Grun, K. Karg, and E. E. Farmer, "Oxylipin analysis methods," *Plant J.*, vol. 45, no. 4, pp. 472–489, 2006, doi: 10.1111/j.1365-313X.2005.02614.x.
- [84] Oh S.F., Vickery T.W., Serhan C.N., "Chiral lipidomics of E-series resolvins: Aspirin and the biosynthesis of novel mediators. Biochim. Biophys. Acta Mol. Cell Biol. Lipids.," *Biochim. Biophys. Acta Mol. Cell Biol. Lipids.*, vol. 1811, pp. 737–747, 2011, doi: doi: 10.1016/j.bbalip.2011.06.007.
- [85] A. K. Pedersen, M. L. Watson, and G. A. FitzGerald, "Inhibition of thromboxane biosynthesis in serum: limitations of the measurement of immunoreactive 6-keto-PGF1 alpha," *Thromb. Res.*, vol. 33, no. 1, pp. 99–103, Jan. 1984, doi: 10.1016/0049-3848(84)90159-2.
- [86] Y. Wang, A. Armando, O. Quehenberger, C. Yan, and E. A. Dennis, "Comprehensive Ultra Performance Liquid Chromatographic Separation and Mass Spectrometric Analysis of Eicosanoid Metabolites Suitable for Human Materials," *J. Chromatogr. A*, vol. 1359, pp. 60–69, Sep. 2014, doi: 10.1016/j.chroma.2014.07.006.
- [87] D. Tsikas and M.-T. Suchy, "Assessment of urinary F(2)-isoprostanes in experimental and clinical studies: mass spectrometry versus ELISA," *Hypertens. Dallas Tex 1979*, vol. 60, no. 2, pp. e14; author reply e15, Aug. 2012, doi: 10.1161/HYPERTENSIONAHA.112.199315.
- [88] M. Aslan, I. Aslan, F. Özcan, R. Eryılmaz, C. O. Ensari, and T. Bilecik, "A pilot study investigating early postoperative changes of plasma polyunsaturated fatty acids after

- laparoscopic sleeve gastrectomy," *Lipids Health Dis.*, vol. 13, p. 62, Apr. 2014, doi: 10.1186/1476-511X-13-62.
- [89] J. Y. Jeremy *et al.*, "Oocyte maturity and human follicular fluid prostanoids, gonadotropins, and prolactin after administration of clomiphene and pergonal," *J. Clin. Endocrinol. Metab.*, vol. 65, no. 3, pp. 402–406, Sep. 1987, doi: 10.1210/jcem-65-3-402.
- [90] A. S. Gandhi, D. Budac, T. Khayrullina, R. Staal, and G. Chandrasena, "Quantitative analysis of lipids: a higher-throughput LC-MS/MS-based method and its comparison to ELISA," *Future Sci. OA*, vol. 3, no. 1, p. FSO157, Mar. 2017, doi: 10.4155/fsoa-2016-0067.
- [91] D. K. Miller *et al.*, "Development of enzyme-linked immunosorbent assays for measurement of leukotrienes and prostaglandins," *J. Immunol. Methods*, vol. 81, no. 2, pp. 169–185, Aug. 1985, doi: 10.1016/0022-1759(85)90202-9.
- [92] M. VanRollins and V. A. VanderNoot, "Simultaneous resolution of underivatized regioisomers and stereoisomers of arachidonate epoxides by capillary electrophoresis," *Anal. Biochem.*, vol. 313, no. 1, pp. 106–116, Feb. 2003, doi: 10.1016/s0003-2697(02)00503-1.
- [93] N. Chiang, E. A. Bermudez, P. M. Ridker, S. Hurwitz, and C. N. Serhan, "Aspirin triggers antiinflammatory 15-epi-lipoxin A4 and inhibits thromboxane in a randomized human trial," *Proc. Natl. Acad. Sci. U. S. A.*, vol. 101, no. 42, pp. 15178–15183, Oct. 2004, doi: 10.1073/pnas.0405445101.
- [94] Z.-R. Tan *et al.*, "Sensitive bioassay for the simultaneous determination of pseudoephedrine and cetirizine in human plasma by liquid-chromatography-ion trap spectrometry," *J. Pharm. Biomed. Anal.*, vol. 42, no. 2, pp. 207–212, Sep. 2006, doi: 10.1016/j.jpba.2006.02.057.
- [95] Y. Satomi, M. Hirayama, and H. Kobayashi, "One-step lipid extraction for plasma lipidomics analysis by liquid chromatography mass spectrometry," *J. Chromatogr. B Analyt. Technol. Biomed. Life. Sci.*, vol. 1063, pp. 93–100, Sep. 2017, doi: 10.1016/j.jchromb.2017.08.020.
- [96] I. Willenberg, A. I. Ostermann, and N. H. Schebb, "Targeted metabolomics of the arachidonic acid cascade: current state and challenges of LC-MS analysis of oxylipins," *Anal. Bioanal. Chem.*, vol. 407, no. 10, pp. 2675–2683, Apr. 2015, doi: 10.1007/s00216-014-8369-4.
- [97] Y. H. Lee, L. Cui, J. Fang, B. S. M. Chern, H. H. Tan, and J. K. Y. Chan, "Limited value of pro-inflammatory oxylipins and cytokines as circulating biomarkers in endometriosis a targeted 'omics study," *Sci. Rep.*, vol. 6, p. 26117, May 2016, doi: 10.1038/srep26117.
- [98] M. Chocholoušková, R. Jirásko, D. Vrána, J. Gatěk, B. Melichar, and M. Holčapek, "Reversed phase UHPLC/ESI-MS determination of oxylipins in human plasma: a case study of female breast cancer," *Anal. Bioanal. Chem.*, vol. 411, no. 6, pp. 1239–1251, Feb. 2019, doi: 10.1007/s00216-018-1556-y.
- [99] W. Wang, S. Qin, L. Li, X. Chen, Q. Wang, and J. Wei, "An Optimized High Throughput Clean-Up Method Using Mixed-Mode SPE Plate for the Analysis of Free Arachidonic Acid in Plasma by LC-MS/MS," *Int. J. Anal. Chem.*, vol. 2015, p. 374819, 2015, doi: 10.1155/2015/374819.
- [100] D. French, "Chapter Five Advances in Clinical Mass Spectrometry," in *Advances in Clinical Chemistry*, vol. 79, G. S. Makowski, Ed., Elsevier, 2017, pp. 153–198. doi: 10.1016/bs.acc.2016.09.003.

- [101] J. Aldana, A. Romero-Otero, and M. P. Cala, "Exploring the Lipidome: Current Lipid Extraction Techniques for Mass Spectrometry Analysis," *Metabolites*, vol. 10, no. 6, p. 231, Jun. 2020, doi: 10.3390/metabo10060231.
- [102] G. Astarita, A. C. Kendall, E. A. Dennis, and A. Nicolaou, "Targeted lipidomic strategies for oxygenated metabolites of polyunsaturated fatty acids," *Biochim. Biophys. Acta*, vol. 1851, no. 4, pp. 456–468, Apr. 2015, doi: 10.1016/j.bbalip.2014.11.012.
- [103] S. Tumanov and J. J. Kamphorst, "Recent advances in expanding the coverage of the lipidome," *Curr. Opin. Biotechnol.*, vol. 43, pp. 127–133, Feb. 2017, doi: 10.1016/j.copbio.2016.11.008.
- [104] J. Sostare *et al.*, "Comparison of modified Matyash method to conventional solvent systems for polar metabolite and lipid extractions," *Anal. Chim. Acta*, vol. 1037, pp. 301–315, Dec. 2018, doi: 10.1016/j.aca.2018.03.019.
- [105] M. Puppolo, D. Varma, and S. A. Jansen, "A review of analytical methods for eicosanoids in brain tissue," *J. Chromatogr. B Analyt. Technol. Biomed. Life. Sci.*, vol. 964, pp. 50–64, Aug. 2014, doi: 10.1016/j.jchromb.2014.03.007.
- [106] Z.-X. Yuan, S. Majchrzak-Hong, G. S. Keyes, M. J. Iadarola, A. J. Mannes, and C. E. Ramsden, "Lipidomic profiling of targeted oxylipins with ultra-performance liquid chromatography-tandem mass spectrometry," *Anal. Bioanal. Chem.*, vol. 410, no. 23, pp. 6009–6029, Sep. 2018, doi: 10.1007/s00216-018-1222-4.
- [107] M. Jelińska, A. Białek, H. Mojska, I. Gielecińska, and A. Tokarz, "Effect of conjugated linoleic acid mixture supplemented daily after carcinogen application on linoleic and arachidonic acid metabolites in rat serum and induced tumours," *Biochim. Biophys. Acta*, vol. 1842, no. 11, pp. 2230–2236, Nov. 2014, doi: 10.1016/j.bbadis.2014.08.013.
- [108] J. Dalli and C. N. Serhan, "Specific lipid mediator signatures of human phagocytes: microparticles stimulate macrophage efferocytosis and pro-resolving mediators," *Blood*, vol. 120, no. 15, pp. e60–e72, Oct. 2012, doi: 10.1182/blood-2012-04-423525.
- [109] A. F. Galvão *et al.*, "Plasma eicosanoid profiles determined by high-performance liquid chromatography coupled with tandem mass spectrometry in stimulated peripheral blood from healthy individuals and sickle cell anemia patients in treatment," *Anal. Bioanal. Chem.*, vol. 408, no. 13, pp. 3613–3623, May 2016, doi: 10.1007/s00216-016-9445-8.
- [110] M. Y. Golovko and E. J. Murphy, "An improved LC-MS/MS procedure for brain prostanoid analysis using brain fixation with head-focused microwave irradiation and liquid-liquid extraction," *J. Lipid Res.*, vol. 49, no. 4, pp. 893–902, Apr. 2008, doi: 10.1194/jlr.D700030-JLR200.
- [111] T. Petta, L. A. B. Moraes, and L. H. Faccioli, "Versatility of tandem mass spectrometry for focused analysis of oxylipids," *J. Mass Spectrom. JMS*, vol. 50, no. 7, pp. 879–890, Jul. 2015, doi: 10.1002/jms.3595.
- [112] D. D. Shinde *et al.*, "LC-MS/MS for the simultaneous analysis of arachidonic acid and 32 related metabolites in human plasma: Basal plasma concentrations and aspirin-induced changes of eicosanoids," *J. Chromatogr. B Analyt. Technol. Biomed. Life. Sci.*, vol. 911, pp. 113–121, Dec. 2012, doi: 10.1016/j.jchromb.2012.11.004.
- [113] K. M. Rund *et al.*, "Development of an LC-ESI(-)-MS/MS method for the simultaneous quantification of 35 isoprostanes and isofurans derived from the major n3- and n6-PUFAs," *Anal. Chim. Acta*, vol. 1037, pp. 63–74, Dec. 2018, doi: 10.1016/j.aca.2017.11.002.

- [114] M. Hennebelle *et al.*, "Altered soluble epoxide hydrolase-derived oxylipins in patients with seasonal major depression: An exploratory study," *Psychiatry Res.*, vol. 252, pp. 94–101, Jun. 2017, doi: 10.1016/j.psychres.2017.02.056.
- [115] G.-Y. Chen and Q. Zhang, "Comprehensive analysis of oxylipins in human plasma using reversed-phase liquid chromatography-triple quadrupole mass spectrometry with heatmap-assisted selection of transitions," *Anal. Bioanal. Chem.*, vol. 411, no. 2, pp. 367–385, Jan. 2019, doi: 10.1007/s00216-018-1446-3.
- [116] S. Medina *et al.*, "A ultra-pressure liquid chromatography/triple quadrupole tandem mass spectrometry method for the analysis of 13 eicosanoids in human urine and quantitative 24 hour values in healthy volunteers in a controlled constant diet," *Rapid Commun. Mass Spectrom. RCM*, vol. 26, no. 10, pp. 1249–1257, May 2012, doi: 10.1002/rcm.6224.
- [117] Yue H., Strauss K.I., Borenstein M.R., Barbe M.F., Rossi L.J., Jansen S.A, "Determination of bioactive eicosanoids in brain tissue by a sensitive reversed-phase liquid chromatographic method with fluorescence detection," *J. Chromatogr. B Anal. Technol. Biomed. Life Sci*, no. 803, pp. 267–277, 2004, doi: doi: 10.1016/j.ichromb.2003.12.027.
- [118] B. Bojko, "Solid-phase microextraction: a fit-for-purpose technique in biomedical analysis," *Anal. Bioanal. Chem.*, vol. 414, no. 24, pp. 7005–7013, Oct. 2022, doi: 10.1007/s00216-022-04138-9.
- [119] C. L. Arthur and Janusz. Pawliszyn, "Solid phase microextraction with thermal desorption using fused silica optical fibers," *Anal. Chem.*, vol. 62, no. 19, pp. 2145–2148, Oct. 1990, doi: 10.1021/ac00218a019.
- [120] Q. Zhang, L. Zhou, H. Chen, C.-Z. Wang, Z. Xia, and C.-S. Yuan, "Solid-phase microextraction technology for in vitro and in vivo metabolite analysis," *Trends Anal. Chem. TRAC*, vol. 80, pp. 57–65, Jun. 2016, doi: 10.1016/j.trac.2016.02.017.
- [121] G. Ouyang, D. Vuckovic, and J. Pawliszyn, "Nondestructive sampling of living systems using in vivo solid-phase microextraction," *Chem. Rev.*, vol. 111, no. 4, pp. 2784–2814, Apr. 2011, doi: 10.1021/cr100203t.
- [122] G. Vas and K. Vékey, "Solid-phase microextraction: a powerful sample preparation tool prior to mass spectrometric analysis," *J. Mass Spectrom. JMS*, vol. 39, no. 3, pp. 233–254, Mar. 2004, doi: 10.1002/jms.606.
- [123] A. Napylov *et al.*, "In Vivo Solid-Phase Microextraction for Sampling of Oxylipins in Brain of Awake, Moving Rats," *Angew. Chem. Int. Ed Engl.*, vol. 59, no. 6, pp. 2392–2398, Feb. 2020, doi: 10.1002/anie.201909430.
- [124] G. Ouyang and J. Pawliszyn, "A critical review in calibration methods for solid-phase microextraction," *Anal. Chim. Acta*, vol. 627, no. 2, pp. 184–197, Oct. 2008, doi: 10.1016/j.aca.2008.08.015.
- [125] H. Sereshti, O. Duman, S. Tunç, N. Nouri, and P. Khorram, "Nanosorbent-based solid phase microextraction techniques for the monitoring of emerging organic contaminants in water and wastewater samples," *Microchim. Acta*, vol. 187, no. 9, p. 541, Sep. 2020, doi: 10.1007/s00604-020-04527-w.
- [126] R. W. Jiang, L. M. Marin, K. Jaroch, W. Zhou, W. L. Siqueira, and J. Pawliszyn, "Proteomic Analysis of Human Saliva via Solid-Phase Microextraction Coupled with Liquid Chromatography–Mass Spectrometry," *Anal. Chem.*, vol. 96, no. 14, pp. 5363–5367, Apr. 2024, doi: 10.1021/acs.analchem.4c00307.

- [127] D. Vuckovic *et al.*, "In vivo solid-phase microextraction for single rodent pharmacokinetics studies of carbamazepine and carbamazepine-10,11-epoxide in mice," *J. Chromatogr. A*, vol. 1218, no. 21, pp. 3367–3375, May 2011, doi: 10.1016/j.chroma.2010.07.060.
- [128] H. Vereb, A. M. Dietrich, B. Alfeeli, and M. Agah, "The Possibilities Will Take Your Breath Away: Breath Analysis for Assessing Environmental Exposure," *Environ. Sci. Technol.*, vol. 45, no. 19, pp. 8167–8175, Oct. 2011, doi: 10.1021/es202041j.
- [129] B. Bojko *et al.*, "Untargeted metabolomics profiling of skeletal muscle samples from malignant hyperthermia susceptible patients," *Can. J. Anaesth. J. Can. Anesth.*, vol. 68, no. 6, pp. 761–772, Jun. 2021, doi: 10.1007/s12630-020-01895-y.
- [130] S. Liu, Y. Huang, J. Liu, C. Chen, and G. Ouyang, "In Vivo Contaminant Monitoring and Metabolomic Profiling in Plants Exposed to Carbamates via a Novel Microextraction Fiber," *Environ. Sci. Technol.*, vol. 55, no. 18, pp. 12449–12458, Sep. 2021, doi: 10.1021/acs.est.1c04368.
- [131] J. Qiu *et al.*, "In vivo tracing of organochloride and organophosphorus pesticides in different organs of hydroponically grown malabar spinach (Basella alba L.)," *J. Hazard. Mater.*, vol. 316, pp. 52–59, Oct. 2016, doi: 10.1016/j.jhazmat.2016.05.024.
- [132] S. De Grazia, E. Gionfriddo, and J. Pawliszyn, "A new and efficient Solid Phase Microextraction approach for analysis of high fat content food samples using a matrix-compatible coating," *Talanta*, vol. 167, pp. 754–760, May 2017, doi: 10.1016/j.talanta.2017.01.064.
- [133] N. Reyes-Garcés *et al.*, "In Vivo Brain Sampling Using a Microextraction Probe Reveals Metabolic Changes in Rodents after Deep Brain Stimulation," *Anal. Chem.*, vol. 91, no. 15, pp. 9875–9884, Aug. 2019, doi: 10.1021/acs.analchem.9b01540.
- [134] A. Roszkowska *et al.*, "*In vivo* solid-phase microextraction sampling combined with metabolomics and toxicological studies for the non-lethal monitoring of the exposome in fish tissue," *Environ. Pollut.*, vol. 249, pp. 109–115, Jun. 2019, doi: 10.1016/j.envpol.2019.03.024.
- [135] E. Sánchez-Palomo, M. C. Díaz-Maroto, and M. S. Pérez-Coello, "Rapid determination of volatile compounds in grapes by HS-SPME coupled with GC–MS," *Talanta*, vol. 66, no. 5, pp. 1152–1157, Jun. 2005, doi: 10.1016/j.talanta.2005.01.015.
- [136] E. Cudjoe, B. Bojko, I. de Lannoy, V. Saldivia, and J. Pawliszyn, "Solid-phase microextraction: a complementary in vivo sampling method to microdialysis," *Angew. Chem. Int. Ed Engl.*, vol. 52, no. 46, pp. 12124–12126, Nov. 2013, doi: 10.1002/anie.201304538.
- [137] O. Coskun, "Separation techniques: Chromatography," *North. Clin. Istanb.*, vol. 3, no. 2, pp. 156–160, Nov. 2016, doi: 10.14744/nci.2016.32757.
- [138] I. Liakh, A. Pakiet, T. Sledzinski, and A. Mika, "Methods of the Analysis of Oxylipins in Biological Samples," *Molecules*, vol. 25, no. 2, p. 349, Jan. 2020, doi: 10.3390/molecules25020349.
- [139] W. Qu *et al.*, "Cytochrome P450 CYP2J9, a new mouse arachidonic acid omega-1 hydroxylase predominantly expressed in brain," *J. Biol. Chem.*, vol. 276, no. 27, pp. 25467–25479, Jul. 2001, doi: 10.1074/jbc.M100545200.
- [140] Kiran Karhale, Nitin B. Kohale, Suraj B. Rathod, Rahul V. jadhav, "Overview an Nano Liquid Chromatography," *Int. J. Humanit. Soc. Sci. Manag. IJHSSM*, vol. 3, no. 2, pp. 401–409, Apr. 2023.

- [141] K. L. Sanders and J. L. Edwards, "Nano-Liquid Chromatography-Mass Spectrometry and Recent Applications in Omics Investigations," *Anal. Methods Adv. Methods Appl.*, vol. 12, no. 36, pp. 4404–4417, Sep. 2020, doi: 10.1039/d0ay01194k.
- [142] A. Andries, J. Rozenski, P. Vermeersch, D. Mekahli, and A. Van Schepdael, "Recent progress in the LC–MS/MS analysis of oxidative stress biomarkers," *ELECTROPHORESIS*, vol. 42, no. 4, pp. 402–428, 2021, doi: 10.1002/elps.202000208.
- [143] K. Sterz, G. Scherer, and J. Ecker, "A simple and robust UPLC-SRM/MS method to quantify urinary eicosanoids," *J. Lipid Res.*, vol. 53, no. 5, pp. 1026–1036, May 2012, doi: 10.1194/jlr.D023739.
- [144] L. Kutzner *et al.*, "Development of an Optimized LC-MS Method for the Detection of Specialized Pro-Resolving Mediators in Biological Samples," *Front. Pharmacol.*, vol. 10, p. 169, 2019, doi: 10.3389/fphar.2019.00169.
- [145] D. Fuchs, M. Hamberg, C. M. Sköld, Å. M. Wheelock, and C. E. Wheelock, "An LC-MS/MS workflow to characterize 16 regio- and stereoisomeric trihydroxyoctadecenoic acids," *J. Lipid Res.*, vol. 59, no. 10, pp. 2025–2033, Oct. 2018, doi: 10.1194/jlr.D087429.
- [146] A. P. Neilson *et al.*, "Effect of fish oil on levels of R- and S-enantiomers of 5-, 12-, and 15-hydroxyeicosatetraenoic acids in mouse colonic mucosa," *Nutr. Cancer*, vol. 64, no. 1, pp. 163–172, 2012, doi: 10.1080/01635581.2012.630168.
- [147] R. Berkecz, M. Lísa, and M. Holčapek, "Analysis of oxylipins in human plasma: Comparison of ultrahigh-performance liquid chromatography and ultrahigh-performance supercritical fluid chromatography coupled to mass spectrometry," *J. Chromatogr. A*, vol. 1511, pp. 107–121, Aug. 2017, doi: 10.1016/j.chroma.2017.06.070.
- [148] L. Kortz, J. Dorow, S. Becker, J. Thiery, and U. Ceglarek, "Fast liquid chromatography-quadrupole linear ion trap-mass spectrometry analysis of polyunsaturated fatty acids and eicosanoids in human plasma," *J. Chromatogr. B Analyt. Technol. Biomed. Life. Sci.*, vol. 927, pp. 209–213, May 2013, doi: 10.1016/j.jchromb.2013.03.012.
- [149] C. Monnin, P. Ramrup, C. Daigle-Young, and D. Vuckovic, "Improving negative liquid chromatography/electrospray ionization mass spectrometry lipidomic analysis of human plasma using acetic acid as a mobile-phase additive," *Rapid Commun. Mass Spectrom. RCM*, vol. 32, no. 3, pp. 201–211, Feb. 2018, doi: 10.1002/rcm.8024.
- [150] D. S. Dumlao, M. W. Buczynski, P. C. Norris, R. Harkewicz, and E. A. Dennis, "High-throughput lipidomic analysis of fatty acid derived eicosanoids and N-acylethanolamines," *Biochim. Biophys. Acta*, vol. 1811, no. 11, pp. 724–736, Nov. 2011, doi: 10.1016/j.bbalip.2011.06.005.
- [151] R. Thakare *et al.*, "Simultaneous LC-MS/MS analysis of eicosanoids and related metabolites in human serum, sputum and BALF," *Biomed. Chromatogr. BMC*, vol. 32, no. 3, Mar. 2018, doi: 10.1002/bmc.4102.
- [152] X. Fu *et al.*, "High Sensitivity and Wide Linearity LC-MS/MS Method for Oxylipin Quantification in Multiple Biological Samples," *J. Lipid Res.*, vol. 63, no. 12, p. 100302, Dec. 2022, doi: 10.1016/j.jlr.2022.100302.
- [153] Napylov A, "Ultra-high performance liquid chromatography-high resolution mass spectrometry method for detection and quantitation of oxylipin in plasma "MSc thesis. Department of Chemistry and Biochemtry, Concordia University Montreal, Quebec, Feb. 2019.
- [154] M. Király, B. Dalmadiné Kiss, K. Vékey, I. Antal, and K. Ludányi, "[Mass spectrometry: past and present]," *Acta Pharm. Hung.*, vol. 86, no. 1, pp. 3–11, 2016.

- [155] G. Zhang, R. S. Annan, S. A. Carr, and T. A. Neubert, "Overview of peptide and protein analysis by mass spectrometry," *Curr. Protoc. Protein Sci.*, vol. Chapter 16, p. Unit16.1, Nov. 2010, doi: 10.1002/0471140864.ps1601s62.
- [156] I. Finoulst, M. Pinkse, W. Van Dongen, and P. Verhaert, "Sample preparation techniques for the untargeted LC-MS-based discovery of peptides in complex biological matrices," *J. Biomed. Biotechnol.*, vol. 2011, p. 245291, 2011, doi: 10.1155/2011/245291.
- [157] M. Vilbaste, E. Tammekivi, and I. Leito, "Uncertainty contribution of derivatization in gas chromatography/mass spectrometric analysis," *Rapid Commun. Mass Spectrom. RCM*, vol. 34, no. 16, p. e8704, Aug. 2020, doi: 10.1002/rcm.8704.
- [158] A. M. Haag, "Mass Analyzers and Mass Spectrometers," *Adv. Exp. Med. Biol.*, vol. 919, pp. 157–169, 2016, doi: 10.1007/978-3-319-41448-5_7.
- [159] M. Commisso, A. Anesi, S. Dal Santo, and F. Guzzo, "Performance comparison of electrospray ionization and atmospheric pressure chemical ionization in untargeted and targeted liquid chromatography/mass spectrometry based metabolomics analysis of grapeberry metabolites," *Rapid Commun. Mass Spectrom. RCM*, vol. 31, no. 3, pp. 292–300, Feb. 2017, doi: 10.1002/rcm.7789.
- [160] E. V. S. Maciel, N. G. Pereira Dos Santos, D. A. Vargas Medina, and F. M. Lanças, "Electron ionization mass spectrometry: Quo vadis?," *Electrophoresis*, vol. 43, no. 15, pp. 1587–1600, Aug. 2022, doi: 10.1002/elps.202100392.
- [161] C. Ho *et al.*, "Electrospray Ionisation Mass Spectrometry: Principles and Clinical Applications," *Clin. Biochem. Rev.*, vol. 24, no. 1, pp. 3–12, Feb. 2003.
- [162] A. Criscuolo *et al.*, "Analytical and computational workflow for in-depth analysis of oxidized complex lipids in blood plasma," *Nat. Commun.*, vol. 13, no. 1, Art. no. 1, Nov. 2022, doi: 10.1038/s41467-022-33225-9.
- [163] S. Hellhake *et al.*, "Non-targeted and targeted analysis of oxylipins in combination with charge-switch derivatization by ion mobility high-resolution mass spectrometry," *Anal. Bioanal. Chem.*, vol. 412, no. 23, p. 5743, 2020, doi: 10.1007/s00216-020-02795-2.
- [164] P. L. Urban, "Quantitative mass spectrometry: an overview," *Philos. Transact. A Math. Phys. Eng. Sci.*, vol. 374, no. 2079, p. 20150382, Oct. 2016, doi: 10.1098/rsta.2015.0382.
- [165] M. Mann and N. L. Kelleher, "Precision proteomics: the case for high resolution and high mass accuracy," *Proc. Natl. Acad. Sci. U. S. A.*, vol. 105, no. 47, pp. 18132–18138, Nov. 2008, doi: 10.1073/pnas.0800788105.
- [166] D. J. Douglas, "Mechanism of the collision-induced dissociation of polyatomic ions studied by triple quadrupole mass spectrometry," *J. Phys. Chem.*, vol. 86, no. 2, pp. 185–191, Jan. 1982, doi: 10.1021/j100391a011.
- [167] H. Khan and J. Ali, "UHPLC/Q-TOF-MS Technique: Introduction and Applications," *Lett. Org. Chem.*, vol. 12, no. 6, pp. 371–378, Jul. 2015.
- [168] M. Tanner and D. Günther, "Short transient signals, a challenge for inductively coupled plasma mass spectrometry, a review," *Anal. Chim. Acta*, vol. 633, no. 1, pp. 19–28, Feb. 2009, doi: 10.1016/j.aca.2008.11.041.
- [169] M. F. L'annunziata, "11 SOLID SCINTILLATION ANALYSIS," in *Handbook of Radioactivity Analysis (Second Edition)*, M. F. L'Annunziata, Ed., San Diego: Academic Press, 2003, pp. 845–987. doi: 10.1016/B978-012436603-9/50016-8.
- [170] J. Ding and Y.-Q. Feng, "Mass spectrometry-based metabolomics for clinical study: Recent progresses and applications," *TrAC Trends Anal. Chem.*, vol. 158, p. 116896, Jan. 2023, doi: 10.1016/j.trac.2022.116896.

- [171] S. Heiles, "Advanced tandem mass spectrometry in metabolomics and lipidomics—methods and applications," *Anal. Bioanal. Chem.*, vol. 413, no. 24, pp. 5927–5948, Oct. 2021, doi: 10.1007/s00216-021-03425-1.
- [172] Y. Qi and D. A. Volmer, "Structural analysis of small to medium-sized molecules by mass spectrometry after electron-ion fragmentation (ExD) reactions," *Analyst*, vol. 141, no. 3, pp. 794–806, Jan. 2016, doi: 10.1039/C5AN02171E.
- [173] T. Baba, J. L. Campbell, J. C. Y. Le Blanc, and P. R. S. Baker, "Structural Identification of Eicosanoids with Ring Structures Using Differential Mobility Spectrometry-Electron Impact Excitation of Ions from Organics Mass Spectrometry," *J. Am. Soc. Mass Spectrom.*, vol. 34, no. 1, pp. 75–81, Jan. 2023, doi: 10.1021/jasms.2c00256.
- [174] D. Balgoma *et al.*, "Quantification of lipid mediator metabolites in human urine from asthma patients by electrospray ionization mass spectrometry: controlling matrix effects," *Anal. Chem.*, vol. 85, no. 16, pp. 7866–7874, Aug. 2013, doi: 10.1021/ac401461b.
- [175] A. Sens *et al.*, "Pre-analytical sample handling standardization for reliable measurement of metabolites and lipids in LC-MS-based clinical research," *J. Mass Spectrom. Adv. Clin. Lab*, vol. 28, pp. 35–46, Apr. 2023, doi: 10.1016/j.jmsacl.2023.02.002.
- [176] T. Martínez-Sena *et al.*, "Monitoring of system conditioning after blank injections in untargeted UPLC-MS metabolomic analysis," *Sci. Rep.*, vol. 9, p. 9822, Jul. 2019, doi: 10.1038/s41598-019-46371-w.
- [177] A. K. Hewavitharana, N. S. Abu Kassim, and P. N. Shaw, "Standard addition with internal standardisation as an alternative to using stable isotope labelled internal standards to correct for matrix effects—Comparison and validation using liquid chromatographytandem mass spectrometric assay of vitamin D," *J. Chromatogr. A*, vol. 1553, pp. 101–107, Jun. 2018, doi: 10.1016/j.chroma.2018.04.026.
- [178] P. Kościelniak, "Calibration methods in qualitative analysis," *TrAC Trends Anal. Chem.*, vol. 150, p. 116587, May 2022, doi: 10.1016/j.trac.2022.116587.
- [179] S. M. Sheik and W. D. S. Cr, "Quality control in clinical biochemistry laboratory: a glimpse," *Int. J. Clin. Diagn. Res.*, vol. 5, no. 5, Art. no. 5, Oct. 2017, doi: 10.12691/ijcdr-5-5-2.
- [180] J. Yang, K. Schmelzer, K. Georgi, and B. D. Hammock, "Quantitative Profiling Method for Oxylipin Metabolome by Liquid Chromatography Electrospray Ionization Tandem Mass Spectrometry," *Anal. Chem.*, vol. 81, no. 19, pp. 8085–8093, Oct. 2009, doi: 10.1021/ac901282n.
- [181] K. M. Rund *et al.*, "Clinical blood sampling for oxylipin analysis effect of storage and pneumatic tube transport of blood on free and total oxylipin profile in human plasma and serum," *Analyst*, vol. 145, no. 6, pp. 2378–2388, Mar. 2020, doi: 10.1039/C9AN01880H.
- [182] E. Koch *et al.*, "Stability of oxylipins during plasma generation and long-term storage," *Talanta*, vol. 217, p. 121074, Sep. 2020, doi: 10.1016/j.talanta.2020.121074.
- [183] K. J. Polinski *et al.*, "Collection and Storage of Human Plasma for Measurement of Oxylipins," *Metabolites*, vol. 11, no. 3, p. 137, Feb. 2021, doi: 10.3390/metabol1030137.
- [184] J. Dorow, S. Becker, L. Kortz, J. Thiery, S. Hauschildt, and U. Ceglarek, "Preanalytical Investigation of Polyunsaturated Fatty Acids and Eicosanoids in Human Plasma by Liquid Chromatography-Tandem Mass Spectrometry," *Biopreservation Biobanking*, vol. 14, no. 2, pp. 107–113, Apr. 2016, doi: 10.1089/bio.2015.0005.

- [185] C. E. Ramsden *et al.*, "Temperature and time-dependent effects of delayed blood processing on oxylipin concentrations in human plasma," *Prostaglandins Leukot. Essent. Fatty Acids*, vol. 150, pp. 31–37, Nov. 2019, doi: 10.1016/j.plefa.2019.09.001.
- [186] H. S. Jonasdottir, H. Brouwers, R. E. M. Toes, A. Ioan-Facsinay, and M. Giera, "Effects of anticoagulants and storage conditions on clinical oxylipid levels in human plasma," *Biochim. Biophys. Acta Mol. Cell Biol. Lipids*, vol. 1863, no. 12, pp. 1511–1522, Dec. 2018, doi: 10.1016/j.bbalip.2018.10.003.
- [187] E. Hewawasam, G. Liu, D. W. Jeffery, B. S. Muhlhausler, and R. A. Gibson, "A stable method for routine analysis of oxylipins from dried blood spots using ultra-high performance liquid chromatography–tandem mass spectrometry," *Prostaglandins Leukot. Essent. Fatty Acids*, vol. 137, pp. 12–18, Oct. 2018, doi: 10.1016/j.plefa.2018.08.001.
- [188] M. G. J. Balvers *et al.*, "Fish oil and inflammatory status alter the n-3 to n-6 balance of the endocannabinoid and oxylipin metabolomes in mouse plasma and tissues," *Metabolomics Off. J. Metabolomic Soc.*, vol. 8, no. 6, pp. 1130–1147, Dec. 2012, doi: 10.1007/s11306-012-0421-9.
- [189] C. Gladine, A. I. Ostermann, J. W. Newman, and N. H. Schebb, "MS-based targeted metabolomics of eicosanoids and other oxylipins: Analytical and inter-individual variabilities," *Free Radic. Biol. Med.*, vol. 144, pp. 72–89, Nov. 2019, doi: 10.1016/j.freeradbiomed.2019.05.012.
- [190] M. Moran-Garrido, S. M. Camunas-Alberca, J. Sáiz, A. Gradillas, A. Y. Taha, and C. Barbas, "Deeper insights into the stability of oxylipins in human plasma across multiple freeze-thaw cycles and storage conditions," *J. Pharm. Biomed. Anal.*, vol. 255, p. 116587, Mar. 2025, doi: 10.1016/j.jpba.2024.116587.
- [191] R. A. Colas, M. Shinohara, J. Dalli, N. Chiang, and C. N. Serhan, "Identification and signature profiles for pro-resolving and inflammatory lipid mediators in human tissue," *Am. J. Physiol. Cell Physiol.*, vol. 307, no. 1, pp. C39-54, Jul. 2014, doi: 10.1152/ajpcell.00024.2014.
- [192] A. Hanif, M. L. Edin, D. C. Zeldin, C. Morisseau, and M. A. Nayeem, "Effect of Soluble Epoxide Hydrolase on the Modulation of Coronary Reactive Hyperemia: Role of Oxylipins and PPARγ," *PLoS ONE*, vol. 11, no. 9, p. e0162147, Sep. 2016, doi: 10.1371/journal.pone.0162147.
- [193] A. Ferdouse, S. Leng, T. Winter, and H. M. Aukema, "The Brain Oxylipin Profile Is Resistant to Modulation by Dietary n-6 and n-3 Polyunsaturated Fatty Acids in Male and Female Rats," *Lipids*, vol. 54, no. 1, pp. 67–80, Jan. 2019, doi: 10.1002/lipd.12122.
- [194] M. Hennebelle *et al.*, "Brain oxylipin concentrations following hypercapnia/ischemia: effects of brain dissection and dissection time," *J. Lipid Res.*, vol. 60, no. 3, pp. 671–682, Mar. 2019, doi: 10.1194/jlr.D084228.
- [195] J. Musakhanian, J.-D. Rodier, and M. Dave, "Oxidative Stability in Lipid Formulations: a Review of the Mechanisms, Drivers, and Inhibitors of Oxidation," *AAPS PharmSciTech*, vol. 23, no. 5, p. 151, May 2022, doi: 10.1208/s12249-022-02282-0.
- [196] I. Pinchuk, H. Shoval, Y. Dotan, and D. Lichtenberg, "Evaluation of antioxidants: scope, limitations and relevance of assays," *Chem. Phys. Lipids*, vol. 165, no. 6, pp. 638–647, Sep. 2012, doi: 10.1016/j.chemphyslip.2012.05.003.
- [197] V. Jannin, J.-D. Rodier, and J. Musakhanian, "Polyoxylglycerides and glycerides: Effects of manufacturing parameters on API stability, excipient functionality and processing," *Int. J. Pharm.*, vol. 466, no. 1, pp. 109–121, May 2014, doi: 10.1016/j.ijpharm.2014.03.007.

- [198] M. van Aardt, S. E. Duncan, T. E. Long, S. F. O'Keefe, J. E. Marcy, and S. R. Sims, "Effect of antioxidants on oxidative stability of edible fats and oils: thermogravimetric analysis," *J. Agric. Food Chem.*, vol. 52, no. 3, pp. 587–591, Feb. 2004, doi: 10.1021/jf030304f.
- [199] N. A. Santos *et al.*, "Commercial antioxidants and thermal stability evaluations," *Fuel*, vol. 97, pp. 638–643, Jul. 2012, doi: 10.1016/j.fuel.2012.01.074.
- [200] F. Shahidi and Y. Zhong, "Lipid oxidation and improving the oxidative stability," *Chem. Soc. Rev.*, vol. 39, no. 11, pp. 4067–4079, Nov. 2010, doi: 10.1039/b922183m.
- [201] R. Vani *et al.*, "Prospects of Vitamin C as an Additive in Plasma of Stored Blood," *Adv. Hematol.*, vol. 2015, p. 961049, 2015, doi: 10.1155/2015/961049.
- [202] M. J. James, R. A. Gibson, and L. G. Cleland, "Dietary polyunsaturated fatty acids and inflammatory mediator production," *Am. J. Clin. Nutr.*, vol. 71, no. 1 Suppl, pp. 343S–8S, Jan. 2000, doi: 10.1093/ajcn/71.1.343s.
- [203] D. R. Johnson and E. A. Decker, "The Role of Oxygen in Lipid Oxidation Reactions: A Review," *Annu. Rev. Food Sci. Technol.*, vol. 6, no. 1, pp. 171–190, 2015, doi: 10.1146/annurev-food-022814-015532.
- [204] G. L. Milne, H. Yin, and J. D. Morrow, "Human biochemistry of the isoprostane pathway," *J. Biol. Chem.*, vol. 283, no. 23, pp. 15533–15537, Jun. 2008, doi: 10.1074/jbc.R700047200.
- [205] D. Praticò and J.-M. Dogné, "Vascular biology of eicosanoids and atherogenesis," *Expert Rev. Cardiovasc. Ther.*, vol. 7, no. 9, pp. 1079–1089, Sep. 2009, doi: 10.1586/erc.09.91.
- [206] Y. Urade and O. Hayaishi, "Prostaglandin D2 and sleep regulation," *Biochim. Biophys. Acta*, vol. 1436, no. 3, pp. 606–615, Jan. 1999, doi: 10.1016/s0005-2760(98)00163-5.
- [207] T. Hattori *et al.*, "G2A Plays Proinflammatory Roles in Human Keratinocytes under Oxidative Stress as a Receptor for 9-Hydroxyoctadecadienoic Acid," *J. Invest. Dermatol.*, vol. 128, no. 5, pp. 1123–1133, May 2008, doi: 10.1038/sj.jid.5701172.
- [208] G. C. Shearer and R. E. Walker, "An overview of the biologic effects of omega-6 oxylipins in humans," *Prostaglandins Leukot. Essent. Fatty Acids*, vol. 137, pp. 26–38, Oct. 2018, doi: 10.1016/j.plefa.2018.06.005.
- [209] E. Ricciotti and G. A. FitzGerald, "Prostaglandins and inflammation," *Arterioscler. Thromb. Vasc. Biol.*, vol. 31, no. 5, pp. 986–1000, May 2011, doi: 10.1161/ATVBAHA.110.207449.
- [210] O. Quehenberger, A. M. Armando, and E. A. Dennis, "High sensitivity quantitative lipidomics analysis of fatty acids in biological samples by gas chromatography-mass spectrometry," *Biochim. Biophys. Acta*, vol. 1811, no. 11, pp. 648–656, Nov. 2011, doi: 10.1016/j.bbalip.2011.07.006.
- [211] N. G. Bazan, V. Colangelo, and W. J. Lukiw, "Prostaglandins and other lipid mediators in Alzheimer's disease," *Prostaglandins Other Lipid Mediat.*, vol. 68–69, pp. 197–210, Aug. 2002, doi: 10.1016/s0090-6980(02)00031-x.
- [212] "JASP A Fresh Way to Do Statistics." Accessed: Jun. 28, 2022. [Online]. Available: https://jasp-stats.org/
- [213] "MetaboAnalyst 6.0: towards a unified platform for metabolomics data processing, analysis and interpretation | Nucleic Acids Research | Oxford Academic." [Online]. Available: https://academic.oup.com/nar/advance-article/doi/10.1093/nar/gkae253/7642060

- [214] N. Psychogios *et al.*, "The human serum metabolome," *PloS One*, vol. 6, no. 2, p. e16957, Feb. 2011, doi: 10.1371/journal.pone.0016957.
- [215] S. Wang, A. Ma, S. Song, Q. Quan, X. Zhao, and X. Zheng, "Fasting serum free fatty acid composition, waist/hip ratio and insulin activity in essential hypertensive patients," *Hypertens. Res. Off. J. Jpn. Soc. Hypertens.*, vol. 31, no. 4, pp. 623–632, Apr. 2008, doi: 10.1291/hypres.31.623.
- [216] O. Quehenberger *et al.*, "Lipidomics reveals a remarkable diversity of lipids in human plasma," *J. Lipid Res.*, vol. 51, no. 11, pp. 3299–3305, Nov. 2010, doi: 10.1194/jlr.M009449.
- [217] K. A. Massey and A. Nicolaou, "Lipidomics of oxidized polyunsaturated fatty acids," *Free Radic. Biol. Med.*, vol. 59, no. 100, pp. 45–55, Jun. 2013, doi: 10.1016/j.freeradbiomed.2012.08.565.
- [218] A. A. Askari, S. Thomson, M. L. Edin, F. B. Lih, D. C. Zeldin, and D. Bishop-Bailey, "Basal and inducible anti-inflammatory epoxygenase activity in endothelial cells," *Biochem. Biophys. Res. Commun.*, vol. 446, no. 2, pp. 633–637, Apr. 2014, doi: 10.1016/j.bbrc.2014.03.020.
- [219] E. D. Thuresson, K. M. Lakkides, and W. L. Smith, "Different catalytically competent arrangements of arachidonic acid within the cyclooxygenase active site of prostaglandin endoperoxide H synthase-1 lead to the formation of different oxygenated products," *J. Biol. Chem.*, vol. 275, no. 12, pp. 8501–8507, Mar. 2000, doi: 10.1074/jbc.275.12.8501.
- [220] S. Viswanathan, B. D. Hammock, J. W. Newman, P. Meerarani, M. Toborek, and B. Hennig, "Involvement of CYP 2C9 in Mediating the Proinflammatory Effects of Linoleic Acid in Vascular Endothelial Cells," *J. Am. Coll. Nutr.*, vol. 22, no. 6, pp. 502–510, Dec. 2003, doi: 10.1080/07315724.2003.10719328.
- [221] J. Seubert *et al.*, "Enhanced Postischemic Functional Recovery in CYP2J2 Transgenic Hearts Involves Mitochondrial ATP-Sensitive K+ Channels and p42/p44 MAPK Pathway," *Circ. Res.*, vol. 95, no. 5, pp. 506–514, Sep. 2004, doi: 10.1161/01.RES.0000139436.89654.c8.
- [222] J. G. Still and F. C. Greiss, "The effect of prostaglandins and other vasoactive substances on uterine blood flow and myometrial activity," *Am. J. Obstet. Gynecol.*, vol. 130, no. 1, pp. 1–8, Jan. 1978, doi: 10.1016/0002-9378(78)90430-1.
- [223] A. Konkel and W.-H. Schunck, "Role of cytochrome P450 enzymes in the bioactivation of polyunsaturated fatty acids," *Biochim. Biophys. Acta*, vol. 1814, no. 1, pp. 210–222, Jan. 2011, doi: 10.1016/j.bbapap.2010.09.009.
- [224] N. Brossard, M. Croset, C. Pachiaudi, J. P. Riou, J. L. Tayot, and M. Lagarde, "Retroconversion and metabolism of [13C]22:6n-3 in humans and rats after intake of a single dose of [13C]22:6n-3-triacylglycerols," *Am. J. Clin. Nutr.*, vol. 64, no. 4, pp. 577–586, Oct. 1996, doi: 10.1093/ajcn/64.4.577.
- [225] J. Suttnar, L. Mášová, and J. E. Dyr, "Influence of citrate and EDTA anticoagulants on plasma malondialdehyde concentrations estimated by high-performance liquid chromatography," *J. Chromatogr. B. Biomed. Sci. App.*, vol. 751, no. 1, pp. 193–197, Feb. 2001, doi: 10.1016/S0378-4347(00)00453-9.
- [226] E. Borras, L. Schrumpf, N. Stephens, B. C. Weimer, C. E. Davis, and E. S. Schelegle, "Novel LC-MS-TOF method to detect and quantify ascorbic and uric acid simultaneously in different biological matrices," *J. Chromatogr. B*, vol. 1168, p. 122588, Apr. 2021, doi: 10.1016/j.jchromb.2021.122588.

- [227] M.-O. Trépanier, M. Eiden, D. Morin-Rivron, R. P. Bazinet, and M. Masoodi, "High-resolution lipidomics coupled with rapid fixation reveals novel ischemia-induced signaling in the rat neurolipidome," *J. Neurochem.*, vol. 140, no. 5, pp. 766–775, 2017, doi: 10.1111/jnc.13934.
- [228] D. A. Sylvestre, Y. Otoki, A. H. Metherel, R. P. Bazinet, C. M. Slupsky, and A. Y. Taha, "Effects of hypercapnia / ischemia and dissection on the rat brain metabolome," *Neurochem. Int.*, vol. 156, p. 105294, Jun. 2022, doi: 10.1016/j.neuint.2022.105294.
- [229] Y. Otoki *et al.*, "Acute Hypercapnia/Ischemia Alters the Esterification of Arachidonic Acid and Docosahexaenoic Acid Epoxide Metabolites in Rat Brain Neutral Lipids," *Lipids*, vol. 55, no. 1, pp. 7–22, Jan. 2020, doi: 10.1002/lipd.12197.
- [230] O. Ousji and L. Sleno, "Identification of In Vitro Metabolites of Synthetic Phenolic Antioxidants BHT, BHA, and TBHQ by LC-HRMS/MS," *Int. J. Mol. Sci.*, vol. 21, no. 24, p. 9525, Dec. 2020, doi: 10.3390/ijms21249525.
- [231] M. A. Nayeem, "Role of oxylipins in cardiovascular diseases," *Acta Pharmacol. Sin.*, vol. 39, no. 7, pp. 1142–1154, Jul. 2018, doi: 10.1038/aps.2018.24.
- [232] L. Ferré-González, C. Peña-Bautista, M. Baquero, and C. Cháfer-Pericás, "Assessment of Lipid Peroxidation in Alzheimer's Disease Differential Diagnosis and Prognosis," *Antioxidants*, vol. 11, no. 3, p. 551, Mar. 2022, doi: 10.3390/antiox11030551.
- [233] T. d. Parker, D. a. Adams, K. Zhou, M. Harris, and L. Yu, "Fatty Acid Composition and Oxidative Stability of Cold-pressed Edible Seed Oils," *J. Food Sci.*, vol. 68, no. 4, pp. 1240–1243, 2003, doi: 10.1111/j.1365-2621.2003.tb09632.x.
- [234] I. Aidos, S. Lourenclo, A. Van Der Padt, J. b. Luten, and R. m. Boom, "Stability of Crude Herring Oil Produced from Fresh Byproducts: Influence of Temperature during Storage," *J. Food Sci.*, vol. 67, no. 9, pp. 3314–3320, 2002, doi: 10.1111/j.1365-2621.2002.tb09585.x.
- [235] E. Koç and B. Karayiğit, "Lipoxygenase activity and antioxidant capacity in pepper (Capsicum annum) exposed to high concentration of copper sulphate," *Environ. Exp. Biol.*, vol. 19, no. 2, Art. no. 2, Oct. 2021, doi: 10.22364/eeb.19.07.
- [236] F. Visioli, R. Bordone, C. Perugini, M. Bagnati, C. Cau, and G. Bellomo, "The Kinetics of Copper-Induced LDL Oxidation Depend upon Its Lipid Composition and Antioxidant Content," *Biochem. Biophys. Res. Commun.*, vol. 268, no. 3, pp. 818–822, Feb. 2000, doi: 10.1006/bbrc.2000.2212.
- [237] M. Kuzuya *et al.*, "Oxidation of low-density lipoprotein by copper and iron in phosphate buffer," *Biochim. Biophys. Acta*, vol. 1084, no. 2, pp. 198–201, Jul. 1991.
- [238] A. Surendran, H. Zhang, T. Winter, A. Edel, H. Aukema, and A. Ravandi, "Oxylipin profile of human low-density lipoprotein is dependent on its extent of oxidation," *Atherosclerosis*, vol. 288, pp. 101–111, Sep. 2019, doi: 10.1016/j.atherosclerosis.2019.07.018.
- [239] H. Yin, J. D. Brooks, L. Gao, N. A. Porter, and J. D. Morrow, "Identification of novel autoxidation products of the omega-3 fatty acid eicosapentaenoic acid in vitro and in vivo," *J. Biol. Chem.*, vol. 282, no. 41, pp. 29890–29901, Oct. 2007, doi: 10.1074/jbc.M703108200.
- [240] P. B. M. C. Derogis *et al.*, "The Development of a Specific and Sensitive LC-MS-Based Method for the Detection and Quantification of Hydroperoxy- and Hydroxydocosahexaenoic Acids as a Tool for Lipidomic Analysis," *PLOS ONE*, vol. 8, no. 10, p. e77561, Oct. 2013, doi: 10.1371/journal.pone.0077561.

- [241] I. Kusumoto, S. Kato, and K. Nakagawa, "Analysis of docosahexaenoic acid hydroperoxide isomers in mackerel using liquid chromatography-mass spectrometry," *Sci. Rep.*, vol. 13, no. 1, p. 1325, Jan. 2023, doi: 10.1038/s41598-023-28514-2.
- [242] L. J. Roberts *et al.*, "Formation of isoprostane-like compounds (neuroprostanes) in vivo from docosahexaenoic acid," *J. Biol. Chem.*, vol. 273, no. 22, pp. 13605–13612, May 1998, doi: 10.1074/jbc.273.22.13605.
- [243] S. Miyamoto, G. R. Martinez, D. Rettori, O. Augusto, M. H. G. Medeiros, and P. Di Mascio, "Linoleic acid hydroperoxide reacts with hypochlorous acid, generating peroxyl radical intermediates and singlet molecular oxygen," *Proc. Natl. Acad. Sci. U. S. A.*, vol. 103, no. 2, pp. 293–298, Jan. 2006, doi: 10.1073/pnas.0508170103.
- [244] S. Miyamoto *et al.*, "Biological hydroperoxides and singlet molecular oxygen generation," *IUBMB Life*, vol. 59, no. 4–5, pp. 322–331, 2007, doi: 10.1080/15216540701242508.
- [245] S. Miyamoto, G. R. Martinez, M. H. G. Medeiros, and P. Di Mascio, "Singlet molecular oxygen generated from lipid hydroperoxides by the russell mechanism: studies using 18(O)-labeled linoleic acid hydroperoxide and monomol light emission measurements," *J. Am. Chem. Soc.*, vol. 125, no. 20, pp. 6172–6179, May 2003, doi: 10.1021/ja0291150.
- [246] S. Miyamoto, G. R. Martinez, A. P. B. Martins, M. H. G. Medeiros, and P. Di Mascio, "Direct evidence of singlet molecular oxygen [O2(1Deltag)] production in the reaction of linoleic acid hydroperoxide with peroxynitrite," *J. Am. Chem. Soc.*, vol. 125, no. 15, pp. 4510–4517, Apr. 2003, doi: 10.1021/ja029262m.
- [247] H. Esterbauer, R. J. Schaur, and H. Zollner, "Chemistry and biochemistry of 4-hydroxynonenal, malonaldehyde and related aldehydes," *Free Radic. Biol. Med.*, vol. 11, no. 1, pp. 81–128, 1991, doi: 10.1016/0891-5849(91)90192-6.
- [248] J. A. Weiny, W. E. Boeglin, M. W. Calcutt, D. F. Stec, and A. R. Brash, "Monolayer autoxidation of arachidonic acid to epoxyeicosatrienoic acids as a model of their potential formation in cell membranes," *J. Lipid Res.*, vol. 63, no. 1, p. 100159, Jan. 2022, doi: 10.1016/j.jlr.2021.100159.
- [249] M. Hennebelle. et al, "Linoleic acid participates in the response to ischemic brain injury through oxidized metabolites that regulate neurotransmission," *Sci Rep*, vol. 7, no. 4342, 2017, doi: doi.org/10.1038/s41598-017-02914-7.
- [250] R. Chaleckis, I. Meister, P. Zhang, and C. E. Wheelock, "Challenges, progress and promises of metabolite annotation for LC-MS-based metabolomics," *Curr. Opin. Biotechnol.*, vol. 55, pp. 44–50, Feb. 2019, doi: 10.1016/j.copbio.2018.07.010.
- [251] A. Martín-Sómer, M. Yáñez, M.-P. Gaigeot, and R. Spezia, "Unimolecular fragmentation induced by low-energy collision: statistically or dynamically driven?," *J. Phys. Chem. A*, vol. 118, no. 46, pp. 10882–10893, Nov. 2014, doi: 10.1021/jp5076059.
- [252] Y. Qi and D. A. Volmer, "Electron-based fragmentation methods in mass spectrometry: An overview," *Mass Spectrom. Rev.*, vol. 36, no. 1, pp. 4–15, Jan. 2017, doi: 10.1002/mas.21482.
- [253] R. N. Hayes and M. L. Gross, "Collision-induced dissociation," *Methods Enzymol.*, vol. 193, pp. 237–263, 1990, doi: 10.1016/0076-6879(90)93418-k.
- [254] Wang, M., Carver, J., Phelan, V. et al, "Sharing and community curation of mass spectrometry data with Global Natural Products Social Molecular Networking," *Nat Biotechnol*, vol. 34, no. 828–837, 2016, doi: doi.org/10.1038/nbt.3597.

[255] Lise Cougnaud, "The effect of diet and probiotic administration on lipid dysregulation and gut microbiota dysbiosis during atherosclerosis development," PhD thesis, Department of Chemistry and Biochemistry, Concordia University 2024.

Appendix A: Supplementary information for Chapter 2

Supplementary Table A1: List of oxylipins evaluated during stability studies in Chapter 2

Full name	Abbreviation	Formula	Precursor	[M-H] ⁻ m/z	Retention time (min.)	FT stability Study (Standard)	FT stability Study (Spiked plasma)	FT stability Study (Non- spiked plasma)	RT stability study (Spiked plasma)
linoleic acid	LA	$C_{18}H_{32}O_2$	Precursor	279.2330	29.78	X	X	X	X
9-hydroxy-10E,12Z,15Z- octadecatrienoic acid	9-HOTrE	C ₁₈ H ₃₀ O ₃	LA	293.2122	18.96	X	X	X	Spiked but below LOQ
13-hydroxy-9Z,11E,15Z- octadecatrienoic acid	13-HOTrE	C ₁₈ H ₃₀ O ₃	LA	293.2122	19.34				X
9-oxo-10E,12Z-octadecadienoic acid	9-oxoODE	$C_{18}H_{30}O_3$	LA	293.2122	22.23	X	X	X	X
13-oxo-9Z,11E-octadecadienoic acid	13-oxoODE	$C_{18}H_{30}O_3$	LA	293.2122	21.75	X	X	X	X
9-hydroxy-10E,12Z-octadecadienoic acid	9-HODE	C ₁₈ H ₃₂ O ₃	DHA	295.2279	21.23	X	X	X	X
13-hydroxy-10E,12Z-octadecadienoic acid	13-HODE	C ₁₈ H ₃₂ O ₃	DHA	295.2279	21.14	X	X	X	X
eicosapentaenoic acid	EPA	$C_{20}H_{30}O_2$	Precursor	301.2173	27.32	X	X	X	X
arachidonic acid	AA	$C_{20}H_{32}O_2$	Precursor	303.2330	29.43	X	X	X	X
12,13-dihydroxy-9Z-octadecenoic acid	12,13- DiHOME	$C_{18}H_{34}O_4$	LA	313.2384	16.92	X	Spiked but below LOQ		Spiked but below LOQ
9,10-dihydroxy-12Z-octadecenoic acid	9,10- DiHOME	C ₁₈ H ₃₄ O ₄	LA	313.2384	17.48	X	Spiked but below LOQ		Spiked but below LOQ
18-hydroxy- 5Z,8Z,11Z,14Z,16Eeicosapentaenoic acid	18-НЕРЕ	C ₂₀ H ₃₀ O ₃	EPA	317.2122	19.45	X	Spiked but below LOQ		X

Full name	Abbreviation	Formula	Precursor	[M-H] ⁻ m/z	Retention time (min.)	FT stability study for pre- extraction loading (Standard)	FT stability study for post- extraction loading (Standard)	FT stability study for pre- extractio n loading (Spiked plasma)	FT stability study for post- extraction loading (Spiked plasma)
11,12-epoxyeicosatetraenoic acid	11,12-EpETE	$C_{20}H_{30}O_3$	EPA	317.2122	22.57	X	Spiked but below LOQ		X
8-hydroxy- 5Z,7E,11Z,14Z,17Zeicosapentaenoic acid	8-НЕРЕ	$C_{20}H_{30}O_3$	EPA	317.2122	20.42	X	Spiked but below LOQ		
15-hydroxy-5Z,8Z,11Z,13E,17Z- eicosapentaenoic acid	15-НЕРЕ	C ₂₀ H ₃₀ O ₃	EPA	317.2122	19.99				X
20-hydroxy-5Z,8Z,11Z,13E,17Z- eicosapentaenoic acid	20-НЕРЕ	C ₂₀ H ₃₀ O ₃	EPA	317.2122	18.93	X	Spiked but below LOQ		Spiked but below LOQ
5-hydroxy-5Z,8Z,11Z,13E,17Z- eicosapentaenoic acid	5-НЕРЕ	C ₂₀ H ₃₀ O ₃	EPA	317.2122	21.12	X	X	X	X
11-hydroxy- 5Z,8Z,12E,14Z,17Zeicosapentaenoic acid	11-НЕРЕ	$C_{20}H_{30}O_3$	EPA	317.2122	20.23	X	Spiked but below LOQ		
5-oxo-eicosatetraenoic acid	5-oxoETE	$C_{20}H_{30}O_3$	AA	317.2122	24.40		X	X	X
12-hydroxy- 5Z,8Z,12E,14Z,17Zeicosapentaenoic acid	12-НЕРЕ	$C_{20}H_{30}O_3$	EPA	317.2122	20.55	X	Spiked but below LOQ		
16-hydroxy- 5Z,8Z,11Z,13 E- eicosatetraenoic acid	16-НЕТЕ	C ₂₀ H ₃₂ O ₃	AA	319.2279	20.68				X
15-hydroxy- 5Z,8Z,11Z,13 E- eicosatetraenoic acid	15-НЕТЕ	C ₂₀ H ₃₂ O ₃	AA	319.2279	21.62		X	X	X
5-hydroxy- 6E,8Z,11Z,14 Z- eicosatetraenoic acid	5-НЕТЕ	$C_{20}H_{32}O_3$	AA	319.2279	23.17		X	X	X

Full name	Abbreviation	Formula	Precursor	[M-H] ⁻ m/z	Retention time (min.)	FT stability study for pre- extraction loading (Standard)	FT stability study for post- extraction loading (Standard)	FT stability study for pre- extractio n loading (Spiked plasma)	FT stability study for post- extraction loading (Spiked plasma)
11-hydroxy- 6E,8Z,11Z,14 Z- eicosatetraenoic acid	11-НЕТЕ	$C_{20}H_{32}O_3$	AA	319.2279	22.60	X	X	X	X
9-hydroxy-5Z,7E,11Z,14Z- eicosatetraenoic acid	9-НЕТЕ	$C_{20}H_{32}O_3$	AA	319.2279	22.86	X	X	X	X
11(12)-epoxy-5Z,8Z,14Z-eicosatrienoic acid	11,12-EET	$C_{20}H_{32}O_3$	AA	319.2279	24.72	X	Spiked but below LOQ		
8(9)-epoxy-5Z,8Z,14Z-eicosatrienoic acid	8,9-EET	C ₂₀ H ₃₂ O ₃	AA	319.2279	25.18	X	Spiked but below LOQ		
15-hydroxy-11Z,13E-eicosadienoic acid	15-HEDE	C ₂₀ H ₃₆ O ₃	AA	323.2592	24.66	X	Spiked but below LOQ		X
docosahexaenoic acid	DHA	C ₂₂ H ₃₂ O ₂	Precursor	327.2330	29.11	X	X	X	X
leukotriene B4	LTB4	$C_{20}H_{32}O_4$	AA	335.2222	16.36	X	X	X	X
8,15-dihydroxy- 5Z,9E,11Z,13 E- eicosatetraenoic acid	8,15-DiHETE	C ₂₀ H ₃₂ O ₄	AA	335.2228	15.55	X	X	X	X
5,15-dihydroxy-6E,8Z,10Z,13E-eicosatetraenoic acid	5,15-DiHETE	C ₂₀ H ₃₂ O ₄	AA	335.2228	15.96	X	X	X	X
5,12-dihydroxy-6E,8Z,10E,14Z-eicosatetraenoic acid	5,12-DiHETE	C ₂₀ H ₃₂ O ₄	AA	335.2228	16.93	X	X	X	X
5,6-dihydroxy-7E,9E,11Z,14Z- eicosatetraenoic acid	5,6-DiHETE	C ₂₀ H ₃₂ O ₄	AA	335.2228	19.81	X	Spiked but below LOQ		
11,12-dihydroxy-5Z,8Z,14Z- eicosatrienoic acid	11,12-DiHET	C ₂₀ H ₃₄ O ₄	AA	337.2384	18.70	X	X	X	
14,15-dihydroxy-5Z,8Z,14Z- eicosatrienoic acid	14,15-DiHET	C ₂₀ H ₃₄ O ₄	AA	337.2384	17.99	X	Spiked but below LOQ		
7-hydroxydocosahexaenoic acid	7-HDHA	C ₂₂ H ₃₂ O ₃	DHA	343.2279	22.86	X	Spiked but below LOQ		

Full name	Abbreviation	Formula	Precursor	[M-H] ⁻ m/z	Retention time (min.)	FT stability study for pre- extraction loading (Standard)	FT stability study for post- extraction loading (Standard)	FT stability study for pre- extractio n loading (Spiked plasma)	FT stability study for post- extraction loading (Spiked plasma)
8-hydroxydocosahexaenoic acid	8-HDHA	$C_{22}H_{32}O_3$	DHA	343.2279	23.01	X	Spiked but below LOQ		
13-hydroxydocosahexaenoic acid	13-HDHA	$C_{22}H_{32}O_3$	DHA	343.2279	22.23	X	X	X	X
11-hydroxydocosahexaenoic acid	11-HDHA	$C_{22}H_{32}O_3$	DHA	343.2279	22.72	X	X	X	X
10-hydroxydocosahexaenoic acid	10-HDHA	$C_{22}H_{32}O_3$	DHA	343.2279	22.42	X	X	X	X
14-hydroxydocosahexaenoic acid	14-HDoHE	$C_{22}H_{32}O_3$	DHA	343.2279	22.46	X	X	X	X
20-hydroxydocosahexaenoic acid	20-HDoHE	$C_{22}H_{32}O_3$	DHA	343.2279	21.45	X	X	X	X
17-hydroxydocosahexaenoic acid	17-HDoHE	$C_{22}H_{32}O_3$	DHA	343.2279	21.96	X	X	X	X
4-hydroxydocosahexaenoic acid	4-HDoHE	$C_{22}H_{32}O_3$	DHA	343.2279	23.75	X	X	X	X
prostaglandin E2	PGE2	C ₂₀ H ₃₂ O ₅	AA	351.2177	10.83	X	Spiked but below LOQ		
prostaglandin D2	PGD2	$C_{20}H_{32}O_5$	AA	351.2177	11.28	X	Spiked but below LOQ		
8-iso-15(R)-prostaglandin F2α	8-iso-15(R)- PGF2α	$C_{20}H_{34}O_5$	AA	353.2334	9.20	X	Spiked but below LOQ		X
8-iso-prostaglandinF2α	8-iso-PGF2α	$C_{20}H_{34}O_5$	AA	353.2334	9.42	X	Spiked but below LOQ		
8-iso-prostaglandinF2β	8-iso-PGF2β	$C_{20}H_{34}O_5$	AA	353.2334	9.49				X
11β-prostaglandinF2α	11β-PGF2α	$C_{20}H_{34}O_5$	AA	353.2334	9.66	X	X		X
15(R)-prostaglandinF2α	15(R)-PGF2α	$C_{20}H_{34}O_{5}$	AA	353.2334	10.38	X	X		X
prostaglandinF2α	PGF2α	$C_{20}H_{34}O_5$	AA	353.2334	10.53	X	Spiked but below LOQ		Spiked but below LOQ
19,20-dihydroxyldocosapentaenoic acid	19,20- DiHDPA	$C_{22}H_{34}O_4$	DHA	361.2379	18.05	X	Spiked but below LOQ		Spiked but below LOQ
prostaglandinF2α ethanolamide	PGF2αEA	C ₂₂ H ₃₉ NO 5	AA	396.2755	7.95	X	Spiked but below LOQ		

Full name	Abbreviation	Formula	Precursor	[M-H] ⁻ m/z	Retention time (min.)	FT stability study for pre- extraction loading (Standard)	FT stability study for post- extraction loading (Standard)	FT stability study for pre- extractio n loading (Spiked plasma)	FT stability study for post- extraction loading (Spiked plasma)
leukotriene D4	LTD4	$\begin{array}{c} C_{25}H_{40}N_2 \\ O_6S \end{array}$	AA	495.2534	12.99	X	Spiked but below LOQ		

 $X = tested \ oxylipins \ in \ various \ stability \ studies. \ RT = Room \ temperature. \ FT = freeze \ and \ thaw$

Supplementary Table A2: Summary of the results of 3-freeze-and-thaw cycle study for oxylipins extracted using SPME from standard mix. The results are shown as mean concentration (ng/mL) \pm SD for oxylipins that failed accepted criteria of concentration within 80-120% of 0-T and ANOVA p value <0.05.

Oxylipins	Control 0-T (ng/mL)	1-FT cycle (ng/mL)	2-FT cycles (ng/mL)	3-FT cycles (ng/mL)	ANOVA p-value
PGE2	9.8±2	13.2±2	11.3±0.8	13.9±2	0.023
AA	34±8	30.5±6	21.1±7	18.3±6	0.048

Supplementary Table A3: Summary of the results of 3-freeze-and-thaw cycle study for oxylipins extracted using SPME from spiked citrate plasma. The results are shown as mean concentration $(ng/mL) \pm SD$ for oxylipins that failed accepted criteria of concentration within 80-120% of 0-T and ANOVA < 0.05

Oxylipins	Control 0-T (ng/mL)	1-FT cycle (ng/mL)	2-FT cycles (ng/mL)	3-FT cycles (ng/mL)	ANOVA p-value
13-HDHA	1.9 ± 0.2	3.1±0.3	2.4±0.1	2.6 ± 0.1	< 0.001
11-HDHA	1.5±0.2	2.2±0.2	1.8±0.2	2.1±0.1	< 0.001

Supplementary Table A4: Peak areas of identified in-house oxylipins for precursors' 3-cycle degradation.

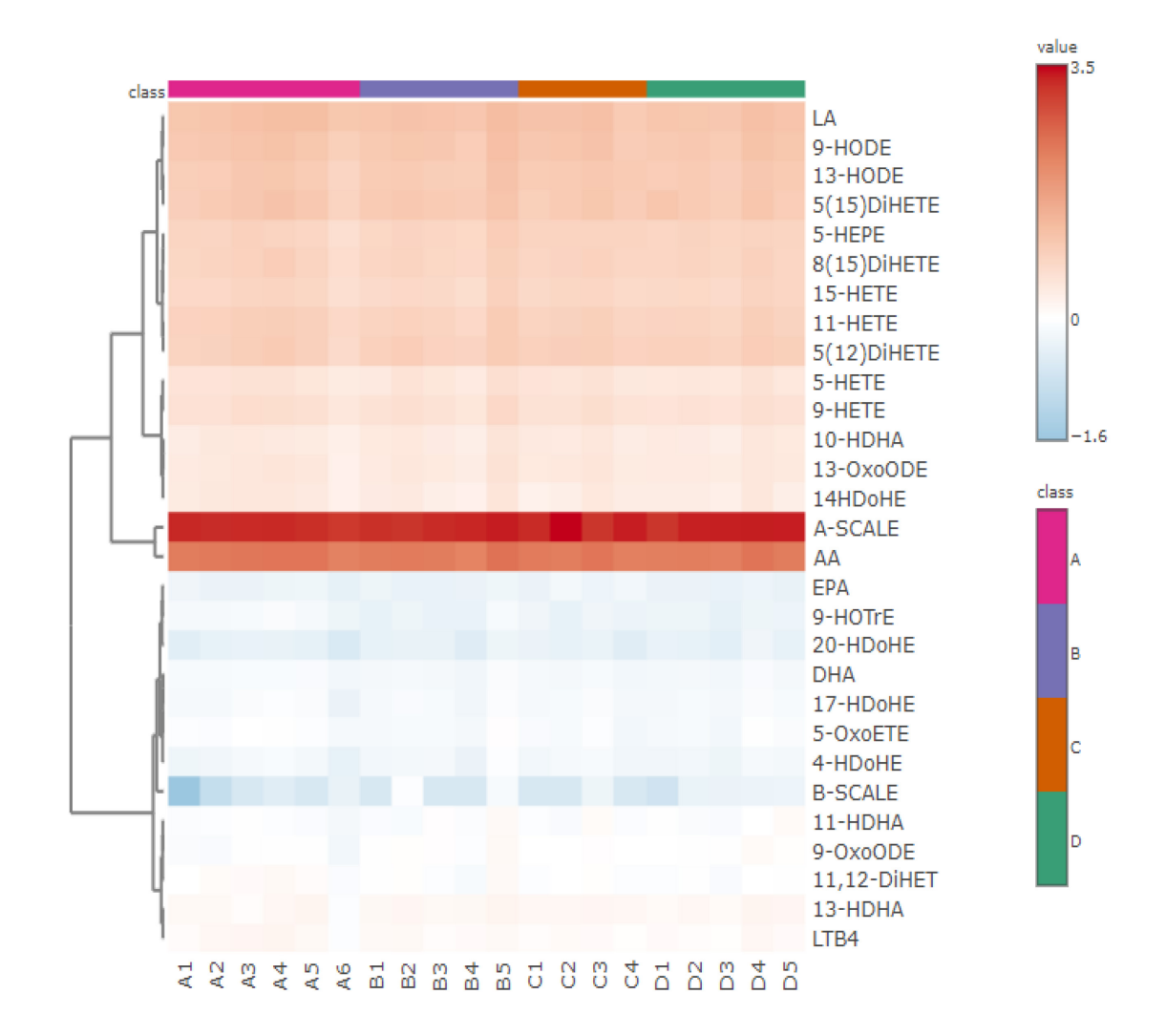
Experimental [M-H]- m/z	Oxylipins	Retention time (min)	Control 0-T	1-FT cycle	2-FT cycles	3-FT cycles	ANOVA p-valve
293.2122	13-oxoODE	21.56	82048±44805	93858±67347	73721±17925	140261±45734	0.376
317.2122	8-HEPE	20.33	14033±3380	12967±26944	21408±4657	24949±2141	0.06
317.2122	5-HEPE	20.98	32641±3605	30056±9647	45418±6974	48508±4792	0.022
343.2279	20-HDoHE	21.26	34791±3907	36016±15741	53462±8925	89783±37537	0.039
343.2279	14-HDoHE	22.02	13269±3517	34070±4767	22987±18191	23412±8102	0.192
343.2279	8-HDHA	23.06	88487±12515	106808±21215	158601±17824	201379±25578	<0.001
343.2279	4-HDoHE	23.64	24468±2584	24675±6602	28111±3224	43358±1253	<0.001

Supplementary Table A5: Summary of the results comparing the concentration of oxylipins of identified from 3-freeze-and-thaw cycle of precursors extracted from standard solution and stored on SPME devices to concentration measured in HDMB.

Known oxylipins	Precursor	Normal concentration in blood (µM) reported in HDMB	Estimated degradation of precursor from our study (%)	How much oxylipin were produced by precursors in our study (µM)	Significant
5-HEPE	EPA	0.007	0.07	0.0120	Yes
4-HDHA	DHA	0.0053	0.007	0.00102	Yes
20-HDHA	DHA	0.00028	0.009	0.00136	Yes
14-HDHA	DHA	0.00164	0.03	0.00409	Yes
8-HEPE	EPA	0.00134	0.0004	0.00601	Yes
8-HDHA	DHA	0.000294	0.1	0.02036	Yes

Supplementary Table A6: Summary of the results of 3-freeze-and-thaw cycle study for oxylipins extracted using SPME from non-spiked citrate plasma. The results are shown as mean concentration (ng/mL) \pm SD for oxylipins that failed the accepted criteria of concentration within 80-120% of 0-T and ANOVA < 0.05.

Oxylipins	Control 0-T (ng/mL)	1-FT cycle (ng/mL)	2-FT cycles (ng/mL)	3-FT cycles (ng/mL)	ANOVA p-value
9-HOTrE	0.7 ± 0.1	0.5±0.1	0.5±0.1	0.5±0.1	0.008
9-oxoODE	0.8 ± 0.1	1.1±0.2	1.0±0.03	1.1±0.1	0.012



Supplementary Figure A1: Heatmap results of 3-cycle freeze-and-thaw stability study for 27 oxylipins extracted on HLB SPME devices from spiked plasma samples. Heatmap was built using log transformation with hierarchical clustering, and Euclidean distance using MetaboAnalyst, where A =Control samples (n=6), B = 1-FT cycles (n=5), C=2-FT cycles (n=4), and D = 3-FT cycles (n=5). The row A-SCALE and B-SCALE were added to the raw data to show all hierarchical maps in this chapter on the same scal

Appendix B: Supplementary information for Chapter 3

Supplementary Table B1: List of oxylipins evaluated during the 3-freeze-and-thaw (FT) cycles stability studies of oxylipins with pre-and post-extraction loading of BHT

Full name	Abbreviation	Formula	Precursor	[M-H] ⁻ m/z	Retention time (min.)	FT stability study for pre- extraction loading (Standard)	FT stability study for post- extraction loading (Standard)	FT stability study for pre- extraction loading (Spiked plasma)	FT stability study for post- extraction loading (Spiked plasma)
linoleic acid	LA	$C_{18}H_{32}O_2$	Precursor	279.2330	29.78	X	X	X	X
9-hydroxy-10E,12Z,15Z- octadecatrienoic acid	9-HOTrE	C ₁₈ H ₃₀ O ₃	LA	293.2122	18.96	X	X	Spiked but below LOQ	Spiked but below LOQ
9-oxo-10E,12Z- octadecadienoic acid	9-oxoODE	$C_{18}H_{30}O_3$	LA	293.2122	22.23	X	X	X	X
13-oxo-9Z,11E- octadecadienoic acid	13-oxoODE	$C_{18}H_{30}O_3$	LA	293.2122	21.75	X	X	X	X
9-hydroxy-10E,12Z- octadecadienoic acid	9-HODE	$C_{18}H_{32}O_3$	DHA	295.2279	21.23	X	X	X	X
13-hydroxy-10E,12Z- octadecadienoic acid	13-HODE	$C_{18}H_{32}O_3$	DHA	295.2279	21.14	X	X	X	X
arachidonic acid	AA	$C_{20}H_{32}O_2$	Precursor	303.2330	29.43	X	X	X	X
12,13-dihydroxy-9Z- octadecenoic acid	12,13-DiHOME	C ₁₈ H ₃₄ O ₄	LA	313.2384	16.92	X	X	Spiked but below LOQ	Spiked but below LOQ
9,10-dihydroxy-12Z- octadecenoic acid	9,10-DiHOME	C ₁₈ H ₃₄ O ₄	LA	313.2384	17.48	X	X	Spiked but below LOQ	Spiked but below LOQ

Full name	Abbreviation	Formula	Precursor	[M-H] ⁻ m/z	Retention time (min.)	FT stability study for pre- extraction loading (Standard)	FT stability study for post- extraction loading (Standard)	FT stability study for pre- extraction loading (Spiked plasma)	FT stability study for post- extraction loading (Spiked plasma)
18-hydroxy- 5Z,8Z,11Z,14Z,16E- eicosapentaenoic acid	18-НЕРЕ	$C_{20}H_{30}O_3$	EPA	317.2122	19.45	X	X	Spiked but below LOQ	Spiked but below LOQ
11,12-epoxyeicosatetraenoic acid	11,12-EpETE	$C_{20}H_{30}O_3$	EPA	317.2122	22.57	X	X	Spiked but below LOQ	Spiked but below LOQ
8-hydroxy- 5Z,7E,11Z,14Z,17Z- eicosapentaenoic acid	8-НЕРЕ	$C_{20}H_{30}O_3$	EPA	317.2122	20.42	X	X	Spiked but below LOQ	Spiked but below LOQ
20-hydroxy- 5Z,8Z,11Z,13E,17Z- eicosapentaenoic acid	20-НЕРЕ	$C_{20}H_{30}O_3$	EPA	317.2122	18.93	X	X	Spiked but below LOQ	Spiked but below LOQ
5-hydroxy- 5Z,8Z,11Z,13E,17Z- eicosapentaenoic acid	5-HEPE	$C_{20}H_{30}O_3$	EPA	317.2122	21.12	X	X	Spiked but below LOQ	Spiked but below LOQ
12-hydroxy- 5Z,8Z,11Z,13 E- eicosatetraenoic acid	12-НЕТЕ	$C_{20}H_{32}O_3$	AA	319.2279	21.93	X	X	X	X
20-hydroxy- 5Z,8Z,11Z,13 E- eicosatetraenoic acid	20-НЕТЕ	$C_{20}H_{32}O_3$	AA	319.2279	19.40	X	X	Spiked but below LOQ	Spiked but below LOQ
15-hydroxy- 5Z,8Z,11Z,13 E- eicosatetraenoic acid	15-HETE	$C_{20}H_{32}O_3$	AA	319.2279	21.62	X	X	X	X
5-hydroxy- 6E,8Z,11Z,14 Z- eicosatetraenoic acid	5-НЕТЕ	$C_{20}H_{32}O_3$	AA	319.2279	23.17			X	X
9-hydroxy-5Z,7E,11Z,14Z- eicosatetraenoic acid	9-НЕТЕ	$C_{20}H_{32}O_3$	AA	319.2279	22.86	X	X	X	X

Full name	Abbreviation	Formula	Precursor	[M-H] ⁻ m/z	Retention time (min.)	FT stability study for pre- extraction loading (Standard)	FT stability study for post- extraction loading (Standard)	FT stability study for pre- extraction loading (Spiked plasma)	FT stability study for post- extraction loading (Spiked plasma)
11(12)-epoxy-5Z,8Z,14Z-eicosatrienoic acid	11,12-EET	$C_{20}H_{32}O_3$	AA	319.2279	24.72	X	X	Spiked but below LOQ	Spiked but below LOQ
15-hydroxy-11Z,13E- eicosadienoic acid	15-HEDE	$C_{20}H_{36}O_{3}$	AA	323.2592	24.66	X	X	Spiked but below LOQ	Spiked but below LOQ
docosahexaenoic acid	DHA	$C_{22}H_{32}O_2$	Precursor	327.2330	29.11	X	X	X	X
leukotriene B4	LTB4	$C_{20}H_{32}O_4$	AA	335.2222	16.36	X	X	X	X
8,15-dihydroxy- 5Z,9E,11Z,13 E- eicosatetraenoic acid	8,15-DiHETE	$C_{20}H_{32}O_4$	AA	335.2228	15.55	X	X	X	X
5,12-dihydroxy- 6E,8Z,10E,14Z- eicosatetraenoic acid	5,12-DiHETE	$C_{20}H_{32}O_4$	AA	335.2228	16.93	X	X	X	X
5,6-dihydroxy-7E,9E,11Z,14Z-eicosatetraenoic acid	5,6-DiHETE	$C_{20}H_{32}O_4$	AA	335.2228	19.81	X	X	Spiked but below LOQ	Spiked but below LOQ
11,12-dihydroxy-5Z,8Z,14Z-eicosatrienoic acid	11,12-DiHET	$C_{20}H_{34}O_4$	AA	337.2384	18.70	X	X	Spiked but below LOQ	Spiked but below LOQ
14,15-dihydroxy-5Z,8Z,14Z- eicosatrienoic acid	14,15-DiHET	C ₂₀ H ₃₄ O ₄	AA	337.2384	17.99	X	X	X	X
8-hydroxydocosahexaenoic acid	8-HDHA	C ₂₂ H ₃₂ O ₃	DHA	343.2279	23.01	X	X	Spiked but below LOQ	Spiked but below LOQ
13-hydroxydocosahexaenoic acid	13-HDHA	C ₂₂ H ₃₂ O ₃	DHA	343.2279	22.23	X	X	X	X

Full name	Abbreviation	Formula	Precursor	[M-H] ⁻ m/z	Retention time (min.)	FT stability study for pre- extraction loading (Standard)	FT stability study for post- extraction loading (Standard)	FT stability study for pre- extraction loading (Spiked plasma)	FT stability study for post- extraction loading (Spiked plasma)
11-hydroxydocosahexaenoic acid	11-HDHA	$C_{22}H_{32}O_3$	DHA	343.2279	22.72	X	X	X	X
16-hydroxydocosahexaenoic acid	16-НДоНЕ	$C_{22}H_{32}O_3$	DHA	343.2279	21.96	X	X	X	X
4-hydroxydocosahexaenoic acid	4-HDoHE	$C_{22}H_{32}O_3$	DHA	343.2279	23.75	X	X	X	X
prostaglandin E2	PGE2	$C_{20}H_{32}O_5$	AA	351.2177	10.83	X	X	Spiked but below LOQ	Spiked but below LOQ
8-iso-15(R)-prostaglandin F2α	8-iso-15(R)- PGF2α	$C_{20}H_{34}O_5$	AA	353.2334	9.20	X	X	X	Spiked but below LOQ
8-iso-prostaglandinF2β	8-iso-PGF2β	$C_{20}H_{34}O_5$	AA	353.2334	9.49	X	X	X	Spiked but below LOQ
11β-prostaglandinF2α	11β-PGF2α	$C_{20}H_{34}O_5$	AA	353.2334	9.66	X	X	X	Spiked but below LOQ
15(R)-prostaglandinF2α	15(R)-PGF2α	$C_{20}H_{34}O_5$	AA	353.2334	10.38	X	X	X	X
prostaglandinF2α	PGF2α	$C_{20}H_{34}O_5$	AA	353.2334	10.53	X	X	X	Spiked but below LOQ
19,20- dihydroxyldocosapentaenoic acid	19,20-DiHDPA	C ₂₂ H ₃₄ O ₄	DHA	361.2379	18.05	X	X	Spiked but below LOQ	Spiked but below LOQ

 $X = tested \ oxylipins \ in \ various \ stability \ studies.$ FT= freeze and thaw

Supplementary Table B2: Summary of the results of the 3-freeze-and-thaw cycle study of pre-loading extraction of BHT(5-h) and identified unstable oxylipins extracted using SPME from standard solution in **Section 2.3.1**. The results are shown as mean concentration (ng/mL) \pm SD for oxylipins that passed the accepted criteria of concentration within 80-120% of 0-T and ANOVA <0.05.

Oxylipins	Control 0-T (ng/mL)	1-FT cycles (ng/mL)	2-FT cycles (ng/mL)	3-FT cycles (ng/mL)	ANOVA p-value
AA	47.9±6	66.8±6	63.1±10	44.6±6	0.162
PGE2	75.2±8	80.9±15	77.6±19	76.8±7	0.936

^{*} The number of replicates was n=4 for all conditions

Supplementary Table B3: Summary of the results of 3- freeze-and-thaw cycle study of post-loading extraction of BHT (5 min.) and identified unstable oxylipins extracted using SPME from standard solution in Section 2.3.1. The results are shown as mean concentration (ng/mL) \pm SD **for** oxylipins that passed the accepted criteria of concentration within 80-120% of 0-T and ANOVA < 0.05.

Oxylipins	Control 0-T (ng/mL)	1-FT cycles (ng/mL)	2-FT cycles (ng/mL)	3-FT cycles (ng/mL)	ANOVA p-value
AA	49.7±18	37.5±25	56.1±43	35.2±33	0.417
PGE2	49.9±12	66.1±9	55.2±19	61.8±7	0.468

^{*} The number of replicates was n=4 for all conditions

Supplementary Table B4: Summary result of the average amount of BHT remaining on SPME fibres (ng) during 3-freeze-and-thaw cycle stability study. In this experiment, pre-extraction loading of BHT (5-h) from standard solution was used.

Antioxidants	Control 0-T (ng)	1-FT cycles (ng)	2-FT cycles (ng)	3-FT cycles (ng)	ANOVA p-value (Control and 3 FT cycles)	ANOVA p-value (3-FT cycles)
BHT	1745±74	1684±226	1534±114	1639±83	0.227	0.404

^{*}The number of replicates was n=4 for all conditions.

Supplementary Table B5: Summary result of the average amount of BHT remaining on SPME fibres (ng) during 3-freeze-and-thaw cycle stability study. In this experiment, post-extraction loading of BHT (5 min.) from standard solution was used.

Antioxidants	Control 0-T (ng)	1-FT cycles (ng)	2-FT cycles (ng)	3-FT cycles (ng)	ANOVA p-value (Control and 3 FT cycles)	ANOVA p-value (3-FT cycles)
BHT	999±313	443±100	386±96	531±115	0.002	0.193

^{*}The number of replicates was n=4 for all conditions.

Supplementary Table B6: Summary result of the average amount of BHT remaining on SPME fibres (ng) during 3-freeze-and-thaw cycle stability study. In this experiment, pre-extraction loading (5-hs) of BHT from spiked citrate plasma was used.

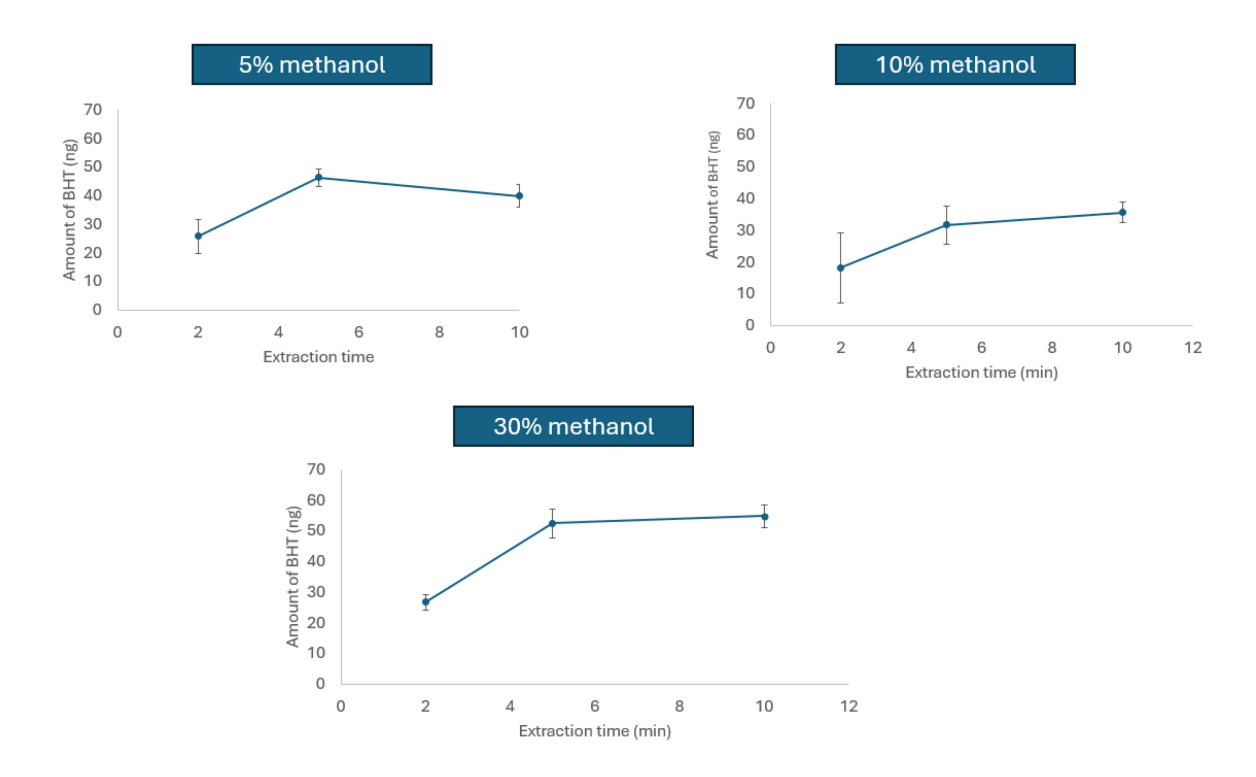
Antioxidants	Control	1-FT cycle	2-FT cycles	3-FT	ANOVA	ANOVA
	0-T	Amount	Amount	cycles	p-value	p-value
	Amount	remaining	remaining	Amount	(Control	(3-FT
	remaining	(ng)	(ng)	remaining	and	cycles)
	(ng)			(ng)	3 FT cycles)	
BHT	472±11	642±52	667±62	657±65	0.001	0.849

^{*}The number of replicates was n=4 for all conditions.

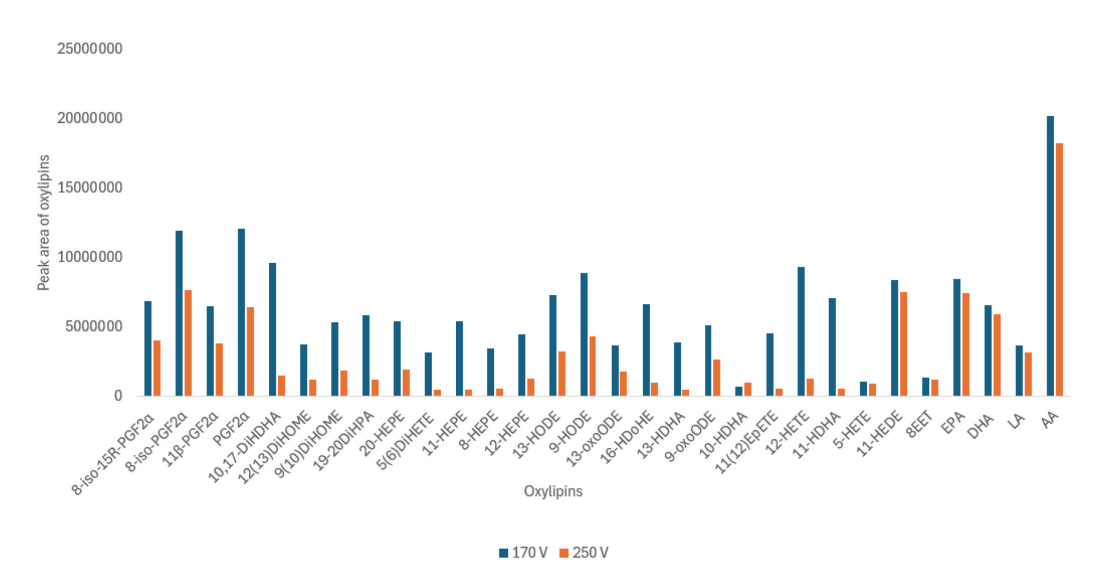
Supplementary Table B7: Summary result of the average amount of BHT remaining on SPME fibres (ng) during 3- freeze-and-thaw cycle stability study. In this experiment, post-extraction loading of BHT (5 min.) from spiked citrate plasma was used.

Antioxidants	Control 0-T Amount (ng)	1-FT cycle Amount (ng)	2-FT cycles Amount (ng)	3-FT cycles Amount (ng)	ANOVA p-Value	ANOVA p-value (3-FT cycles)
BHT	157±40	293±126	386±126	337.±39	0.025	0.485

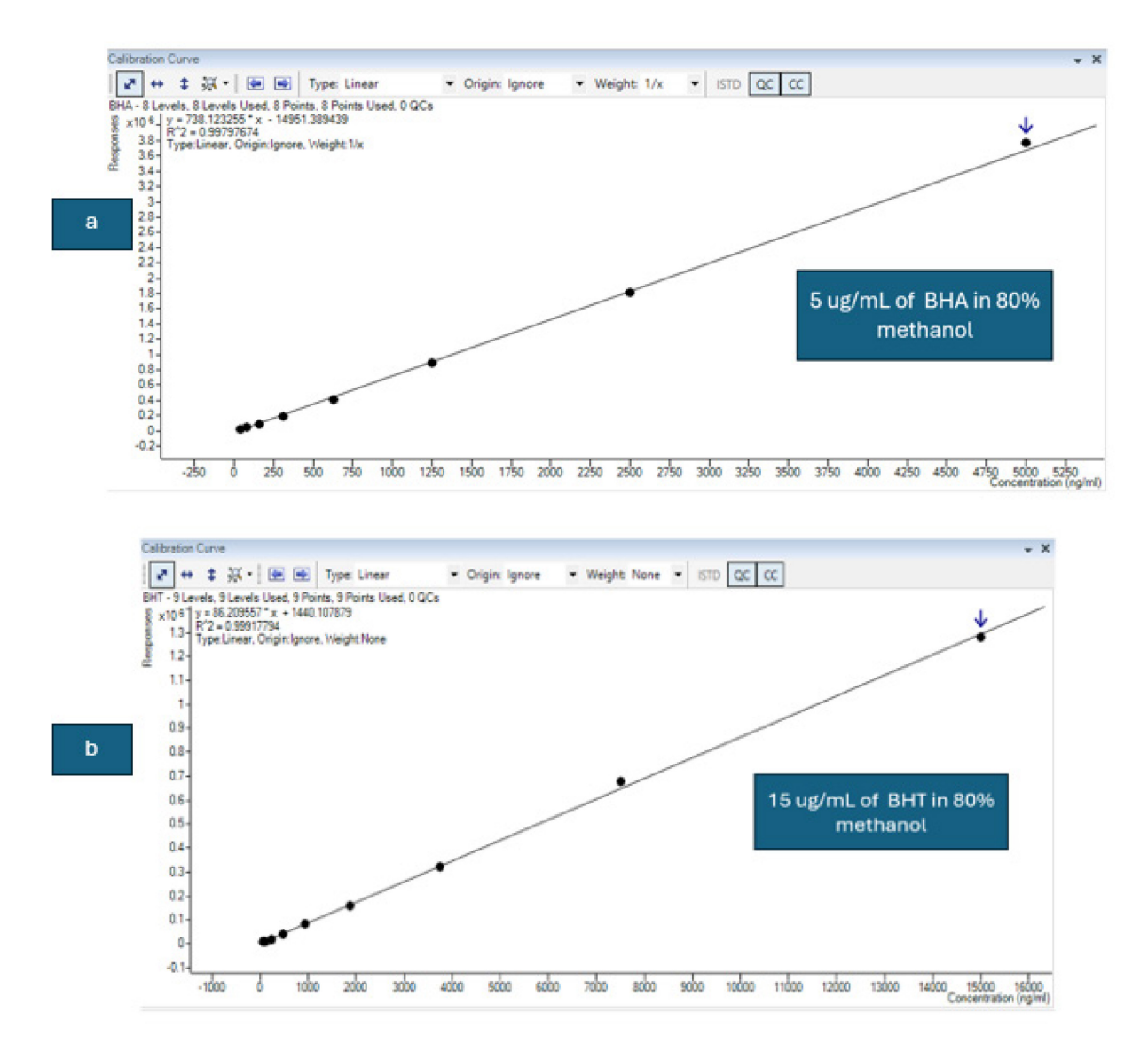
^{*}The number of replicates was n=4 for all conditions



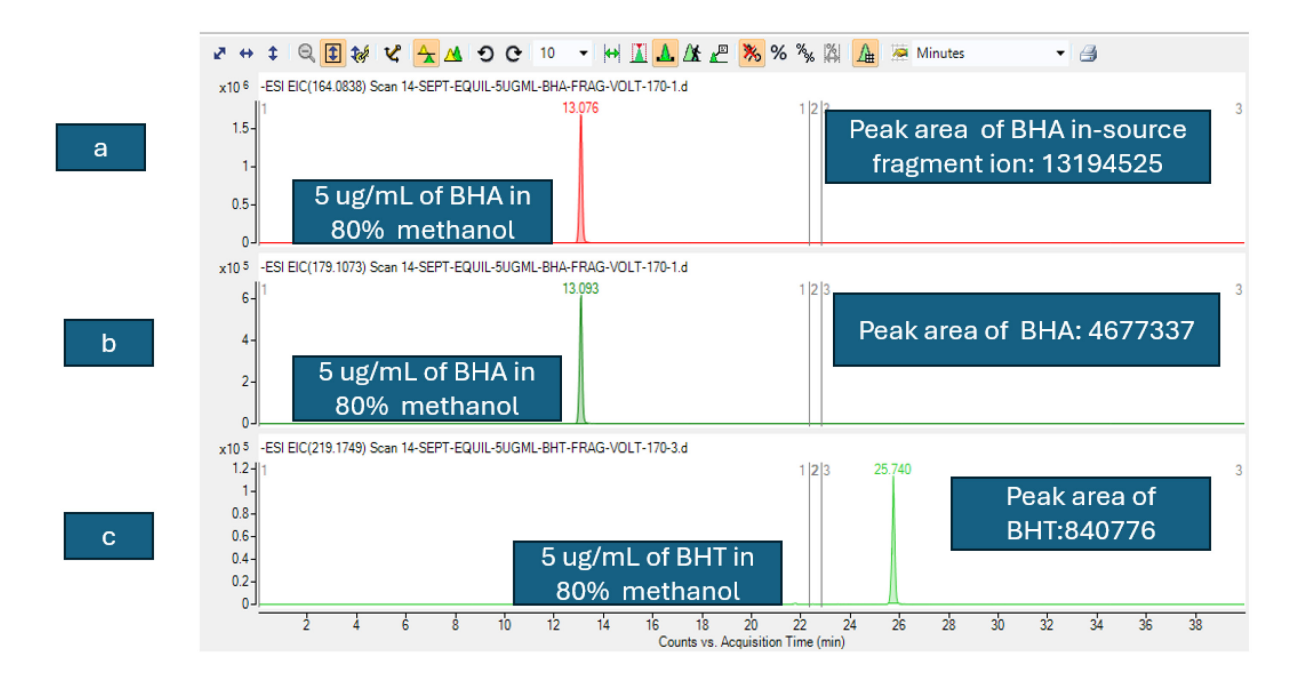
Supplementary Figure B1: Optimization of % composition of organic solvent for the post-extraction loading of BHT on SPME fibre (n=2). BHT was extracted from 1 μ g/mL of standard solutions prepared in 5%, 10% or 30% methanol. Amount of BHT loaded on SPME devices was analyzed on LC-MS using the oxylipin method.



Supplementary Figure B2: Effects of the fragmentor voltage on the peak area of oxylipins. A 100 ng/mL standard mix of oxylipins in 100% methanol was analyzed on LC-MS, and all ESI settings were kept as described in Section 3.2.6 except fragmentor voltage which varied from 170-250V. Number of replicates is shown =1. The initial fragmentor setting of oxylipins LC-MS assay was set at 250 V, showing that the fragmental voltage at 170V was suitable for the analysis of oxylipins.



Supplementary Figure B3: Calibration curve of BHA and BHT analyzed on LC-MS using oxylipin method where $a=5~\mu g/mL$ BHA standard in 80% methanol and $b=15~\mu g/mL$ BHA standard in 80% methanol.



Supplementary Figure B4: Extracted ion chromatogram of 5 μ g/mL BHT and BHA standard in 80% methanol on LC-MS using C18 oxylipin method with optimization of fragmental voltage to 170V.Where (a) EIC of in-source fragment in m/z 164.0838 (b)EIC of m/z of BHA 179.1073 (c)EIC of m/z of BHT 219.1749.

Appendix C: Supplementary information for Chapter 4

Supplementary Table C1: List of oxylipins for forced degradation study.

Full name	Abbreviation	Formula	Precursor	[M-H]- m/z	Retention time (min.)
linoleic acid	LA	$C_{18}H_{32}O_2$	Precursor	279.2330	29.38
9-hydroxy-10E,12Z,15Z-octadecatrienoic acid	9-HOTrE	C ₁₈ H ₃₀ O ₃	LA	293.2122	18.61
9-oxo-10E,12Z-octadecadienoic acid	9-oxoODE	$C_{18}H_{30}O_3$	LA	293.2122	21.73
13-oxo-9Z,11E-octadecadienoic acid	13-oxoODE	C ₁₈ H ₃₀ O ₃	LA	293.2122	21.22
eicosapentaenoic acid	EPA	$C_{20}H_{30}O_2$	Precursor	301.2173	26.99
arachidonic acid	AA	$C_{20}H_{32}O_2$	Precursor	303.2330	28.11
11,12-epoxyeicosatetraenoic acid	11,12-EpETrE	$C_{20}H_{30}O_3$	EPA	317.2122	22.02
5-oxo-eicosatetraenoic acid	5-oxoETE	$C_{20}H_{30}O_3$	AA	317.2122	23.89
15-hydroxy- 5Z,8Z,11Z,13 E-eicosatetraenoic acid	15-НЕТЕ	$C_{20}H_{32}O_3$	AA	319.2279	21.01
12-hydroxy- 6E,8Z,11Z,14 Z-eicosatetraenoic acid	12-НЕТЕ	C ₂₀ H ₃₂ O ₃	AA	319.2279	21.25
9-hydroxy-5Z,7E,11Z,14Z-eicosatetraenoic acid	9-НЕТЕ	C ₂₀ H ₃₂ O ₃	AA	319.2279	21.58
docosahexaenoic acid	DHA	C ₂₂ H ₃₂ O ₂	Precursor	327.2330	28.72
leukotriene B4	LTB4	C ₂₀ H ₃₂ O ₄	AA	335.2222	15.23
13-hydroxydocosahexaenoic acid	13-HDHA	C ₂₂ H ₃₂ O ₃	DHA	343.2279	21.56
11-hydroxydocosahexaenoic acid	11-HDHA	C ₂₂ H ₃₂ O ₃	DHA	343.2279	22.36
16-hydroxydocosahexaenoic acid	16-НДоНЕ	C ₂₂ H ₃₂ O ₃	DHA	343.2279	21.24

Full name	Abbreviation	Formula	Precursor	[M-H] ⁻ m/z	Retention time (min.)
4-hydroxydocosahexaenoic acid	4-HDoHE	$C_{22}H_{32}O_3$	DHA	343.2279	23.41
prostaglandin E2	PGE2	C ₂₀ H ₃₂ O ₅	AA	351.2177	10.58
11β-prostaglandin F2α	11-PGF2α	C ₂₀ H ₃₄ O ₅	AA	353.2334	9.27

Supplementary Table C2: Summary of the results of the forced degradation of AA when stored at various degradation conditions. The results are shown in % as compared to peak area of AA in the control sample.

[M-H] ⁻ m/z	rt (min.)	Control (%)	3-days 37°C (%)	3-days 50°C (%)	5-days UV (%)	7-days UV (%)	3 hours CuSO ₄ Case A (%)	6 hours CuSO ₄ Case A (%)	3 hours CuSO ₄ Case B (%)	6 hours CuSO ₄ Case B (%)	Identified oxylipins
303.2330	28.11	100	80	1	82	72	98	156	NA	NA	AA
303.2330	29.41	NA	NA	NA	4	43	NA	NA	NA	NA	Unknown
271.2432	16.03	NA	NA	0.1	NA	NA	NA	NA	NA	NA	Unknown
271.2432	17.49	NA	NA	0.04	NA	NA	NA	NA	NA	NA	Unknown
271.2432	18.35	NA	NA	0.1	NA	NA	NA	NA	NA	NA	Unknown
287.2381	11.19	NA	NA	0.03	NA	NA	NA	NA	NA	NA	Unknown
287.2381	16.09	NA	NA	0.1	NA	NA	NA	NA	NA	NA	Unknown
287.2381	16.61	NA	NA	0.1	NA	NA	NA	NA	NA	NA	Unknown
315.1996	16.67	NA	NA	0.4	NA	NA	NA	NA	NA	NA	Unknown
315.1996	17.19	NA	NA	0.2	NA	NA	NA	NA	NA	NA	Unknown
315.1996	17.64	NA	NA	0.1	NA	NA	NA	NA	NA	NA	Unknown
315.1996	17.84	NA	NA	0.1	NA	NA	NA	NA	NA	NA	Unknown
315.1996	18.12	NA	NA	0.6	NA	NA	NA	NA	NA	NA	Unknown
315.1996	18.62	NA	NA	0.1	NA	NA	NA	NA	NA	NA	Unknown
315.1996	19.10	NA	NA	0.1	NA	NA	NA	NA	NA	NA	Unknown

[M-H] ⁻		Control	3-days 37°C	3-days 50°C	5-days UV	7-days UV	3 hours CuSO ₄ Case A	6 hours CuSO ₄ Case A	3 hours CuSO ₄ Case B	6 hours CuSO ₄ Case B	Identified
m/z	rt (min.)	(%)	(%)	(%)	(%)	(%)	Case A (%)	(%)	(%)	(%)	oxylipins
317.2116	17.24	NA	17	NA	NA	NA	NA	NA	NA	NA	Unknown
317.2116	18.76	NA	44	NA	NA	NA	NA	NA	NA	NA	Unknown
317.2122	14.93	NA	NA	0.1	NA	NA	NA	NA	NA	NA	Unknown
317.2122	15.81	NA	NA	0.1	NA	NA	NA	NA	NA	NA	Unknown
317.2122	16.79	NA	NA	0.1	NA	NA	NA	NA	NA	NA	Unknown
317.2122	17.43	NA	NA	0.1	NA	NA	NA	NA	NA	NA	Unknown
317.2122	17.64	NA	NA	0.1	NA	NA	NA	NA	NA	NA	Unknown
317.2122	20.12	NA	NA	0.2	NA	NA	NA	NA	NA	NA	Unknown
319.2279	17.27	NA	NA	0.1	NA	NA	NA	NA	NA	NA	Unknown
319.2279	20.15	NA	NA	0.1	NA	NA	NA	NA	NA	NA	15-HETE
319.2279	21.08	NA	NA	0.1	NA	NA	NA	NA	NA	NA	8/12-HETE
319.2279	22.48	NA	NA	0.1	NA	NA	NA	NA	NA	NA	14,15-EET
319.2279	23.14	NA	NA	0.03	NA	NA	NA	NA	NA	NA	Unknown
321.2436	12.71	NA	NA	0.1	NA	NA	NA	NA	NA	NA	Unknown
321.2436	24.75	NA	NA	0.1	NA	NA	NA	NA	NA	NA	Unknown
321.2436	26.56	NA	NA	0.2	NA	NA	NA	NA	NA	NA	Unknown
333.2071	10.97	NA	NA	0.1	NA	NA	NA	NA	NA	NA	Unknown
333.2071	11.21	NA	NA	0.3	NA	NA	NA	NA	NA	NA	Unknown
333.2071	11.40	NA	NA	0.1	NA	NA	NA	NA	NA	NA	Unknown
333.2071	12.11	NA	NA	0.04	NA	NA	NA	NA	NA	NA	Unknown
333.2071	12.53	NA	NA	0.2	NA	NA	NA	NA	NA	NA	Unknown
333.2071	13.66	NA	NA	0.2	NA	NA	NA	NA	NA	NA	Unknown
333.2071	14.09	NA	NA	0.03	NA	NA	NA	NA	NA	NA	Unknown
333.2071	15.58	NA	NA	0.1	NA	NA	NA	NA	NA	NA	Unknown
333.2071	17.84	NA	NA	0.1	NA	NA	NA	NA	NA	NA	Unknown
335.2228	9.13	NA	NA	0.04	NA	NA	NA	NA	NA	NA	Unknown

			3-days	3-days	5-days	7-days	3 hours CuSO ₄	6 hours CuSO ₄	3 hours CuSO ₄	6 hours CuSO ₄	
[M-H]-		Control	37°C	50°C	UV	UV	Case A	Case A	Case B	Case B	Identified
m/z	rt (min.)	(%)	(%)	(%)	(%)	(%)	(%)	(%)	(%)	(%)	oxylipins
333.2071	15.58	NA	NA	0.1	NA	NA	NA	NA	NA	NA	Unknown
335.2228	9.47	NA	NA	0.03	0.01	5	NA	NA	NA	NA	Unknown
335.2228	9.82	NA	NA	0.2	NA	NA	NA	NA	NA	NA	Unknown
335.2228	11.06	NA	NA	0.1	NA	NA	NA	NA	NA	NA	Unknown
335.2228	11.49	NA	NA	0.04	NA	NA	NA	NA	NA	NA	Unknown
335.2228	12.14	NA	NA	0.1	NA	NA	NA	NA	NA	NA	Unknown
335.2228	13.81	NA	NA	0.5	NA	NA	NA	NA	NA	NA	Unknown
335.2228	13.93	NA	NA	2	NA	NA	NA	NA	NA	NA	Unknown
335.2228	14.75	NA	NA	0.04	NA	NA	NA	NA	NA	NA	Unknown
335.2228	15.90	NA	NA	0.1	NA	NA	NA	NA	NA	NA	Unknown
335.2228	16.38	NA	NA	0.1	NA	NA	NA	NA	NA	NA	Unknown
349.2020	6.94	NA	NA	0.1	NA	NA	NA	NA	NA	NA	Unknown
349.2020	7.27	NA	NA	0.1	NA	NA	NA	NA	NA	NA	Unknown
349.2020	7.53	NA	NA	0.1	NA	NA	NA	NA	NA	NA	Unknown
349.2020	13.38	NA	NA	0.04	NA	NA	NA	NA	NA	NA	Unknown
349.2020	15.39	NA	NA	0.1	NA	NA	NA	NA	NA	NA	Unknown
349.2020	16.77	NA	NA	0.1	NA	NA	NA	NA	NA	NA	Unknown
351. 2177	6.66	NA	NA	0.1	NA	NA	NA	NA	NA	NA	Unknown
351. 2177	7.23	NA	NA	0.04	NA	NA	NA	NA	NA	NA	Unknown
351. 2177	7.82	NA	NA	0.03	NA	NA	NA	NA	NA	NA	Unknown
351. 2177	8.93	NA	NA	0.1	NA	NA	NA	NA	NA	NA	Unknown
351. 2177	9.58	NA	NA	0.03	NA	NA	NA	NA	NA	NA	PGE2
351. 2177	10.75	NA	NA	0.1	NA	NA	NA	NA	NA	NA	LXA4
351. 2177	11.50	NA	NA	0.1	NA	NA	NA	NA	NA	NA	Unknown
351. 2177	9.58	NA	NA	0.03	NA	NA	NA	NA	NA	NA	PGE2
351. 2177	12.05	NA	NA	0.03	NA	NA	NA	NA	NA	NA	Unknown

[M-H] ⁻ m/z	rt (min.)	Control (%)	3-days 37°C (%)	3-days 50°C (%)	5-days UV (%)	7-days UV (%)	3 hours CuSO ₄ Case A (%)	6 hours CuSO ₄ Case A (%)	3 hours CuSO ₄ Case B	6 hours CuSO ₄ Case B (%)	Identified oxylipins
351. 2177	13.82	NA	NA	0.1	NA	NA	NA	NA	NA	NA	Unknown
Estimated mass balance		100	141	9	86	120	98	156	27	NA	

Supplementary Table C3: Summary of the results of the forced degradation of LA when stored at various degradation conditions. The results are shown in % as compared to peak area of LA in the control samples

[M-H] ⁻ m/z	rt (min.)	Control (%)	3-days 37°C (%)	3-days 50°C (%)	5-days UV (%)	7-days UV (%)	3 hours CuSO ₄ Case A (%)	6 hours CuSO ₄ Case A (%)	3 hours CuSO ₄ Case B (%)	6 hours CuSO ₄ Case B (%)	Identified oxylipins
279.2330	29.38	100	110	64	92	88	95	89	48	5	LA
293.2122	15.33	NA	0.3	NA	12	12	NA	NA	NA	NA	Unknown
293.2122	19.13	NA	4	NA	1	1	NA	NA	NA	NA	Unknown
293.2122	22.92	NA	0.3	NA	NA	NA	NA	NA	NA	NA	Unknown
293.2122	26.91	NA	1	NA	NA	NA	NA	NA	NA	NA	Unknown
293.2122	14.04	NA	NA	NA	0.4	NA	NA	NA	NA	NA	Unknown
295.2278	20.74	NA	0.2	1	0.2	0.3	NA	NA	NA	NA	9-HODE
295.2278	20.89	NA	NA	1	0.2	NA	NA	NA	NA	NA	13-HODE
315.1966	12.19	NA	0.3	NA	0.1	0.1	NA	NA	NA	NA	Unknown
315.1966	14.58	NA	0.1	NA	0.1	0.1	NA	NA	NA	NA	Unknown
367.1925	20.07	NA	NA	23	NA	NA	NA	NA	NA	NA	Unknown
Estimated mass balance			116	89	107	102	95	89	48	5	

Supplementary Table C4: Summary of the results of the forced degradation of DHA when stored at various degradation conditions. The results are shown in % as compared to peak area of DHA in the control samples

[M-H] ⁻ m/z	rt (min.)	Control	3-days 37°C (%)	3-days 50°C (%)	5-days UV (%)	7-days UV (%)	3 hours CuSO ₄ Case A (%)	6 hours CuSO ₄ Case A (%)	3 hours CuSO ₄ Case B (%)	6 hours CuSO ₄ Case B (%)	Identified oxylipins
327.2330	28.72	100	111	64	96	103	87	93	0.4	4	DHA
315.1966	14.29	NA	0.1	2	NA	NA	NA	NA	NA	NA	Unknown
315.1966	17.13	NA	NA	2	NA	NA	NA	NA	NA	NA	Unknown
315.1966	18.07	NA	0.1	1	0.03	NA	NA	NA	NA	NA	Unknown
315.1966	18.28	NA	NA	0.4	NA	NA	NA	NA	NA	NA	Unknown
315.1966	18.58	NA	0.1	2	0.04	0.01	NA	NA	NA	NA	Unknown
315.1966	18.82	NA	NA	0.1	NA	NA	NA	NA	NA	NA	Unknown
317.2116	16.22	NA	NA	0.3	NA	NA	NA	NA	NA	NA	Unknown
317.2116	18.12	NA	NA	0.3	NA	NA	NA	NA	NA	NA	Unknown
317.2116	19.44	NA	NA	0.3	NA	NA	NA	NA	NA	NA	Unknown
317.2116	20.59	NA	NA	1	NA	NA	NA	NA	NA	NA	Unknown
317.2116	20.84	NA	NA	0.1	NA	NA	NA	NA	NA	NA	Unknown
317.2116	21.58	NA	NA	0.2	NA	NA	NA	NA	NA	NA	Unknown
319.2279	20.66	NA	NA	0.2	NA	NA	NA	NA	NA	NA	Unknown
319.2279	22.96	NA	NA	0.2	NA	NA	NA	NA	NA	NA	Unknown
319.2279	23.92	NA	NA	0.4	NA	NA	NA	NA	NA	NA	Unknown
333.2071	11.19	NA	NA	0.4	NA	NA	NA	NA	NA	NA	Unknown
333.2071	11.48	NA	NA	1	NA	NA	NA	NA	NA	NA	Unknown
333.2071	12.37	NA	NA	0.2	NA	NA	NA	NA	NA	NA	Unknown
333.2071	12.85	NA	NA	1	NA	NA	NA	NA	NA	NA	Unknown
333.2071	14.07	NA	NA	1	NA	NA	NA	NA	NA	NA	Unknown
333.2071	14.64	NA	NA	0.2	NA	NA	NA	NA	NA	NA	Unknown
333.2071	15.91	NA	NA	0.2	NA	NA	NA	NA	NA	NA	Unknown

[M-H] ⁻ m/z	rt (min.)	Control (%)	3-days 37°C (%)	3-days 50°C (%)	5-days UV (%)	7-days UV (%)	3 hours CuSO ₄ Case A (%)	6 hours CuSO ₄ Case A (%)	3 hours CuSO ₄ Case B	6 hours CuSO ₄ Case B (%)	Identified oxylipins
335.2228	9.44	NA	NA	0.2	NA	NA	NA	NA	NA	NA	Unknown
335.2228	10.01	NA	NA	0.3	NA	NA	NA	NA	NA	NA	Unknown
335.2228	12.39	NA	NA	0.2	NA	NA	NA	NA	NA	NA	Unknown
335.2228	13.71	NA	NA	0.2	NA	NA	NA	NA	NA	NA	Unknown
335.2228	14.21	NA	NA	1	NA	NA	NA	NA	NA	NA	Unknown
335.2228	14.38	NA	NA	2	NA	NA	NA	NA	NA	NA	Unknown
335.2228	14.85	NA	NA	0.3	NA	NA	NA	NA	NA	NA	Unknown
335.2228	16.29	NA	NA	0.2	NA	NA	NA	NA	NA	NA	8,15- DiHETE
335.2228	16.77	NA	NA	0.4	NA	NA	NA	NA	NA	NA	Unknown
335.2228	17.14	NA	NA	0.2	NA	NA	NA	NA	NA	NA	Unknown
343.2279	16.15	NA	0.1	NA	0.01	0.1	NA	NA	NA	NA	Unknown
343.2273	23.39	NA	NA	NA	NA	NA	6	1	10	ND	Unknown
343.2279	24.16	NA	0.1	NA	0.1	NA	NA	NA	NA	NA	Unknown
351.2177	11.79	NA	NA	0.2	NA	NA	NA	NA	NA	NA	Unknown
351.2177	14.11	NA	NA	0.4	NA	NA	NA	NA	NA	NA	Unknown
Estimated mass balance		100	111	84	96	103	93	94	10	4	

Supplementary Table C5: Summary of the results of the forced degradation of EPA when stored at various degradation conditions. The results are shown in % as compared to peak area of EPA in the control samples

0.4 m				3-days		7-days	3 hours CuSO ₄	6 hours CuSO ₄	3 hours CuSO ₄	6 hours CuSO ₄	1146-1
[M-H] ⁻ m/z	rt (min.)	Control (%)	3-days 37°C (%)	50°C (%)	5-days UV (%)	UV (%)	Case A	Case A	Case B (%)	Case B	Identified oxylipins
301.2173	26.99	100	110	49	92	102	115	110	9	8	EPA
264.1582	23.89	NA	0.7	NA	NS	NA	NA	NA	NA	NA	Unknown
264.1582	23.91	NA	NA	NA	0.2	NA	NA	NA	NA	NA	Unknown
269.2275	21.31	NA	0.1	NA	NA	NA	NA	NA	NA	NA	Unknown
269.2275	21.67	NA	0.1	NA	NA	NA	NA	NA	NA	NA	Unknown
269.2275	22.84	NA	0.1	NA	NA	NA	NA	NA	NA	NA	Unknown
269.2275	25.03	NA	0.1	NA	0.3	NA	NA	NA	NA	NA	Unknown
269.2275	22.17	NA	NA	NA	0.1	0.2	NA	NA	NA	NA	Unknown
293.1760	17.83	NA	0.3	NA	0.1	NA	NA	NA	NA	NA	Unknown
293.1760	19.17	NA	4	NA	0	2	NA	NA	NA	NA	Unknown
293.1760	29.02	NA	23	NA	9	11	NA	NA	NA	NA	Unknown
293.1760	15.33	NA	NA	NA	8	6	NA	NA	NA	NA	Unknown
295.2278	18.38	NA	NA	0.3	NA	NA	NA	NA	NA	NA	Unknown
295.2278	20.88	NA	0.2	NA	NA	NA	NA	NA	NA	NA	9-HODE
295.2278	23.66	NA	0.2	NA	NA	NA	NA	NA	NA	NA	Unknown
313.2384	16.30	NA	0.4	NA	NA	NA	NA	NA	NA	NA	Unknown
315.1966	12.20	0.3	NA	NA	NA	NA	NA	NA	NA	NA	Unknown
315.1966	14.59	0.3	0.3	0.1	0.1	NA	NA	NA	NA	NA	Unknown
315.1966	17.42	0.3	0.3	NA	NA	NA	NA	NA	NA	NA	Unknown
315.1966	18.38	NA	0.2	NA	NA	NA	NA	NA	NA	NA	Unknown
315.1966	18.58	0.4	0.2	NA	NA	NA	NA	NA	NA	NA	Unknown
315.1966	21.84	NA	NA	0.1	0.2	NA	NA	NA	NA	NA	Unknown
317.2122	16.55	0.1	NA	NA	NA	NA	NA	NA	NA	NA	Unknown
317.2122	17.26	0.1	NA	NA	NA	NA	NA	NA	NA	NA	Unknown

				3-days		7-days	3 hours CuSO ₄	6 hours CuSO ₄	3 hours CuSO ₄	6 hours CuSO ₄	
[M-H] ⁻		Control	3-days	50°C	5-days	UV	Case A	Case A	Case B	Case B	Identified
m/z	rt (min.)	(%)	37°C (%)	(%)	UV (%)	(%)	(%)	(%)	(%)	(%)	oxylipins
317.2122	18.41	0.2	NA	NA	NA	NA	NA	NA	NA	NA	20-HEPE
317.2122	18.76	0.1	NA	NA	NA	NA	NA	NA	NA	NA	Unknown
317.2122	19.73	0.1	NA	NA	NA	NA	NA	NA	NA	NA	11-HEPE
317.2122	20.18	0.1	NA	NA	NA	NA	NA	NA	NA	NA	12-HEPE
317.2122	20.92	0.4	NA	NA	NA	NA	NA	NA	NA	NA	Unknown
317.2122	21.18	0.3	NA	NA	NA	NA	NA	NA	NA	NA	Unknown
317.2122	21.44	0.1	NA	NA	NA	NA	NA	NA	NA	NA	Unknown
317.2122	21.87	NA	0.2	NA	NA	NA	NA	NA	NA	NA	Unknown
333.2071	11.48	0.1	NA	NA	NA	NA	NA	NA	NA	NA	Unknown
333.2071	11.74	0.1	NA	NA	NA	NA	NA	NA	NA	NA	Unknown
333.2071	13.11	0.1	NA	NA	NA	NA	NA	NA	NA	NA	Unknown
333.2071	14.34	0.1	NA	NA	NA	NA	NA	NA	NA	NA	Unknown
335.2228	16.89	NA	0.2	NA	NA	NA	NA	NA	NA	NA	Unknown
335.2228	28.21	NA	0.4	NA	NA	NA	NA	NA	NA	NA	Unknown
335.2228	10.31	0.1	NA	NA	NA	NA	NA	NA	NA	NA	Unknown
335.2228	10.59	0.8	NA	NA	NA	NA	NA	NA	NA	NA	Unknown
335.2228	12.69	0.1	NA	NA	NA	NA	NA	NA	NA	NA	Unknown
335.2228	14.47	0.3	NA	NA	NA	NA	NA	NA	NA	NA	Unknown
351.2177	25.09	0.1	NA	NA	NA	NA	NA	NA	NA	NA	Unknown
351.2177	22.41	NA	NA	NA	0.1	NA	NA	NA	NA	NA	Unknown
351.2177	23.75	NA	NA	NA	0.2	NA	NA	NA	NA	NA	Unknown
351.2177	16.02	NA	NA	NA	0.1	NA	NA	NA	NA	NA	Unknown
351.2177	28.59	NA	NA	NA	0.1	NA	NA	NA	NA	NA	Unknown
353.2334	24.79	NA	NA	NA	7	NA	NA	NA	NA	NA	Unknown
413.1980	15.74	NA	0.2	NA	NA	NA	NA	NA	NA	NA	Unknown
413.1980	16.30	NA	2	NA	NA	NA	NA	NA	NA	NA	Unknown

				3-days		7-days	3 hours CuSO ₄	6 hours CuSO ₄	3 hours CuSO ₄	6 hours CuSO ₄	
[M-H] ⁻		Control	3-days	50°C	5-days	UV	Case A	Case A	Case B	Case B	Identified
m/z	rt (min.)	(%)	37°C (%)	(%)	UV (%)	(%)	(%)	(%)	(%)	(%)	oxylipins
413.1980	17.05	NA	11	NA	NA	NA	NA	NA	NA	NA	Unknown
413.1980	17.33	NA	1	NA	NA	NA	NA	NA	NA	NA	Unknown
413.1980	17.63	NA	2	NA	NA	NA	NA	NA	NA	NA	Unknown
413.1980	18.06	NA	0.3	NA	NA	NA	NA	NA	NA	NA	Unknown
Estimated											
mass											
balance		113	157	50	120	120	115	110	9	18	

Supplementary Table C6: Summary of the results of the forced degradation of PGE2 when stored at various degradation conditions. The results are shown in % as compared to peak area of PGE2 in the control samples

Reactions	[M-H] ⁻ m/z	rt (min.)	Control (%)	3-days 37°C (%)	3-days 50°C (%)	5-days UV (%)	7-days UV (%)	Identified oxylipins
	351.2177	10.58	100	46	6	75	2	PGE2
Hydrolysis	315.1966	12.01	NA	0.4	1	NA	NA	Unknown
Hydrolysis	315.1966	14.29	NA	0.3	1	NA	NA	Unknown
Hydrolysis	315.1966	18.61	NA	NA	0.7	NA	0.3	Unknown
Hydrolysis	315.1966	10.28	NA	1	NA	2	NA	Unknown
Hydrolysis	315.1966	13.24	NA	0.6	NA	NA	NA	Unknown
Hydrolysis	315.1966	13.59	NA	15	NA	6	NA	Unknown
Hydrolysis	315.1966	15.12	NA	0.9	NA	NA	NA	Unknown
Redox	333.2071	10.28	NA	0.01	NA	0.7	NA	Unknown
Redox	333.2071	13.24	NA	0.3	63	NA	NA	Unknown
Redox	333.2071	13.62	NA	7	19	3	NA	PGJ2
Redox	333.2071	13.87	NA	0.9	NA	NA	NA	Unknown
Redox	333.2071	15.13	NA	0.4	NA	NA	NA	Unknown
Hydrolysis	317.2166	20.27	NA	NA	0.6	NA	NA	Unknown
Hydrolysis	317.2122	13.60	NA	0.5	NA	0.2	NA	Unknown
Hydrolysis	317.2122	20.94	NA	0.2	NA	0.2	NA	Unknown
Hydrolysis	317.2122	18.40	NA	NA	NA	0.1	NA	Unknown
Hydrolysis	317.2122	21.86	NA	NA	NA	0.1	NA	Unknown
Reduction	335.2228	13.59	NA	NA	NA	0.1	NA	8-iso-PGA1
Reduction	335.2228	15.25	NA	NA	NA	0.4	NA	8,15-DiHETE
Reduction	335.2228	15.95	NA	NA	NA	0.2	NA	LTB4
Unknown	343.2273	20.55	NA	NA	NA	NA	2	Unknown

	[M-H] ⁻		Control	3-days	3-days 50°C	5-days	7-days UV	
Reactions	m/z	rt (min.)	(%)	37°C (%)	(%)	UV (%)	(%)	Identified oxylipins
Unknown	343.2273	22.33	NA	NA	NA	NA	30	Unknown
Unknown	343.2273	24.16	NA	0.4	NA	0.4	0.3	Unknown
Unknown	343.2273	22.80	NA	NA	1	NA	NA	Unknown
Reduction	352.2255	23.39	NA	NA	0.4	NA	NA	Unknown
Reduction	353.2334	24.78	NA	1	NA	NA	41	Unknown
Oxidation	367.2126	20.45	NA	2	NA	14	NA	Unknown
Oxidation	367.2126	24.11	NA	NA	NA	0.2	NA	Unknown
Reduction	352.2253	14.14	NA	0.4	NA	0.5	NA	Unknown
Reduction	369.2283	14.95	NA	0.1	NA	NA	0.2	Unknown
Reduction	369.2283	21.64	NA	NA	NA	NA	0.2	Unknown
Reduction	369.2283	26.49	NA	NA	NA	NA	2	Unknown
Estimated mass								
balance			100	80	94	102	77	

Supplementary Table C7: Summary of the results of the forced degradation of 13-HDHA when stored at various degradation conditions. The results are shown in % as compared to peak area of 13-HDHA in the control samples.

Reactions	[M-H] ⁻ m/z	rt (min.)	Control (%)	3-days 37°C (%)	3-days 50°C (%)	5-days UV (%)	7-days UV (%)	Identified oxylipins
	343.2279	21.56	100	112	NA	104	98	13-HDHA
Isomerization	343.2279	24.12	NA	2	NA	1	NA	Unknown
Isomerization	343.2279	22.17	NA	NA	NA	2	NA	7-HDHA
Unknown	293.2122	18.39	NA	NA	2	NA	NA	Unknown
Unknown	293.2122	22.10	NA	NA	3	NA	NA	Unknown
Ketone formation	313.2384	16.24	NA	NA	3	NA	NA	12,13-DiHOME
Reduction	335.2228	10.33	NA	NA	2	NA	NA	Unknown
Reduction	335.2228	14.38	NA	NA	3	NA	NA	Unknown
Unknown	351.2177	19.59	NA	NA	0.9	NA	NA	Unknown
Unknown	351.2177	20.47	NA	NA	0.8	NA	NA	Unknown
Unknown	351.2177	21.01	NA	NA	0.9	NA	NA	Unknown
Unknown	351.2177	21.38	NA	NA	0.8	NA	NA	Unknown
Reduction	355.1691	13.81	NA	NA	2	NA	NA	Unknown
Reduction	355.1691	15.22	NA	NA	2	NA	NA	Unknown
Unknown	413.1981	15.75	NA	NA	2	NA	NA	Unknown
Unknown	413.1981	16.31	NA	NA	21	NA	NA	Unknown
Unknown	413.1981	17.05	NA	NA	99	NA	NA	Unknown
Unknown	413.1981	17.31	NA	NA	12	NA	NA	Unknown
Unknown	413.1981	17.62	NA	NA	14	NA	NA	Unknown
Unknown	413.1981	18.05	NA	NA	3	NA	NA	Unknown
Unknown	413.1981	18.47	NA	NA	1	NA	NA	Unknown
Estimated mass balance			100	114	173	107	98	

Supplementary Table C8: Summary of the results of the forced degradation of 11-HDHA when stored at various degradation conditions. The results are shown in % as compared to peak area of 11-HDHA in the control samples.

Reactions	[M-H] ⁻ m/z	rt (min.)	Control (%)	3-days 37°C (%)	3-days 50°C (%)	5-days UV (%)	7-days UV (%)	Identified oxylipins
	343.2273	22.36	100	115	49	96	91	11-HDHA
Isomerization	343.2273	21.11	NA	1	NA	1	1	Unknown
Isomerization	343.2273	21.89	NA	NA	NA	1	NA	10-HDHA
Isomerization	343.2273	24.14	NA	NA	NA	NA	2	Unknown
Isomerization	343.2273	15.88	NA	NA	2	NA	2	Unknown
Unknown	293.2122	18.12	NA	NA	4	NA	NA	Unknown
Unknown	293.2122	18.37	NA	NA	4	NA	NA	Unknown
Unknown	293.2122	18.83	NA	NA	2	NA	NA	13-HOTrE
Unknown	313.2384	16.28	NA	NA	16	NA	NA	12,13-DіНоМЕ
Redox	317.2116	15.37	NA	NA	3	NA	NA	Unknown
Redox	317.2116	16.24	NA	NA	3	NA	NA	Unknown
Redox	317.2116	18.09	NA	NA	6	NA	NA	Unknown
Redox	317.2116	18.47	NA	NA	2	NA	NA	Unknown
Redox	317.2116	20.18	NA	NA	2	NA	NA	9-HEPE
Redox	317.2116	20.60	NA	NA	14	NA	NA	5-HEPE
Redox	317.2116	20.86	NA	NA	4	NA	NA	Unknown
Redox	317.2116	21.56	NA	NA	2	NA	NA	Unknown
Redox	317.2116	21.82	NA	NA	52	NA	NA	Unknown
Reduction	319.2279	17.71	NA	NA	2	NA	NA	Unknown
Reduction	319.2279	19.11	NA	NA	2	NA	NA	Unknown
Reduction	319.2279	20.47	NA	NA	1	NA	NA	Unknown
Reduction	319.2279	20.65	NA	NA	4	NA	NA	Unknown
Reduction	319.2279	22.71	NA	NA	2	NA	NA	5-HETE

Reactions	[M-H] ⁻ m/z	rt (min.)	Control (%)	3-days 37°C (%)	3-days 50°C (%)	5-days UV (%)	7-days UV (%)	Identified oxylipins
Reduction	319.2279	22.98	NA	NA	4	NA	NA	Unknown
Reduction	319.2279	23.66	NA	NA	1	NA	NA	14,15-EET
Reduction	319.2279	24.08	NA	NA	3	NA	NA	11/15-HEDE
Redox	333.2071	11.18	NA	NA	6	NA	NA	Unknown
Redox	333.2071	11.48	NA	NA	9	NA	NA	Unknown
Redox	333.2071	11.65	NA	NA	3	NA	NA	Unknown
Redox	333.2071	12.37	NA	NA	2	NA	NA	Unknown
Redox	333.2071	12.85	NA	NA	9	NA	NA	Unknown
Redox	333.2071	13.47	NA	NA	2	NA	NA	Unknown
Redox	333.2071	14.04	NA	NA	10	NA	NA	Unknown
Oxidation	335.2228	9.41	NA	NA	3	NA	NA	Unknown
Oxidation	335.2228	9.99	NA	NA	5	NA	NA	Unknown
Oxidation	335.2228	10.33	NA	NA	32	NA	NA	Unknown
Oxidation	335.2228	11.30	NA	NA	3	NA	NA	Unknown
Oxidation	335.2228	12.38	NA	NA	5	NA	NA	Unknown
Oxidation	335.2228	14.23	NA	NA	17	NA	NA	Unknown
Oxidation	335.2228	14.37	NA	NA	41	NA	NA	Unknown
Oxidation	335.2228	15.31	NA	NA	2	NA	NA	5,15-DiHETE
Oxidation	335.2228	16.27	NA	NA	3	NA	NA	Unknown
Oxidation	335.2228	16.75	NA	NA	3	NA	NA	Unknown
Oxidation	335.2228	28.22	NA	NA	2	NA	NA	Unknown
Redox	351.2177	6.82	NA	NA	4	NA	NA	Unknown
Redox	351.2177	7.32	NA	NA	1	NA	NA	Unknown
Redox	351.2177	9.11	NA	NA	3	NA	NA	Unknown
Redox	351.2177	9.26	NA	NA	3	NA	NA	Unknown
Redox	351.2177	11.78	NA	NA	1	NA	NA	LXB4
Redox	351.2177	14.09	NA	NA	2	NA	NA	Unknown

Reactions	[M-H] ⁻ m/z	rt (min.)	Control (%)	3-days 37°C (%)	3-days 50°C (%)	5-days UV (%)	7-days UV (%)	Identified oxylipins
Redox	351.2177	19.60	NA	NA	2	NA	NA	Unknown
Redox	351.2177	20.46	NA	NA	1	NA	NA	Unknown
Redox	351.2177	21.01	NA	NA	2	NA	NA	Unknown
Redox	351.2177	21.40	NA	NA	2	NA	NA	Unknown
Redox	351.2177	22.52	NA	NA	1	NA	NA	Unknown
Hydrolysis	379.2484	23.66	NA	NA	2	NA	NA	Unknown
Hydrolysis	379.2484	24.19	NA	NA	5	NA	NA	Unknown
Hydrolysis	379.2484	24.89	NA	NA	2	NA	NA	Unknown
Hydrolysis	379.2484	25.21	NA	NA	2	NA	NA	Unknown
Hydrolysis	379.2484	25.63	NA	NA	21	NA	NA	Unknown
Estimated mass balance			100	116	372	98	95	

Supplementary Table C9: Summary of the results of the forced degradation of 9-oxoODE when stored at various degradation conditions. The results are shown in % as compared to peak area of 9-oxoODE in the control samples.

Reactions	[M-H] ⁻ m/z	rt (min.)	Control (%)	3-days 37°C (%)	3-days 50°C (%)	5-days UV (%)	7-days UV (%)	Identified oxylipins
	293.2122	21.73	100	112	85	26	12	9-oxoODE
Isomerization	293.2122	22.23	NA	NA	NA	37	39	unknown
Isomerization	293.2122	23.08	NA	NA	NA	14	12	unknown
Isomerization	293.2122	21.53	NA	NA	NA	25	46	unknown
Estimated mass								
balance			100	112	85	103	109	

Supplementary Table C10: Summary of the results of the forced degradation of 9-HoTrE when stored at various degradation conditions. The results are shown in % as compared to peak area of 9-HoTrE in the control samples.

Reactions	[M-H] ⁻ m/z	rt (min.)	Control (%)	3-days 37°C (%)	3-days 50°C (%)	5-days UV (%)	7-days UV (%)	Identified oxylipins
	293.2122	18.61	100	119	78	99	97	9-HoTrE
Estimated mass								
balance		NA	100	119	78	99	97	

Supplementary Table C11: Summary of the results of the forced degradation of 15-HETE when stored at various degradation conditions. The results are shown in % as compared to peak area 15-HETE in the control samples

Reactions	[M-H] ⁻ m/z	rt (min.)	Control (%)	3-days 37°C (%)	3-days 50°C (%)	5-days UV (%)	7-days UV (%)	Identified oxylipins
	319.2279	20.42	100	5	0	88	91	15-HETE
Hydrolysis	301.2173	26.96	NA	31	NA	NA	NA	Unknown
Reduction	303.2330	29.48	NA	17	NA	2	2	Unknown
Redox	315.1966	16.67	NA	NA	5	NA	NA	Unknown
Redox	315.1966	17.62	NA	NA	2	NA	NA	Unknown
Redox	315.1966	17.85	NA	NA	2	NA	NA	Unknown
Redox	315.1966	19.07	NA	NA	1	NA	NA	Unknown
Redox	317.2122	15.78	NA	NA	2	NA	NA	Unknown
Redox	317.2122	17.41	NA	NA	1	NA	NA	Unknown
Redox	317.2122	17.63	NA	NA	2	NA	NA	Unknown
Redox	317.2122	17.99	NA	NA	2	NA	NA	Unknown
Redox	317.2122	20.07	NA	NA	4	NA	NA	Unknown
Redox	333.2071	11.18	NA	NA	4	NA	NA	Unknown
Redox	333.2071	12.52	NA	NA	2	NA	NA	PGJ2

	[M-H] ⁻	rt	Control	3-days 37°C	3-days 50°C	5-days	7-days UV	Identified
Reactions	m/z	(min.)	(%)	(%)	(%)	UV (%)	(%)	oxylipins
Redox	333.2071	13.67	NA	NA	2	NA	NA	Unknown
Redox	333.2071	14.24	NA	NA	3	NA	NA	Unknown
Redox	333.2071	15.55	NA	NA	2	NA	NA	Unknown
Redox	335.2228	10.06	NA	NA	10	NA	NA	Unknown
Redox	335.2228	11.03	NA	NA	2	NA	NA	Unknown
Redox	335.2228	12.09	NA	NA	3	NA	NA	Unknown
Redox	335.2228	13.79	NA	NA	7	NA	NA	Unknown
Redox	335.2228	13.92	NA	NA	22	NA	NA	Unknown
Redox	335.2228	14.30	NA	6	NA	NA	NA	8,15-DiHETE
Oxidation	351.2177	8.89	NA	NA	1	NA	NA	Unknown
Oxidation	351.2177	10.70	NA	NA	1	NA	NA	LXA4
Oxidation	351.2177	11.49	NA	NA	1	NA	NA	Unknown
Oxidation	351.2177	13.78	NA	NA	1	NA	NA	Unknown
Oxidation	351.2177	15.79	NA	3	NA	NA	NA	Unknown
Oxidation	351.2177	17.38	NA	11	NA	NA	NA	Unknown
Oxidation	351.2177	23.36	NA	2	NA	NA	NA	Unknown
Hydrolysis	355.2490	21.51	NA	11	NA	NA	NA	Unknown
Hydrolysis	355.2490	24.33	NA	5	NA	NA	NA	Unknown
Estimated mass balance			100	88	82	90	93	

Supplementary Table C12: Summary of the results of the forced degradation of 5-oxoETE stored at various degradation conditions. The results are shown in % as compared to peak area 5-oxoETE in the control samples.

Reactions	[M-H] ⁻ m/z	rt (min.)	Control (%)	3-days 37°C (%)	3-days 50°C (%)	5-days UV (%)	7-days UV (%)	Identified oxylipins
	317.2122	23.89	100	104	40	42	22	5-oxoETE
Isomerization	317.2122	20.74	NA	2	1	3	NA	Unknown
Isomerization	317.2122	21.70	NA	1	NA	1	NA	11,12- EpETE
Isomerization	317.2122	23.68	NA	NA	NA	NA	12	Unknown
Isomerization	317.2122	24.14	NA	NA	NA	13	19	Unknown
Isomerization	317.2122	24.28	NA	NA	NA	6	11	Unknown
Isomerization	317.2122	24.68	NA	NA	NA	8	8	Unknown
Reduction	319.2279	23.94	4	4	NA	NA	NA	Unknown
Hydrolysis/Redox	335.2228	10.38	NA	NA	44	NA	NA	Unknown
Estimated mass balance			104	107	85	73	72	

Supplementary Table C13: Summary of the results of the forced degradation of 13-oxoODE when stored at various degradation conditions. The results are shown in % as compared to peak area 13-oxoODE in the control samples.

Reactions	[[M-H] ⁻ m/z	rt (min.)	Control (%)	3-days 37°C (%)	3-days 50°C (%)	5-days UV (%)	7-days UV (%)	Identified oxylipins
	293.2122	21.22	100	110	69	18	16	13-oxoODE
Isomerization	293.2122	21.52	NA	NA	3	48	44	Unknown
Isomerization	293.2122	21.04	NA	NA	NA	34	42	Unknown
Isomerization	293.2122	22.47	NA	NA	NA	2	2	Unknown
Isomerization	293.2122	22.84	NA	NA	NA	10	9	Unknown
Estimated mass balance			100	110	72	112	113	

Supplementary Table C14: Summary of the results of the forced degradation of 4-HDoHE when stored at various degradation conditions. The results are shown in % as compared to peak area 4-HDoHE in the control samples.

Reactions	[M-H] ⁻ m/z	rt (min.)	Control (%)	3-days 37°C (%)	3-days 50°C (%)	5-days UV (%)	7-days UV (%)	Identified oxylipins
	343.2279	23.41	100	110	103	93	94	4-HDoHE
Isomerization	343.2279	24.15	NA	1	NA	NA	2	Unknown
Estimated								
mass								
balance			100	111	103	93	96	

Supplementary Table C15: Summary of the results of the forced degradation of 11,12-EpETE when stored at various degradation conditions. The results are shown in % as compared to peak area 11,12-EpETE in the control samples.

Reactions	[M-H] ⁻ m/z	rt (min.)	Control (%)	3-days 37°C (%)	3-days 50°C (%)	5-days UV (%)	7-days UV (%)	Identified oxylipins
	317.2122	22.01	100	87	107	97	91	11,12-EpETE
Isomerization	317.2122	16.34	NA	3	NA	NA	NA	Unknown
Isomerization	317.2122	18.21	NA	3	NA	NA	NA	Unknown
Isomerization	317.2122	20.75	NA	12	NA	NA	NA	Unknown
Hydrolysis	299.2016	18.01	NA	4	NA	NA	NA	Unknown
Hydrolysis	299.2016	18.69	NA	2	NA	NA	NA	Unknown
Estimated mass balance				105	107	97	91	

Supplementary Table C16: Summary of the results of the forced degradation of LTB4 stored when stored at various degradation conditions. The results are shown in % as compared to peak area LTB4 in the control samples

Reactions	[M-H] ⁻ m/z	rt (min.)	Control (%)	3-days 37°C (%)	3-days 50°C (%)	5-days UV (%)	7-days UV (%)	Identified oxylipins
	335.2228	15.23	100	8	66	101	8	LTB4
Isomerization	335.2228	11.06	NA	2	NA	NA	NA	Unknown
Isomerization	335.2228	11.49	NA	1	NA	NA	NA	Unknown
Isomerization	335.2228	12.16	NA	3	NA	NA	NA	Unknown
Isomerization	335.2228	13.67	NA	1	NA	NA	NA	Unknown
Isomerization	335.2228	13.84	NA	14	NA	NA	NA	Unknown
Isomerization	335.2228	14.63	NA	2	NA	NA	NA	Unknown
Isomerization	335.2228	14.94	NA	1	1	NA	2	5,15-DiHETE
Isomerization	335.2228	15.88	NA	2	NA	NA	NA	5,12-DiHETE
Isomerization	335.2228	16.38	NA	5	NA	NA	NA	Unknown
Isomerization	335.2228	22.87	NA	NA	2	NA	NA	Unknown
Dehydration	317.2122	14.92	NA	2	NA	NA	NA	Unknown
Dehydration	317.2122	15.82	NA	2	NA	NA	NA	Unknown
Dehydration	317.2122	16.79	NA	2	NA	NA	NA	Unknown
Dehydration	317.2122	17.46	NA	1	NA	NA	NA	Unknown
Dehydration	317.2122	17.67	NA	3	NA	NA	NA	Unknown
Dehydration	317.2122	17.98	NA	2	NA	NA	NA	20-НЕРЕ
Dehydration	317.2122	20.15	NA	6	NA	NA	NA	Unknown
Dehydration	317.2122	20.43	NA	2	NA	NA	NA	Unknown
Dehydration	317.2122	21.13	NA	3	NA	NA	NA	Unknown
Redox	351.2177	8.85	NA	1	NA	NA	NA	Unknown
Redox	351.2177	8.94	NA	2	NA	NA	NA	Unknown
Redox	351.2177	9.59	NA	2	NA	NA	NA	PGE2
Redox	351.2177	10.76	NA	2	NA	NA	NA	Unknown

Desetions	[M-H] ⁻	rt (min)	Control	3-days 37°C	3-days 50°C	5-days	7-days	Identified
Reactions	m/z	(min.)	(%)	(%)	(%)	UV (%)	UV (%)	oxylipins
Redox	351.2177	11.56	NA	1	NA	NA	NA	Unknown
Redox	351.2177	13.83	NA	2	NA	NA	NA	Unknown
Redox	351.2177	22.89	NA	NA	50	NA	NA	Unknown
Hydrolysis	353.2333	13.08	NA	NA	2	NA	NA	Unknown
Hydrolysis	353.2333	21.19	NA	NA	14	NA	NA	Unknown
Hydrolysis	353.2333	22.22	NA	NA	24	NA	NA	Unknown
Hydrolysis	353.2333	26.68	NA	NA	1	NA	NA	Unknown
Hydrolysis	371.2439	22.90	NA	NA	8	NA	NA	Unknown
Hydrolysis	371.2439	23.84	NA	NA	5	NA	NA	Unknown
Hydrolysis	371.2439	24.48	NA	NA	2	NA	NA	Unknown
Hydrolysis	371.2439	25.35	NA	NA	3	NA	NA	Unknown
Estimated mass								
balance				153	180	10	90	

Supplementary Table C17: Summary of the results of the forced degradation of 16-HDoHE stored at various degradation conditions. The results are shown in % as compared to peak area 16-HDoHE in the control samples.

[M-H] ⁻	rt	Control	3-days 37°C	3-days 50°C	5-days	7-days	Identified
m/z	(min.)	(%)	(%)	(%)	UV (%)	UV (%)	oxylipins
343.2279	21.24	100	96	94	60	66	16-HDOHE
Estimated mass balance		100	96	94	60	66	

Supplementary Table C18: Summary of the results of the forced degradation of 12-HETE when stored at various degradation conditions. The results are shown in % as compared to peak area 12-HETE in the control samples.

Reactions	[M-H] ⁻ m/z	rt (min.)	Control (%)	3-days 37°C (%)	3-days 50°C (%)	5-days UV (%)	7-days UV (%)	Identified oxylipins
	319.2279	21.25	100	110	0	100	93	12-HETE
Isomerization	319.2279	17.29	NA	NA	2	NA	NA	Unknown
Isomerization	319.2279	20.19	NA	NA	5	NA	NA	Unknown
Isomerization	319.2279	20.52	NA	1.7	NA	7	NA	15-HETE
Reduction	287.2381	11.20	NA	NA	2	NA	NA	Unknown
Reduction	287.2381	16.05	NA	NA	3	NA	NA	Unknown
Reduction	287.2381	16.60	NA	NA	2	NA	NA	Unknown
Hydrolysis	301.2173	23.42	NA	NA	8	NA	NA	Unknown
Hydrolysis	301.2173	25.19	NA	NA	7	NA	NA	Unknown
Hydrolysis	301.2173	25.37	NA	NA	7	NA	NA	Unknown
Hydrolysis	301.2173	25.88	NA	NA	6	NA	NA	Unknown
Hydrolysis	301.2173	26.04	NA	NA	3	NA	NA	Unknown
Hydrolysis	301.2173	26.29	NA	NA	39	NA	NA	Unknown
Reduction	303.2330	28.31	NA	NA	14	NA	NA	Unknown
Reduction	303.2330	28.52	NA	NA	9	3	2	Unknown
Reduction	303.2330	28.91	NA	NA	44	NA	5	Unknown
Redox	317.2116	14.90	NA	NA	3	NA	NA	Unknown
Redox	317.2116	15.79	NA	NA	6	NA	NA	Unknown
Redox	317.2116	16.81	NA	NA	3	NA	NA	Unknown
Redox	317.2116	17.42	NA	NA	2	NA	NA	Unknown
Redox	317.2116	17.64	NA	NA	3	NA	NA	Unknown
Redox	317.2116	20.12	NA	NA	8	NA	NA	Unknown
Redox	333.2228	10.95	NA	NA	7	NA	NA	Unknown
Redox	333.2228	11.19	NA	NA	11	NA	NA	Unknown

	[M-H] ⁻	rt	Control	3-days 37°C	3-days 50°C	5-days	7-days	Identified
Reactions	m/z	(min.)	(%)	(%)	(%)	UV (%)	UV (%)	oxylipins
Redox	333.2228	11.39	NA	NA	2	NA	NA	Unknown
Redox	333.2228	12.09	NA	NA	2	NA	NA	Unknown
Redox	333.2228	12.52	NA	NA	7	NA	NA	PGJ2
Redox	333.2228	13.12	NA	NA	2	NA	NA	Unknown
Redox	333.2228	13.66	NA	NA	9	NA	NA	Unknown
Redox	333.2228	14.09	NA	NA	2	NA	NA	Unknown
Redox	333.2228	15.54	NA	NA	4	NA	NA	Unknown
Redox	333.2228	17.84	NA	NA	2	NA	NA	Unknown
Redox	335.2228	16.35	NA	NA	5	NA	NA	Unknown
Redox	335.2490	20.13	NA	7	NA	3	NA	Unknown
Redox	335.2490	24.52	NA	NA	NA	2	NA	Unknown
Oxidation	351.2177	6.66	NA	NA	6	NA	NA	Unknown
Oxidation	351.2177	7.21	NA	NA	3	NA	NA	Unknown
Oxidation	351.2177	7.82	NA	NA	2	NA	NA	Unknown
Oxidation	351.2177	8.26	NA	NA	2	NA	NA	Unknown
Oxidation	351.2177	8.92	NA	NA	4	NA	NA	Unknown
Oxidation	351.2177	9.57	NA	NA	2	NA	NA	PGE2
Oxidation	351.2177	10.73	NA	NA	4	NA	NA	Unknown
Oxidation	351.2177	11.52	NA	NA	2	NA	NA	Unknown
Oxidation	351.2177	12.07	NA	NA	2	NA	NA	Unknown
Oxidation	351.2177	13.79	NA	NA	3	NA	NA	Unknown
Estimated mass balance			100	119	256	109	101	

Supplementary Table C19: Summary of the results of the forced degradation of 9-HETE when stored at various degradation conditions. The results are shown in % as compared to peak area 9-HETE in the control samples.

Reactions	[M-H] ⁻ m/z	rt (min.)	Control (%)	3-days 37°C (%)	3-days 50°C (%)	5-days UV (%)	7-days UV (%)	Identified oxylipins
	319.2279	21.58	100	54	21	96	91	9-HETE
Reduction	323.2592	12.51	NA	2	NA	NA	NA	Unknown
Reduction	323.2592	19.26	NA	2	NA	NA	NA	Unknown
Dehydration	301.2173	17.81	NA	1	NA	NA	NA	Unknown
Dehydration	301.2173	21.59	NA	16	7	NA	NA	Unknown
Dehydration	301.2173	23.40	NA	NA	2	NA	NA	Unknown
Dehydration	301.2173	25.17	NA	6	4	NA	NA	Unknown
Dehydration	301.2173	25.38	NA	4	2	NA	NA	Unknown
Dehydration	301.2173	25.60	NA	2	2	NA	NA	Unknown
Dehydration	301.2173	25.89	NA	8	7	NA	NA	Unknown
Estimated mass balance			100	95	45	96	91	

Supplementary Table C20: Summary of the results of the forced degradation of $11\text{-PGF}2\alpha$ when stored at various degradation conditions. The results are shown in % as compared to peak area $11\text{-PGF}2\alpha$ in the control samples.

	[M-H] ⁻	rt	Control	3-days 37°C	3-days 50°C	5-days UV	7-days UV	Identified
Reactions	m/z	(min.)	(%)	(%)	(%)	(%)	(%)	oxylipins
	353.2334	9.27	100	129	148	95	NA	11-PGF2α
Hydrolysis/Dehydration	297.1861	10.55	NA	NA	NA	NA	0.3	Unknown
Hydrolysis/Dehydration	297.1861	19.27	NA	0.4	ND	ND	NA	Unknown
Hydrolysis/Dehydration	297.1861	18.97	NA	NA	0.4	NA	NA	Unknown
Hydrolysis/Dehydration	315.1966	10.83	NA	NA	ND	ND	NA	Unknown
Hydrolysis/Dehydration	315.1966	15.68	NA	NA	2	ND	NA	Unknown
Hydrolysis/Dehydration	315.1966	18.98	NA	NA	10	NA	NA	Unknown
Hydrolysis/Dehydration	315.1966	10.29	NA	NA	NA	NA	0.5	Unknown
Hydrolysis/Dehydration	315.1966	13.61	NA	NA	NA	NA	3	Unknown
Dehydration/Reduction	333.2071	10.55	NA	NA	NA	NA	72	PGE2
Dehydration/Reduction	333.2071	15.67	NA	2	NA	NA	NA	Unknown
Estimated mass balance			100	132	160	95	76	

Supplementary Table C21: Summary of the results of the forced degradation of PGE2 using SCIEX Zeno trap when stored at 3 days 50°C (%). The results are shown in % as compared to peak area PGE2 in the control samples.

[M-H] ⁻ m/z	Rt (min.)	3-days 50°C (%)	Identified oxylipins
351.2177	14.80	14	PGE2
243.1961	23.94	16	Unknown
243.1961	19.29	23	Unknown
315.1958	17.50	243	Unknown
243.1961	16.52	48	Unknown
315.1958	16.31	483	Unknown
365.2323	17.17	13	Unknown
			Unknown
351.2169	14.65	14	Unknown
351.1781	18.03	18	Unknown
349.2012	14.22	26	Unknown
349.2012	14.14	18	
349.2012	13.80	26	Unknown
333.2063	17.77	1149	PGJ2
333.2068	17.50	411	Unknown
333.2063	14.80	26	Unknown
321.1731	29.37	31	Unknown
321.1731	28.83	19	Unknown
309.1699	18.22	67	Unknown
309.1699	17.80	84	Unknown
309.1699	17.44	36	Unknown
307.1574	28.45	59	Unknown
307.1574	28.36	79	Unknown
307.1574	27.10	66	Unknown
307.1574	26.99	40	Unknown
337.2358	18.86	181	Unknown
297.1340	8.87	193	Unknown
253.1442	15.56	613	Unknown
297.1341	7.08	579	Unknown
297.1341	7.35	1425	Unknown
365.2323	27.50	24	Unknown
339.1440	10.15	18	Unknown
321.1732	29.51	49	Unknown
311.1495	16.11	18	Unknown
295.1546	19.14	66	Unknown
295.1546	15.99	25	Unknown
293.1783	23.91	43	Unknown
Estimated mass balance		4660	

Supplementary Table C22: Summary of the results of the forced degradation of EPA using SCIEX Zeno trap when stored at 3-days 50°C (%). The results are shown in % as compared to peak area **EPA** in the control samples

[M-H] ⁻ m/z	rt (min.)	3-days 50°C	Identified oxylipins
301.2174	28.94	1	EPA
297.1347	8.13	4	Unknown
297.1348	7.88	15	Unknown
299.2019	26.71	1	Unknown
299.2592	26.44	7	Unknown
301.2174	29.39	0.6	Unknown
313.1808	22.38	4	Unknown
313.2172	30.61	0.3	Unknown
315.1815	16.36	8	Unknown
315.1937	18.41	0.3	Unknown
315.1952	22.82	0.3	Unknown
315.1952	24.66	0.7	Unknown
315.1952	22.88	0.3	Unknown
317.2117	25.06	0.3	Unknown
317.2119	25.40	0.3	Unknown
317.2119	25.30	0.1	Unknown
329.1756	15.20	0.3	Unknown
335.2260	20.60	0.3	Unknown
351.1789	18.06	0.3	Unknown
357.1550	7.37	5	Unknown
365.1947	19.01	0.2	Unknown
371.2439	22.92	4	Unknown
413.1969	20.10	6	Unknown
473.2176	20.26	5	Unknown
Estimated			
mass			
balance		64	

Supplementary Table C23: Summary of the results of the forced degradation of DHA using SCIEX Zeno trap when stored at 3 days 50°C (%). The results are shown in % as compared to peak area DHA in the control samples

[M-H] ⁻ m/z	rt (min.)	3-days 50°C (%)	Identified oxylipins
327.2330	30.62	2	DHA
297.1344	8.68	48	Unknown
315.1956	18.46	4	Unknown
315.1956	21.81	1	Unknown
315.1956	20.94	3	Unknown
315.1956	22.20	4	Unknown
315.1956	7.45	12	Unknown
Estimated			
mass			
balance		74	

Supplementary Table C24: Summary of the results of the forced degradation pathway using SCIEX Zeno trap and SCIEX OS software for DHA when stored at 3 days 50°C (%).

- 1	rt	Neutral	Average	[M-H] ⁻	D 4		Б.
Formular	(min.)	mass	mass	m/z	Reaction	Adducts	Peak area
$C_{20}H2_{8}O_{3}$	21.81	316.2	316.39	315.1957	Ethyl to alcohol	M-H	6.50E+04
$C_{20}H_{28}O_3$	20.94	316.2	316.39	315.1965	Ethyl to alcohol	М-Н	1.50E+05
$C_{20}H_{28}O_3$	22.20	316.2	316.38	315.1965	Ethyl to alcohol	М-Н	1.65E+05
$C_{20}H_{28}04$	18.46	316.2	316.37	315.1956	Ethyl to alcohol	М-Н	1.79E+05

Supplementary Table C25: Summary of the results of the forced degradation pathway using SCIEX Zeno trap and SCIEX OS software for EPA when stored at 3 days 50°C (%).

Formula	rt (min.)	Neutral mass	Average mass	[M-H] ⁻ m/z	Reaction	Adducts	Peak area
C ₂₀ H3 ₂ O ₄	20.60	336.23	336.42	335.2226	Oxidation and internal hydrolysis	М-Н	3.51E+04
$C_{20}H_{30}O_3$	22.26	318.22	318.39	317.2122	Oxidation and internal hydrolysis	М-Н	6.71E+04
$C_{20}H_{28}O_3$	22.82	316.2	316.38	315.1952	Ketone formation	М-Н	4.33E+04
$C_{20}H_{28}O_4$	24.66	316.2	316.38	315.1952	Ketone formation	М-Н	8.39E+04
$C_{20}H_{30}O_3$	23.59	318.22	318.39	317.2122	Oxidation	М-Н	4.07E+04
$C_{20}H_{30}O_3$	25.06	318.22	318.39	317.2122	Oxidation	М-Н	3.39E+04
$C_{20}H_{30}O_4$	25.40	318.22	318.39	317.2122	Oxidation	М-Н	1.43E+04
$C_{18}H_{36}O_3$	26.44	300.27	300.41	299.2592	Loss of 1.9581	М-Н	8.36E+05
$C_{16}H_{28}O_6$	16.36	316.19	316.31	315.1815	Gain of 13.9641	М-Н	1.03E+06
$C_{15}H_{22}O_6$	7.88	298.14	298.27	297.1348	Loss of 4.025	М-Н	1.86E+06
$C_{20}H_{32}O_4$	20.60	336.23	334.42	335.2226	Oxidation and internal hydrolysis	М-Н	3.51E+04
$C_{20}H_{30}O_3$	25.40	318.22	318.39	317.2119	Oxidation	M-H	3.12E+04
$C_{20}H_{30}O_3$	25.28	318.22	318.37	317.2119	Oxidation	М-Н	1.43E+04
$C_{20}H_{30}O_3$	25.06	318.22	318.38	317.2117	Oxidation	М-Н	3.39E+04
$C_{20}H_{30}O_3$	23.59	318.22	318.38	317.2122	Oxidation	М-Н	4.07E+04
$C_{20}H_{30}O_3$	22.26	318.22	318.39	317.2121	Oxidation	М-Н	6.71E+04

Formula	rt (min.)	Neutral mass	Average mass	[M-H] ⁻ m/z	Reaction	Adducts	Peak area
$C_{20}H_{28}O_3$	24.66	316.2	316.38	315.1959	Ketone formation	M-H	8.39E+04
$C_{20}H_{28}O_3$	22.88	316.2	316.38	315.1952	Ketone formation	М-Н	4.33E+04
$C_{20}H_{28}O_3$	18.41	316.2	316.38	315.1937	Ketone formation	M-H	3.46E+04
$C_{21}H_{30}O_2$	30.61	314.22	314.39	313.2172	Loss of O+formylation	M-H	3.55E+04
$C_{20}H_{26}O_3$	22.38	314.19	314.35	313.1808	Loss of O+bis-ketone formation	M-H	4.61E+05
$C_{20}H_{28}O_2$	26.71	300.21	300.28	299.2019	Desaturation	M-H	1.44E+05
$C_{20}H_{36}O_{6}$	22.92	372.25	372.42	371.2439	gain of 70	M-H	5.02E+05
$C_{24}H_{30}O_6$	20.26	414.2	414.4	413.2176	Gain of 111.9792	M-H	6.30E+05
$C_{15}H_{22}O_6$	7.37	298.14	298.29	357.1550	Loss of 4.08	M+CH ₃ COO-	5.74E+05
$C_{24}H_{30}O6$	20.10	414.2	414.4	413.1969	Gain of 111.9796	M-H	7.96E+05
$C_{15}H_{22}O_6$	8.13	298.14	298.26	297.1347	Loss of 4.0826	M-H	5.47E+05
$C_{20}H_{26}O_4$	15.20	330.18	330.33	329.1756	Bis-ketone formation	M-H	3.42E+04
$C_{19}H_{28}O_6$	18.06	352.19	352.36	351.1789	Tetra-oxidation and demethylation	M-H	3.85E+04
$C_{20}H_{30}O_6$	19.01	366.2	366.37	365.1947	Tetra-oxidation	M-H	2.54E+04

Supplementary Table C26: Summary of the results of the forced degradation pathway using SCIEX Zeno trap and SCIEX OS software for PGE2 when stored at 3 days 50°C (%).

Formula	rt (min.)	Neutral mass	Average mass	[M-H] ⁻ m/z	Reaction	Adducts	Peak area
					Demethylation and		
$C_{19}H_{30}O_{7}$	17.77	370.19	370.37	369.1822	di-0xidation	М-Н	4.12E+04
$C_{14}H_{28}O_3$	23.94	244.2	244.32	243.1961	Loss of 108.0216	М-Н	3.36E+04
$C_{14}H_{28}O_3$	19.29	244.2	244.34	243.1961	Loss of 108.0216	М-Н	4.70E+04
$C_{20}H_{30}O_4$	17.50	334.21	334.38	315.1958	Loss of water	M-H-H ₂ 0	5.04E5
$C_{13}H_{24}O_4$	16.52	244.17	244.28	243.1960	Loss of 108.0577	М-Н	1.00E+06
$C_{16}H_{28}O_{6}$	16.31	316.19	316.33	315.1810	Loss of 36.0367	М-Н	1.00E+06

		Neutral	Average	[M-H] ⁻			
Formula	rt (min.)	mass	mass	m/z	Reaction	Adducts	Peak area
$C_{21}H_{34}O_5$	17.17	366.24	366.42	365.2323	Methylation	М-Н	2.60E+04
					Demethylation and		
$C_{19}H_{28}O_6$	18.03	352.19	352.35	351.1781	methylene to ketone	М-Н	3.68E+04
$C_{20}H_{30}O_5$	14.22	350.21	350.4	349.2012	Desaturation	М-Н	5.45E+04
$C_{20}H_{30}O_5$	14.14	350.21	350.4	349.2012	Desaturation	М-Н	3.70E+04
$C_{20}H_{30}O_5$	13.80	350.21	350.38	349.2012	Desaturation	М-Н	5.27E+04
$C_{20}H_{30}O_4$	17.77	334.21	334.4	333.2068	Loss of water	М-Н	2.38E+06
$C_{20}H_{30}O_4$	17.50	334.21	334.38	333.2063	Loss of water	М-Н	8.51E+05
$C_{20}H_{30}O_4$	14.80	334.21	334.39	333.2061	Loss of water	М-Н	5.34E+04
					Loss of O+ethyl		
$C_{18}H_{26}O_5$	29.37	322.18	322.32	321.1732	ether to acid	М-Н	6.40E+04
					Loss of O+ethyl		
$C_{18}H_{26}O_5$	28.83	322.31	321.17	321.1730	ether to acid	М-Н	3.91E+04
	10.00	210.10	210.24	200 1 600	loss of O+ehyl	3.6.77	1 405 : 05
$C_{17}H_{26}O_5$	18.22	310.18	310.34	309.1699	ketone to acid	М-Н	1.40E+05
$C_{17}H_{26}O_5$	17.80	310.18	310.33	309.1699	Loss of O+ehyl ketone to acid	М-Н	1.73E+05
C1/1126O5	17.00	310.10	310.33	307.1077	Loss of O+ehyl	141-11	1.73L+03
$C_{17}H_{26}O_5$	17.44	310.18	310.33	309.1699	ketone to acid	М-Н	7.40E+04
					Loss of O+ehyl		
$C_{17}H_{24}O_5$	28.45	308.16	308.3	307.1576	ketone to acid	М-Н	1.22E+05
					Loss of O+propyl		
$C_{17}H_{24}O_5$	28.36	308.16	308.3	307.1575	ether to acid	М-Н	1.63E+05
	27.10	200.16	200.20	207.1575	Loss of O+propyl	N 11	1.275+05
$C_{17}H_{24}O_5$	27.10	308.16	308.29	307.1575	ether to acid	М-Н	1.37E+05
$C_{17}H_{24}O_5$	26.99	308.16	308.28	307.1574	Loss of O+propyl ether to acid	М-Н	8.19E+04
C ₁₇ Π ₂₄ U ₅	20.99	300.10	300.20	307.1374	Loss of	IVI-II	0.17E±04
$C_{20}H_{34}O_4$	18.86	338.24	338.42	337.2358	O+hydrogenation	М-Н	3.74E+05
$C_{15}H_{22}O_6$	8.87	298.14	298.26	297.1340	Loss of 54.0837	M-H	4.00E+05
$C_{14}H_{22}O_4$	15.56	254.15	254.26	253.1442	Loss of 98.0735	M-H	1.27E+06
C ₂₁ H ₃₄ O ₅	27.50	366.24	366.43	365.2322	Methylation	M-H	5.00E+04

		Neutral	Average	[M-H]-			
Formula	rt (min.)	mass	mass	m/z	Reaction	Adducts	Peak area
$C_{17}H_{24}O_{7}$	10.15	340.15	340.34	339.1440	Tert-butyl to acid	М-Н	3.75E+04
					Loss of O+ethyl		
$C_{18}H_{26}O_5$	29.51	322.18	322.31	321.1731	ether to acid	M-H	1.02E+05
$C_{16}H_{24}O_{6}$	16.11	312.16	312.32	311.1495	Propyl ketone to acid	М-Н	3.69E+04
					Loss of O+propyl		
$C_{16}H_{24}O_5$	19.14	296.16	296.3	295.1546	ketone acid	М-Н	1.37E+05
					Loss of O+propyl		
$C_{16}H_{24}O_5$	15.99	296.16	296.31	295.1545	ketone acid	M-H	5.19E+04
					Loss of O		
					andO+ethylone to		
$C_{17}H_{26}O_4$	23.91	294.19	294.32	293.1783	acid	М-Н	8.79E+04

Supplementary Table C27: Summary table of identified unknown oxylipins from mice plasma samples in comparison to the forced degradation in standard solution. The masses and retention times of the unknown in the plasma diet sample were compared to see if there will be correlation in the forced degradation study in standard solution.

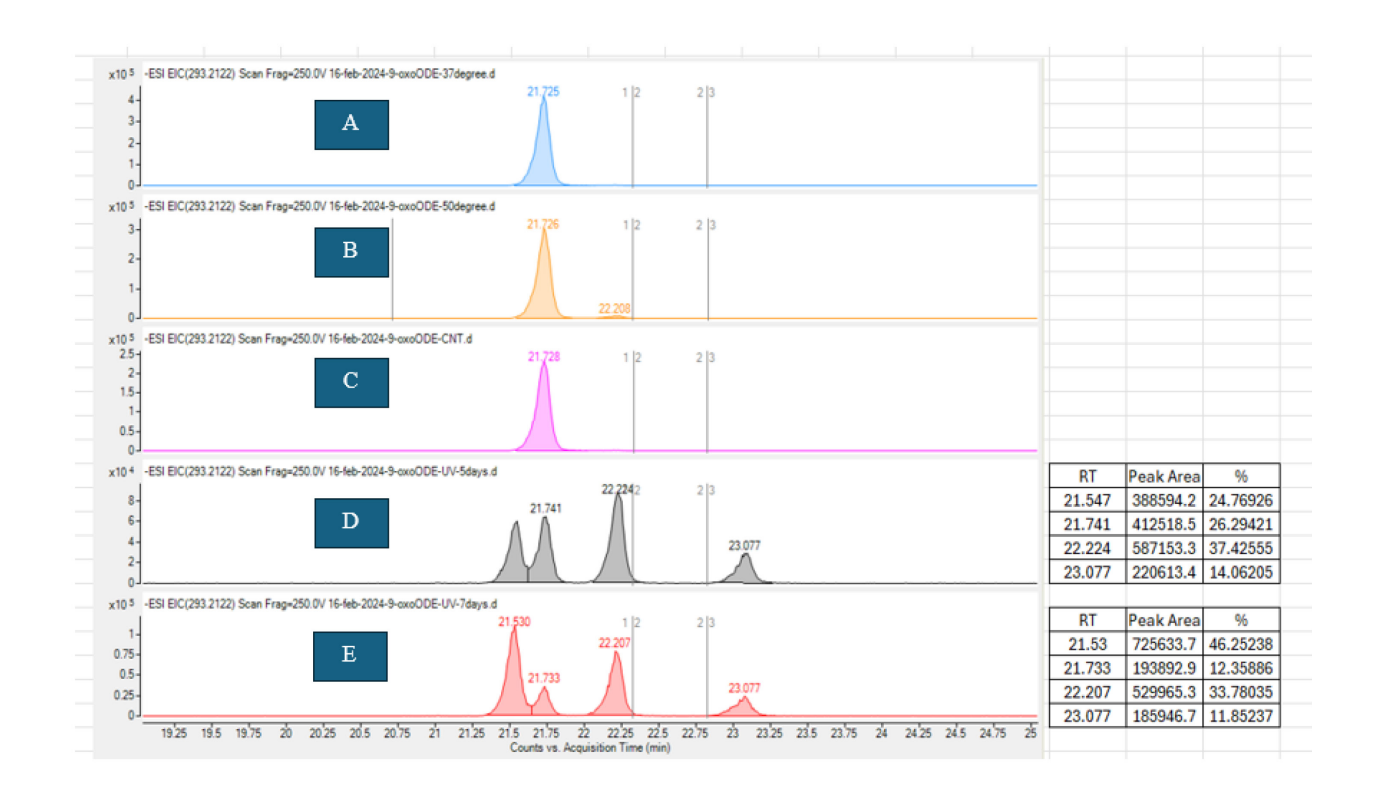
[M-H] ⁻		Detection in forced degradation of	
m/z	rt (min.)	standard	
293.2122	19.97	PGE2 ¹	
301.2173	21.70	X	
301.2173	25.50	X	
313.2384	9.23	X	
313.2384	14.29	X	
313.2384	22.06	X	
315.1966	14.18	X	
315.1966	17.01	DHA ²	
315.1966	18.45	PGE2, EPA, DHA ²	
317.2116	14.17	X	
317.2116	16.11	DHA^2	
335.2228	12.17	DHA^2	
335.2228	12.48	X	
335.2228	27.81	X	
337.2348	14.52	X	
353.2334	18.80	X	
353.2334	24.90	X	
353.2334	24.24	X	
353.2334	27.91	X	
359.2228	26.59	X	
359.2228	26.90	X	

^{*}Where X means not present. Where *1 is SCIEX and *2 is Agilent TOF instrumentation.

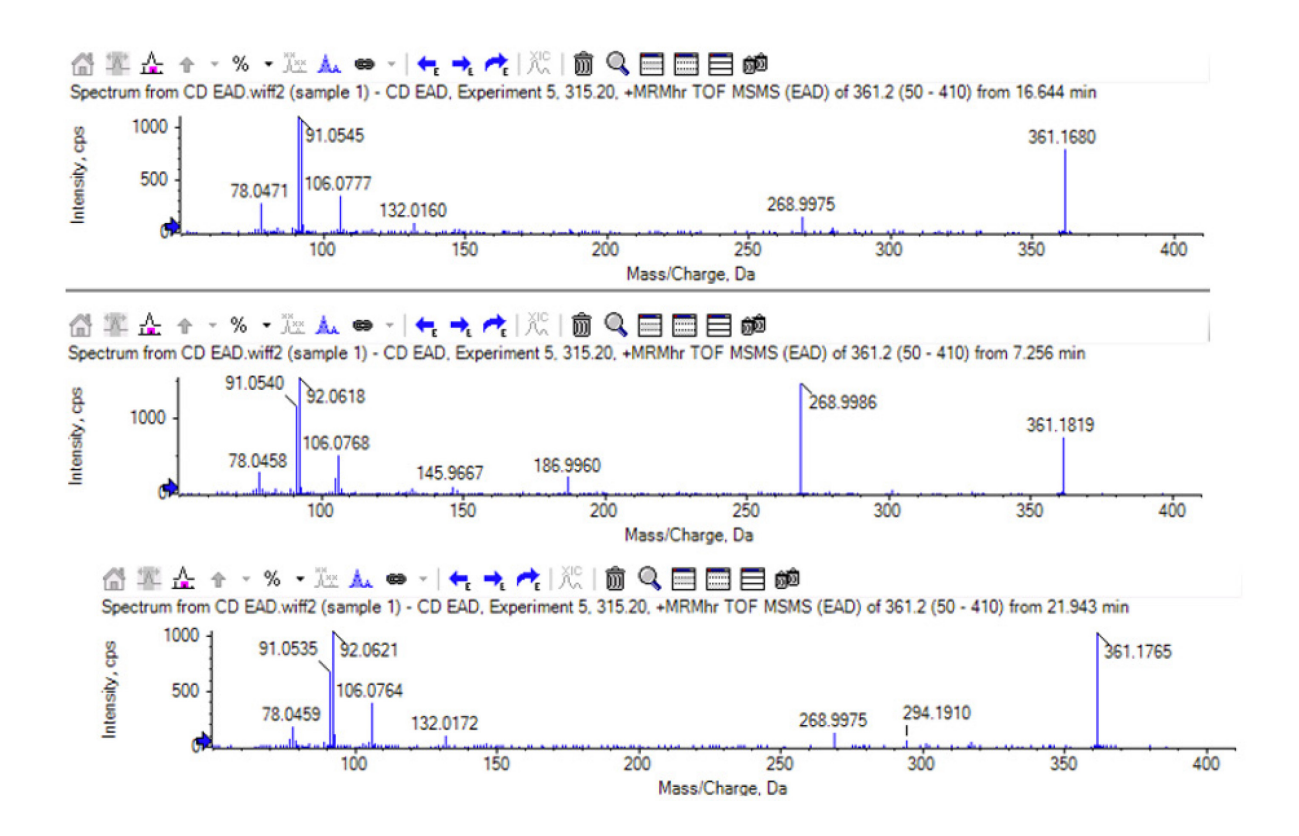
Supplementary Table C28: Summary table of identified unknown oxylipin from mice plasma samples with comparison to the forced degradation in standard solution

Mass in Agilent (CID) Mass in SCIEX (EAD)		SCIEX rt (min.) EAD	Identified oxylipins
293.2122	339.1940	16.59	NA
293.2122	339.1940	18.15	NA
293.2122	339.1940	18.64	NA
293.2122	339.1940	19.32	NA
293.2122	339.1940	20.27	NA
293.2122	339.1940	21.55	NA
293.2122	339.1940	22.36	13-HoTrE
301.2173	347.1990	21.63	NA
313.2384	359.2200	12.62	NA
313.2384	359.2200	13.54	NA
313.2384	359.2200	13.78	NA
313.2384	359.2200	19.26	NA
313.2384	359.2200	30.89	NA
315.1966	361.1790	16.64	NA
315.1966	361.1790	7.26	NA
315.1966	361.1790	21.94	NA
317.2116	363.1910	24.14	NA
335.2228	381.2070	22.21	NA
335.2228	381.2070	30.21	NA
335.2228	381.2070	30.62	NA
337.2348	383.2160	32.16	NA
337.2348	383.2160	30.21	NA
337.2348	383.2160	25.34	NA
337.2348	383.2160	22.39	NA
353.2334	399.2150	18.44	NA
353.2334	399.2150	32.16	NA
353.2334	399.2150	22.21	NA
353.2334	399.2150	22.95	NA
353.2334	399.2150	24.39	NA
353.2334	399.2150	27.91	NA
359.2228	405.2040	26.97	NA
359.2228	405.2040	29.95	NA
359.2228	405.2040	29.25	NA
359.2228	405.2040	29.48	NA

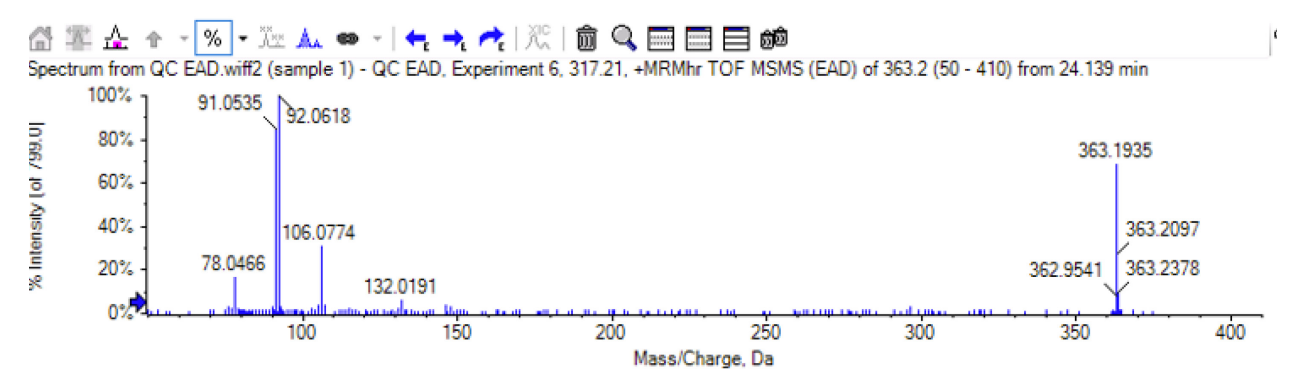
^{*}Where NA means not identified.



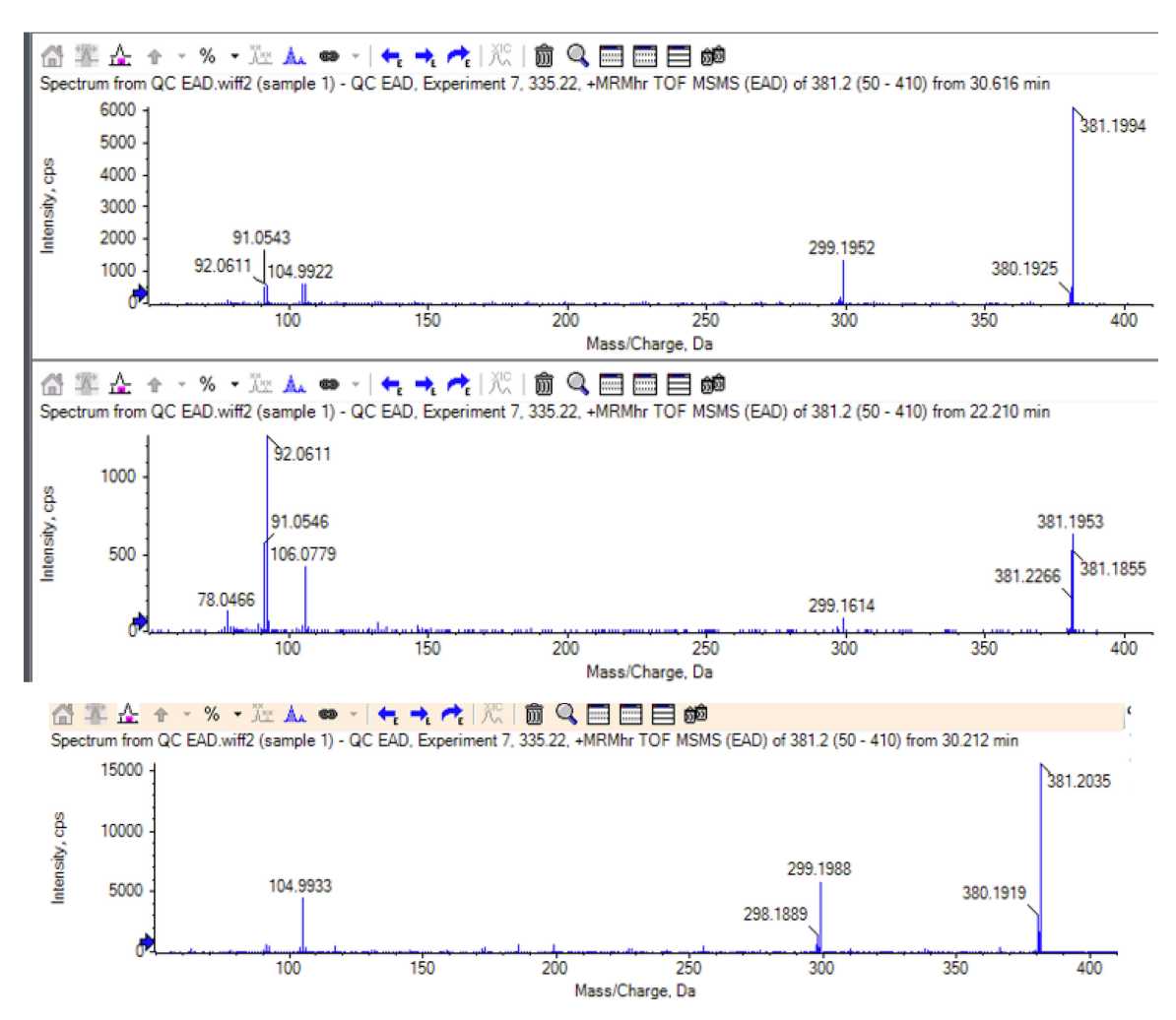
Supplementary Figure C1: Chromatogram of 9-oxoODE various forced degradation conditions. Where (A) 3-days 37°C (B) 3-days 50°C (C) control (D) 5-days UV (E) 7-days UV



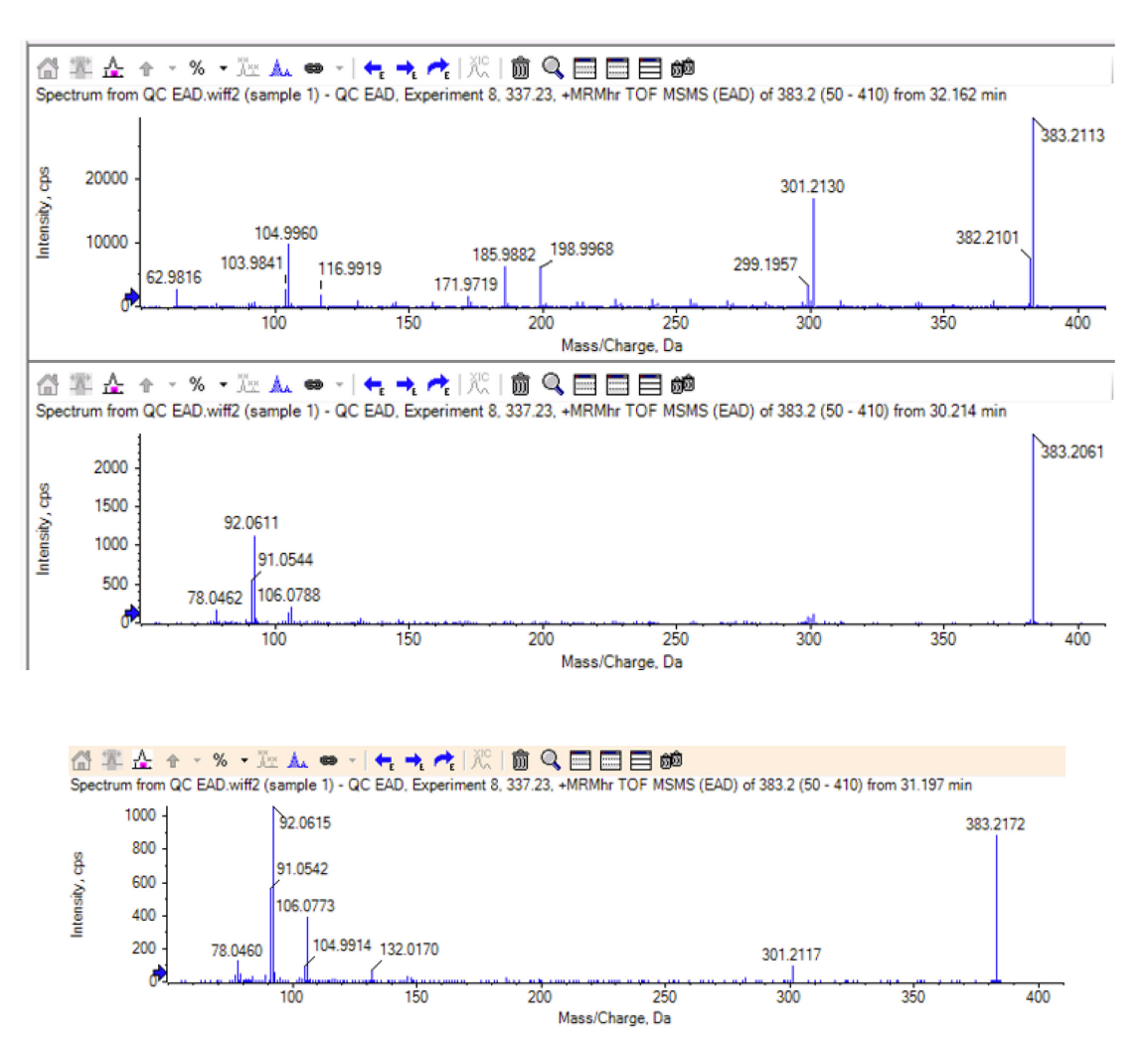
Supplementary Figure C2: EAD MS/MS spectra results for unknowns with m/z 361.1790 in plasma of mouse fed control chow diet (CD) analyzed on ZenoTOF 7600 instrument in positive ESI mode.



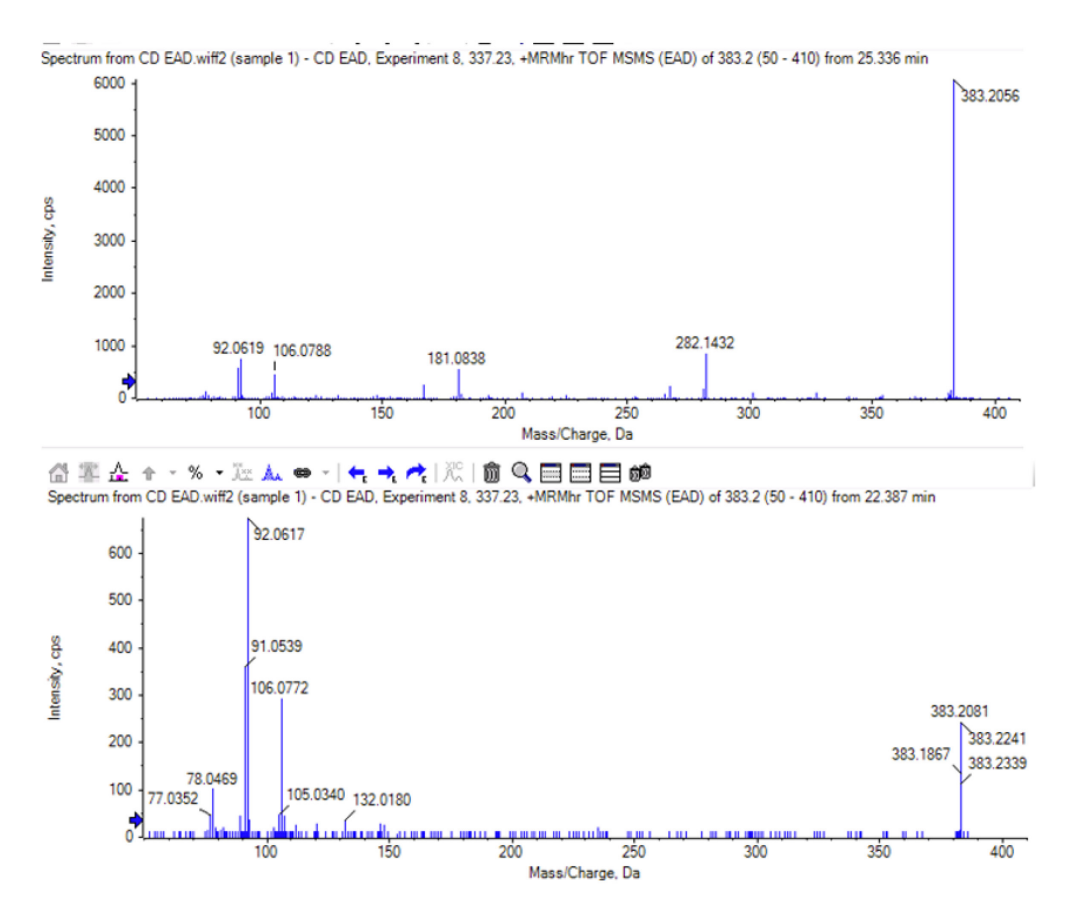
Supplementary Figure C3: EAD MS/MS spectrum of an unknown with m/z 363.1910 and retention time of 24.1 min in pooled sample of murine plasma analyzed on ZenoTOF 7600 instrument in positive ESI mode.



Supplementary Figure C4: EAD MS/MS spectra results for unknowns with m/z 381.2070 in pooled sample of murine plasma analyzed on ZenoTOF 7600 instrument in positive ESI mode.



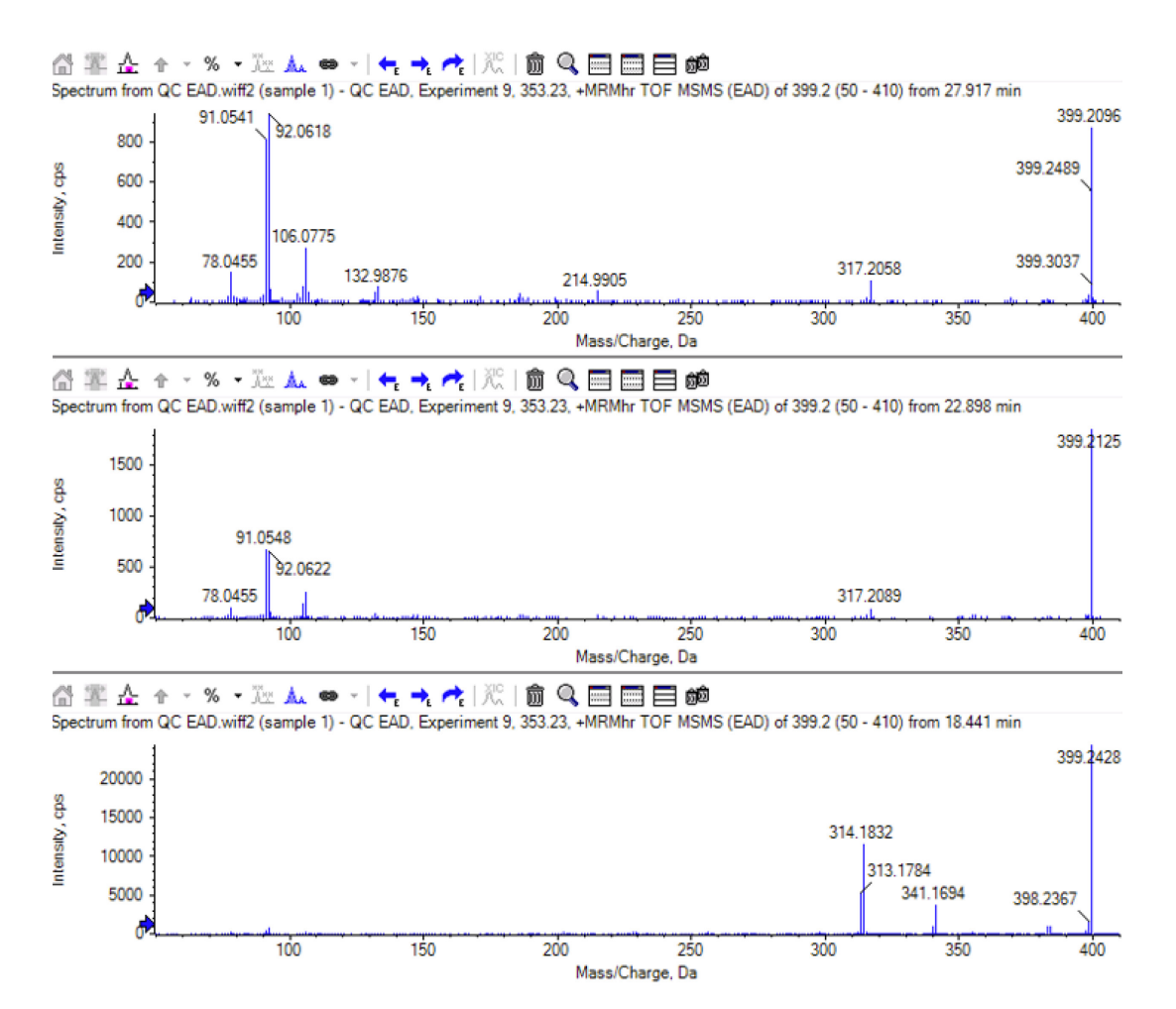
Supplementary Figure C5: EAD MS/MS spectra results for unknowns with m/z 383.2113 in pooled sample of murine plasma analyzed on ZenoTOF 7600 instrument in positive ESI mode.

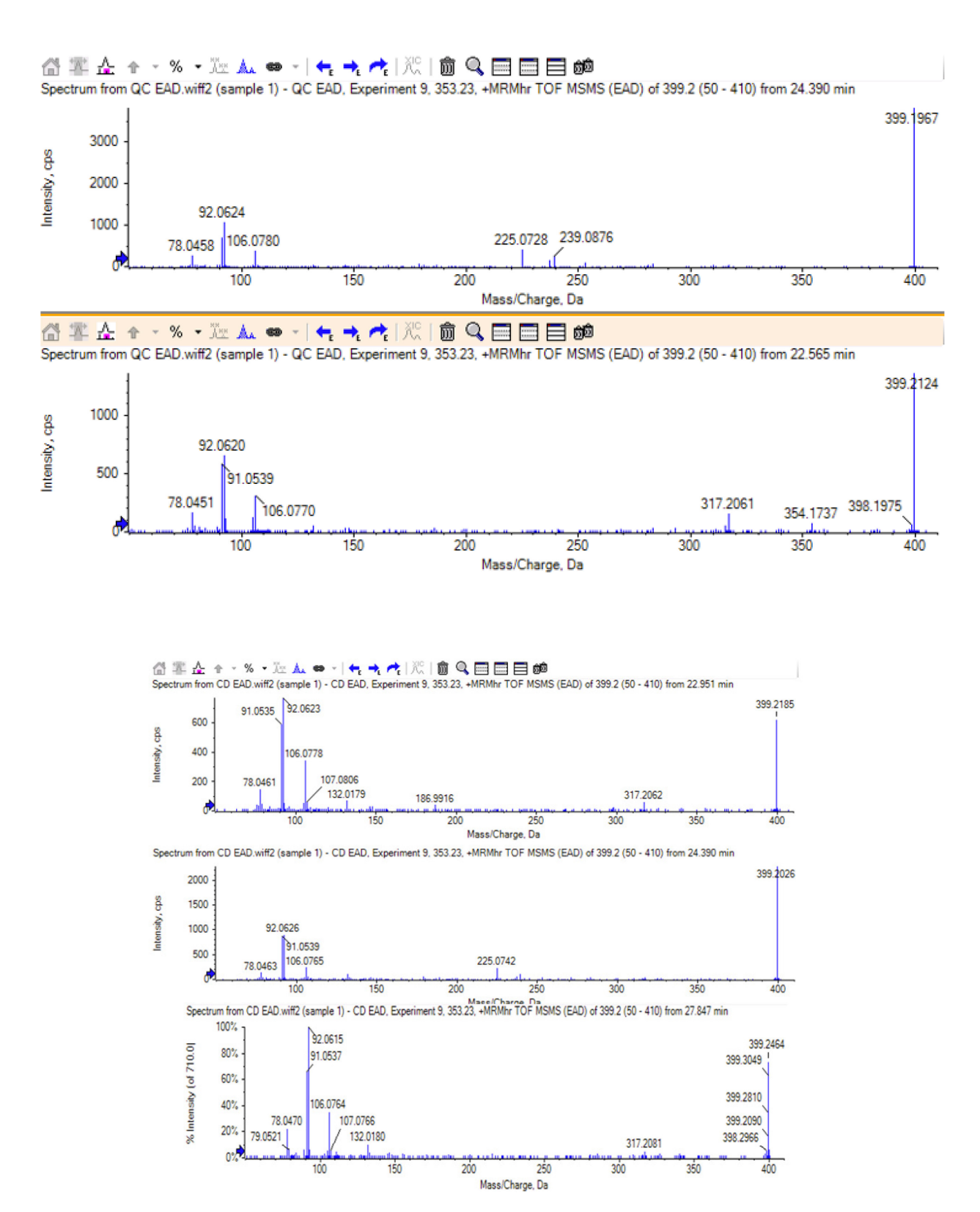


Supplementary Figure C6: EAD MS/MS spectra results for unknowns with m/z 383.2113 in plasma of mouse fed control chow diet (CD) analyzed on ZenoTOF 7600 instrument in positive ESI mode

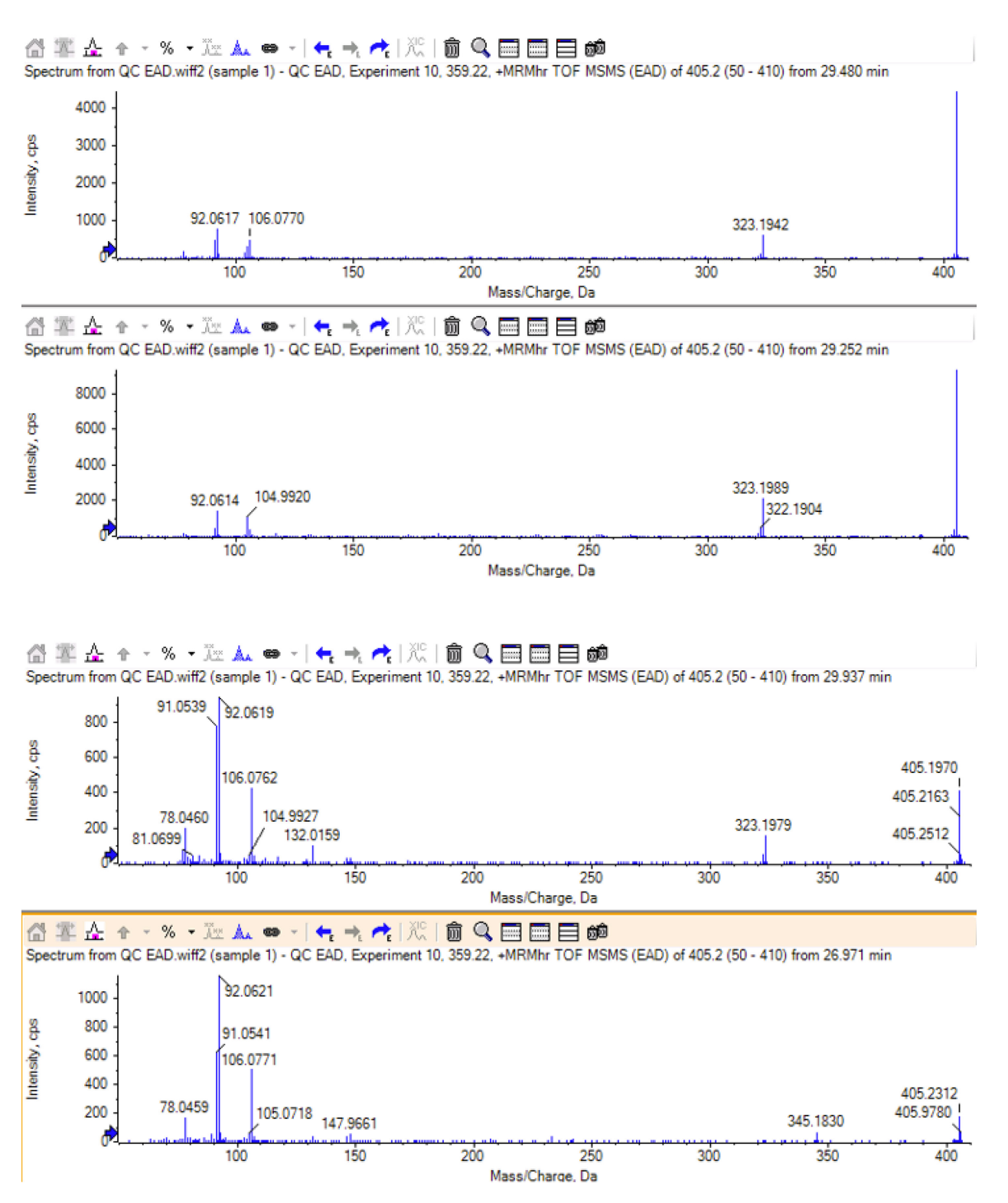
.

.





Supplementary Figure C7: EAD MS/MS spectra results for unknowns with m/z 399.2150 in plasma of mouse fed control chow diet (CD) analyzed on ZenoTOF 7600 instrument in positive ESI mode.



Supplementary Figure C8: EAD MS/MS spectra results for unknowns with m/z 405.2040 in pooled sample of murine plasma analyzed on ZenoTOF 7600 instrument in positive ESI mode.